SAIMM
JOURNAL OF THE SOUTHERN AFRICAN INSTITUTE OF MINING AND METALLURGY
FOUNDED 1894
VOLUME 116 NO. 5 MAY 2016

www.PatersonCooke.com

*** WINNER of the 2015 SAICE – SAFCEC award for BEST INTERNATIONAL PROJECT: The Khouribga to Jorf Lasfar Slurry Pipeline Project in Morocco.**

Global Leaders in Slurry Systems Engineering

- Long Distance Slurry Pipelines
- Process Engineering
- Mine Backfill and Pastefill
- Mine Tailings Systems
- Field Services
- Plants and Products
- Marine and Coastal
- Specialist Engineering
- Laboratories
- Courses

Established in 1991 in Cape Town, Paterson & Cooke is a recognised leader in the design of slurry pipeline systems and associated technologies. We have consistently expanded our range of specialist expertise so that we can offer complete solutions to our Clients.

We engineer systems that work by taking the time to understand the complex process environment and site specific needs in which our systems operate. This includes a thorough appreciation of the upstream and downstream requirements as well as ensuring proper characterisation of the material properties in our world class slurry process laboratories at our various offices.

We are specialists and have made it our business to be the best.

South African Offices

CAPE TOWN
Paterson & Cooke Consulting Engineers (Pty) Ltd
Sunrise Park, Prestige Drive, Sunrise Circle,
Ndabeni, 7405, Cape Town, South Africa

Tel +27 (0) 21 531 2955
Fax + 27 (0) 86 546 9876
CapeTown@PatersonCooke.com

JOHANNESBURG
Paterson & Cooke Field Services
Unit 19, Norma Jean Square, 244 Jean Avenue,
Centurion, 0157, South Africa

Tel +27 (0) 86 010 6129
Fax +27 (0) 86 546 9876
Johannesburg@PatersonCooke.com

PATERSON & COOKE

AUSTRALIA | CANADA | CHILE | SOUTH AFRICA | UNITED KINGDOM | USA

UNIVERSITY OF THE WITWATERSRAND, JOHANNESBURG

SCHOOL OF CHEMICAL AND METALLURGICAL ENGINEERING

Innovative engineering

The School of Chemical and Metallurgical Engineering at Wits has embarked on a programme to increase its research and postgraduate teaching in the disciplines of mineral processing and extractive metallurgy, as well as its services to the mining sector. The endeavour follows the recent awarding of a SARChI-NRF-funded chair to Professor Selo Ndlovu, a chair in hydrometallurgy and sustainable development. Included in the programme are the appointments of individuals who will support Professor Ndlovu and efforts to upgrade facilities and equipment. The appointments will add emphasis to the School's support of mining and metallurgical industries in South Africa. They include:

Marek Dworzanowski as a visiting adjunct professor and Director of Research in the School. A registered professional engineer, Professor Dworzanowski was previously employed at Anglo American. His areas of speciality are physical beneficiation and hydrometallurgy across numerous commodities.

Dr Victor Ross as a visiting adjunct professor and Director of Industrial and Commercial Liaison (Metallurgical Engineering). Professor Ross has worked previously at Mintek, De Beers and Lonmin.

Dr Tom Hara as a visiting adjunct professor and Director of Industrial Liaison Development (Pyrometallurgical Industries). Professor Hara was previously employed at Anglo American as Research Manager of Projects in its coal business unit.

Henry Simonsen as a visiting adjunct professor and Director of Academic and Commercial Partnerships. A specialist in engineering economics with experience in corporate finance, Professor Simonsen joins the school from Te-Con Consultants, where, as managing member, he undertook the techno-economic evaluation of mining, processing and energy projects.

Walter Purcell as a visiting professor in applied industrial metals and minerals. Professor Purcell joins the School from the Department of Chemistry at the University of the Free State. He is a specialist with extensive knowledge of and experience in the extraction chemistries of several industrially important metals, including Zr, Hf, Ta, Nb and the rare earth elements.

George Panopoulos as a visiting lecturer and Manager of the Development of New Short Courses. George is an independent consultant with extensive industrial experience in mineral processing and extractive metallurgy. He worked for many years at Zincor.

Alain Kabemba as a visiting senior lecturer. A registered professional engineer, Alain has over seventeen years technical experience in process engineering, mineral processing, process design, project controls and due-diligence studies on major operations (gold, PGMs, rare earth metals, base metals and industrial minerals) across several continents. Alain held managerial posts at Tenova Mining and Minerals.

Patrick Swan as a visiting lecturer in lubrication tribology and in failure analysis of materials and mechanical systems. Patrick works as an independent consultant. He has over 30 years' experience in both fields and serves as a technical expert in related legal cases.

Paul Chego as a lecturer. An nGAP (new generation of academic professional) appointment, Paul is a Wits graduate. He is working towards a PhD in chemical engineering in the ImWaRu (Industrial and Mining Water Research) Unit in the School. His research interests centre on renewable energy obtained from wastewater and water remediation.

Lehlohonolo Mokhahlane as a lecturer in mineralogy. Lehlohonolo is a qualified hydrogeologist with over 5 years' experience in geochemical processes. His fields of research include underground coal gasification, the leaching dynamics of coal-ash landfills, acid mine drainage and groundwater systems. He has worked as a hydrogeologist in the Department of Water Affairs (Lesotho) and at Eskom.

Dr David Whitefield as a senior lecturer in physical metallurgy. A graduate of the School, Dr Whitefield is a specialist in hardmetals, cermets and various ceramic materials. He joins his alma mater from De Beers (Research Laboratories). Prior to De Beers he worked at Ultramet and Boart Longyear.

Paul den Hoed as a senior lecturer in pyrometallurgy. Paul, an ex-Mintekker, joins the School from Anglo American, where he worked at its research facility in Crown Mines. Paul has specialist knowledge in the performance of refractories, in fluidisation and its applications, in the reduction and chlorination of oxide minerals, and in the roasting of base metal sulfides.

The School believes that these appointments will improve its ability to train postgraduate students effectively; provide specialised and dedicated training courses for industry; offer contract research, consultancy services and ad-hoc investigation opportunities for industry; increase its research output; and raise its standing in the profession and amongst its peers.

Address enquiries to:
Ms Ntokozo Dube, Postgraduate Course Coordinator:
ntokozo.dube@wits.ac.za / 011-717-7521
Professor Herman Potgieter, Head of School:
herman.potgieter@wits.ac.za / 011-717-7510

www.wits.ac.za/chemmet

OFFICE BEARERS AND COUNCIL FOR THE 2015/2016 SESSION

Honorary President
Mike Teke
President, Chamber of Mines of South Africa

Honorary Vice-Presidents
Mosebenzi Zwane
Minister of Mineral Resources, South Africa

Rob Davies
Minister of Trade and Industry, South Africa

Naledi Pandor
Minister of Science and Technology, South Africa

President
R.T. Jones

President Elect
C. Musingwini

Vice-Presidents
S. Ndlovu
A.S. Macfarlane

Immediate Past President
J.L. Porter

Honorary Treasurer
C. Musingwini

Ordinary Members on Council
Z. Botha
V.G. Duke
I.J. Geldenhuys
M.F. Handley
W.C. Joughin
M. Motuku
D.D. Munro
G. Njowa
A.G. Smith
M.H. Solomon
J.D. Steenkamp
M.R. Tlala
D. Tudor
D.J. van Niekerk

Past Presidents Serving on Council
N.A. Barcza
R.D. Beck
J.R. Dixon
M. Dworzanowski
F.M.G. Egerton
H.E. James
G.V.R. Landman
J.C. Ngoma
S.J. Ramokgopa
M.H. Rogers
G.L. Smith
W.H. van Niekerk

Branch Chairmen

Botswana	L.E. Dimbungu
DRC	S. Maleba
Johannesburg	I. Ashmole
Namibia	N.M. Namate
Northern Cape	C.A. van Wyk
Pretoria	P. Bredell
Western Cape	A. Mainza
Zambia	D. Muma
Zimbabwe	S. Ndiyamba
Zululand	C.W. Mienie

Corresponding Members of Council

Australia:	I.J. Corrans, R.J. Dippenaar, A. Croll, C. Workman-Davies
Austria:	H. Wagner
Botswana:	S.D. Williams
United Kingdom:	J.J.L. Cilliers, N.A. Barcza
USA:	J-M.M. Rendu, P.C. Pistorius

PAST PRESIDENTS

*Deceased

* W. Bettel (1894–1895)
* A.F. Crosse (1895–1896)
* W.R. Feldtmann (1896–1897)
* C. Butters (1897–1898)
* J. Loevy (1898–1899)
* J.R. Williams (1899–1903)
* S.H. Pearce (1903–1904)
* W.A. Caldecott (1904–1905)
* W. Cullen (1905–1906)
* E.H. Johnson (1906–1907)
* J. Yates (1907–1908)
* R.G. Bevington (1908–1909)
* A. McA. Johnston (1909–1910)
* J. Moir (1910–1911)
* C.B. Saner (1911–1912)
* W.R. Dowling (1912–1913)
* A. Richardson (1913–1914)
* G.H. Stanley (1914–1915)
* J.E. Thomas (1915–1916)
* J.A. Wilkinson (1916–1917)
* G. Hildick-Smith (1917–1918)
* H.S. Meyer (1918–1919)
* J. Gray (1919–1920)
* J. Chilton (1920–1921)
* F. Wartenweiler (1921–1922)
* G.A. Watermeyer (1922–1923)
* F.W. Watson (1923–1924)
* C.J. Gray (1924–1925)
* H.A. White (1925–1926)
* H.R. Adam (1926–1927)
* Sir Robert Kotze (1927–1928)
* J.A. Woodburn (1928–1929)
* H. Pirow (1929–1930)
* J. Henderson (1930–1931)
* A. King (1931–1932)
* V. Nimmo-Dewar (1932–1933)
* P.N. Lategan (1933–1934)
* E.C. Ranson (1934–1935)
* R.A. Flugge-De-Smidt (1935–1936)
* T.K. Prentice (1936–1937)
* R.S.G. Stokes (1937–1938)
* P.E. Hall (1938–1939)
* E.H.A. Joseph (1939–1940)
* J.H. Dobson (1940–1941)
* Theo Meyer (1941–1942)
* John V. Muller (1942–1943)
* C. Biccard Jeppe (1943–1944)
* P.J. Louis Bok (1944–1945)
* J.T. McIntyre (1945–1946)
* M. Falcon (1946–1947)
* A. Clemens (1947–1948)
* F.G. Hill (1948–1949)
* O.A.E. Jackson (1949–1950)
* W.E. Gooday (1950–1951)
* C.J. Irving (1951–1952)
* D.D. Stitt (1952–1953)
* M.C.G. Meyer (1953–1954)
* L.A. Bushell (1954–1955)
* H. Britten (1955–1956)
* Wm. Bleloch (1956–1957)
* H. Simon (1957–1958)
* M. Barcza (1958–1959)
* R.J. Adamson (1959–1960)
* W.S. Findlay (1960–1961)
D.G. Maxwell (1961–1962)
* J. de V. Lambrechts (1962–1963)
* J.F. Reid (1963–1964)
* D.M. Jamieson (1964–1965)
* H.E. Cross (1965–1966)
* D. Gordon Jones (1966–1967)
* P. Lambooy (1967–1968)
* R.C.J. Goode (1968–1969)
* J.K.E. Douglas (1969–1970)
* V.C. Robinson (1970–1971)
* D.D. Howat (1971–1972)
J.P. Hugo (1972–1973)
* P.W.J. van Rensburg (1973–1974)
* R.P. Plewman (1974–1975)
* R.E. Robinson (1975–1976)
* M.D.G. Salamon (1976–1977)
* P.A. Von Wielligh (1977–1978)
* M.G. Atmore (1978–1979)
* D.A. Viljoen (1979–1980)
* P.R. Jochens (1980–1981)
G.Y. Nisbet (1981–1982)
A.N. Brown (1982–1983)
* R.P. King (1983–1984)
J.D. Austin (1984–1985)
H.E. James (1985–1986)
H. Wagner (1986–1987)
* B.C. Alberts (1987–1988)
C.E. Fivaz (1988–1989)
O.K.H. Steffen (1989–1990)
* H.G. Mosenthal (1990–1991)
R.D. Beck (1991–1992)
J.P. Hoffman (1992–1993)
* H. Scott-Russell (1993–1994)
J.A. Cruise (1994–1995)
D.A.J. Ross-Watt (1995–1996)
N.A. Barcza (1996–1997)
* R.P. Mohring (1997–1998)
J.R. Dixon (1998–1999)
M.H. Rogers (1999–2000)
L.A. Cramer (2000–2001)
* A.A.B. Douglas (2001–2002)
S.J. Ramokgopa (2002-2003)
T.R. Stacey (2003–2004)
F.M.G. Egerton (2004–2005)
W.H. van Niekerk (2005–2006)
R.P.H. Willis (2006–2007)
R.G.B. Pickering (2007–2008)
A.M. Garbers-Craig (2008–2009)
J.C. Ngoma (2009–2010)
G.V.R. Landman (2010–2011)
J.N. van der Merwe (2011–2012)
G.L. Smith (2012–2013)
M. Dworzanowski (2013–2014)
J.L. Porter (2014–2015)

Honorary Legal Advisers
Van Hulsteyns Attorneys

Auditors
Messrs R.H. Kitching

Secretaries
The Southern African Institute of Mining and Metallurgy
Fifth Floor, Chamber of Mines Building
5 Hollard Street, Johannesburg 2001 • P.O. Box 61127, Marshalltown 2107
Telephone (011) 834-1273/7 • Fax (011) 838-5923 or (011) 833-8156
E-mail: journal@saimm.co.za

Typeset and Published by
The Southern African Institute of Mining and Metallurgy
P.O. Box 61127
Marshalltown 2107
Telephone (011) 834-1273/7
Fax (011) 838-5923
E-mail: journal@saimm.co.za

Printed by
Camera Press, Johannesburg

Advertising Representative
Barbara Spence
Avenue Advertising
Telephone (011) 463-7940
E-mail: barbara@avenue.co.za
The Secretariat
The Southern African Institute of Mining and Metallurgy

ISSN 2225-6253 (print)
ISSN 2411-9717 (online)

SAIMM
JOURNAL OF THE SOUTHERN AFRICAN INSTITUTE OF MINING AND METALLURGY
VOLUME 116 NO. 5 MAY 2016

Contents

Journal Comment

Slope Stability 2016

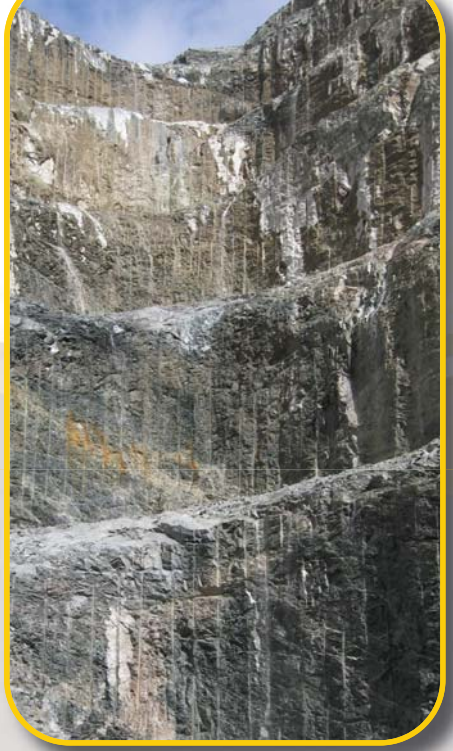

The papers in this *Journal* issue are selected from the proceedings of the Slope Stability Symposium held in Cape Town in October 2015. The symposium was organized by the SAIMM in conjunction with the South African Institute of Rock Engineering (SANIRE). This was the sixth event in this international symposium series, which originated in Cape Town in 2006 and has subsequently been held in Perth, Santiago, Vancouver, and Brisbane. A total of 222 delegates attended from the following countries: Argentina, Australia, Botswana, Brazil, Canada, Chile, the DRC, France, Italy, Lesotho, Madagascar, Namibia, Dominican Republic, Russia, Saudi Arabia, South Africa, Spain, Switzerland, The Netherlands, Turkey, United Kingdom, the USA, and Vientiane. This is the only international event that is dedicated to slope stability in mining and is therefore well attended by authors, delegates, and sponsors.

Optimized slope angles due to improved data, analysis and interpretation, and risk management can result in significant cost savings. This event brings together researchers, consultants, mine operators, and service providers to share newly developed methods and technologies that can improve slope designs and slope management.

One keynote presentation by a well-established contributor to slope stability research is included in this *Journal*. L. Lorig presents methodologies for taking extreme seismic and rainfall events into account in slope design, and discusses the relevance of each in mining.

Slope design methodologies are discussed by M.H. Fillion and J. Hadjigeorgiou, who illustrate the effect of level of confidence in the data on slope design, and give examples of how improved data can result in less conservative designs. D. Wines compares two- and three-dimensional slope analyses, and shows that a true representation of the 3D nature of the structures is often critical in providing realistic stability estimates.

W. Newcomen and G. Dick have updated their strain-based failure prediction approach. The method for setting slope monitoring movement thresholds based on rock mass rating and total strain is now based on over 100 failures in various geological environments.

Two papers deal with the geotechnical management of slopes. M. Bester and co-authors discuss a mine-to-design reconciliation process in which various technologies are implemented to measure the performance of a slope relative to the design and allow for feedback into the mine design cycle. P.J.H. de Graaf and S.D.N. Wessels provide details of the geotechnical management system implemented in the iron ore mines in the Pilbara, Western Australia.

R. Armstrong

ARE YOU READY FOR THE UPTURN?

EXPLORATION • MINING • TAILINGS AND WASTE • WATER • ENVIRONMENTAL AND SOCIAL IMPACT ASSESSMENT • GEOTECHNICAL • CIVIL AND STRUCTURAL •ENGINEERING INFRASTRUCTURE • GIS AND REMOTE SENSING

For information, visit our website www.srk.co.za or contact the SRK office to speak to Celeste Birch on +27 11 441 1111

srk consulting resourceful | experienced | worldwide

Electronic Communication

During September 2009, a delightful experiment was conducted to demonstrate how slow South Africa's data transfer services were. A carrier pigeon called Winston was able to transfer 4 GB of data across the 80 km between Howick and Hillcrest, Durban in just over two hours, whereas Telkom's ADSL service was able to complete only 4% of the transfer in that time. Since then, fibre-optic connections to the internet have improved the situation considerably, at least in some wealthier areas of the country. The bigger limitation is now on the human end, not just the technical capacity.

I remember, as a child in the 1960s and 1970s, that my father wrote letters at least once a week to his mother in England. On Sundays, around lunchtime, we would drive to the mail sorting office and deliver the latest air-mail letter for despatch on the Sunday evening overseas flight to London. A reply would arrive a few days later; this turnaround time allowing for quite a reasonable conversation to take place.

When I started work, in the mid 1980s, most formal communication took place by hand-written or typed letters, delivered to office in-boxes by messengers, and a response time of a few weeks was expected. People with desk-bound jobs could also be reached by fixed-line telephones for more immediate interaction. Telex machines were still used, albeit only occasionally, but soon thereafter faded away. My first business cards contained a telex address, before the widespread advent of more modern technologies. Fax machines opened up the possibility of faster international communication, but it took a while for this to become widespread, as fax technology was often treated as a centralized resource that was tightly controlled. In our case, a manager had to sign off all faxes before they were sent.

Yet, even with paper-based communication conducted at a fairly sedate pace, it was possible to fall behind in one's work. I had a colleague whose in-tray became stacked perilously high. One day, he simply moved the entire contents of his in-tray to his out-tray (which must have overwhelmed the poor messenger). The remarkable thing was that most of it never came back to him.

E-mail became mainstream in the 1990s (although it was first used in a very limited form in 1971) and this introduced some wonderful efficiencies to communication. It became possible to write to someone on the other side of the world and to send documents or photographs (with no loss in quality), and to get a reply by the next day. Unsurprisingly, by 1997, e-mail volume overtook that of postal mail ('snail mail'). E-mail remains the most important form of business communication to this day. I enjoy this asynchronous mode of communication that allows one to write at a time convenient to you, and for the recipient to be able to respond at a time convenient to them. E-mail has become almost universal, with 2.6 billion people being reachable via e-mail. Recent estimates indicate that over 200 billion e-mail messages are sent and received daily. No wonder that most of us experience this as a flood of messages.

But there is a downside to the convenience of e-mail. Because it is so easy to use, e-mail has proliferated to the extent that it has become almost unmanageable for many people. Spam and other unwanted mail accounts for at least as much traffic as meaningful mail. People are often automatically copied in on correspondence that they are only peripherally involved in, but presumably are expected to read. People have got used to expecting an almost immediate response to messages, and this results in the 'tyranny of the urgent over the important'. A great deal of stress is caused by this.

If one is away travelling, or even in extended meetings, the backlog of correspondence can seem unmanageable. It is sometimes necessary to declare an 'e-mail amnesty' where (like my former colleague) all mail in the overflowing in-box is simply removed. Some people are brave enough to simply delete it all, in the expectation that anything really important will be asked for again. When I have had to resort to this sort of tactic, I have simply moved the messages into a '2016' folder, for example, where they could be found again if necessary.

It is certainly true that the past few decades have brought about vast changes. We have seen, or are busy seeing, the obsolescence of the telex, fax, landline phone calls, voice messages, and postal services.

The advent of social media and instant messaging has placed even more pressure on people. New diagnosable disorders have come into being around the worry that can arise from being 'disconnected' even for short periods, and from the feelings of inadequacy, jealousy, anxiety, and depression that often result from the daily unhealthy self-comparisons people make to others online.

Facebook (publicly launched in 2006) is by far the largest of the social networks, having 1.59 billion active users who use the system at least once a month. In the USA, for example, where 85% of adults use the internet, 72% of

Electronic Communication *(continued)*

internet users use Facebook, compared to the 23% who use Twitter (which has 320 million users worldwide). Initially, Facebook was used purely for social and recreational purposes, but it has now become essential to business too. A social media report by Sensis in 2015 reported that nearly half of all Australians access one or more social networking sites every day. The report also found that Australians now spend an average of 8.5 hours per week on Facebook alone, with 24% checking social media more than five times a day. Seven out of ten people used a smartphone to access their accounts.

The rise of smartphones has led to people being reachable for communication throughout their waking hours. Accompanying this, there has been a massive shift from voice communication to text communication, with instant messaging growing enormously. The short message service (SMS) has largely been superseded by instant messaging systems, as they offer almost free communication and are much more flexible to use. The number of SMS messages on the Vodacom network in South Africa peaked in 2012, and since then has been declining by about 14% year-on-year. The number of SMS messages sent annually per subscriber has declined from 245 in 2011 to 110 in 2016.

The most globally popular instant messaging service, WhatsApp, was launched in 2009. In 2013, WhatsApp became the most popular mobile instant messenger in South Africa. WhatsApp reached 1 billion users in February 2016, with 70% of those using the service daily. WhatsApp is a cross-platform instant messaging service, available on most smartphones and computers. This system transmits more than 34 billion messages per day (with a peak throughput of 64 billion messages on a single day). The system is also used to share about 700 million photographs per day. We are told that the average user spends 195 minutes per week on WhatsApp. The average number of messages received by WhatsApp users is 2200 per month, with 1200 being sent per month. WhatsApp was bought by Facebook in 2014. Despite this, Facebook has its own Messenger instant messaging system as well, and this has 900 million users. Snapchat (which supposedly does not store messages or photographs) is increasingly being used by younger people, with about 200 million daily active users.

LinkedIn (launched in 2003) is the system of choice for professional networking, allowing people to stay in touch with their network of business contacts. LinkedIn has 433 million users, with about 25% of those (that is, over 100 million) using it at least once a month. Of all the social networks, this one seems to me to be the least demanding of one's time (unless one is actively in the job market). As your circumstances change, a simple update can be done. Otherwise, you can simply wait to receive occasional updates about the career movements of your friends and colleagues.

Instagram is widely used for sharing photographs. It has 400 million active (at least monthly) users.

Skype (launched in 2003) is widely used for video and voice chatting. It relies on a reasonably good internet connection to work well, requiring about 30 MB per minute of video (*i.e.*, about 4 Mbps). It has 300 million monthly active users, with 4.9 million of those being active daily. Skype was bought by Microsoft in 2011. By 2014, Skype had taken over 40% of the market share of international calls. More recently, services such as WhatsApp, WeChat, Telegram, and others, also let one make Skype-like voice and video calls to other users, using VOIP (voice-over-internet-protocol), on top of their picture messaging and group chat capabilities.

My personal pattern is to receive over 120 e-mail messages per day, about 30 WhatsApp messages, about 2 SMS messages (usually banking-related), about 4 phone calls, and about 0.2 printed letters (usually bills). In addition to this, there is a seemingly endless stream of items on my Facebook news feed (literally uncountable items which I don't ever get to see), and I hardly ever get to see what is sent to my Instagram (which I check occasionally) or Twitter accounts.

On top of this, there is the vast amount of news that one is tempted to try to keep up with. Also, the vast personal library that is the internet makes huge quantities of information available just waiting to be explored. Collectively, we carry out 3.5 billion Google searches per day.

Our challenge seems to be how we manage today's communication media, instead of letting it control us. In addition to our e-mail service and website, SAIMM currently has a presence on Facebook, LinkedIn, and Twitter. I would be interested to hear which of these communication channels you find most effective.

R.T. Jones
President, SAIMM

PAPERS IN THIS EDITION

Papers – Slope Stability Conference

These papers will be available on the SAIMM website
http://www.saimm.co.za

Papers of General Interest

Paper – Furnace Tapping Conference

http://dx.doi.org/10.17159/2411-9717/2016/v116na1

Implications of collecting additional data for slope design in an open pit operation

by M.-H. Fillion* and J. Hadjigeorgiou*

Synopsis

Geotechnical stability analysis and design in open pit mines requires access to representative geological, structural, hydrogeological, and rock mass models. The quality and quantity of collected geomechanical data used to build such models can have significant implications in the design of safe and economically viable slopes. Data collection is a continuous process throughout the life of a mine. The process starts from exploration to conceptual/preliminary feasibility, feasibility, design and construction, operations (early production/late production), and mine closure.

As geomechanical data is often limited at an early stage of a project, the estimated variability of the geotechnical factors may be larger than the actual data variability. This can potentially result in a conservative selection of the pit slope angle. Collecting additional geomechanical data at later stages of the mine development may contribute to reducing the uncertainty associated with the geotechnical properties and a steeper slope angle may be used for the design. This can result in significant economic benefits.

This paper investigates the impact of access to new data over time, following a series of geomechanical data collection campaigns, on design decisions. This is illustrated by comparing the resulting slope design, at three stages of the mine project, at a South African open pit mine. To demonstrate this, a series of slope stability analyses were performed using limit equilibrium tools. For each project stage, the slope angle design was modified until a similar probability of failure of 5% or less was obtained. The corresponding factor of safety distributions for each project stage were then compared to evaluate the impact of collecting additional data on the resulting slope design.

The results showed that data variability can differ significantly from one project stage to another. Data variability may be greater at more advanced project stages (*i.e.* a wider distribution of the factor of safety). Furthermore, the results showed that, even for the cases with greater variability, steeper slope angles were possible at more advanced stages for the proposed design requirement (probability of failure < 5%). In this investigation, as more data became available, the uncertainty associated with data variability could be sufficiently reduced to allow the selection of less conservative slope angles. This can be used as a managerial tool in developing data collection strategies and allocating the necessary funds, and can lead to important economic benefits to the mining operation.

Keywords

slope stability, factor of safety, probability of failure, open pit mining, uncertainty, data variability, project stages.

Introduction

In an open pit mine operation, the results of the geotechnical stability analyses conducted for the design of safe and economically viable slopes can be significantly influenced by the quality and quantity of the geomechanical data. Data collection is a continuous process throughout the timeline of a mine operation (from exploration to conceptual/preliminary feasibility, feasibility, design and construction, operations (early production/late production), and mine closure). It has been generally assumed that the level of confidence in the data should increase from one project stage to another.

It is recognized that, in most cases, the quality and quantity of geotechnical data used for the country rock model and subsequently for slope design is generally inferior to the reserve data used to define the orebody (Hadjigeorgiou, 2012; Haile, 2004; Read and Stacey, 2009; Steffen, 1997). This implies that the level of confidence in the data used for the geotechnical design is potentially less than for the data used for resource and reserve estimation. The absence of quality data may make it difficult to quantify the impact of potential instability and may result in accidents, loss of life, equipment loss, and temporary or permanent closure of an access ramp. Steffen (1997) was arguably one of the first to articulate the specificity of geomechanical data for open pit design. Terbrugge *et al.* (2009) proposed general guidelines for possible, probable, and proven slope angle, similarly to the standards for reporting exploration data (*e.g.* JORC, 2012).

Terbrugge *et al.* (2009) and Steffen (2014) suggested that because data is limited at an early stage of a project, the estimated variability of the geotechnical factors may be greater than the actual data variability, resulting in a conservative selection of the slope angle. Collection of additional data at later stages may contribute to reducing the

* *University of Toronto, Canada.*

 ISSN 2225-6253. This paper was first presented at the, International Symposium on Slope Stability in Open Pit Mining and Civil Engineering 2015, *12–14 October 2015, Cape Town Convention Centre, Cape Town.*

uncertainty associated with the geotechnical properties and a steeper slope angle may be used for the design, which results in economic benefits.

This paper investigates the impact of collecting additional data on the resulting slope design at three different project stages of an open pit mine. The results of an actual case study are compared to the approach proposed by Terbrugge *et al.* (2009) to investigate the relevance and impact of additional data collection for this site.

Case study – Mine A

Mine A was selected as a case study because of the quantity and quality of the available geotechnical data. Mine A is an open pit mine operated by Anglo American in South Africa.

Geology

Three versions of the 3D country rock model are available at Mine A. The N-S section is presented as an example in Figure 1. The first version (Figure 1a) is a 2007 model, the second (Figure 1b) is a 2009 model, and the third is a 2012 model (Figure 1c). For the three models, six geotechnical domains are defined. Geotechnical domains are areas of the proposed pit with similar geological, structural, and material property characteristics (Read and Stacey, 2009). The water table, for a pit approximately 400 m deep, was added to the 2009 and 2012 models. For the 2012 model, a weathered horizon, located 0–60 m from the slope limit, was introduced to the model. The rock mass properties in each geotechnical domain vary according to the structural volume (*i.e.* the location within the pit area) (Mine A, 2012). Major structures were introduced in the updated 2012 model (Figure 1c).

Geotechnical properties database

Geotechnical properties are available for three different project stages at Mine A. The first stage is a geotechnical investigation for Cut 3 (Anon., 1999a, 1999b); the second stage is a pit slope design study for Cuts 4 and 5 (Anon., 2008); and the last stage includes the geotechnical properties used for a slope optimization study (Mine A, 2012). Table I shows the total number of data for different geotechnical properties at the three project stages. As shown in Table I, the quantity of data collected generally increases from the early stage (Cut 3) to the more advanced project stage (slope optimization study). As more data becomes available, the corresponding uncertainty associated with the geotechnical properties should be reduced. However, other factors than additional data (*e.g.* the methods of analysis, the interpretation of data, the interpretation of other sources of information, the judgmental inputs, *etc.*) can also contribute to the changes in the strength parameters used at the various project stages. For this case study, the strength parameters used for the Cut 3 slope design were based on the

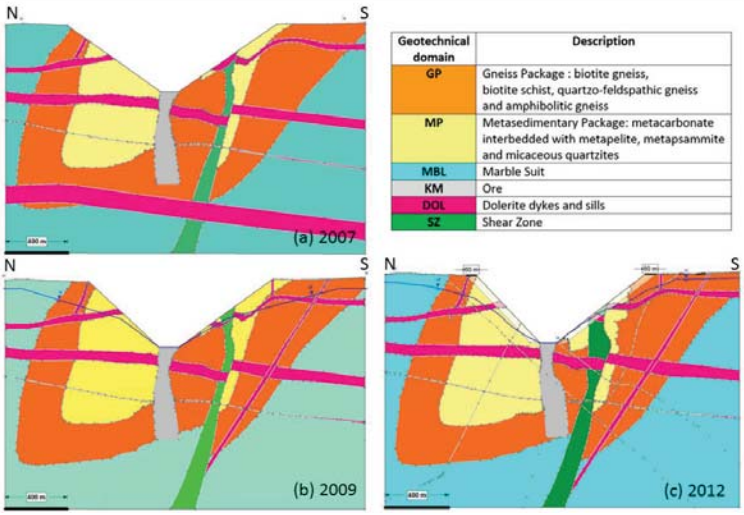

Figure 1—3D country rock models at Mine A: (a) 2007 model with dry conditions, (b) 2009 model with water table, and (c) 2012 model with water table and 60 m weathered horizon

Table I

Quantity of geotechnical data collected at the three different project stages

Geotechnical properties	Total number of data		
	Cut 3 (Consultant A, 1999a)	Cut 4&5 (Consultant A, 2008)	Optimization (Mine A database, unpublished results)
RMR	192	14482	≈ 30000
UCS	212	2052	2147
Triaxial	7	1053	1058
Brazilian	172	977	977
Density	838	2795	2869
Poisson's ratio	112	1980	2772
Young's modulus	112	2029	2717

geotechnical properties collected, on the back-analyses of slope failures, and sensitivity analyses were also performed to determine the impact of using different strength parameters (Anon., 1999a). For the Cut 4 and 5 stage, the estimation of the rock mass strength parameters was based on the more recent version of the drill-hole log database (2007 version) and on the results of the laboratory testing programme. Mohr-Coulomb parameters (cohesion and friction angle) based on the Hoek-Brown criterion were estimated to represent the rock mass strengths (Anon., 2008). For the optimization stage, strength parameters were determined from the updated geotechnical database and the data was weighted based on the percentage of each rock type per geotechnical domain (structural volume). The project resulted in the re-defining of domains for the pit (Ekkerd, 2012).

Uncertainty in geotechnical engineering

Uncertainty in geotechnical data can be due to the natural variability caused by random processes (aleatory) or to lack of information (epistemic). The natural variability in rock mass parameters is due to the processes of formation and continuous modification over geological history, which result in a variation in properties from one spatial location to another over the micro and macro scales (spatial variability), variability in properties at a single location over time (temporal variability), or both. In this case the variability is considered aleatory because it is typically represented as a random process over the project area. As this variability is inherent in the material, additional data will not eliminate the uncertainty, but will allow a better understanding of it. The epistemic uncertainty is due to a lack of data, limited information about events and processes, or lack of understanding of the process. With additional data, the epistemic uncertainty due to the lack of knowledge may be reduced to give a better understanding of the true variability (aleatory uncertainty) of the geotechnical data. For the geotechnical data collection process, the epistemic uncertainty is a combination of the site characterization uncertainty and the parameter uncertainty. The site characterization uncertainty refers to the accuracy of the geological model, which is affected by data and exploration uncertainties (measurement errors, data handling/transcription, and inadequate data coverage). The parameter uncertainty results from the inaccuracy in determining geotechnical parameters from test data. Statistical estimation errors and transformation errors (*i.e.* transforming intact rock parameters to rock mass parameters) are the major components of the parameter uncertainty, both of which become less important as additional data is collected (Christian and Baecher, 2003; Christian, 2004; Hadjigeorgiou and Harrison, 2012; Langford, 2013).

In this paper, in addition to the aleatory uncertainty inherent in the geotechnical domains, both the site characterization uncertainty and the parameter uncertainty will be addressed by including the geological model geometry and the geotechnical properties in the data analysis process.

Data analysis

Reliability-based design

In the process of designing optimal (safe and economic) slopes for an open pit mine, deterministic and probabilistic slope stability analyses can be conducted in order to determine the appropriate slope angle. Deterministic approaches are traditionally used and consider only a single set of representative parameters. The results of deterministic slope stability analyses are expressed in terms of a factor of safety (FoS), which compares the slope capacity (resisting forces) with the driving forces acting on the slope (gravity and water pressure). Since deterministic approaches provide only a first-moment approximation of the mean response, they can miss the true failure mechanism. In order to address this issue, conservative values are generally selected to ensure an adequate performance of the pit slope, which can result in unnecessary costs. Reliability methods, in conjunction with more traditional design methods (deterministic methods), can provide a better understanding of the design performance by quantifying the uncertainty in both the loads and resistances acting on a system. These consist of performing probabilistic slope stability analyses to determine a statistically based criterion, the probability of failure (PoF) that can be assessed with respect to a prescribed failure mode. The probability of failure is the probability (%) that the FoS will be unity or less. FoS and PoF values associated with a certain pit slope angle can be compared to the acceptance criteria for the corresponding slope scale (bench, inter-ramp, overall) and the resulting consequences of failure (low, moderate, high). Acceptance criteria allow the mine management to define the required level of performance of a slope against instability and/or failure. The level of acceptance may vary, depending upon the importance of the slope. Reliability-based design can provide a better understanding of the risk and a more economic design (Christian, 2004; Langford, 2013; Langford and Diederichs, 2011; Priest and Brown, 1983; Read and Stacey, 2009).

For this paper, both limit equilibrium probabilistic and deterministic slope stability analyses were conducted and the results of the deterministic approach are compared to the results obtained from finite element slope stability analyses.

Limit equilibrium analyses

Slope stability analyses were conducted using Slide (Rocscience 2010). Slide is a 2D limit equilibrium slope stability software package that can be used for circular-type failures with circular or non-circular failure surfaces. Other software can also be used for slope stability analyses. Deterministic and probabilistic slope stability analyses were conducted with Slide. Considering the overall slope failure scale, the proposed design requirement for the probabilistic slope stability analyses is PoF < 5%. Typical FoS and PoF acceptance criteria values are proposed in Read and Stacey (2009). It is suggested that for an overall slope scale with high consequences of failure, the maximum PoF should be 5%. Christian (2004) also provides details about the f-N diagrams (*i.e.* annual probability of failure *vs* risk cost or number of lives) that can be used in decision-making regarding the acceptable PoF. It is suggested that typical values for the PoF for mine pit slopes are in the range of 1–10%. The PoF approach does not take into account the consequences of failure or the impact of mitigating measures. Risk-based designs can be undertaken to allow mine

management to assess a slope design in terms of acceptance criteria that include safety or economic impacts to relate the PoF results with annual impacts.

Because the number of equations of equilibrium available is smaller than the number of unknowns in slope stability problems, all equilibrium methods of slope stability analysis employ a series of assumptions to solve the problem. Duncan (1996) suggests that these assumptions do not have a significant effect on the FoS if the method satisfies all conditions of equilibrium (Janbu, 1954; Morgenstern and Price, 1965; Spencer, 1967). In the case of force equilibrium methods (Bishop, Ordinary/Fellenius) the value of the FoS can be significantly affected by the assumed inclinations of the side forces between slices (Duncan, 1996). Because those methods satisfy all conditions of equilibrium, the Janbu's corrected, Morgenstern and Price, and Spencer's methods were used with the non-circular path search option. For each slope, 20 000 surfaces were analysed. The optimize function was used to optimize the shape of the failure surface. The PoF values for the critical failure surface were calculated using 10 000 Monte Carlo simulations with a normal distribution assigned to the input parameters. Monte Carlo analysis is a random or pseudo-random sampling technique allowing the calculation of the PoF directly (Langford, 2013). It is assumed that for a given stability analysis each variable takes a single value selected randomly from its measured distribution, independently from the other variables. In certain cases, it can also account for the dependency between variables using coefficients of correlation during the sampling process. The group of randomly selected parameters is combined with the fixed input data to generate a single value of FoS. A large number of FoS values is obtained by repeating this process (*e.g.* 10 000 times for this specific case) and the FoS values can be plotted in histogram form (Priest and Brown, 1983). A series of slope stability analyses were conducted for different slope angles. The slope angle was modified (increased or reduced) until a PoF of 5% or less was obtained. The 10 000 FoS values were then exported from Slide into MATLAB (Mathworks, 2014) in order to fit a probability distribution to the FoS values and compare the resulting distribution at each project stage. For indicative purposes only, the kernel smoothing function estimate was used to fit the histograms of the FoS values. The kernel smoothing function estimate returns a probability density estimate for the sample (represented by a vector of data). The estimate is based on a normal kernel function, and is evaluated at 100 equally spaced points that cover the range of the data in the vector.

Failure surfaces at the overall slope failure scale for two different slopes were analysed at Mine A for each of the three project stages (Cut 3, Cuts 4 and 5, Optimization). The north and south faces were analysed for a pit approximately 425 m deep. The Mohr-Coulomb strength criterion was derived from the available data at each of the three project stages (Anon., 1999a, 1999b, 2008; Mine A, 2012) and was used for the analyses. The input parameters (cohesion, friction angle, and unit weight) used in Slide for the three different project stages are presented in Table II. Since no specific properties were available regarding the phreatic surface for the Cut 3 stage, all analyses were conducted for drained conditions. For more advanced project stages, the hydrogeological model was refined and water properties became available. The groundwater model presented in Figure 2 was used for the Cut 4 and 5 stage and a phreatic surface was established at the Optimization stage (see Figure 1c).

Finite element slope stability analyses

Deterministic finite element slope stability analyses using the shear strength reduction (SSR) method were conducted in Phase2 (Rocscience, 2011) to compare the results obtained from the deterministic analyses conducted with Slide. It is recognized that elastoplastic finite element analyses agree well with the results of conventional equilibrium analyses of slope stability (Duncan, 1996). Phase2 allows determination of the strength reduction factor (SRF), which is considered equivalent to the FoS in Slide. Probabilistic slope stability analyses were not conducted in Phase2 due to the considerable amount of time required. The selected analysis type is plane strain with the Gaussian Elimination solver type and an initial SRF of 1. The gravity field stress type is used with the actual ground surface, total stress ratio of 1 and locked-in horizontal stress of zero. Field stress and body force is used as the initial element loading with an isotropic elastic type. The material type is plastic and the Mohr-Coulomb failure criterion is used. The elastic properties (Young's modulus, Poisson's ratio) are also from the mine's database (Anon., 1999a, 1999b, 2008), but the values for the Optimization stage are from Anon. (2009a, 2009b). The Young's modulus and Poisson's ratio used in Phase2 for the three project stages are presented in Table III. The same elastic properties were used for both the fresh and weathered horizons at the Optimization stage. The dilatation angle and residual tensile strength are assumed to be zero. Residual cohesion and friction angle are assumed to be equivalent to peak values. A uniform mesh type is used with six-noded triangular elements and a number of elements set to 3000. The SSR search area window was used to limit the calculations to the slope section analysed.

Results

Deterministic values of the FoS were obtained for the critical failure surface. The mean FoS value as well of the PoF were obtained from the probabilistic analyses of the critical failure surface. Table IV presents the FoS and PoF results for the different pit sections at the three stages. Since the results obtained with the three equilibrium methods (Janbu's corrected, Morgenstern-Price, and Spencer's methods) are similar, and for simplification purposes, only the results for the Janbu's corrected method are presented in Table IV. The explanation of the small differences obtained with the different methods is beyond the scope of this work. For comparison purposes, the SRF obtained using Phase2 is also presented in Table IV and is similar to the FoS obtained with Slide. Figure 3 shows the FoS distributions of the two different sections for the three project stages. Table IV shows that higher slope angles are possible at more advance project stages. Furthermore, for the Cut 4 and 5 and Optimization stages, there is a zero or close to zero PoF for steeper slope angle than for the Cut 3 stage. Even with a zero probability of failure, the slope angle was not further increased in order to

Table II

Input parameters used in Slide for the three project stages at Mine A

Geotechnical domains		Slide parameters	Cut 3		Cut 4&5		Optimization			
							North		South	
			Average	Std. dev.	Average	Std. dev	Average	Std. dev.	Average	Std. dev
GP	Fresh	Cohesion (kPa)	134.9	111.4	675.4	202.6	894.0	141.0	900.0	177.0
		Friction angle (°)	32.1	3.7	40.2	4.0	50.0	1.9	50.0	1.7
		Unit weight (kN/m³)	27.9	1.4	27.6	1.7	27.3	1.4	27.3	1.4
	Weathered	Cohesion (kPa)	N/A				516.0	226.0	449.0	213.0
		Friction angle (°)					39.0	8.2	38.0	9.1
		Unit weight (kN/m³)					27.3	1.4	27.3	1.4
MP	Fresh	Cohesion (kPa)	260.0	60.0	471.1	141.3	804.0	227.0	785.0	243.0
		Friction Angle (°)	25.5	2.3	38.5	3.9	49.0	3.5	48.0	3.2
		Unit weight (kN/m³)	26.8	0.5	27.3	1.9	27.6	1.4	27.6	1.4
	Weathered	Cohesion (kPa)	N/A				363.0	167.0	368.0	144.0
		Friction angle (°)					38.0	8.5	40.0	5.7
		Unit weight (kN/m³)					27.6	1.4	27.6	1.4
DOL	Fresh	Cohesion (kPa)	250.0	75.0	952.5	285.8	1473.0	358.0	1473.0	358.0
		Friction angle (°)	40.1	4.0	43.6	4.4	54.0	3.0	54.0	3.0
		Unit weight (kN/m³)	29.3	0.2	27.7	2.3	28.5	1.4	28.5	1.4
	Weathered	Cohesion (kPa)	N/A				556.0	227.0	556.0	227.0
		Friction angle (°)					44.0	6.3	44.0	6.3
		Unit weight (kN/m³)					28.5	1.4	28.5	1.4
MBL	Fresh	Cohesion (kPa)	410.2	123.1	410.2	123.1	981.0	209.0	1027.0	260.0
		Friction angle (°)	37.4	3.7	37.4	3.7	54.0	3.1	53.0	2.9
		Unit weight (kN/m³)	27.2	0.2	28.0	1.6	28.1	1.4	28.1	1.4
	Weathered	Cohesion (kPa)	N/A				569.0	218.0	549.0	118.0
		Friction angle (°)					44.0	12.6	44.0	3.3
		Unit weight (kN/m³)					28.1	1.4	28.1	1.4
SZ	Fresh	Cohesion (kPa)	338.0	101.4	338.0	101.4	919.0	174.0	818.0	240.0
		Friction angle (°)	33.5	3.4	33.5	3.4	50.0	1.7	49.0	2.8
		Unit weight (kN/m³)	28.0	0.5	28.0	1.6	27.3	1.4	27.3	1.4
	Weathered	Cohesion (kPa)	N/A				513.0	226.0	374.0	138.0
		Friction angle (°)					39.0	8.5	38.0	5.5
		Unit weight (kN/m³)					27.3	1.4	27.3	1.4
KM	Fresh	Cohesion (kPa)	707.0	212.1	707.0	212.1	871.0	479.0	871.0	479.0
		Friction angle (°)	39.1	3.9	39.1	3.9	50.0	4.3	50.0	4.3
		Unit weight (kN/m³)	25.7	1.0	26.4	0.9	27.4	1.4	27.4	1.4
	Weathered	Cohesion (kPa)	N/A				87.10	479.0	871.0	479.0
		Friction angle (°)					50.0	4.3	50.0	4.3
		Unit weight (kN/m³)					27.4	1.4	27.4	1.4

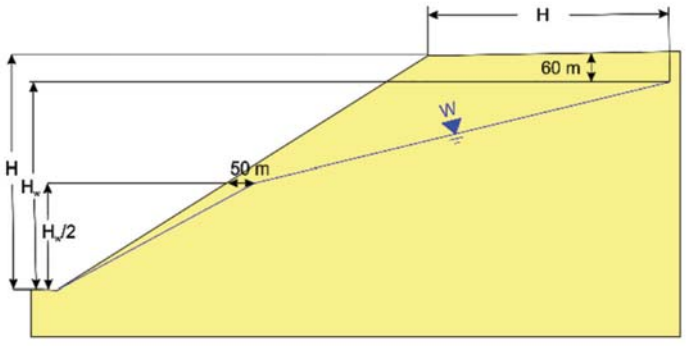

Figure 2—Groundwater model for the Cut 4 and5 stage (modified from Anon., 2008)

Table III

Input parameters used in Phase2 for the three project stages at Mine A

Geotechnical domains	Phase 2 parameters	Cut 3	Cut 4 and 5	Optimization
GP	Young modulus (GPa)	57.02	63.26	17.80
	Poisson ratio	0.20	0.26	0.23
	Tensile strength (MPa)	13.95	12.00	20.00
MP	Young modulus (GPa)	64.12	61.35	11.20
	Poisson ratio	0.20	0.24	0.24
	Tensile strength (MPa)	16.52	12.00	20.00
DOL	Young modulus (GPa)	100.00	88.72	11.20
	Poisson ratio	0.26	0.28	0.24
	Tensile strength (MPa)	27.74	21.00	40.00
MBL	Young modulus (GPa)	81.41	81.41	13.30
	Poisson ratio	0.35	0.35	0.24
	Tensile strength (MPa)	11.23	7.00	10.00
SZ	Young modulus (GPa)	44.90	44.90	14.50
	Poisson ratio	0.22	0.22	0.23
	Tensile strength (MPa)	16.00	16.00	16.00
KM	Young modulus (GPa)	27.58	35.57	13.30
	Poisson ratio	0.21	0.25	0.24
	Tensile strength (MPa)	8.68	8.00	20.00

Table IV

Factor of safety (FoS) and probability of failure (PoF) results for the different sections and stages at Mine A

Project stage	Section	Slope angle (°)	FoS (Slide) Janbu's method		SRF (Phase2)	PoF (%) (Slide)
			Deterministic	Mean		
Cut 3	North	36	1.19	1.20	1.14	3.5
(Anon., 1999a and b)	South	35	1.13	1.13	1.12	3.4
Cut 4 and 5	North	43	1.70	1.71	1.70	0.0
(Anon., 2008)	South	36	1.81	1.82	1.78	0.0
Optimization	North	47	1.57	1.60	1.65	2.8
(Mine A, 2012)	South	38	1.94	1.95	1.89	0.0

remain representative of the real designed slope angle at the corresponding project stage. Note that the PoF is close to zero only for the type of failure analysed (*i.e.* circular slope failure); it may be higher for other type of failures (planar, wedge, rockfall, toppling) that are not analysed in this paper.

Figure 3 shows that the FoS distribution becomes wider from the Cut 3 to the Cut 4 and 5 stage, with higher mean FoS at the Cut 4 and 5 stage. However, at the Optimization stage, the FoS distribution for the South section is narrower than for the Cut 4 and 5 stage with a higher mean FoS (Figure 3b). For the North section, the FoS distribution becomes wider, with a smaller mean FoS value (Figure 3a).

Discussion

Theoretical slope design variation through project stages

Currently, there are two issues that merit consideration in construction of a reliable geotechnical model that can be used for slope design. The first deals with the use of appropriate guidelines in data collection, and the second is that geomechanical data is sometimes collected without a strategy for subsequent analysis. Terbrugge *et al.* (2009) and Steffen (2014) suggest that, similarly to resource and reserve estimation, confidence categories should also be defined for slope design (*i.e.* possible, probable, and proven slope angles). They suggest that with relatively little data at the early stages of a design process, the likely range of slope angles will be widely spread, and, as more data becomes available during more mature stages, the spread of data reduces and can provide sufficient reliability for mine planning. Effectively, as shown in Figure 4a, the level of confidence in the geotechnical data is less for the conceptual stage, which results in a wider precision range and a more conservative slope angle than for the pre-feasibility and the feasibility studies. By collecting additional information, the level of confidence in the data increases and the precision range can be reduced. Then, a steeper slope angle can be selected for the slope design. Steeper slope angles are economically attractive because steepening a slope even by a

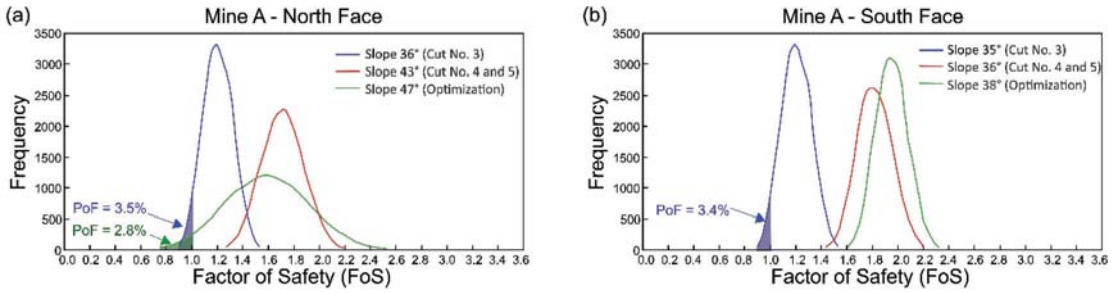

Figure 3—Factor of safety (FoS) distribution at Mine A for the Cut 3, Cut 4 and 5, and Optimization stages for (a) the North Face section and (b) the South Face section

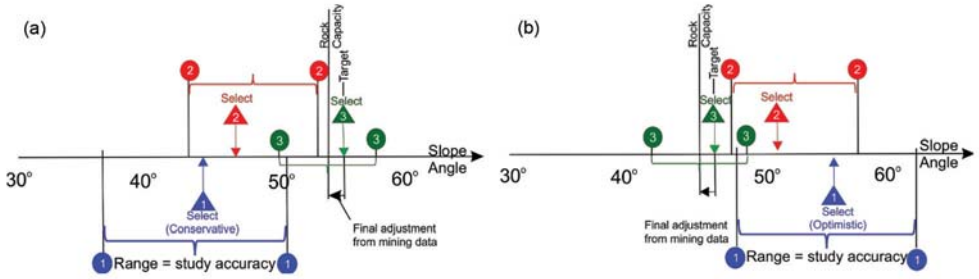

Figure 4—Precision range for the slope angle at different project stages. (a) Conservative slope angle selected at the beginning of the project and (b) optimistic slope angle selected at the beginning of the project (modified from Terbrugge *et al.*, 2009)

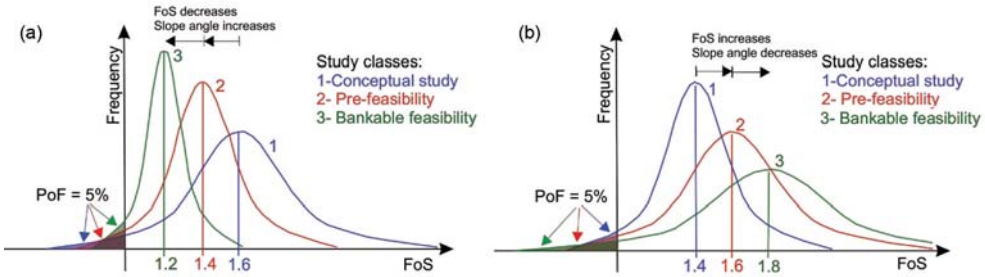

Figure 5—Slope design improvement with additional data. (a) Conservative slope angle selected at the beginning of the project and (b) optimistic slope angle selected at the beginning of the project (modified from Terbrugge *et al.*, 2009)

small increment can have a considerable impact on the return of the operation through increased ore recovery and/or reduced stripping (Read and Stacey, 2009). Figure 5a shows the relationship between the FoS and the PoF as the level of confidence in the data increases from the conceptual to the feasibility study. As shown in Figure 5a, the FoS decreases as the slope angle increases from the conceptual to the feasibility stage. However, the positive impact of additional information (*i.e.* an increased level of confidence in the geotechnical data) is that the PoF is the same, which results in economic benefits.

However, as the project progresses and the quantity and quality of the available information improve, steeper slope angles are not always achievable. In some cases, an 'optimistic' slope angle may be selected at an early stage (Figure 4b) because the allowance for uncertainty is insufficient and does not represent the true variability of the data. With additional data collection, the 'epistemic' uncertainty due to lack of knowledge may be reduced to give a better understanding of the true variability (aleatory uncertainty) of the geotechnical data. The greater variability of the data at later stages of a project may result in a flatter slope angle, as shown in Figure 5b.

In the following section, the slope design of the mine case study through different project stages is compared to the approach presented in Figure 5. Figures 5a and 5b are idealized conceptual representations of the slope design process in terms of uncertainty of the geotechnical information available through the project stages. In a real case situation, there are many other factors (methods of analysis, acceptance criteria, interpretation of data, judgemental inputs, interpretation of other sources of information, *etc.*), apart from the amount of data, that have an influence on the slope design angle.

Slope design variation through the three project stages

A potential contribution of this paper was to determine, through a case study analysis, how the increasing availability of data caused technical modifications in an open pit. This can be achieved by looking at the influence of additional information on the slope design from early project stages to more mature stages. The stability analyses were performed with real geomechanical data for different project stages and for two different sections of the pit, the North and the South faces. The results do not follow exactly the same trend suggested by Terbrugge *et al.* (2009) and Steffen (2014). The other factors not related to the amount of data were not accounted for in the interpretations. The real mine data was compared with the idealized conceptual representations relative to the spread of the FoS distribution (wide or narrow FoS distribution), the variation of the mean FoS value, and the change in the slope angle design through the three project stages.

Spread of the FoS distribution

The wider FoS distribution obtained from the early Cut 3 stage to the more advanced Cut 4 and 5 stage for the North and South faces suggests that, in this particular case study, the additional data allowed the epistemic uncertainty associated with the lack of knowledge to be reduced and a better idea of the natural variability of the data to be obtained. Since the uncertainty associated with data variability increases, the FoS distribution is wider. This is similar to the FoS distribution presented in Figure 5b, except that the slope angle is not reduced at the more advanced stage. For the Optimization stage, the FoS distribution of the South slope is narrower than for the previous stage, with a higher mean FoS and a steeper slope angle. This is similar to the approach presented in Figure 5a, except that the mean FoS is not reduced. For the North slope, the FoS distribution at the Optimization stage is wider than for the two previous stages, which is similar to Figure 5b, but the mean FoS is slightly less than for the previous stage (Cut 4 and 5 stage).

The Optimization stage resulted in re-defining geotechnical domains for the pit. For example, for the six geotechnical domains, two different data-sets are used, one for the fresh rock and one for the weathered rock (*i.e.* the horizon located 0–60 m from the slope limit, as shown with light colours in Figure 1c). Different rock properties were assigned to the geotechnical domains for the fresh and weathered rocks, depending on their structural domain. The structural domains are assigned depending on the slope orientation (*e.g.* N, SE, S, SSW, and WSW). This is why the geotechnical properties of the North slope are slightly different to those for the South slope. The definition of more geotechnical domains at the Optimization stage may have contributed, for the South slope, to reduce the uncertainty associated with data variability in each domain and this may explain the narrower FoS distribution. The wider FoS distribution for the North slope is probably due to the location of the critical failure surface. Indeed, for the North slope, the critical failure surface is located in the weathered horizon (Figure 6a) instead of in the fresh rock as it is the case for the South slope (Figure 6b). Since the standard deviation is generally higher for the properties in the weathered horizon, this can explain the higher variability in the resulting distribution for the FoS in the North slope.

Variation of mean FoS value

For the two early stages, the FoS distribution was similar to Figure 5b, *i.e.* a wider distribution at the more advanced stage (Cuts 4 and 5 stage) with a higher mean FoS value. However, the slope angle is steeper for the more advanced project stage. Terbrugge *et al.* (2009) suggested that when more information about the true variability of the data is available (*i.e.* the epistemic uncertainty is reduced), higher mean FoS are obtained at later stages because the insufficient allowance for uncertainty at the previous stage caused the selection of an optimistic slope angle at the beginning of the project (Figures 4b and 5b). For that particular case, very little data was available at the early stage and, even if the data variability increases at the Cut 4 and 5 stage, the availability of additional data resulted in higher average estimates for cohesion and friction angle, which resulted in more stable slopes (*i.e.* higher mean FoS values). For the Optimization stage, the FoS distributions and the variation of the mean FoS values are different for the North and South slopes, *i.e.* a wider FoS distribution with decreasing mean FoS for the North slope and a narrower FoS distribution with an increasing mean FoS for the South slope. For that particular case, the location of the critical failure surface

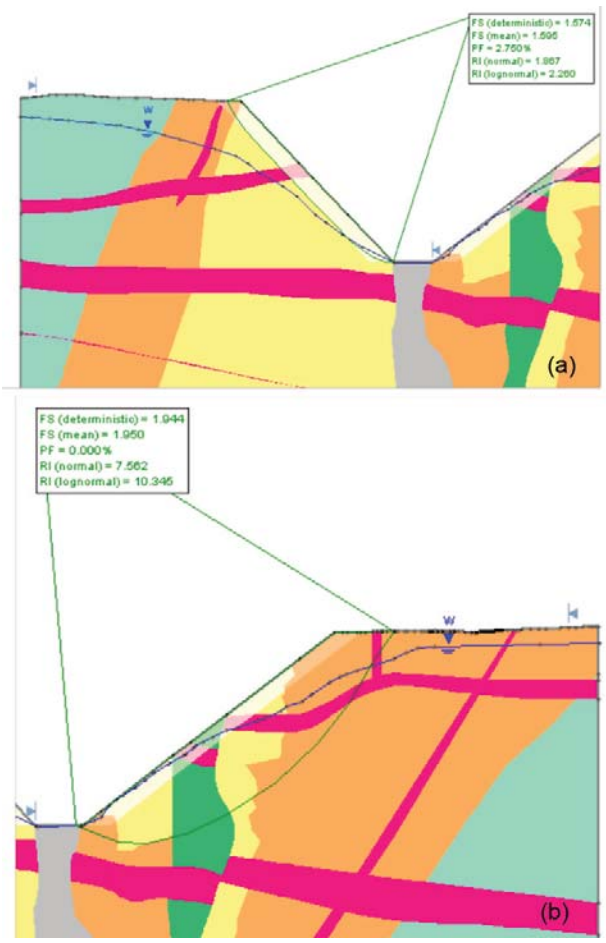

Figure 6—Critical failure surface at the Optimization stage for (a) the North section (critical failure surface located in weathered rock) and (b) the South section (critical failure surface located in fresh rock)

(Figure 6a and 6b) may also explain the variation of the mean FoS value. Dividing the domains in fresh and weathered horizons may have contributed to an estimate of higher cohesion and friction angle values for the fresh rock (the smaller values being characteristic of weathered rocks), which may have resulted in smaller FoS values for the North slope and higher FoS values for the South slope, with their critical failure surface located in weathered and fresh rocks respectively.

Change in the slope angle design

For the two early stages (Cut 3 and Cut 4 and 5), even if the FoS distribution and the mean FoS values are similar to the trend proposed in Figure 5b, the steeper slope angle obtained is different to that in the approach proposed by Terbrugge *et al.* (2009). Effectively, the wider FoS distribution with a higher mean FoS at the Cut 4 and 5 stage is obtained for a steeper slope angle (43° for the North section and 36° for the South section, compared to 36° and 35° respectively for the North and South faces at the Cut 3 stage). For that particular case, the additional data collected at the Cut 4 and 5 stage resulted in higher average estimates for cohesion and friction angle, which allowed for stable slopes at steeper angles.

For the Optimization stage, the re-definition of the geotechnical domains in fresh and weathered rocks indicated that some steeper slope angles are viable in a number of domains (Mine A, 2012). This was observed for the North and South slopes, *i.e.* 47° and 38° at the Optimization stage *vs* 43° and 36° at the Cut 4 and 5 stage for the North and South slopes respectively.

Implications of collecting additional data on the slope design

The results obtained from the case study show that the data variability can differ significantly from one project stage to another. The results also show that data variability may be greater at more advanced project stages (*i.e.* a wider distribution of the FoS) even if a conservative slope angle is selected at the beginning of a project. Effectively, for both analysed sections, steeper slope angles are possible at more advanced stages for the proposed design requirement (PoF < 5%), even for the cases with larger variability. This suggests that with more data available at later project stages, the uncertainty associated with data variability can be sufficiently reduced to allow the selection of less conservative slope angles.

Limitations of the slope stability analyses

The previous interpretations assume that the input parameters are representative of the variability of the rock properties. The input parameter distributions have a direct effect on the calculated FoS values and on the corresponding FoS distributions. For any mining project, the amount of available data is often insufficient and the confidence levels on the input data are often unknown or assessed without using a rigorous statistical method. The consequence is that the removal or addition of a small quantity of data could significantly change the results of the rock characterization process. Even if expert judgement is normally included in the process, this method is subjective and hence susceptible to change. Therefore, rigorous data quality checks and confidence assessment of the characterization results are required to enable reliable interpretations of the modelling results.

Conclusions

This paper provided an assessment of the implications of collecting additional data on the resulting slope angle design for a mine case study. In this particular case study, even if the confidence levels in the modelling input parameters were not rigorously assessed (as this is generally the reality in mining geotechnics), the mine had a comprehensive database that met all good practice criteria. Probabilistic and deterministic slope stability analyses were conducted for three different project stages, the quantity of available data increasing from the early stage to the more advanced stage. For each section analysed, the slope angle was adjusted until a probability of failure smaller than 5% (considering a potential overall slope failure) was obtained for the critical failure surface and the frequency distribution for the corresponding factors of safety was obtained.

The result showed that the variability of the input data can be significantly different from one project stage to another, resulting either in a wider or in a narrower FoS distribution for a more advanced project stage. Effectively, in some cases, a wider distribution for the FoS values was obtained at subsequent stages, which implies that data variability may be larger at more advanced project stages. The results for this case study further demonstrated that, for the proposed design requirement (PoF < 5%), steeper slope angles were possible at more advanced stages, even for the cases with larger variability. This supports the generally accepted concept that collecting additional data may sufficiently reduce the uncertainty associated with data variability to support the decision of selecting less conservative slope angles. Other factors such as the methods of analysis, the acceptance criteria, the interpretation of data, the judgemental inputs, the interpretation of other sources of information, *etc.* can also have an effect on the uncertainty of the slope design. Assessing the level of confidence in all parameters used for modelling is required to obtain a reliable slope angle design. The selection of steeper and reliable slope angles can lead to important economic benefits to the mining operation. Assessing the impact of additional data collection may help in allocating the funds to develop data collection strategies.

Acknowledgements

The authors gratefully acknowledge Anglo American Corporation for providing data for this study and for their support of this project.

References

Anonymous. 2009a. Three-dimensional numerical modelling for country rock stability studies. *Consultant's Report* no. ISA-495. Santiago, Chile. 70 pp.

Anonymous. 2009b. Bench-scale and inter-ramp configuration analysis for the southwest design sectors. *Consultant's Report* no. ISA-548. Santiago, Chile. 17 pp.

Anonymous. 1999a. Determination of the slope angles for the southern slopes of Cut 3. *Consultant's Report* no. 173849/1. South Africa. 59 pp.

Anonymous. 1999b. Determination of the slope angles for the northern slopes of Cut 3. *Consultant's Report* no. 173849/2. South Africa. 23 pp.

Anonymous. 2008. Open pit slope design Cuts 4 and 5. *Consultant's Report* no. 173849. South Africa. 37 pp.

Christian, J.T. 2004. Geotechnical engineering reliability: how well do we know what we are doing? *Journal of Geotechnical and Geoenvironmental Engineering*, vol. 130. pp. 985-1003.

Christian, J.T. and Baecher, G.B. 2003. Reliability and Statistics in Geotechnical Engineering. Wiley, Chichester, UK.

Duncan, J. 1996. State of the art: limit equilibrium and finite-element analysis of slopes. *Journal of Geotechnical Engineering*, vol. 122, no. 7. pp. 577–596.

Hadjigeorgiou, J. 2012. Where do the data come from? *Proceedings of the Sixth International Seminar on Deep and High Stress Mining*, Perth, Australia, 28-30 March 2012. Potvin, Y. (ed.). pp. 259–278.

Hadjigeorgiou, J. and Harrison, J.P. 2012. Uncertainty and sources of error in rock engineering. *Harmonising Rock Engineering and the Environment*. Quian, Q. and Zhou, Y. (eds.). Taylor and Francis, London. pp. 2063–2067.

Haile, A. 2004. A reporting framework for geotechnical classification of mining projects. *AuSIMM Bulletin*, no. 5. pp. 30-37.

Janbu, N. 1954. Application of composite slip surfaces for stability analysis. *Proceedings of the European Conference on Stability of Earth Slopes*, Stockholm. vol. 13. pp. 43–49.

JORC. 2012. Australian Joint Ore Reserves Committee. Australasian Code for Reporting of Exploration Results, Mineral Resources and Ore Reserves. The Joint Ore Reserves Committee of the Australasian Institute of Mining and Metallurgy, Australian Institute of Geoscientists and Minerals Council of Australia. http://www.jorc.org/docs/JORC_code_2012.pdf.

Langford, J.C. 2013. Application of reliability methods to the design of underground structures. PhD thesis, Queen's University, Kingston, Ontario, Canada.

Langford, J.C. and Diederichs, M.S. 2011. Application of reliability methods in geological engineering design. *Proceedings of the Pan-Am CGS Geotechnical Conference*, Toronto, ON, Canada, October 2011. 8 pp.

Mathworks. 2014. MATLAB Version R2014a, Language of technical computing. Natick, MA, USA. http://www.mathworks.com

Mine, A. 2012. 2011. K01/K02 Slope optimisation. Note for the record. *Internal report*. South Africa. 64 pp.

Morgenstern, N.R. and Price, V.E. 1965. The analysis of the stability of general slip surfaces. *Geotechnique*, vol. 15. pp. 79–93.

Priest, D.S. and Brown, E.T. 1983. Probabilistic stability analysis of variable rock slopes. *Transactions of the Institute of Mining and Metallurgy*, vol. 92. pp. A1–A12.

Read, J. and Stacey, P. 2009. Guidelines for Open Pit Slope Design. CRC Press/Balkema. 496 pp.

Rocscience Inc. 2010. Slide version 6.0, 2D Limit equilibrium slope stability software, Toronto, Ontario, Canada. https://www.rocscience.com

Rocscience Inc. 2011. Phase2 version 8.0, Advanced finite element analysis for excavations and slopes. Toronto, Ontario, Canada. https://www.rocscience.com

Spencer, E. 1967. A method of analysis of the stability of embankments assuming parallel interslice forces. *Geotechnique*, vol. 17. pp. 11–26.

Steffen, O.K.H. 1997. Planning of open pit mines on a risk basis. *Journal of the South.African Institute of Mining and Metallurgy*, vol. 97, no. 2. pp. 47–56.

Steffen, O.K.H. 2014. Risk management in geotechnical engineering and open pit mine planning. *Proceedings of the First International Congress on Mine Design and Empirical Methods*, Lima, Peru, 9-11 June. International Society for Rock Mechanics.

Terbrugge, P.J., Contreras, L.F., and Steffen, O.K.H. 2009. Value and risk in slope design. *Proceedings of the Slope Stability Conference*, Santiago, Chile, 9-11 November. ◆

http://dx.doi.org/10.17159/2411-9717/2016/v116n5a2

A framework for managing geotechnical risk across multiple operations

by P.J.H. de Graaf* and S.D.N. Wessels†

Synopsis

Rio Tinto's Western Australian expansion, combined with mining within structurally complex geology and increasingly below the water table, presents challenges in effective slope management to ensure safe and economic mining.

The Geotechnical Management System (GMS) was developed by Rio Tinto Iron Ore (RTIO) to manage geotechnical risks identified during the design process and implementation, and to ensure feedback based on the 'as-found' conditions. The GMS utilizes a risk-based approach to geotechnical risk management and is centred on the geotechnical risk and hazard assessment management system (GRAHAMS). GRAHAMS is used to assess pre- and post-control risk for future potential risks (planned slopes), current risks (as-built slopes), and actual geotechnical hazards (realized risks) identified in the pit. This serves as a core operational risk management tool in identifying and prioritizing key risk sectors and management of critical controls. The system's database reporting functionality supports effective communication of operational risks to operational personnel, as well as reporting the risk profile across operations to management.

A rigorous engagement process between design engineers and site-based engineers is implemented to ensure that key design assumptions, limitations, risks, and opportunities are understood by the site teams. This information, together with mine plan schedule details, is used to assess the design risk and develop appropriate controls. These controls typically include slope performance monitoring and slope reconciliation. The design feedback loop is closed through sharing of key slope performance and reconciliation data with the design teams.

The GMS has been successfully implemented in RTIO pits and is fundamental to successful geotechnical slope management. Improved characterization of design assumptions has allowed for re-assessment of the pit design and improved hazard management in high-risk pits. The GMS, GRAHAMS, and other processes reduce the incidence of unexpected slope instability. Improved understanding of rock mass conditions has allowed for economic optimization through redesign of slopes, allowing for an improved understanding of risk and fewer unexpected conditions (surprises), hence an increased realized value.

Keywords
open pit mining, slope management, geotechnical risk, hazard assessment.

Introduction

Rio Tinto Iron Ore (RTIO) operations are located in the Pilbara Region of Western Australia, approximately 1000 km north of Perth (Figure 1). They comprise 16 iron ore mines and three port facilities, supported by a 1700 km rail network. In 2009, 170 Mt were produced from the 100 operating pits, increasing to 350 Mt/a from over 120 pits in 2016. Since 2007 RTIO has commissioned five new mines.

Background

The geology of the Pilbara is structurally complex with multiple deformation events resulting in significant folding and faulting. The complex structure (often resulting in bedding dipping adversely into the pit void), major expansions below the water table, and detrital sequences present a challenging geotechnical environment to design and implement mine slopes while maximizing ore recovery. Orebodies typically comprise multiple ore pods, resulting in multi-pit mines, where a number of pits can be active at one time (depending on product quality requirements).

Most mines have site-based geotechnical engineers with support from a Perth geotechnical team. Before 2010, geotechnical risk management at RTIO Pilbara Operations was site-based. The skill and experience of geotechnical teams across the Pilbara varied and most geotechnical engineers had less than five years of experience. The situation was further exacerbated by the Australian mining boom, resulting in a scarcity of qualified and experienced geotechnical engineers, limited across-site support, and lack of standardization of systems and tools. Slope management systems were variable, with the level of rigour depending upon the experience of the site-based engineers. This resulted in inconsistencies in perceived levels of risk, and consequently it was difficult for a holistic business risk profile (and prioritization) to be communicated to management.

* *De Beers Group of Companies, previously Rio Tinto Iron Ore.*
† *Rio Tinto Iron Ore.*
 This paper was first presented at the, International Symposium on Slope Stability in Open Pit Mining and Civil Engineering 2015, *12–14 October 2015, Cape Town Convention Centre, Cape Town.*

A framework for managing geotechnical risk across multiple operations

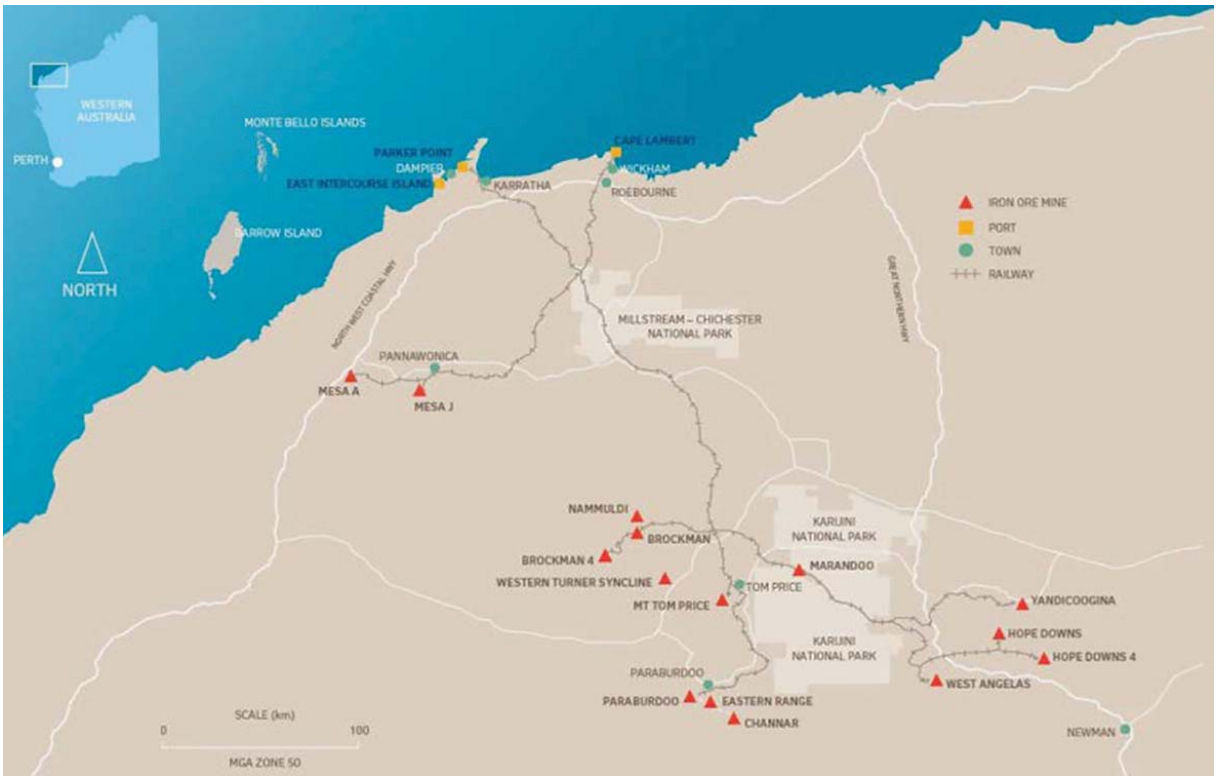

Figure 1—Rio Tinto Iron Ore operations in the Pilbara, Western Australia

A Technical Services Geotechnical Assurance group was established to provide across-site support, with responsibility for the development and commissioning of standardized tools and systems to manage geotechnical risk across the Pilbara Operations. The focus of this team is to protect the mine plan and ensure 'zero harm' safety outcomes during production ramp-up.

In early 2010, two events prompted a review of the RTIO geotechnical management systems:

(1) The introduction of a new Rio Tinto corporate standard: 'D3 Management of pit slopes, stockpiles, spoil and waste dumps'
(2) A significant slope instability at the West Angelas mine (described by Joass *et al.*, 2013).

The outcome of the review highlighted the need for improved management of geotechnical risk, including clarity of design recommendations for implementation and effective reconciliation of key design assumptions with improved slope performance, slope monitoring alarm notification, and system health monitoring.

It was clear that a more structured approach was required to ensure transparent, auditable, and sustainable geotechnical risk management. In particular, a scalable system was needed to cope with the planned ramp-up and increased risk associated with (i) additional pits, (ii) wider geographical spread of operations, and (iii) increased vertical advance rates below the water table.

The approach to remediate the slope monitoring system shortcomings has been presented previously (de Graaf and Wessels, 2013).

This paper addresses the improved risk-based geotechnical management system (GMS) implemented across the RTIO Pilbara Operations.

The need for slope management

Effective slope management is an obvious prerequisite and enabler for safe and economic open pit operation – the scope of which can be significant. Statutory and corporate governance provide a framework with which operations must comply.

Regulations and corporate standards require that appropriate slope designs are developed and implemented. The legislative requirements principally focus on the safety requirements and penalties in the case of noncompliance and/or adverse findings. Although the key focus of the corporate standard is the management of slope-related risks, (which may exceed the local legislative requirements, depending on the jurisdiction), a well-managed slope provides the added advantage of satisfying shareholders' demands for maximizing profit through efficient mining.

Legislative requirements

RTIO's Pilbara mines are governed by the Western Australian *Mines Safety and Inspection Act* (1994) (MSIA) and the *Mines Safety and Inspection Regulations* (1995) (MSIR). Regulation 13.8 of those regulations pertains specifically to the application of sound geotechnical engineering practice in open pit mines.

Experience and professional judgement are important aspects of geotechnical engineering that are not easily

quantified, but which can contribute significantly to the formulation of various acceptable and equally viable solutions to a particular mining problem. Management at each mining operation should recognize, identify, and address the geotechnical issues that are unique to each mine, using current geotechnical knowledge, methodology, and software and hardware appropriate to the situation. On this basis, the then WA Department of Minerals and Energy (DME) issued guidelines 'Geotechnical Considerations in Open Pit Mines' (1999), specifically to provide further explanation of the requirements of Regulation 13.8 and provide examples of good geotechnical engineering practice. The DME also encourages the application of current geotechnical knowledge, methodology, instrumentation, and 'ground support and reinforcement' techniques and hardware to the practical solution of geotechnical engineering issues in open pit mining.

Corporate standards

Rio Tinto Safety Standard '*D3: Management of pit slopes, stockpiles, spoil and waste dumps*' (2010) provides a corporate standard for management of geotechnical hazards across all Rio-managed operations. The standard covers all geotechnical activities related to open pit mining, from design through implementation and verification. The application of the standard ensures that mines are designed, constructed, operated, and decommissioned on the basis of defensible, rigorous, and verifiable approaches to the management of business risks and achievement of Rio Tinto's business objectives. The standard requires that:

- Pit slope and dump design follow an engineering process that results in a geometry that meets safety and economic objectives, and is adopted in support of mine planning, mine development, and closure
- Implementation encompasses the application of the design, and geotechnical hazard management systems and processes that are put in place to support mine operations through to closure, and post-closure
- Verification involves applying monitoring and measurement processes and systems to reconcile the implemented design performance and conformance, with the design
- Design, implementation, and verification are part of a holistic process for the creation of slopes that promote both safety and economic mining goals.

To achieve these objectives, it is necessary to formalize the management of geotechnical and associated risks across business units and employ robust processes and systems for managing risks. The standard mandates the development and implementation of slope and dump management plans. These are equivalent to ground control management plans, which are recommended in the DME (1999) guidance note, or Code of Practice as required in other jurisdictions.

The overall objective for regulators is to ensure a safe working environment, and consequently the slope design must take into account the *in situ* conditions and planned mining strategy, and demonstrate that geotechnical risks are appropriately managed, whereas corporate standards combine the safety and economic requirements and maximize profit by ensuring designs are optimized.

Risk-based approach

The evaluation and management of risk is an ongoing function throughout the life of a mining project. Uncontrolled slope instability can have significant safety and economic impacts, and consequently typically features in the top ten risks for most open pit operations. Lack of certainty of design and mine plan inputs and assumptions presents a risk of adverse outcomes; but also may present upside potential or opportunity if more favourable outcomes are realized. Sharon (2009) describes risk management as the culture, process, and structure directed toward realizing potential opportunities while managing adverse effects. It is the authors' opinion that risk management requires end-to-end integration and needs to be maintained current with changing conditions and ongoing evaluation of effectiveness of controls.

To effectively use a risk management process it is important to understand the principles that underlie effective risk management. The international risk standard ISO 31000:2009 *Risk Management - Principles and Guidelines* includes a set of eleven principles for consideration. Hillson (2011) provides an excellent summary of and commentary on these principles: 'Each of which tells us something important about risk management, and together they set a challenging target for organisations who want to manage risk well. Some of them are obvious, but others may need a little explanation. Risk management should:

1) create and protect value. Risk management helps us to optimize our performance. It also protects value by minimizing the effect of downside risk, avoiding waste and rework.
2) be an integral part of all organizational processes. Risk management is not a stand-alone activity, and it should be 'built-in not bolt-on'. Everything we do should take account of risk.
3) be a part of decision-making. When we are faced with important situations that involve significant uncertainty, our decisions need to be risk-informed.
4) explicitly addresses uncertainty. All sources and forms of uncertainty need to be considered, not just 'risk events'. This includes ambiguity, variability, complexity, change etc.
5) be systematic, structured and timely. The risk process should be conducted in a disciplined way to maximise its effectiveness and efficiency.
6) be based on the best available information. We will never have perfect information, but we should always be sure to use every source, being aware of its limitations.
7) be tailorable. There is no 'one-size-fits-all' approach that suits everyone. We need to adjust the process to match the specific risk challenge that we face.
8) take human and cultural factors into account. Risk is managed by people, not processes or techniques. We need to recognize the existence of different risk perceptions and risk attitudes.
9) be transparent and inclusive. We must communicate honestly about risk to our stakeholders and decision-makers, even if the message is unwelcome to some.

10) be dynamic, iterative and responsive to change. Risk changes constantly, and the risk process needs to stay up to date, reviewing existing risks and identifying new ones.
11) facilitate continual improvement of the organisation. Our management of risk should improve with time as we learn lessons from the past in order to benefit the future.'

These principles make risk management more effective; they have been central to the practical development of the approach described in this paper, and are in alignment with corporate risk management requirements.

The geotechnical management plans of some large open pit operations rely almost exclusively on 'slope displacement' action plans based on experience rather than risk assessment. Good examples of geotechnical risk management and mitigation systems for large open pits are presented by Bye *et al.* (2005), Hearth (2007), and Ginting *et al.* (2011).

These approaches are appropriate where resources and personnel are focused on a single pit environment. However, due to the wide geographical spread of pits at individual mine operations and across the Pilbara, a risk-based approach was needed to prioritize and allocate resources. To give an indication of the substantial spatial challenges, the current Paraburdoo Mine produces >20 Mt/a ore from 30 pits spread along 34 km of the Central and Eastern Range ridge line. A scalable yet flexible system was needed to evaluate and manage geotechnical risk. Furthermore, a standardized reporting approach to quantify, prioritize, and track implementation of controls, and which would also allow for reporting on risk type across the Pilbara operations, was required.

Hamman (2009) and Canbulat *et al.* (2013) present pit risk rating systems that can be used to evaluate the geotechnical risk 'status' of mines. This information can then be used to rate an individual mine within a company against others, or internally to determine whether geotechnical management has improved over time. These tools were developed to provide a high-level business-wide risk overview. The principal limitation of these systems is that the entire operation is evaluated in a single risk assessment. There is no provision for evaluating individual slope sectors and various modes of instability; consequently there is limited scope to use these tools to evaluate appropriate levels of control to be used for operational risk management.

Sharon (2009) suggests that operational risk management requires collaborative exchanges involving the development of risk assessments and evolution of improved and sustainable management practices; and that the principal goals of a geotechnical management programme are achieved with an effective performance monitoring system, developed jointly with the mine operators. The authors have extended this approach such that the justification and deployment of monitoring systems is risk-based. This provides a defensible justification for short- and long-term planning as well as budget planning.

Design, implementation, and verification

RTIO has developed a slope management framework in compliance with legislative and corporate governance requirements. This process aligns with the robust engineering design principles of ensuring that the design loop is closed through operational feedback, where input and outputs of each stage are aligned to enable effective engineering optimization. This can be displayed as a diagram representing a design-implementation-verification cycle (Figure 2). This is an iterative process that should be worked through a number of times as mining progresses to ensure that the slope design process is honed.

The geotechnical management system

The large number of operational pits across RTIO's 16 operations in the Pilbara requires a standardized and risk-based approach to managing geotechnical risks to ensure

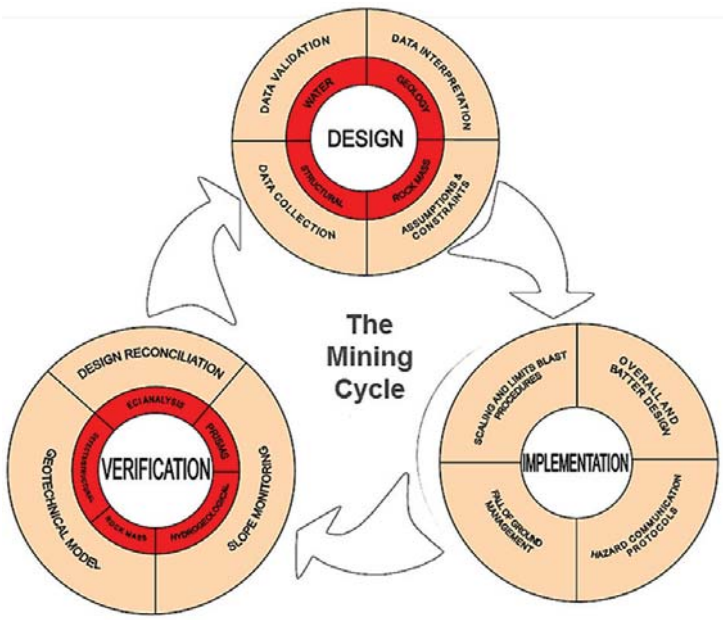

Figure 2—Design-implementation-verification work cycle (adapted from Hutchinson and Diederichs, 1996)

resources and effort are focused in the right areas. A standardized approach facilitates the reporting, management, and auditing of geotechnical risks across the multiple operations to a centralized management.

RTIO developed a systematic framework to ensure that potential geotechnical risks are identified early and rigorously evaluated to allow effective controls to be identified and implemented. Figure 3 illustrates the geotechnical management system (GMS) developed by RTIO in alignment with the design-implementation-verification work cycle.

Geotechnical design

Geotechnical design is undertaken in line with the corporate study progression guidelines and is commensurate with the level of risk associated with the design and rock mass conditions. As most significant designs are undertaken by Perth-based engineers and consultants, a rigorous design engagement process with site-based engineers is implemented to ensure that key design assumptions, limitations, risks, and opportunities are understood by the site teams. All designs are based on the following mine design principles:

- Satisfy Western Australian MSIA and MSIR requirements
- Satisfy Rio Tinto corporate slope and waste dump safety standard
- Satisfy RTIO geotechnical design acceptance criteria
- Must be operationally achievable (comply with minimum mining width and equipment limitations)
- Design flexibility reflects the current data confidence, topographical constrains
- Most acceptable safe economic outcome (ore recovery *vs* waste)
- Achievable to full depth based upon current orebody knowledge and life-of-mine directives
- Designs based on industry-accepted practice, geotechnical design methods, and independently peer reviewed as required
- Design risks must be acceptable to the business. Areas of geotechnical uncertainty and knowledge limits, along with any known/recommended actions and their timelines, must be communicated by the design team.

Departures from the design principles are justified by risk assessment and supported by an appropriate management plan.

Implementation

Geotechnical slope management systems that ensure safe operations at RTIO mine sites include technical procedures and systems (administered by the Technical Services group), and safe work procedures and systems mandated by Operations. One of the main technical systems is the geotechnical risk and hazard management system (GRAHAMS). This is a database of all the geotechnical risks on site and is the 'core' of the GMS. GRAHAMS includes functionality to assess and manage the current potential (as-built slope) and future potential (design slope) risks, leading to the development of monitoring plans and associated area management plans. Responses to conditions exceeding monitoring thresholds or other indications of slope instability are documented in geotechnical trigger action response plans (TARPs). Geotechnical hazards are communicated with hazard alert and maps, while the face risk assessment procedure and geotechnical awareness training provide non-geotechnical personnel with the knowledge to ensure a safe working environment.

Verification

Slope reconciliation is an essential component of the design process to confirm design parameters used in the feasibility studies. Verification of these parameters is a key step in

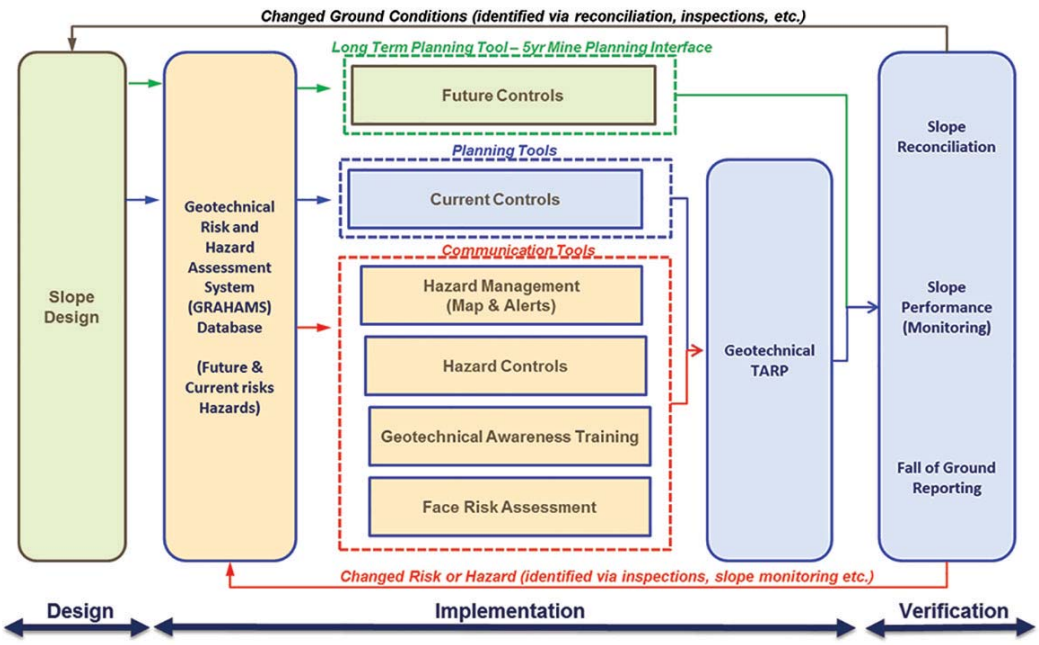

Figure 3—RTIO Geotechnical Management System

ensuring that the original design assumptions and recommendations are valid and that the design remains suitable for current conditions.

The geotechnical reconciliation process is the last step of the GMS and is designed to close the loop by providing feedback into the design process. This reconciliation process aims to compare all major input parameters utilized in slope design studies with current conditions. Any significant differences between observed and accepted design parameters are highlighted – these may present a risk or an opportunity. Negative reconciliation triggers design remediation studies, while positive reconciliation presents an opportunity to optimize the design.

GMS requirements

Systems engineering encourages the use of tools and methods to better comprehend and manage complexity in systems, but requires that the process is well documented and supported with appropriate training and routine checking (ensuring effective implementation) and periodic review to identify areas of improvement to fine-tune the system. The GMS is a management plan, backed by an organized system of supporting documents describing the design, implementation, and verification to maintain safe operations. This is to ensure that the system is sustainable. Figure 4 illustrates this framework.

Essential aspects of the RTIO GMS include:

1. *Documentation*—The primary document is the Slope and Dump Management Plan; this outlines the integration of all geotechnical risk management throughout the design, implementation, and verification process. Other key documents include the geotechnical trigger action response plan and various technical guidance notes covering key aspects of the work cycle and functional use of the tools and systems. These documents include:
   (a) Appointments of mandatory accountable roles: registered manager, quarry manager, qualified (geotechnical) individual(s), and individuals authorized to make changes to designs (slope/dump/ blast *etc.*).
   (b) RACI matrices identifying roles and accountabilities for all elements of the work flow
2. Systems and tools—includes:
   (a) Mine design approval system, managing and tracking approval of the 'design of record' as well as a repository of supporting technical information pertaining to the design
   (b) Geotechnical hazard and risk management (GRAHAMS)
   (c) Face risk assessment system, ensuring operational risks are appropriately addressed when working on foot adjacent to slopes.
3. *Training*—Basic geotechnical hazard awareness training for all personnel, and advanced training for supervisors and personnel working in higher risk areas

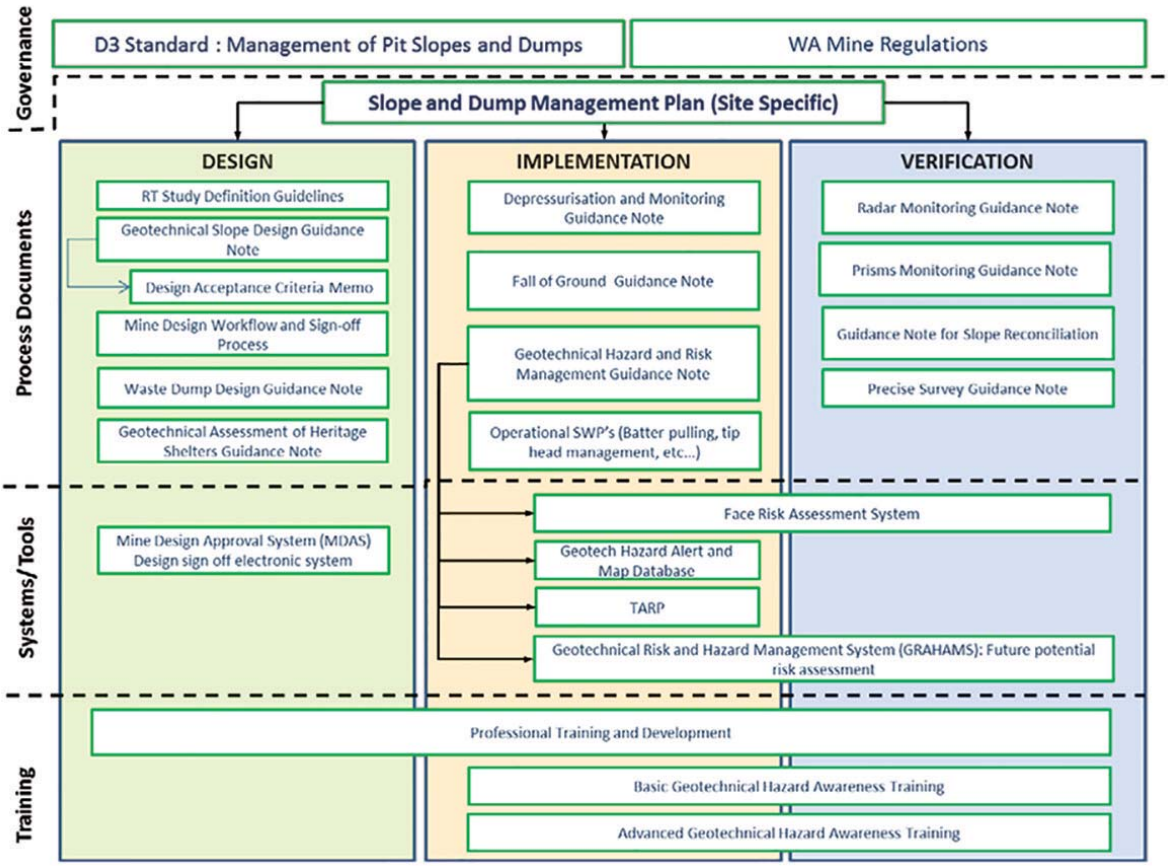

Figure 4—Summary of governance requirements and RTIO GMS supporting framework of documentation, systems, and training

4. *Regular audits and reviews*—Routine reviews and internal checks are undertaken by the assurance team. Rio Tinto HSE undertakes (external) system and compliance audits (similar to other HSE Stand requirements). External technical reviews are undertaken annually.

It is imperative that the GMS is 'live' and owned and operated by the site teams – significant effort is expended in rolling out and implementing the system to ensure that all parties understand their accountabilities and roles in maintaining the system.

GRAHAMS

The GRAHAMS (see Figure 3) is a tool that was developed by RTIO to capture all the geotechnical risk assessments, consisting of a SQL database with an MS Access front end.

Risk assessments are conducted for predetermined risk assessment slope sectors (RASSs). These generally align with the slope design sectors. Failure mechanisms, geological structures, geology, and slope orientation can all play a role in the determination of the RASS boundaries. Risk assessments are done for three scale scenarios for each RASS, *i.e.* multi-batter, batter scale, and rockfalls. Dump risks are also assessed.

The risk assessment methodology is compliant with the Rio Tinto 5×5 qualitative risk assessment matrix; considering the consequence and likelihood of a scenario to derive the risk level. As a minimum, the safety and economic risk are assessed, but the system also allows for other impacts to be evaluated, *e.g.* reputational, environmental, community *etc.*

The data capture form of the GRAHAMS is shown in Figure 5. The first section of the inputs relates to the information regarding the hazard, including a description, details of the scale (multi-batter, batter, or rockfall), the likelihood of the hazard eventuating, and the controls in place to prevent the hazard. In the second part (which is the main section to be populated) particulars of the specific scenario are recorded. These include a description, the current controls, and assessment of the risk (likelihood and consequences). If applicable, the future controls are listed, as well as the predicted risk.

Two periods are considered for the risk assessments – current and future potential. The difference and the need for current and future potential assessments are illustrated in Figure 5.

Current potential risk assessments assess the risk related to current slope geometry, projected to include planned mining for the next 6 months, and future potential assessments evaluate the complete height of the final (yet to be excavated) slope. This approach ensures that controls are commensurate with the level of risk posed to current operations, while planning and preparations can be done for future controls.

Critical controls are those controls that, should they be lost or become inactive, the risk level will immediately change to high or critical. Examples of critical controls are slope radar, automated prism monitoring, or a physical barrier. Critical controls are identified and tagged during the assessment process. This tagging allows the critical controls to be summarized in a separate report. Operations and line management should be aware of the critical controls. When a critical control is compromised the geotechnical team should be informed and evacuation of the area should be considered.

Reporting of risk levels can be carried at different levels (refer to Figure 6): per slope sector in a pit, per pit in a mining area, per mining area in a mining operation, or per operation across all the sites. In Figure 6 the top graphic shows the risk profile across all operations, while the pie charts shows the detail of a specific mine operation. This flexibility provides management with the opportunity to identify areas with elevated risk and allocate resources accordingly. For mine managers it provides a dashboard summary that indicates the risk profile across the different mining areas; and for general managers it provides an overview across the Pilbara operations.

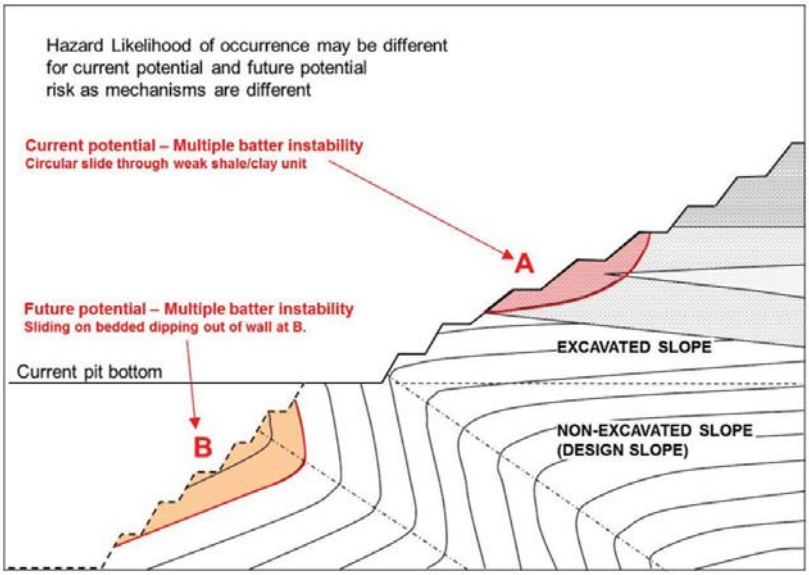

Figure 5—Schematic illustrating geometrical relationships between current and future potential assessments

Figure 6—Example GRAHAMS report output. These example charts are for illustrative purposes only and are not representative of the actual RTIO risk profiles

Risk assessments are carried out by defining the geotechnical hazard and assessing both consequences and probability of occurrence. The current risk is assessed, *i.e.* the existing controls are taken into account, and when the assessed current risk level is considered unacceptably high, the predicted risk is assessed with the inclusion of future controls.

Slope monitoring plan

As an outcome of the GRAHAMS, all mining areas are risk-assessed and ranked. This provides the basis for decisions regarding the level of resources and management required for each mining area. Best practice for slope performance monitoring is through a multi-layered approach whereby additional controls are implemented depending on the slope risk level. Basic monitoring for low-risk slopes may include infrequent berm inspections, whereas radar may be used for critical risk slopes where near-real-time monitoring is warranted. As the slope risk increases, improved data accuracy and frequency of readings are required, *e.g.* manually read crack pins are much less accurate than prism readings, while slope radar can provide 'sub-millimetre' accuracy. Table I details the RTIO risk-based hierarchical approach to slope monitoring systems.

RTIO uses the GRAHAMS output to implement this risk approach. Current and future controls needed to mitigate elevated risk profiles are identified during the risk assessment process. Accountabilities and frequency of current controls (where applicable) are summarized in the 'geotechnical monitoring plan' – an output from the GRAHAMS. Controls with recurring frequencies, *e.g.* monthly inspections and weekly monitoring, can be tabulated with the target frequency and dates as an output from GRAHAMS. Confirmation that a control was implemented, *e.g.* an inspection conducted, can be recorded in the system. A change in the monitoring schedule will automatically determine future implementation dates. This is an important planning tool for the site geotechnical team and also serves as auditable evidence that controls were in place. The 'future controls' requirements are included in the budgeting process to ensure availability when required. A summary of critical controls and accountabilities provides the opportunity to

Table I

RTIO risk-based approach to slope monitoring

Slope risk	Monitoring method	Monitoring frequency	Access required
Low risk	Berm inspections (crack inspections)	Increasing monitoring frequency (some can be alarmed if approxiate telemetry and alert systems are in place)	Access to berms
	Manually read crack monitors or surface extensometers		Access to berms
Moderate risk	Laser scanners		Access to berms (install/maintenance)
	Inclinometers		Access to berms (readings)
	TDR/VWP		Access to berms (readings)/telemetry
	Automated surface extensometers		Access to berms (readings)/telemetry
	Manually read prisms		Initial access to berms (install/targets)
High risk	ATS Prisms (Automated Total Station)	Required near real time telemetry and alarms (*i.e.* alert, alarm, evacuation)	Access to berms (install/maintenance)
Critical risk (Safety, crtical, monitoring)	Radar		Remote
	Automated surface extensometers with local or remote alarms		Remote

closely monitor these controls to ensure they are in place. This provides a robust, reliable, auditable, risk-based system for early detection of slope instability.

Hazard management

Communication of geotechnical hazards to operational personnel forms an important part of the management of geotechnical hazards. Personnel working in the pit and near slopes need to be aware of geotechnical hazards in or near their working area.

When a geotechnical hazard is identified on a RTIO operation, the details are documented in a hazard alert, including a description of the hazard, the controls that are in place (if any), needs for further controls, and the level of the risk posed by the hazard. Controls are discussed and approved by the quarry manager, who is accountable for the safe working environment on a Western Australian mine site. Hazard maps are mandatory documents for all RTIO Pilbara mine operations to communicate geotechnical hazards and are displayed in crib rooms, information centres, and other locations around the site, allowing all pit personnel access to the information.

It is expected that personnel and supervisors working in the pit will consult the hazard map to familiarize themselves with the geotechnical hazards in their working area before each shift.

The hazard alerts (and the hazard database) are part of GRAHAMS. There is a direct link between the risk assessments conducted for each RASS and the hazard alert. When a new hazard alert is generated in GRAHAMS, the user is prompted to review the risk assessment for that RASS and for the scale applicable in the hazard alert. This will ensure that the learnings from the hazard are incorporated into the risk assessment and that GRAHAMS is a live database that is updated with current slope performance.

Working near slopes

A face risk assessment (FRA) must be completed before work on foot less than 10 m from the slope can start. The process starts with consultation of the geotechnical hazard map. If a geotechnical hazard exists for the work area, the hazard level and associated hazard number should be noted in order to confirm that all required controls are in place. The level of risk indicated by the hazard map combined with the outcome of the FRA will determine the level of controls required before work can start.

A FRA is an onsite assessment of the face directly above the area where the work is taking place. The results determine the job hazard analysis (JHA) risk assessment, sign-off level requirements, and actions that must be completed prior to work commencing. Sign-off of the JHA indicates that effective controls have been identified. The FRA is valid for only one shift as conditions may change between shifts and will require reassessment. If conditions are observed to change during the shift a new FRA should be completed.

Training

Effective management of geotechnical risks requires that the workforce is trained and aware of geotechnical hazards. RTIO developed two levels of geotechnical awareness training to ensure we have 'Trained Eyes Everywhere' and to support the geotechnical teams.

Basic geotechnical hazard awareness training is provided to all mine operations personnel. This training provides the basics of geotechnical awareness in the open pit mining environment. The main focus of the training provides knowledge on (i) how to identify signs of instability, (ii) how to and to whom to report hazards, and (iii) where to find the information regarding the site's geotechnical hazards.

The advanced geotechnical awareness training targets supervisors and personnel that will work on foot within 10 m of batter faces or highwalls. The training provides more detail on types of monitoring and effectiveness of controls that can be implemented to mitigate geotechnical hazards. It also focuses on the FRA system and provides information on how each of the parameters listed in the FRA should be assessed. This empowers non-geotechnical personnel with the knowledge to effective conduct face risk assessments.

Both the training sessions are competency-tested. The qualifications are managed through the RTIO mandatory competencies system and refresher training is required every two years. The training packages were initially classroom-based but have since been developed into web-based interactive audiovisual training packages to ensure standardized delivery of training content and streamlined course administration.

Slope reconciliation

Dixon *et al.* (2011), describe RTIO's approach to prioritizing and determining the level of rigour required for slope reconciliation – a key control in the verification of the design. This is a subset of the geotechnical management system described in this paper.

Geotechnical slope reconciliation is an integral part of the GMS, as illustrated in Figure 3. The process is a feedback loop from field implementation, including field assessment and audit of the results back to the design. Geotechnical reconciliation addresses the following risks:

- Unexpected instability due to inappropriate design (design uncertainty not considered)
- Unexpected instability due to lack of regular monitoring of all areas of the pit slope (design uncertainty not managed appropriately)
- Sub-optimal slope design, where the design may be overly conservative (design uncertainty results in conservatism).

The geotechnical reconciliation process evaluates all major input parameters utilized in slope design studies. Any significant differences between observed and accepted design parameters shall be highlighted and if significant, reassessment of the design shall be undertaken.

Reconciliation provides a formalized process for continually re-assessing the geotechnical risk of the entire pit area to avoid 'surprises' and allow early identification of risk to operational processes. The process also results in increased confidence when estimating geotechnical risk as data uncertainty is reduced. The aim is to provide sufficient early warning of changed conditions to enable options to be assessed for:

- Remediation by design to prevent development of instability in the first place. The end result is improved safety and productivity
- Design optimization to improve ore recovery or reduce waste stripping
- Modification and /or improvement to design implementation practices.

Assurance

To demonstrate ongoing performance of the GMS, and ensure compliance with legislative and corporate standards as well as internal operating requirements, regular audits and reviews are undertaken. These comprise both internal and external reviews:

- Internal reviews:
  - Technical Services geotechnical assurance team – Monthly to quarterly site visits are conducted to confirm effective implementation of systems. Technical support is provided to the operations teams by means of operational risk management and design advice. This regular engagement also provides an opportunity to identify areas for system improvement. Bi-annual GRAHAMS moderation reviews are undertaken to ensure consistency in approach and identify any critical risks that would benefit from Independent Technical Review Team (ITRT) review.
- External reviews:
  - Rio Tinto HSE audits – System and compliance audits (similar to other HSE Standard requirements) every second year. Slope and dump management plans and operation compliance to the D3 standard requirements are assessed either by corporate Technology and Innovation (T&I) or other business unit geotechnical engineers
  - External (independent) technical reviews are undertaken in alternate years to the HSE audits. These reviews focus on the effectiveness of the implementation of the SDMP and supporting systems, as well as the designs. To date a pool of six external reviewers, familiar with the D3 and WA regulations, are rotated to provide these reviews
  - DMP Mines Inspector visits – At least annual site visits are undertaken by the Special Geotechnical Inspector to confirm conformance to the Act and regulations. Periodic 'geotechnical considerations' audits covering the standards associated with the safe development, operation, and closure of open pit operations from a geotechnical perspective are also undertaken.

Peer review is a fundamental risk management process that must be in place. Peer reviews are hierarchical, as the level of expertise required to undertake a technical review must be commensurate with the level of risk and complexity associated with the project (Table II). A key aspect of this is 'independent' review, where an individual not directly involved in the development (or outcomes) of the design is engaged as a 'fresh set of eyes' to critically review the work. Critical-risk projects and operations require ITRT review; that is, a team of external subject matter experts to provide advice and guidance on technical issues.

Conclusions

Effective management of the geotechnical risks across the 100 operational and 160 additional planned pits within the RTIO Pilbara Operations portfolio has required a risk-based approach to systematically identify potential hazards, evaluate the business risk (safety, economic, environmental, reputational, *etc.*), and define appropriate slope management controls. The risk-based framework is in alignment with the business risk management strategy, and provides the basis for defining the level of rigour required for slope management, as well as for prioritizing deployment of resources.

This facilitates better understanding of design and orebody knowledge risks and opportunities, leading to

Table II

RTIO risk-based geotechnical review framework

Geotechnical risk (GRAHAMS)	RTIO geotechnical reviews		
	Mine operations		Design
Critical	2-yearly external (independent) reviews (incl. operational designs).	SDMPs reviewed and signed off by geotechnical 'Qualified Individuals' and nominated D3 managers.	Independent Technical Review Team (ITRT) – typically external
High			Independent technical peer review
Moderate			Technical peer review
Low			Technical peer review

improved hazard management across operations and focused attention on areas of elevated risk. Reporting on the geotechnical risk status on an individual pit basis, or grouped by mine operation or Pilbara-wide, is an important tool in managing geotechnical risks across multiple operations, where the mine output is blended to achieve the required marketable product specifications. Interruptions in supply (through slope instability) can significantly impact the blended product quality.

The geotechnical management system (GMS) has been successfully implemented across RTIO mine operations and is fundamental to effective geotechnical slope management in a multi-pit – multi-operations environment. Additionally, the system provides an auditable process with demonstrated compliance with WA mines regulations and Rio Tinto's corporate health and safety standard D3 'Management of pit slopes, stockpiles, spoil and waste dumps'.

Acknowledgements and disclaimer

The contributions of colleges in developing, maintaining and improving the GMS are acknowledged. In particular Julian Venter's contributions in the initial system inception, and Tim Johnson's role in the system documentation and rollout is recognized. The shared vision of the members of the assurance and operations teams over the years has contributed to the deployment of sustainable risk management system. Furthermore, permission from Rio Tinto management, to publish this work is also gratefully acknowledged.

All opinions and conclusions drawn in this paper are those of the authors alone and it should not be assumed that any views expressed herein are also necessarily those of RTIO and/or the individual mine owners.

References

Bye, A., Little, M., and Mossop, D. 2005. Slope stability risk management at Anglo Platinum's Sandsloot open pit. *Proceedings of the Institute of Quarrying and ASPASA 36th Annual Conference and Exhibition*, Birchwood, Gauteng, South Africa, 3–5 March 2005.

Canbulat, I., Hoelle, J., and Emery, J. 2013. Risk management in open cut coal mines. *International Journal of Mining Science and Technology*, vol. 23, no. 3, May 2013. pp. 369–374.

De Graaf, P.J.H. and Wessels, S.D.N. 2013. Slope monitoring and data visualisation state-of-the-art – advancing to Rio Tinto Iron Ore's Mine of the Future™. *Proceedings of the International Symposium on Slope Stability in Open Pit Mining and Civil Engineering (Slope Stability 2013)*, Brisbane, Australia, 25–27 September 2013. Dight, P.M. (ed.). Australian Centre for Geomechanics, Perth. pp. 803–814.

Department of Minerals and Energy Western Australia. 1999. Guideline – Geotechnical Considerations in Open Pit Mines. Government Printer, Perth.

Dixon, R.A., Johnson, T.M., de Graaf, P.J.H., Wessels, S.D.N., and Venter, J. 2011. Risk based geotechnical slope reconciliation at Rio Tinto Iron Ore, Pilbara Operations. *Proceedings of Slope Stability 2011: the International Symposium on Rock Slope Stability in Open Pit Mining and Civil Engineering*, Vancouver, Canada, 18–21 September 2011. CIM, Montreal.

Ginting, A., Stawski, M., and Widiadi, R. 2011. Geotechnical risk management and mitigation at Grasberg open pit, PT Freeport Indonesia. *Proceedings of Slope Stability 2011: the International Symposium on Slope Stability in Open Pit Mining and Civil Engineering*, Vancouver, Canada, 12–21 September 2011. CIM, Montreal.

Herath, A. 2007. Pit slope management strategy at Mt Keith nickel operation, Western Australia, *Proceedings of the International Symposium on Soil and Rock Engineering*, Colombo, Sri Lanka, 6–11 August 2007. Sri Lankan Geotechnical Society

Hamman, E. 2009. Qualitative geotechnical hazard and risk assessment. *Slope Stability 2009: Proceedings of the International Symposium on Slope Stability in Open Pit Mining and Civil Engineering*, Santiago, Chile, 9–11 November 2009.

Hillson, D. 2011. Risk Management Principles Part 1: ISO31000:2009. *Risk Doctor Briefing*, August 2011

Hutchinson, D. and Diederichs, M. 1996. Cable Bolting in Underground Mines. BiTech Publishers, Richmond, BC, Canada. 401 pp.

Joass, G., Dixon, R., Sikma, T., Wessels, S., Lapwood, J., and de Graaf, P. 2013. Risk management and remediation of the north wall slip, West Angelas mine, Western Australia. *Slope Stability 2013: Proceedings of the International Symposium on Slope Stability in Open Pit Mining and Civil Engineering*, Brisbane, Australia, 25–27 September 2013. Dight, P.M. (ed.). Australian Centre for Geomechanics, Perth.

Sharon, B. 2009. Risk management – geomechanics application for open pit slope design and performance. *Slope Stability 2009: Proceedings of the International Symposium on Slope Stability in Open Pit Mining and Civil Engineering*, Santiago, Chile, 9–11 November 2009.

Western Australia Government. 1994. Mines Safety and Inspection Act 1994. Government Printer, Perth.

Western Australia Government. 1995. Mines Safety and Inspection Regulations 1995. Government Printer, Perth. ◆

http://dx.doi.org/10.17159/2411-9717/2016/v116n5a3

An update to the strain-based approach to pit wall failure prediction, and a justification for slope monitoring

by W. Newcomen* and G. Dick*

Synopsis

Effective management and mitigation of pit slope instability in open pit mines begins with a comprehensive slope monitoring programme. The ability to differentiate between non-critical pit wall movements due to rebound or relaxation of the excavated slopes and movements that may be indicative of slope failure is important for maintaining a safe working environment and maximizing production. Slope failure prediction methods using velocity, acceleration, and strain criteria have been introduced and put into practice over the past few decades. Forty-eight slope failures with surface monitoring data are presented and assessed using the strain-based failure prediction approach, with consideration of the quality of the rock mass and the potential failure mechanism. The results indicate that the strain-based approach can be used to provide general guidance regarding strain thresholds for pit walls for a variety of failure modes in diverse geological environments. The advantages and potential drawbacks of the strain-based and other slope failure prediction methods are discussed. The importance of implementing a pit slope monitoring and performance evaluation system early in mine development is also emphasized.

Keywords

open pit slopes, slope monitoring, failure prediction, pit wall strain, strain criteria, strain thresholds.

Introduction

The successful prediction of the Manefay Slide pit slope failure at Bingham Canyon at 9:30 am on 10 April 2013 (Engineering and Mining Journal, 2014) highlighted the importance of having a comprehensive slope monitoring system that provides an accurate prediction of the time of failure of an open pit slope. Using most of the geotechnical monitoring tools available, the time of the failure was predicted within hours and equipment and personnel were evacuated from the pit well in advance of the failure. From a time to slope failure perspective, the monitoring system in place was a success.

There are two general groups interested in monitoring pit walls, with slightly different objectives in mind when the monitoring system is being set up. There are those at the mine site that have to implement the pit slope design, monitoring protocols, and the action response plans, and there are those designing the slopes (often consultants) who regularly visit the mine but may not be responsible for the day-to-day activities.

The 'implementers' are primarily concerned about safety. Most mining operations go to great lengths to maintain a safe working environment and generally this is a mandate of management and the mine workforce. A comprehensive slope monitoring programme will allow personnel to work more comfortably in areas within the pit that are less stable than others. The mine operation is also keenly interested in optimizing ore recovery and managing risk. Retrieving the last loads of ore often requires that mining be carried out in areas that have a higher risk associated with them, such as the last few benches of the slope in an area generally more confined than the upper portions of the pit. A slope monitoring system allows miners to work confidently below pit walls that are deforming but are not progressing towards catastrophic failure. Confidence in the pit wall behaviour allows mining to be carried out for as long as possible, resulting in optimized extraction of the mineral resources. There are significant economic benefits associated with being able to stay in an area and continue mining as long as possible. The 'mine and monitor' approach is commonly used in mature mines where slopes are in various stages of instability and where there is a comprehensive experience base in the behaviour of the pit walls.

On the other side of the team are the 'designers'. Their motivation for monitoring is often to test or confirm the pit slope design. Depending on the design approach used, performance monitoring may be a fundamental component of the design. Confirmation that the wall is stable or deforming at a manageable rate is a key aspect of providing

* *BGC Engineering Inc.*

confidence in the design process. If there is a high degree of uncertainty in the design there should be an associated requirement for more comprehensive monitoring. If a particular mode of instability is of concern or has been predicted, early implementation of a pit slope monitoring system will allow this potential to be tested. Slope deformation monitoring is important to test the design. If the design requires modifications by means of step-ins, pushbacks, or slope flattening this can be justified by the results of the monitoring data, with the ultimate goal being to keep the pit slope movement rates or total displacements within pre-defined levels estimated during the design stage.

The implementers and the designers must work together during the planning, operating, and closure stages as future plans are generally influenced by previous pit wall performance. During all stages of mining there has to be a 'meeting of minds' between these two groups so that the safety, risk management, and design objectives of the operation are achieved. This is where the mine planners must balance the competing objectives of the various groups. Economics often plays a large role; for example, implementation of a comprehensive and expensive slope monitoring system may be justified if significant economic benefits from mining more aggressively in certain areas can be shown during the planning stages. Conversely, a simpler monitoring system may be appropriate during closure, as the risks may be lower at this stage of mining.

Monitoring tools

Surface and subsurface instrumentation are common in the slope monitoring programmes of most large open pit mines. Proactive mines will implement surface monitoring systems as the pit wall is developed instead of waiting until an instability occurs, recognizing that it is generally easier and more efficient to install surface instrumentation as the slope is mined. The focus of this paper is on surface displacement monitoring, as surface displacement acceleration is generally the main precursor to slope failure (Read and Stacey, 2009). Surface displacements are still the primary means by which mining operations evaluate the stability of a slope and are also generally easier to monitor than subsurface movements.

There are two main categories of pit wall surface deformation monitoring: point monitoring (prisms, extensometers, GPS) and area monitoring (laser scanning, photogrammetry, radar). Slope monitoring instrumentation can be further classified based on the time at which the monitoring data becomes available: background, extended data update times, and active, short-, or near real-time data updates. The monitoring method(s) selected by the mine should follow a risk-based approach where instrumentation is determined based on the slope risk and consequence of failure (de Graaf and Wessels, 2013).

Large open pit mines generally utilize multiple slope-monitoring instrumentation systems to manage the risk of slope instabilities. The sophisticated multi-system monitoring programme in place at Bingham Canyon (Doyle and Reese, 2011) included visual field inspections and spotters to monitor changing slope conditions, robotic total stations to survey over 200 optical prisms strategically located throughout the open pit area, and two types of ground-based slope stability radar to actively monitor specific slope instabilities. Visual inspections complemented with prism surveying, however, still appear to be the industry standard in some jurisdictions (Nunoo *et al.*, 2015).

Area-based (radar and laser) monitoring methods are typically employed when point monitoring systems are no longer effective, *i.e.* when slope deformations are large and the installation of prisms is no longer safe or practical. Transition from one monitoring system to another must take into consideration the limitations of each system. It is often desirable to have multiple monitoring systems or sufficient overlap of the systems to overcome and understand their limitations.

Utilizing the monitoring data

Slope instability triggers can be identified by comparing pit slope movements (velocities, displacements, and vectors) to mining activities (blasting and excavating), precipitation events, runoff, and pore pressures. It is important to identify and understand the triggers so that appropriate movement rate thresholds can be developed that take into consideration the various factors contributing to slope movements. It also allows background movements, generally due to slope rebound, relaxation, or creep, to be quantified and filtered out of the overall movements, allowing anomalous slope movements attributed to degradation of the rock mass or the presence of an unanticipated geological feature to be better identified.

Maximum velocities, accelerations, or total movements, generally based on experience at operating mines using historical monitoring data or experience in similar geological environments, can then be used to establish trigger action response plans (TARPs) to guide mining operations during periods of increased slope displacement. The TARPs are used to guide mine operators regarding which unstable areas can be accessed, who is allowed to access these areas, and what kind of equipment can be used to work in these areas. The response plans and/or thresholds may be modified as experience is gained in mining adjacent to the area of instability.

Monitoring data can also be compared to displacements predicted by numerical models to confirm that the pit slope is performing or responding as predicted. Anomalous movements, potentially indicative of the onset of failure, may be detected that require a reassessment of the design assumptions. By monitoring the pit slopes and comparing the movements to those that would be expected for a potential mode of instability, the designers can determine if their assumptions are correct or require modification, possibly resulting in changes to the pit slope geometry.

Strain-based approach to failure prediction

The use of strain measurements to predict the onset of failure of a geological material is not a new concept. This approach has been used in underground applications by means of measuring convergence, and is also routinely measured during testing of geological materials to understand the conditions leading to failure. Pit slope design practitioners have proposed strain limits to define the onset of tension cracking, steady-state movement, and the onset of progressive slope failure (Zavodni, 2001). Building on that

initial work, using a relatively small data-set of twelve slope failures collected from various sources, the proposed strain limits were tested and compared to the quality of the rock mass (the rock mass rating (RMR), as defined by Bieniawski, 1976) to see if a correlation could be developed between RMR and strain thresholds (Brox and Newcomen, 2003). Due to the limited size of the database, pit slopes experiencing a variety of failure mechanisms and in different stages of instability (*e.g.* initial cracking, steady state, and progressive) were grouped together.

The key conclusion of that work was that the strain at 'failure' is generally influenced by the quality of the rock and that, in general, the lower the rock quality the higher the potential strain at failure. The results of that study suggested that the deformability of the rock mass, which can be estimated from the RMR, plays a primary role in the amount of strain a pit wall can accommodate prior to failing. However, those assessments also indicated that the failure mode must be considered when assigning the allowable strain in a pit slope. For example, much smaller movements are tolerable in a pit wall susceptible to planar failure than one susceptible to toppling. In other words, different strain threshold values are appropriate for different failure modes when defining allowable 'strain at failure'. An extensive evaluation of a toppling and a planar failure in the north wall of the Nchanga pit (Wessels *et al.*, 2009) was conducted to test the slope collapse strain criteria originally proposed by Brox and Newcomen (2003). That evaluation concluded that there was not a significant difference between the strain at the onset of tension cracking, progressive failure, or collapse for the two failure mechanisms at that site. That work highlighted the potential complexity of trying to apply strain thresholds to the various stages of slope instability, which may be poorly defined in some cases. However, due to the limited data-set, it cannot definitively be concluded that different strain thresholds should not be applied to different failure mechanisms.

Other pertinent conclusions from the original work (Brox and Newcomen, 2003) included the need for a clearer definition of 'failure' of a pit wall, as steady-state movements due to primary rock mass creep, for example, are not as critical as secondary creep leading to the onset of failure and collapse of the pit wall (Figure 1). For the purpose of this paper, failure was more precisely defined as 'complete collapse of the pit wall', which differs from the original work where the case histories presented included some failures that did not progress to complete collapse. As a result, those case histories were taken out of the database, which was then updated to include slope collapses documented by Whittall *et al.* (2015) as part of a pit wall failure runout prediction study. Thus, the database presented is more rigorous in its definition of failure and also contains a larger number of failures for the four failure modes presented.

Consistent with the previous work by Brox and Newcomen (2003), the 'strain' in the pit slope was defined as the total movement measured at the surface divided by the height of the slope below the prism. This is an approximation of strain and does not represent the actual strain at surface or in the pit wall. This approach probably underestimates the actual strain; however, it is simple to calculate and considered accurate enough to approximate the surface strain, as long as the surface slope monitoring system was implemented relatively soon after mining was started.

Using these definitions, a revised RMR *vs* strain plot was developed from the updated database using only slope instabilities with well-defined failure mechanisms that resulted in complete collapse of the pit wall (Figure 2). To further explore the relationship between RMR and strain at collapse, the data was divided into two groups:

- Planar and wedge failures
- Rock mass and toppling failures.

Failures with complex or poorly defined failure modes were generally eliminated from the data; however, rock mass failures were included, which still tend to be used as a catch-all phrase for failures that are poorly defined. Nonetheless, the divisions noted above were used to produce Figures 3 and 4. Although there is a large amount of scatter in the plots, there also appears to be some trends, as discussed below.

Figure 3 indicates that planar failure generally occurs at the lowest strains and can occur over a relatively wide range – up to 1.5 orders of magnitude for a given RMR. Several slopes that experienced planar failure collapsed at strains of between 0.03% and 0.06%. The maximum strain measured for a planar failure was about 3%. The data for the wedge failures indicates a minimum strain of 0.2% and a maximum strain of 6%; two cases observed had strains greater than 3%. The range of strain for a given RMR is smaller for wedge failures than for planar failures, with only about one order of magnitude between the upper collapse and the planar/wedge boundary. The results suggest that 3% may be a reasonable maximum threshold to use for prediction of planar and wedge failures in poor- to fair-quality rocks.

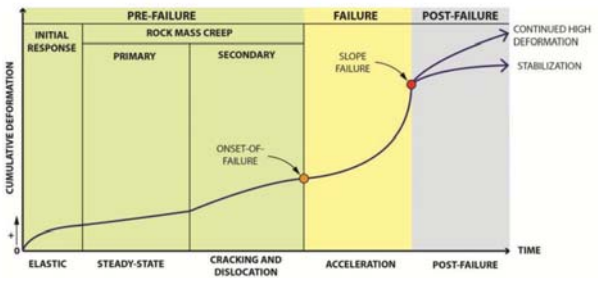

Figure 1—Schematic deformation *vs* time curve leading to failure (after Zavodni and Broadbent, 1980; Varnes, 1982; Martin, 1993; Sullivan, 1993, 2007; and Mercer, 2006)

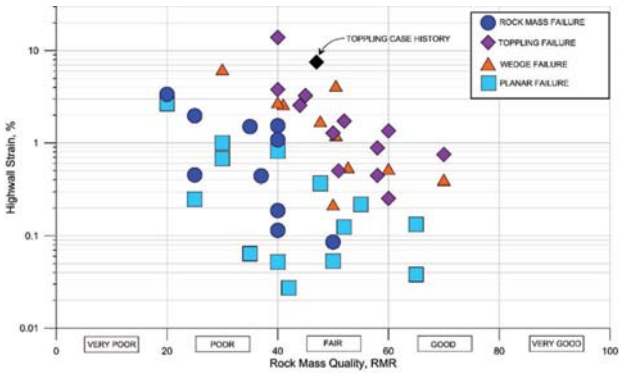

Figure 2—RMR *vs* surface pit wall strain at collapse

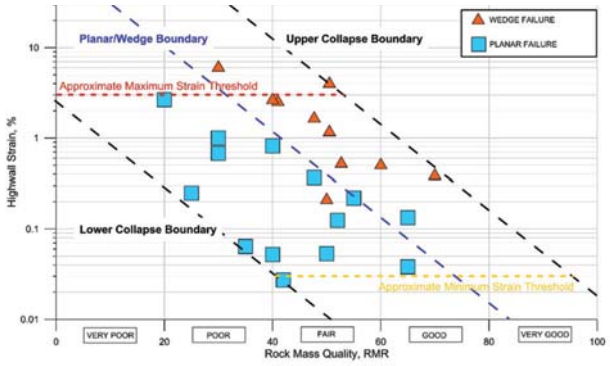

Figure 3—Strain *vs* RMR for planar and wedge failures

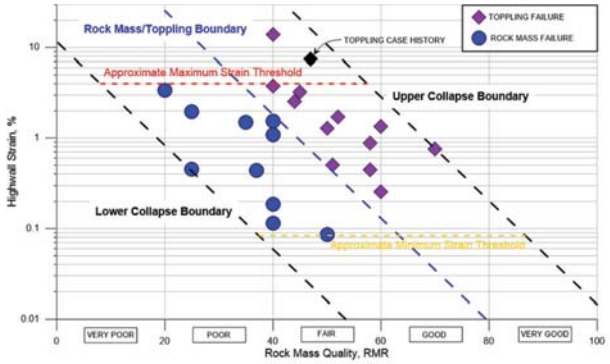

Figure 4—Strain *vs* RMR for rock mass and toppling failures

Figure 4 indicates that rock mass failures can occur over a relatively wide range – up to 1.5 orders of magnitude for a given RMR. One pit wall experiencing rock mass failure collapsed with a strain of less than 0.1%. The maximum strain measured for a rock mass failure was about 3%. The highest strain was observed for a toppling failure, with almost 15% strain measured at failure; however, the strain was less than 4% for most failures. The minimum strain for the toppling failures was between 0.2% and 0.3%. The range of strain for a given RMR appears to be smaller for toppling than for rock mass failure, with only about one order of magnitude between the upper collapse and the rock mass/toppling boundary. The results for the rock mass and toppling failures suggest that 4% may be a reasonable maximum strain threshold to use for prediction of non-kinematic failures in poor- to fair- quality rocks.

Surprisingly, the results presented indicate that strain to collapse for the rock mass failures documented is lower than the strain for wedge-type failures for a particular RMR value, and is within similar ranges to those measured for planar failures. It would generally be expected that rock mass failures would occur in weak and deformable rock masses, resulting in higher strains leading up to collapse of a slope. This may simply be due to the limited data-set used in this study or to the use of 'rock mass failure' terminology as a catch-all for otherwise undefined failures. There is also a possibility that rock mass failure involves more internal strain that is not captured by measuring surface deformations. Further review of the database and/or additional data is required to evaluate this apparent inconsistency.

The results suggest that if the RMR of a pit slope can be estimated it can be used to define a range of strains that could typically be expected at collapse for a particular failure mechanism. The plots in Figures 3 and 4 indicate that there is a relatively well-defined boundary between the planar and wedge failures, and between the toppling and rock mass failures. Based on the data evaluated for this study, it is reasonable starting point to assume that 4% could be used as the maximum strain at which a pit slope failure could occur, regardless of the failure mode. It is noteworthy that this is twice the maximum strain value of 2% previously suggested by Brox and Newcomen (2003) and four times the strain value of 1% originally proposed by Zavodni (2001).

Assuming that pit wall movements can be projected forward and used to estimate the strain in the slope at some future point in time, the maximum strain thresholds proposed could be used for contingency planning. However, since the minimum strain at failure varies substantially and also appears to be sensitive to the failure mode, slope designers, and those responsible for implementing the designs, must have an understanding of the potential failure mode early on so that proper protocols are in place in the event that a slope progresses to complete collapse closer to the minimum strain threshold. This highlights the importance of establishing a reliable geotechnical data acquisition programme early on in the mine life.

The strain-based approach to failure prediction provides a reasonable 'first check' in the evaluation of the stability of a pit slope, and can be used to determine if further attention regarding monitoring is necessary. It could also be incorporated into the TARP for a particular slope instability, for example by specifying a maximum displacement of the slope at which further evaluations or more detailed stability assessments are required.

Other approaches to failure prediction

Inverse velocity

The Fukuzono (1985) inverse velocity method for predicting the time of pit slope failure has become a widely applied failure prediction method in the mining industry. One of the most notable applications of the inverse velocity method for failure prediction is by Rose and Hungr (2007), where the time of slope failure was successfully predicted in three open pit mines by linearly extrapolating the inverse velocity *versus* time trend to zero. The power of the inverse velocity method lies in its simplicity; however, care must be taken when applying this method as it is highly dependent on the user's understanding of the data source. Successive progressive-regressive phases of pit slope movement also complicate the use of this method.

One limitation of the inverse velocity method is the linear extrapolation of the inverse velocity *versus* time trend to zero. In reality, the inverse velocity is never zero since the velocity at failure is not infinite. In addition, the velocity at failure varies with the geological environment, failure mechanism, instability size, and slope angle. Depending on their understanding and experience at a particular site, those

trying to predict when the failure is going to occur may have confidence in establishing a non-zero inverse velocity as the point of failure to ensure a more conservative time-of-failure prediction.

When conducting inverse velocity analysis, those analysing the monitoring data must also consider what data to include and exclude in their analysis and what data smoothing is required, especially when using ground-based radar measurements. Dick *et al.* (2015) provide recommendations on the application of the inverse velocity method in real time, based on the back-analysis of several slope failures monitored using ground-based radar. To improve the reliability of the inverse velocity analysis, they recommend including only data following the estimated onset of progressive deformation (Zavodni and Broadbent, 1980) and updating the analyses if a change in the accelerating deformation trend is observed. This is a significant limitation to the approach, as the onset of progressive deformation is not always obvious until failure is well underway.

Acceleration and velocity

Catastrophic pit wall failures are generally preceded by a significant increase in displacement rates; thus, accelerating pit slope displacements should be considered as an indication that failure is underway (Figure 1). Federico *et al.* (2012) present a collection of 38 case studies where the velocity and acceleration of a rock slope trending towards failure were measured, and proposed that there is a relationship between acceleration and velocity just prior to failure. The slope failures presented in the assessment range from natural slopes in clay shales to limestone quarry slopes and highly altered pit slopes in intrusive rocks. A wide range of failure mechanisms were included in the variety of cases presented, including one waste rock dump failure.

The proposed relationship between acceleration and velocity appears to be reasonable and therefore was further investigated. A modified version of the Federico *et al.* (2012) relationship between velocity and acceleration during slope failure is shown in Figure 5. Five case histories from the pit slope failure strain database (indicated by blue squares) were added and the waste dump failure was removed from the data-set. The additional case histories fall within reasonable proximity to the best fit trend line shown.

The ability of point-based monitoring systems to measure slope displacements, and thus calculate velocities and accelerations up to the point of failure, however, requires further scrutiny. For example, during pit wall failure it is unlikely that slope monitoring prisms could be accurately surveyed. However, area-based radar monitoring systems are able to collect data within seconds of slope collapse and should yield more insight to the validity of this approach to failure prediction, as long as the radar data can be corrected for the difference between the line of sight and the failure movement direction.

Selected slope failure case histories used to develop Figure 5 were reviewed in terms of the geology and potential failure modes. Pit wall failures in claystone, limestone, shale, and sandstone (sedimentary rocks), which are likely to be more prone to kinematically possible failures, appear to have generally lower velocities and lower associated accelerations. Failures in rock masses with less predictable or more complex geological structure (*e.g.* porphyry copper deposits) appear to have significantly higher velocities and accelerations. This may be a function of the failure mode and could possibly be related to the amount of strain at failure or strain build-up; however, the ability of the failure to deform internally also probably plays a role in the mobility and speed of the failure. The failures presented in Figure 5 may need to be further divided into brittle and ductile rock types, possibly using RMR to guide these divisions, to see if certain groupings become apparent and to determine if separate best fit trend lines are needed for these two groupings.

Velocity and acceleration data from area-based radar monitoring of a toppling instability in a pit wall excavated in deformable granitic rocks that appeared to be trending towards failure was used to test the relationship proposed by Federico *et al.* (2012), as illustrated on Figure 6. For reference, this toppling instability case has been plotted on

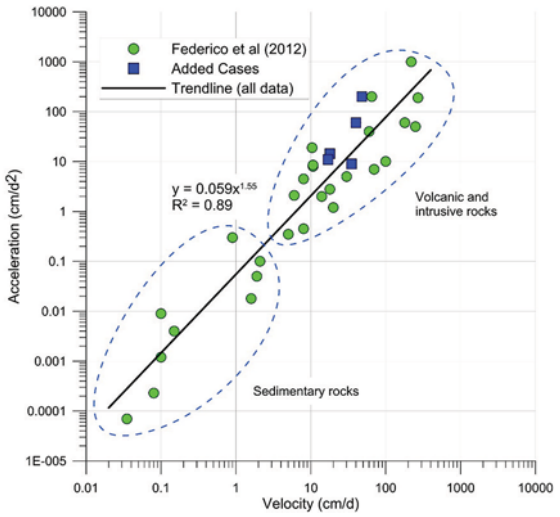

Figure 5—Proposed relationship between velocity and acceleration at failure (modified after Federico *et al.* (2012), with additional case histories)

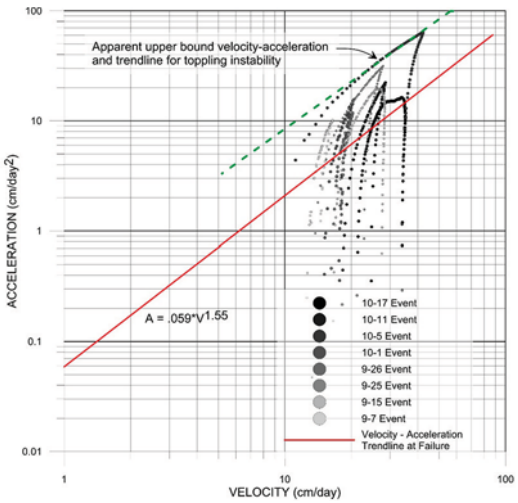

Figure 6—Plot of velocity *vs* acceleration for toppling instability monitored using radar data

Figures 2 and 4. The maximum strain measured for this pit wall was about 8%, which is twice as high as the recommended maximum strain of 4% for this failure mode, but less than half the strain of 15% measured for another toppling failure in the database.

The velocity and acceleration data (Figure 6) recorded by radar for this instability were smoothed using a 12-hour moving average to reduce the 'noise' in the radar measurements. As a result of the data smoothing technique, the velocity and acceleration values are lower than what was recorded incrementally. However, the smoother trend allows the important patterns in the data to be captured and results in less ambiguity when identifying the curve transition at the maximum recorded values.

It can be seen in Figure 6 that the pit slope of interest experienced eight periods of accelerating movements, with peak velocities of over 40 cm/d and accelerations in excess of 60 cm/d^2. Higher velocities were measured during each subsequent movement event, confirming that the pit wall was accelerating as the pit was mined and suggesting that progressive failure might be underway. The velocity *vs* acceleration curves were plotted for each movement event and compared with the 'failure trend line' from Figure 5. The velocity-acceleration curves from the radar monitoring data crossed the trend line on all occasions; however, the toppling slope did not collapse as predicted, in spite of apparent progressive slope deformations.

Our assessment of this case history suggests that additional work is required to confirm the usefulness of this failure prediction tool, or that possibly the failure trend line needs additional calibration with monitoring data from more case histories. Figure 4 also indicates that the strain estimated for the toppling failure far exceeded the maximum strain threshold value for the toppling failures in the database and was close to the upper collapse boundary for that failure mode. Thus, collapse of the slope was anticipated for this particular pit slope using the strain-based approach to failure prediction.

Of potential significance is that the velocity-acceleration curves for the movement events of the toppling failure case history (Figure 6) appear to asymptotically approach a line that is parallel to the failure trend line developed from the modified database. It is unclear if this is a result of the data smoothing techniques applied to the radar data, or an indication that the slope of the failure trend line is accurate but modifications are required to the intercept on the acceleration axis. Alternatively, the data used in Figure 5 may need to be sorted by failure mode or rock type to develop failure trend lines for smaller data subsets (*e.g.* planar and wedge *vs* rock mass and toppling failures, or brittle *vs* ductile failures). With further sorting of this data it is possible that the velocity-acceleration approach to failure prediction could be used in conjunction with the strain-based approach to failure prediction presented in this paper.

Conclusions

The strain-based approach to failure prediction shows promise as a tool for developing a range of strain thresholds that could be experienced prior to slope collapse for various failure modes based on the quality of the rock mass. Planar slope failures generally experienced the lowest strain prior to collapse, and toppling failures generally experienced the highest strain. Surprisingly, the strain to collapse for the documented rock mass failures is lower than the strain for wedge-type failures for a particular RMR value; however, this may simply be due to the limited data-set used in this study.

The advantages of the strain-based failure prediction approach are:

- It is simple to use
- It can be used as a planning tool and to guide instrumentation selection
- It can be used as a first check to evaluate the slope risk level and to guide instrumentation
- Potential minimum strain thresholds can be assigned according to the anticipated failure mechanism
- Maximum strain thresholds appear to apply to most failure mechanisms.

The disadvantages of this approach are:

- Slope monitoring must be initiated early on in the development of the pit to accurately estimate the strain
- The strain at depth or along the failure plane are not captured
- If there are changes to the rock mass strength/quality over time due to deformation or to changes in the geology as the pit wall gets higher, this method of failure prediction requires caution, particularly if the RMR decreases at depth
- Predicting the strain to collapse for a particular rock mass requires an understanding of the potential failure mode of the pit slope.

The strain-based approach to failure prediction needs to be further tested by adding more data to the plots to further calibrate the strains for different failure mechanisms and a wider range of rock qualities. Comparison with other methods of rock mass classification may also yield further insight.

The inverse velocity method is useful as a failure prediction tool and is still the industry standard; however, the data requires a considerable amount of smoothing to get the inverse velocity plots to converge. Higher confidence in the failure prediction time is attained the closer the pit wall is to actual collapse. Displacement *vs* time plots can also be used to predict the time to failure and should still be reviewed as part of evaluations to identify when the pit wall is accelerating and trending towards collapse. The displacement *vs* time plots are also helpful to define the onset of failure (Figure 1).

The velocity-acceleration failure prediction method proposed by Federico e*t al.* (2012) appears to have some limitations and requires more case histories to refine the currently proposed trend line. Further sorting of the data by failure mode, and possibly differentiating between brittle and ductile rock masses, may provide additional insight. If information on the failure mode and rock quality can be determined for those case histories, the velocity-acceleration method of failure prediction could possibly be used in conjunction with the strain-based approach presented in this paper.

Although the definition of 'collapse' of a pit slope is relatively straightforward, this still may not accurately reflect the behaviour of toppling or rock mass failures and may

explain why there is still a significant amount of scatter in this data-set. Thus, further review of the failure case histories is required to determine if the term 'collapse' is appropriate for these failure modes.

The methods of predicting when a pit slope is going to collapse, as discussed here, require that accurate pit slope monitoring information be collected. The use of multiple methods of slope monitoring data collection and assessment is encouraged to test the usefulness of the various methods. Thus, it is proposed that all of the methods presented in this paper be used to assess failures so that decisions made regarding mitigation and risk management are well informed, increasing the confidence of the mine operators that have to work in close proximity to unstable pit slopes.

References

Bieniawski, Z.T. 1976. Rock mass classification in rock engineering. *Exploration for Rock Engineering*. vol. 1. Bieniawski, Z.T. (ed.). Balkema, Cape Town. pp. 97–106.

Brox, D. and Newcomen, W. 2003. Utilizing strain criteria to predict highwall stability performance. *Proceedings of ISRM 2003 -Technology Roadmap for Rock Mechanics*, Sandton, South Africa. 8–12 September. South African Institute of Mining and Metallurgy, Johannesburg.

Carter, R.A. 2014. Recovering from Bingham Canyon's record-setting 2013 slide. *Engineering and Mining Journal*, 6 May 2014. pp 46–47.

De Graaf, P. and Wessels, S. 2013. Slope monitoring and data visualization state-of-the-art - advancing to Rio Tinto Iron Ore's Mine of the Future. *International Symposium on Slope Stability in Open Pit Mining and Civil Engineering*, Brisbane. Australian Centre for Geomechanics, Perth. pp. 803–814.

Dick, G.J., Eberhardt, E., Cabrejo-Lievano, A.G., Stead, D., and Rose, N.D. 2015. Development of an early-warning time-of-failure analysis methodology for open pit mine slopes utilizing ground-based slope stability radar. *Canadian Geotechnical Journal*, vol. 52, no. 4. pp. 515–529.

Doyle, J.B. and Reese, J.D. 2011. Slope monitoring and back analysis of the east fault failure, Bingham Canyon Mine, Utah. *Proceedings of Slope Stability 2011: International Symposium on Rock Slope Stability in Open Pit Mining and Civil Engineering*, 18–21 September. Vancouver, Canada. Canadian Rock Mechanics Association.

Federico, A., Popescu, M., Elia, G., Fidelibus, C., Interno, G., and Murianni, A. 2012. Prediction of time to slope failure: a general framework. *Environmental Earth Science*, vol. 66, no. 1. pp. 245–256.

Fukuzono, T. 1985. A new method for predicting the failure time of a slope. *Proceedings of the Fourth International Conference and Field Workshop on Landslides*. Japan Landslide Society, Tokyo. pp. 145–150.

Martin, D.C. 1993. Time dependent deformation of rock slopes. PhD thesis, University of London.

Mercer, K.G. 2006. Investigation into the time dependent deformation behaviour and failure mechanisms of unsupported rock slopes based on the interpretation of observed deformation behaviour. PhD thesis, University of the Witwatersrand, Johannesburg, South Africa.

Nunoo, S., Tannant, D.D., and Newcomen, H.W. 2015. Slope monitoring practices at open pit porphyry mines in British Columbia, Canada. *International Journal of Mining, Reclamation and Environment*, vol. 30, no. 3. pp. 245–256.

Read, J. and Stacey, P. 2009. Guidelines for Open Pit Slope Design. CSIRO Publishing, Collingwood, Victoria, Australia.

Rose, N. D. and Hungr, O. 2007. Forecasting potential rock slope failure in open pit mines using the Inverse-velocity method. *International Journal of Rock Mechanics and Mining Sciences*, vol. 44. pp. 308–320.

Sullivan, T.D. 1993. Understanding pit slope movements. *Proceedings of the Conference on Geotechnical Instrumentation and Monitoring in Open Pit and Underground Mining,* Kalgoorlie, Western Australia, 21–23 June. Szwedzicki, T. (ed.). Balkema, Rotterdam. pp. 435–445.

Sullivan, T.D. 2007. Hydromechanical coupling and pit slope movements. *Proceedings of Slope Stability 2007*, Perth, WA, 12-14 September. Australian Centre for Geomechanics, Perth. pp. 3–43.

Varnes, D.J. 1982. Time-deformation relations in creep to failure of earth materials. *Proceedings of the Seventh Southeast Asian Geotechnical Conference*, Hong Kong, 22-26 November. McFeat-Smith, I. and Lumb, P. (eds.). Southeast Asian Geotechnical Society, Bangkok, Thailand. pp. 107–130.

Wessels, S. 2009. Monitoring and Management of a Large Open Pit Failure. MSc thesis, University of the Witswatersrand, Johannesburg.

Whittal, J., Eberhardt, E., Hungr, O., and Stead, D. 2015. Runout of open pit slope failures using and abusing the Fahrböschung angle. *Proceedings of Slope Stability 2015: International Symposium on Slope Stability in Open Pit Mining and Civil Engineering*, Cape Town, South Africa, 12–14 October. Southern African Institute of Mining and Metallurgy, Johannesburg.

Zavodni, Z.M. and Broadbent, C.D. 1980. Slope failure kinematics. *CIM Bulletin,* vol. 73, no. 816. pp. 69–74.

Zavodni, Z.M. 2001. Time-dependent movements of open pit slopes. *Proceedings of Slope Stability in Surface Mining*, Denver, Colorado. Hustrulid, W.A., McCarter, M.K., and Van Zyl, D.J.A. (eds.), SME, Littleton, CO. pp. 81–87. ◆

Mining for the Future 2016

The Future for Mining starts Now

12–13 September 2016
Electra Mining, Nasrec, Johannesburg

BACKGROUND

Globally the mining industry is in a crisis with declining productivity and many mining operations are no longer sustainable at the current commodity prices. The mining organisation as we know it will have to change and become agile to adapt to uncertainty relating to commodity prices, more difficult ore bodies, skills shortages and growing expectations from all stakeholders. New technologies, mining methods, organisational design philosophies, scenario planning, big data and the digital revolution are all opportunities for the mining industry to reinvent itself.

ABOUT THE EVENT

The Southern African Institute of Mining and Metallurgy brings you two days of high impact Forums with top industry Keynote speakers talking about the concept of Mining for the Future. Panel discussions, case studies and networking opportunities will bring the future of mining to you now. Join the Forums to interact and network with industry thought leaders and experts who will discuss topical issues and solutions that work now. Register to attend one or all three forums at a cost of R450.00 per forum.

WHO SHOULD ATTEND

- New Technology Managers
- IM Managers
- CEO
- COO
- R&D Managers
- Resource Managers
- Mine Managers
- Safety Managers
- Engineering Manager
- HR Managers
- MTS Managers
- Solution Architects
- Mining Consultants

EXHIBITION/SPONSORSHIP

Sponsorship opportunities are available. Companies wishing to sponsor or exhibit should contact the Conference Co-ordinator.

For further information contact:
Camielah Jardine
Tel: (011) 834-1273/7
E-mail: camielah@saimm.co.za
Website: http://www.saimm.co.za

SAIMM
THE SOUTHERN AFRICAN INSTITUTE OF MINING AND METALLURGY

Conference Announcement

http://dx.doi.org/10.17159/2411-9717/2016/v116n5a4

Designing for extreme events in open pit slope stabilty

by L. Lorig*

Synopsis

Two types of extreme event, earthquakes and rainfall, potentially affect open pit slope stability. In the case of earthquakes, there are rather well-developed analysis procedures and acceptability criteria. The analysis procedures relate mainly to selection of the dynamic loading either through design earthquakes and/or pseudo-static seismic coefficients. The acceptance criteria are typically expressed in terms of a minimum safety factor in pseudo-static analyses. The acceptance criteria are often promulgated by governments despite the fact that no open pit slope has ever been adversely affected by an earthquake. This paper explains why open pit slopes are seemingly more resistant to dynamic loads than natural landforms, which can experience catastrophic landslides.

Extreme rainfall events are much more likely to cause open pit slope problems than earthquakes. Two types of problem are common – slope erosion and slope instability. Slope erosion is often mitigated by appropriate surface water controls. Slope instability due to elevated transient water pressures is more difficult to mitigate. Analysis procedures and acceptability criteria are rare. This paper will discuss the mechanisms for rainfall-induced slope instability, as well as analysis methods. Examples will be discussed and analysis methods are proposed.

Keywords
slope stabililty, analysis methods, acceptability criteria, extreme rainfall.

Introduction

Two types of extreme event, earthquakes and rainfall, potentially affect open pit slope stability. In the case of earthquakes, there are rather well-developed analysis procedures and acceptability criteria. The analysis procedures relate mainly to selection of the dynamic loading either through design earthquakes and/or pseudo-static seismic coefficients. The acceptance criteria are typically expressed in terms of a minimum safety factor in pseudo-static analyses. The acceptance criteria are often promulgated by governments (*e.g.*, Peru, Chile) despite the fact that no open pit slope has ever been adversely affected by an earthquake. This paper explains why open pit slopes are seemingly more resistant to dynamic loads than natural landforms, which can experience catastrophic landslides.

Extreme rainfall events are much more likely to cause open pit slope problems when compared to earthquakes. Two types of problems are common – slope erosion and slope instability. Slope erosion is often mitigated by appropriate surface water controls. Slope instability due to elevated transient water pressures is more difficult to mitigate. Analysis procedures and acceptability criteria are rare, but do exist. In Peru, for example, slopes are required by law to be designed for a 100-year storm.

Thus it seems that there is disproportional design attention given to these two extreme events. Large slope displacements and even failure are often preceded by periods of heavy rainfall, yet little, if any design attention is paid to rainfall (or in some cases snowmelt). If nothing else, this paper aims to raise awareness of the need to consider the impact of the amount and rate of rainfall in the design process.

Earthquakes and open pits

Failure of rock slopes is a complex phenomenon, often involving failure of rock bridges and sliding on pre-existing joints. Stress changes are induced in slopes by earthquake movements. Combined with existing static stresses, these additional dynamic stresses may exceed the available strength along a potential sliding surface (formed of the rock bridges and pre-existing joints) and cause failure. These failures can either be in the form of slides and rockfalls, where the material is broken into a large number of small pieces, or coherent slides, where a few large blocks translate or rotate on deep-seated failure surfaces. Glass (2000) notes that while shallow slides and rockfalls

* *Itasca.*

are quite common during earthquakes (Harp and Jibson, 1995, 1996), the correlation of seismic shaking with open pit slope failures is much less compelling, and he is not aware of any large, deep, coherent open pit slope failures that have been attributed to earthquake-induced shaking. Although earthquakes apparently pose a low-probability risk to open pit mines, given their relatively shorter design lifetime in comparison to natural slopes, and small landslides and rockfalls cause little disruption to mining operations, a deep coherent failure could still have a profound effect.

Because mining regulations often require investigation of slope stability in response to earthquake loading, relatively simple quasi-static analyses are typically carried out for open pit mines. It is widely recognized (*e.g.* Kramer, 1996) that the quasi-static analysis of the effect of seismic shaking on stability of slopes is inadequate and incorrect (and usually too conservative). Thus, open pit mine designers often defer to empirical evidence when considering seismic hazard in open pit slope design.

It is important to understand and explain the relatively good performance of open pit slopes as opposed to extensive evidence of landslides during historical earthquakes, but also to determine the conditions when open pit slope stability can be at risk during the seismic shaking. Damjanac *et al.* (2013) provide, based on a mechanistic approach (using numerical models), a rationale for why field observations indicate relatively small effects of earthquakes on the stability of open pit slopes, and also investigate the level of conservatism in the predictions of the quasi-static analyses as a function of important ground motion parameters.

Large open pits versus natural slopes

The main differences between large open pit slopes and natural slopes that are believed to be reasons for better performance of large open pit slopes during earthquakes are summarized below (after Damjanac *et al.*, (2013).

a. Infrequent occurrence of strong earthquakes during the mine's lifetime. The life of a mine is relatively short compared to the recurrence periods of large earthquakes ($M_w \geq 6.5$). Natural slopes are hit by numerous strong earthquakes, resulting in damage accumulation and gradual reduction in the safety margin
b. Natural slopes exist at a wide range of conditions and wide range of factors of safety (FoS), with some of them being metastable (close to FoS = 1.0) under static conditions. Typically, open pits are designed to have a static FoS of around 1.2 or greater. As a result, some natural slopes are likely to fail when subject to additional dynamic loading from earthquakes
c. Earthquakes cause failure of some of the natural slopes that are close to static equilibrium. However, most natural slopes do not fail. In fact, a small fraction of all natural slopes fail during even very strong earthquakes.
d. Open pits are typically excavated in relatively strong, competent rocks. Natural slopes are comprised of rock and soil with different states of degradation and weathering and are susceptible to softening mechanisms.
e. As explained later, topographic amplification is greater in natural slopes than in open pits
f. Also, as explained later, wave amplification due to heterogeneities is much greater in natural slopes than open pits.

For the reasons described above, natural slopes are at a disadvantage when subjected to seismic loading, both in terms of higher additional demand induced by dynamic stresses and lower extra capacity available in material strength to meet that demand. In the following sections, these factors are quantified. For the same magnitude earthquake, the actual shaking and dynamic stresses induced in the slope are functions of slope geometry (surface topography) and geological profile (variation of mechanical properties with depth). Both these effects are studied using two- and three-dimensional numerical models as described below.

Induced dynamic stresses caused by seismic shaking

One aspect of the problems caused by earthquakes is the increased demand due to induced dynamic stresses caused by seismic shaking. This can be due to either geometric effects (topographic amplification) or material heterogeneity (*e.g.*, softer material underlain by hard rock). Both of these effects are evaluated in this section by means of continuum elastic numerical simulations. Damjanac *et al.* (2013) investigated conditions when dominant wavelengths and the characteristic height of the pit are large relative to any structure in the rock mass, which can be approximated as a continuum. The finite-difference software packages *FLAC* (Itasca, 2011) and *FLAC3D* (Itasca, 2012) were used in the study.

Topographic amplification

It has been observed in many earthquakes that the formation geometry plays a critical role in site response and may lead to trapping of seismic energy in a certain region or channelling it away. This can lead to amplification of ground motion in some areas while moderating it in others (Raptakis *et al.*, 2000; Bouckovalas and Kouretzis, 2001; Assimaki and Kausel, 2007). The effect of topography on wave amplification is investigated for both two- and three-dimensional geometries as explained in Appendix A.

Stiffness contrast

Another reason for amplification of seismic waves is the presence of heterogeneities (*e.g.*, typically softer materials on top of more competent rock). Seismic waves propagating downward after reflection at the free surface are trapped between the free surface and more competent rock, leading to a very high amplification ratio. In Appendix B, the effect of both horizontal layering and vertical heterogeneities (*e.g.*, orebody) is examined.

Dynamic safety factor

The reduction in FoS due to additional demand induced by seismic shaking is quantified and correlated with different earthquake intensity parameters. A suite of real ground motions was selected with a wide range of peak ground accelerations (PGAs), peak ground velocities (PGVs), durations of shaking, and frequency content. The model geometry is the same as for 2D elastic simulations (Appendix A) with a slope height of 500 m. The analysis is carried out

for two different overall slope angles: 45° and 35°. The rock is modelled as a dry elasto-plastic material using a Mohr-Coulomb yield criterion with strength values corresponding to typical values for fractured rock. For the 45° slope, a cohesion of 0.5 MPa and a friction angle of 45° is used. For the 35° slope, a cohesion of 0.37 MPa and a friction angle of 37° is used. A Poisson's ratio of 0.2 is used for both cases. The lateral stress is initialized using a lateral stress coefficient of =0.25. These parameters result in a static factor of safety (FoS_s) of 1.5 for both slopes.

To calculate the dynamic factor of safety (FoS_d), a threshold displacement (D_t) above which the slope is considered to have failed is chosen. This chosen displacement corresponds to shear strains that are expected to cause significant loss in rock mass strength. Two values are considered: D_t = 0.5 m and D_t =1.0 m. A dynamic analysis is performed using each ground motion (both horizontal and vertical components) and the maximum displacement on slope is monitored. If the displacement is less than the threshold, strength properties (cohesion and friction angle) are reduced in increments and the analysis is rerun until the permanent earthquake-induced displacements are greater than the threshold. This strength reduction factor is denoted as the FoS_d for that ground motion. A typical displacement contour plot for maximum displacement D_t = 1.0 m is shown in Figure 1. A typical plot of maximum displacement as a function of strength reduction factor highlighting the calculation of FoS_d is shown in Figure 2.

The FoS_d is then normalized by the FoS_s, and the ratio is correlated with different earthquake intensity parameters.

The following earthquake intensity parameters are correlated with the dynamic factor of safety.

1. Peak ground acceleration (PGA): maximum value of absolute acceleration. The correlation is shown in Figure 3 for D_t = 1.0 m
2. Peak ground velocity (PGV): maximum value of absolute velocity. The correlation is shown in Figure 4 for D_t = 1.0 m
3. Arias intensity (I_a): time integral of square of ground acceleration (in m/s²):

$$I_a = \frac{\pi}{2g}\int_0^{T_d} a(t)^2\,dt$$

where g is the acceleration due to gravity and $a(t)$ is the acceleration at time instant t.

The correlation is shown in Figure 5 for D_t = 1.0 m.

4. Power: time integral of square of ground velocity:

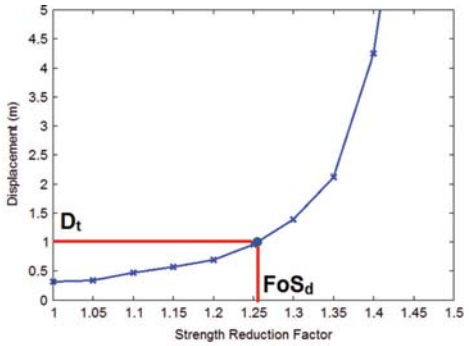

Figure 2—Observed maximum displacement in the numerical model as a function of strength reduction factor

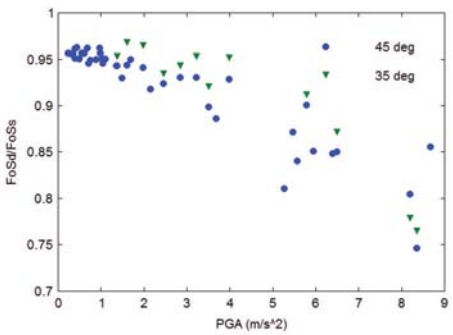

Figure 3—Correlation of normalized dynamic factor of safety with PGA for D_t = 1.0 m

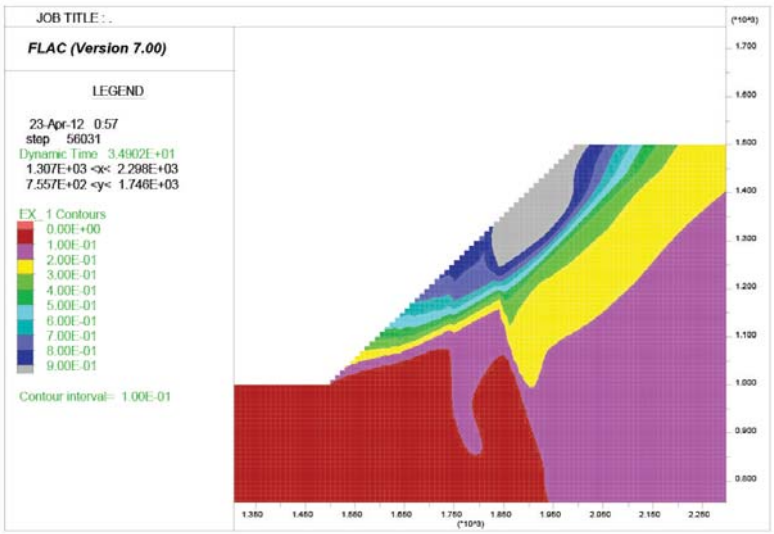

Figure 1—Displacement contour plot for peak displacement for D_t = 1.0 m

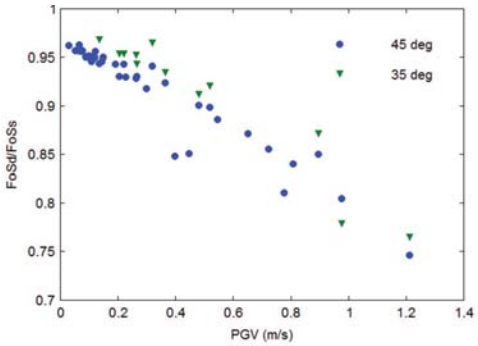

Figure 4—Correlation of normalized dynamic factor of safety with PGV for D_t = 1.0 m

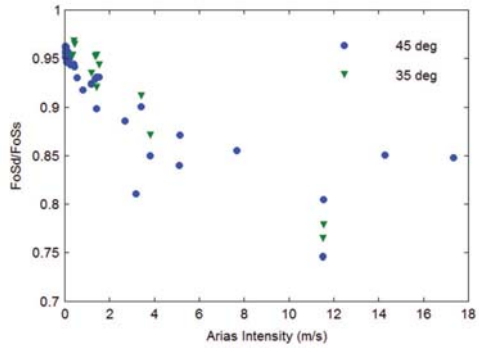

Figure 5—Correlation of normalized dynamic factor of safety with Arias intensity for D_t =1.0 m

$$Power = \int_0^{T_d} V(t)^2 dt$$

where $V(t)$ is the velocity at time instant t.

The correlation is shown in Figure 6 for D_t = 1.0 m.

5. Cumulative absolute velocity (CAV): time integral of absolute value of acceleration

$$CAV = \int_0^{T_d} |a(t)| dt$$

The correlation is shown in Figure 7 for D_t = 1.0 m.

The correlation of normalized dynamic factor of safety with both Arias intensity and cumulative absolute velocity (CAV) is poor. Some correlation is obtained with peak ground acceleration (PGA), but the scatter increases significantly for higher levels of PGA. The best correlation is obtained with PGV and power, with PGV performing slightly better. Good correlation is obtained for both levels of threshold displacement (0.5 m and 1 m) when PGV is used. Thus, PGV is found to be a better indicator of seismic damage to slopes than PGA, which is used in conventional methods.

Conventional pseudo-static approach

The results from numerical analysis are compared with the pseudo-static approach commonly employed for determining the dynamic factor of safety for slopes. The pseudo-static method involves running a static analysis with a horizontal component of acceleration a_h, = $k_s g$ where k_s is the seismic coefficient and is correlated with earthquake magnitude (Pyke, 2001) and peak ground acceleration. To compare the results directly, pseudo-static analyses were carried out and the factor of safety was calculated for different seismic coefficients. The results are shown in Figure 8.

For every earthquake motion used in numerical analysis in the previous section, a dynamic factor of safety was determined. Using the chart in Figure 8, a seismic coefficient that would give the same factor of safety in pseudo-static analysis for that earthquake was determined. These seismic

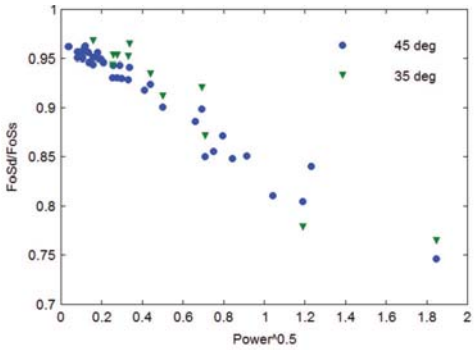

Figure 6—Correlation of normalized dynamic factor of safety with power for D_t = 1.0 m

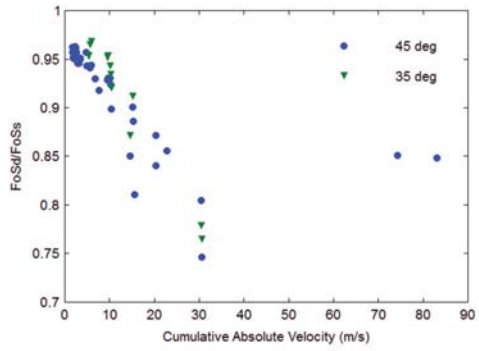

Figure 7—Correlation of normalized dynamic factor of safety with cumulative absolute velocity for D_t = 1.0 m

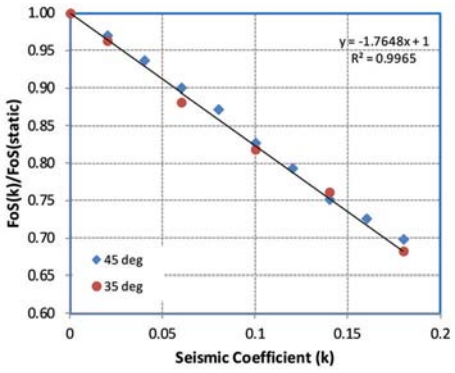

Figure 8—Normalized FoS from pseudo-static analyses as a function of seismic coefficient

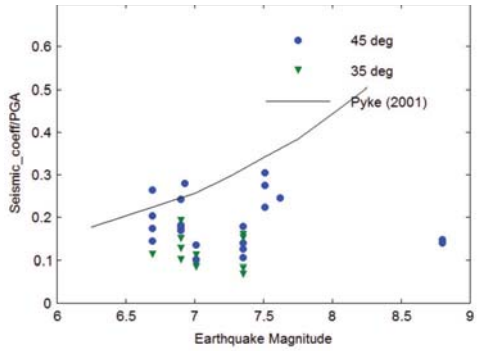

Figure 9—Comparison between numerical results and recommendations by Pyke (2001) for normalized seismic coefficient as a function of earthquake magnitude for D_t = 1.0 m

coefficients are normalized by PGA and plotted against the earthquake magnitude. The cases with very low PGA are excluded as they are prone to large errors when normalized. The results are compared with recommendations by Pyke (2001) as shown in Figure 9.

The results indicate that there is no significant correlation between the seismic coefficient and earthquake magnitude. However, for the most part, the recommendation by Pyke (2001) corresponds to the upper bound and is conservative. While this approach may work fine for low-magnitude earthquakes, it can lead to an over-conservative design for larger-magnitude earthquakes. As discussed in the next section, using another ground motion parameter such as PGV instead of magnitude may help in better estimation of the dynamic factor of safety for such cases. It is logical that PGV might be better because velocity relates directly to stress.

Improved pseudo-static approach

As discussed above, Damjanac *et al.* (2013) reported results for a two-dimensional fully dynamic study involving homogeneous slopes 500 m high at 35° and 45° slope angles for 20 recorded ground motions (for earthquakes covering ranges of magnitudes, durations, and epicentre distances). The study showed that reduction in the dynamic factor of safety (FoS_d) does not correlate well with the PGA and event magnitude. Consequently, the charts and empirical formulae for calculation of pseudo-static seismic coefficient currently used in industry for pit design and assessment of the seismic hazard are inadequate. The study also showed that currently used seismic coefficients typically overestimate the seismic hazard for the pit slopes. However, in a few cases, that hazard is underestimated. Full dynamic analyses indicate that reduction in the FoS due to dynamic loading best correlates with PGV, which is one of the earthquake intensity measures. The pseudo-static seismic coefficients that result in the same FoS as calculated from full dynamic analysis for the considered ground motions are shown in Figure 10. as functions of PGV. Clearly, the correlation is very good. More research is needed to generalize the process into a more accurate and rigorous, but simple, methodology for calculating seismic coefficient to be used in the pit design and assessment of the earthquake hazard.

Extreme rainfall and open pits

Extreme rainfall events are among the most common causes of slope instability in open pits. As discussed in this section, extreme rainfall can adversely affect both soil and rock slopes, although the mechanisms are different.

Soil slopes

Soil slopes are affected by extreme rainfall in one of two ways – erosion and/or loss of apparent cohesion (suction).

Erosion

Soil erosion due to rainfall is probably the most common consequence of an extreme rainfall event. An example of soil erosion is shown in Figure 11. Erosion is probably best handled by providing an effective surface water management system.

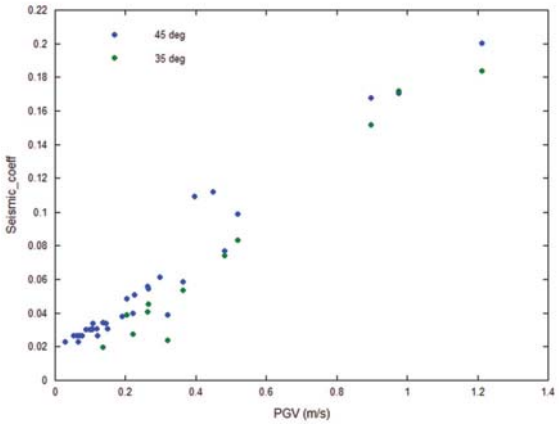

Figure 10—Correlation between peak ground velocity (PGV) and equivalent seismic coefficient for use in pseudo-static analyses

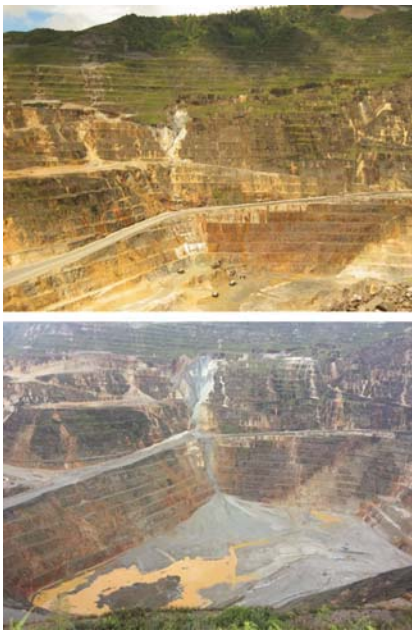

Figure 11—Erosion effects of extreme rainfall, before (above) and after (below). Photographs courtesy of John Read

Stability in unsaturated conditions

The presence of capillary pressure in unsaturated soils can have a major impact on the stability of a slope. Capillary forces hold fine particles together and can impart additional cohesion to the soil. The apparent cohesion provided by the capillary forces usually decreases as the soil saturation increases. With saprolites and other granular soils, strong negative pore pressures (soil suction) are developed when the moisture content is below about 85%. This behaviour explains why many saprolite slopes remain stable at slope angles and heights greater than would be expected from typical effective stress analysis. It also explains why these slopes may fail after prolonged rainfall even without the development of excess pore pressures or reaching 100% saturation (Fourie and Haines, 2007). While a rainfall event of low intensity and long duration may under certain conditions be beneficial to the stability of the slope, a high-intensity, short-duration event may promote a buildup of saturation and induce slope failure. Detournay and Hart (2008) provide the theoretical background and use numerical simulations with *FLAC* (Itasca, 2011) to illustrate the relationship between rate of infiltration from precipitation and stability in a silty slope. They used a simplified framework, based on Mohr-Coulomb model for the soil, generalized Bishop effective stress (Nuth and Laloui, 2007; Wang *et al.*, 2015), and van Genuchten laws relating capillary pressure and permeability to saturation (van Genuchten, 1980) to show the impact of intensity and duration of a rainfall event on the stability of a slope. Generic geometry and material properties were used for the slope. It was shown that a rainfall event of low intensity and long duration was not detrimental to slope stability, provided that the additional cohesion imparted to the soil by the capillary forces was sufficient. On the other hand, a rainfall event of high intensity and short duration was responsible for slope failure (see Figure 12). In this case, the behaviour was explained by an increase in soil saturation (see Figure 13) accompanied by a decrease in the capillary forces, intensity, causing an apparent decrease in soil cohesion. A similar discussion and example is provided by Garcia *et al.* (2011).

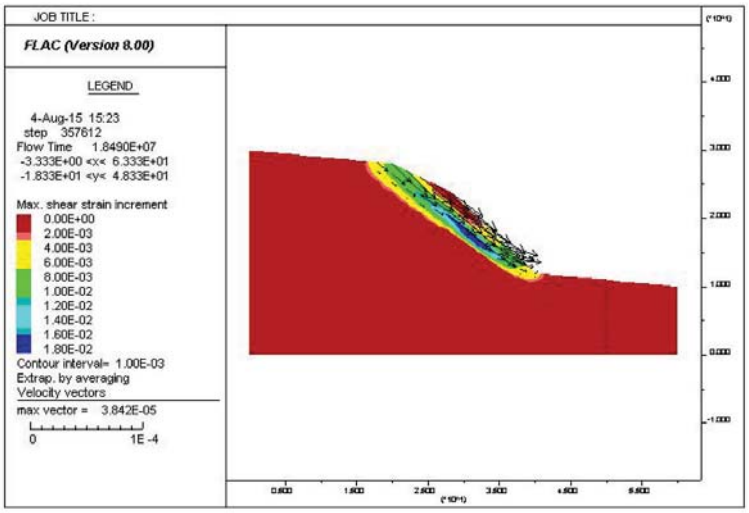

Figure 12—Velocity vectors after the high-intensity, short-duration rainfall event, showing slope failure

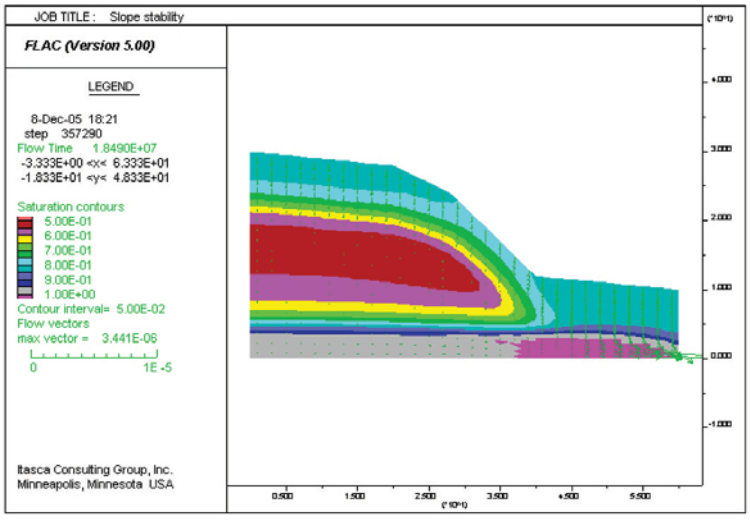

Figure 13—Saturation contours and flow vectors after the second rainfall event

Predicting rainfall-induced slope instability using simplified methods

Numerical analyses, such as shown in the previous section, are complex due to the nonlinearity of the hydraulic and soil constitutive behaviour at play. In addition, the actual geometry of the slope may add another level of complexity. A simplified approach to handle the problem is desirable, if practical guidance is to be the outcome of the analysis.

One possibility is to simplify the geometry of the problem, without compromise to the established hydraulic and soil behaviour. For example, the case of an infinite slope has been adopted by several authors, including Fourie (1996), Iverson (2000), Collins (2004), and Tsai *et al.* (2008), to name a few.

Fourie (1996) provides a methodology based on statistical rainfall records together with a simplified method to simulate the rate of infiltration. The methodology includes rainfall intensity, duration, and antecedent conditions in assessing slope stability based on Pradel and Raad's (1993) approximate method. The process starts with the rainfall data expressed in terms of rainfall intensity, duration, and return period (Figure 14).

The next step is to determine the minimum rainfall intensity (I_{min}) that exceeds the infiltration rate of the soil and must last long enough (T_{min}) to saturate the soil to a depth z_w measured perpendicular to the slope.

$$T_{\min} = \frac{(\theta_s - \theta_0)}{k}\left[z_w - \left(\frac{S + z_w}{S}\right)\right]$$

$$I_{\min} = k\left[\frac{z_w + S}{z_w}\right]$$

where θ_s and θ_o are the saturated and *in situ* volumetric water content respectively, k is the coefficient of hydraulic conductivity of the soil in the wetted zone and S is the wetting-front capillary suction (metres of water).

The relations are shown for a hypothetical example in Figure 14 where all rainfall events with an intensity and duration that plot within the box in the top right-hand corner will be sufficient to saturate soil to a depth z_w. The final step is to compute the safety factor of the slope for the saturated soil depth, z_w. Within the saturated depth, the matric suction (capillary pressure) should be reduced to a minimum value.

Rock slopes

The behaviour of rock slopes is significantly different from that of soil slopes during extreme rainfall events. Whereas soil slopes may fail due to loss of apparent cohesion, rock slopes generally fail due to high transient water pressures in open fractures, particularly tension-induced fractures (tension cracks) as described below. Transient pressures equivalent to 40 m of water have been measured at some mines.

Transient water pressure in tension cracks

Consider, for example, the steady-state condition shown in Figure 15. Under steady-state conditions, the pressure at any point along a structure is approximated by the product of the vertical depth below the groundwater table and the unit weight of water. Under transient conditions, a tension crack

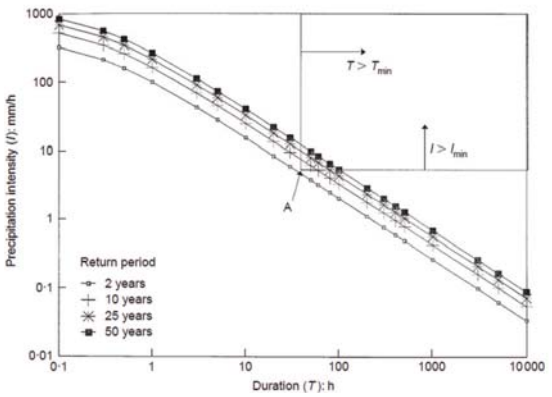

Figure 14—Example of relationship between rainfall intensity, duration, and return period (after Fourie, 1996)

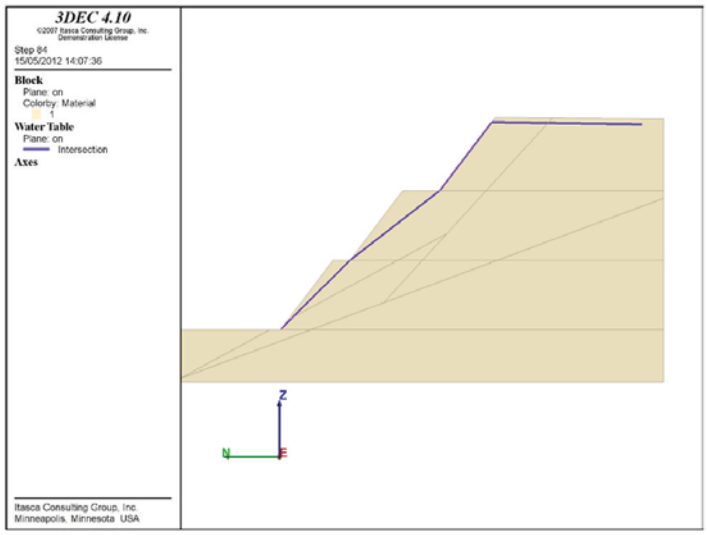

Figure 15—Steady-state situation with a groundwater table (blue line)

may quickly fill with water, producing the condition shown in Figure 16. The water pressure in the tension crack in Figure 16 is significantly higher than in Figure 15. In this particular case, the slope in Figure 15 had a safety factor of 1.18, whereas the slope in Figure 16 had a safety factor of 1.01.

Seasonal infiltration effects

In most cases when we consider extreme rainfall events, we think about durations of days or weeks. However, extreme rainfall events can also be seasonal, with rainfall occurring over months. This section discusses the effect of seasonal rainfall on a slope simulated as an equivalent continuum.

The effect of seasonal infiltration in a rock slope was examined by Hazzard *et al.* (2011) by alternating the rate of infiltration between zero for six months, and twice the average infiltration rate for six months. Example pore pressure histories are shown in Figure 17 for models with $k = 10^{-6}$ m/s and $k = 10^{-8}$ m/s. It is clear that the high-permeability model is affected greatly by the seasonal variations, whereas the low-permeability model is not. To examine the effect of the seasons on FoS, four different scenarios were simulated to consider different offsets for the start of the wet season. The FoS for the different seasonal simulations in one model are shown in Figure 18. Factors of safety were calculated nine months after each excavation. Depending on the start of the wet season, this may or may not correspond to peak transient pore pressures. However, it is possible to construct an envelope encompassing the minimum FoS for the four different scenarios; then it is possible to pick the peak pressure state for each excavation stage. Next, it is possible to calculate the average FoS over stages 1 to 6 for this minimum envelope and compare the results to the FoS calculated for a constant infiltration rate. Such an analysis clearly shows that the seasonal variations essentially have no effect on the FoS for low permeabilities and/or high excavation rates. However, for high permeabilities and/or low excavation rates, the seasonality may result in a decrease in FoS of up to 8%. Similar results are obtained for the other infiltration rates, except that as q

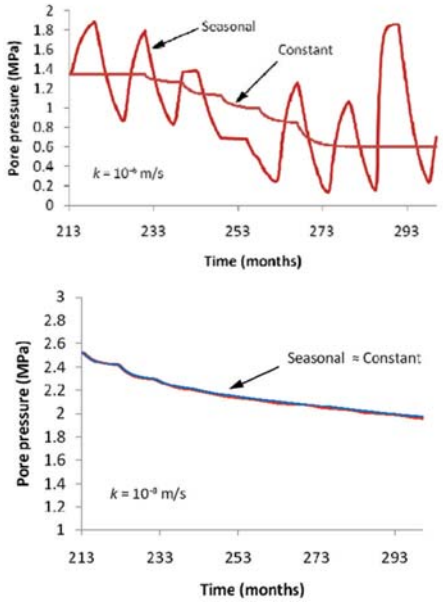

Figure 17—Example pore pressures for seasonal infiltration variation compared with constant rate for the model with $k = 10^{-6}$ m/s (upper) and $k = 10^{-8}$ m/s (lower). n = 1%. The history point is located 400 m below the ground surface and 150 m from the slope face

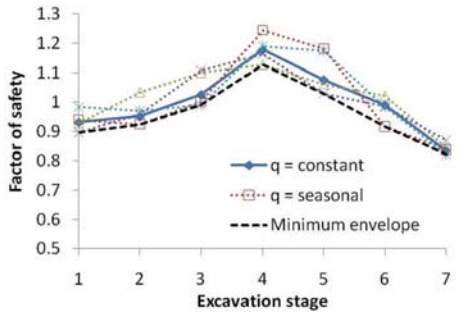

Figure 18—Factors of safety for different seasonal simulations in the model with $k = 10^{-6}$ m/s, n = 1%

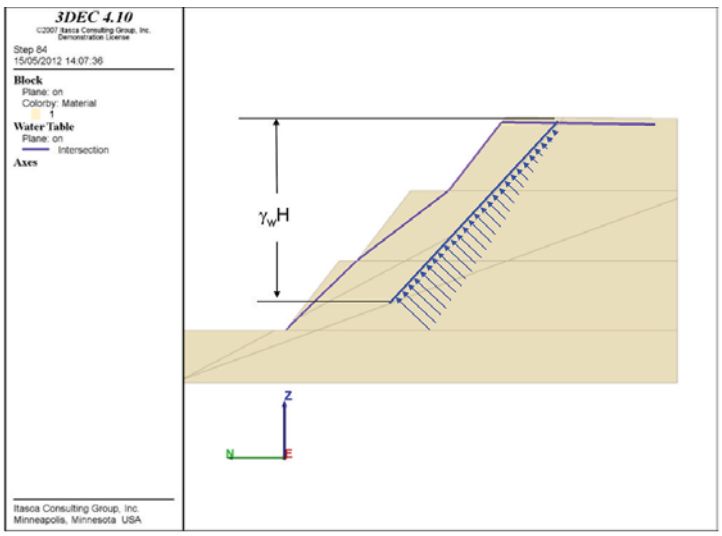

Figure 16—Transient water pressure distribution in tension crack

decreases, the effect of seasonality becomes even less severe. For q = 0.3 m/a, the maximum decrease in FoS caused by seasonality is only about 2.5% compared to constant q.

Concluding remarks

When it comes to earthquakes, it appears that stability analyses are largely unnecessary unless required by law. Possible exceptions might include mined slopes on the sides of steep, elevated topography where amplification affects may be important. If dynamic analyses are performed, time-domain numerical analyses are preferred over pseudo-static analyses due to their inherent ability to reproduce transient seismic forces. If pseudo-static analyses are performed, consider selecting seismic coefficients using peak particle velocity (PPV) rather than peak ground acceleration (PGA).

Designing for extreme rainfall events starts with designing stable slopes for 'normal' conditions such that tension cracks are minimized to the extent practicable and thus limiting the opportunities for water to enter cracks. The next step is to provide good surface drainage so that water does not erode and/or infiltrate slopes. Even with these mitigation measures, there is a need to consider the possibility that extreme rainfall may adversely affect slopes. Selection of appropriate acceptability criteria for extreme rainfall depends on risk tolerance, but it seems that a safety factor of at least unity under extreme rainfall conditions (*e.g.*, 24-hour duration and 100-year return period) is a reasonable starting point. Stability of soil slopes can by evaluated using an approximate method described in the paper or numerical models. For hard rock slopes, the rainfall-induced transient pressures should be considered either in an equivalent continuum rock mass and/or in explicit discontinuities.

Acknowledgements

The author would like to acknowledge Itasca colleagues Branko Damjanac, Christine Detournay, Roger Hart, Varun, Pedro Velasco and others for their important contributions to this paper. The author would also like to thank the Large Open Pit Consortium and Commonwealth Scientific Industrial and Research Organization (CSIRO) for the financial support provided for the study of earthquake effects on large open pits. Finally, the author would like to thank professional colleagues, including Alan Guest, John Read, Peter Stacey, and Christian Holland, Geoff Beale and others, that provided valuable insights.

References

Assimaki, D. and Kausel, E. 2007. Modified topographic amplification factors for a single-faced slope due to kinematic soil-structure interaction. *Journal of Geotechnical and Geoenvironmental Engineering*, vol. 133, no. 11. pp. 1414–1431.

Bouckovalas, G.D. and Kouretzis, G. 2001. Review of soil and topography effects in the September 7, 1999 Athens (Greece) earthquake. *Proceedings of the Fourth International Conference on Recent Advances in Geotechnical Earthquake Engineering and Soil Dynamics and Symposium in Honor of Professor W. D. Liam Finn*, San Diego, California, 26–31 March.

Collins, B. and Znidarcic, D. 2004. Stability analyses of rainfall induced landslides. *Journal of Geotechnical and Geoenvironmental Engineering*, vol. 130, no. 4. pp. 362-372. DOI: 10.1061/(ASCE)1090-0241(2004)130:4(362)

Damjanac, B., Varun, and L. Lorig. 2013. Seismic stability of large open pit slopes and pseudo-static analysis. *Proceedings of the International Symposium on Slope Stability in Open Pit Mining and Civil Engineering (Slope Stability 2013)*, Brisbane, Australia, September, 2013. Dight, P. (ed.). Australian Centre for Geomechanics, Perth, Australia. pp. 1203–1216,

Detournay, C. and Cundall, P. 2001. Numerical modeling of unsaturated flow in porous media using *FLAC. FLAC and Numerical Modeling in Geomechanics. Proceedings of the 2nd International FLAC Symposium*, Lyon, France, 29-31 October 2001. Billaux, D., Detournay, C., Hart, R., and Rachez, X. (eds.). A.A. Balkema, Lisse.

Detournay, C. and Hart, R. 2008. Stability of a slope in unsaturated conditions. *Continuum and Distinct Element Numerical Modeling in Geo-Engineering. Proceedings of the 1st International FLAC / DEM Symposium*, Minneapolis, August 2008. Sainsbury, D., Hart, R., Detournay, C., and Nelson, M. (eds.). Paper no. 03-03. Itasca Consulting Group, Minneapolis.

Fourie, A.B. 1996. Predicting rainfall-induced slope instability. *Geotechnical Engineering*, vol. 119, no. 4. pp. 211–218.

Fourie, A.B. and Haines, A. 2007. Obtaining appropriate design parameters for slopes in weathered saprolites. *Slope Stability 2007. Proceedings of 2007 International Symposium on Rock Slope Stability in Open Pit Mining and Civil Engineering*. Potvin, Y. (ed.). Australian Centre for Geomechanics, Perth. pp. 105–116.

Garcia, E.F., Riveros, C.A., and Builes, M. A. 2011. Influence of rainfall intensity on infiltration and deformation of unsaturated soil slopes. *Dyna*, no. 170. pp. 116–124.

Glass, C.E. 2000. The influence of seismic events on slope stability. *Slope Stability in Surface Mining*. Society for Mining, Metallurgy and Exploration, Littleton, CO. pp. 97–105.

Harp, E.L. and Jibson, R.W. 1995. Inventory of landslides triggered by the 1994 Northridge, California earthquake. US Geological Survey open file Report 95–213. 17 pp.

Harp, E.L. and Jibson, R.W. 1996. Landslides triggered by the 1994 Northridge, California earthquake. *Bulletin of the Seismological Society of America*, vol. 86, no. 1B. pp. S319–S332.

Hazzard, J., Damjanac, B., Lorig, L., and Detournay, C. 2011. Guidelines for groundwater modelling in large open pit mine design. *Slope Stability 2011: Proceedings of the International Symposium on Rock Slopes in Open Pit Mining and Civil Engineering*, Vancouver, September 2011. Eberhardt, E. and Stead, D. (eds.). Canada Rock Mechanics Association, Vancouver. Paper no. 114.

Itasca Consulting Group, Inc. 2011. *FLAC*: Fast Lagrangian Analysis of Continua, version 7.0. User's manual.

Itasca Consulting Group, Inc. 2012. *FLAC3D*: Fast Lagrangian Analysis of Continua in 3D, version 5.0. User's manual.

Iverson, R.M. 2000. Landslide triggering by rain infiltration. *Water Resources Research*, vol. 36, no. 7. pp. 1897–1910.

Kramer, S. L. 1996. Geotechnical Earthquake Engineering. Prentice-Hall.

Nuth, M. and Laloui, L. 2007. Effective stress concept in unsaturated soils: clarification and validation of a unified framework. *International Journal for Numerical and Analytical Methods in Geomechanics*, vol. 32. pp. 771–-801.

Pradel, D. and Raad, G. 1993. Effect of permeability on surficial stability of homogeneous slopes. *Journal of Geotechnical Engineering*, vol. 119, no. 2. pp. 315–332.

Pyke, R. 2001. Selection of seismic coefficients for use in pseudo-static analyses. TAGAsoft Limited. www.tagasoft.com/discussion/article2.html

Raptakis, D., Chavez-Garcia, F.J., Makra, K., and Pitilakis, K. 2000. Site effects at Euroseistest-I. Determination of the valley structure and confrontation of observations with 1D analysis. *Soil Dynamics and Earthquake Engineering*, vol. 19. pp. 1–22.

Tsai, T-L., Chen, H-E., and Yang, J-C. 2008. Numerical modeling of rainstorm-induced shallow landslides in saturated and unsaturated soils. *Environmental Geology*, vol. 55. pp. 1269–1277.

Van Genuchten, M.Th. 1980. A closed form equation for predicting the hydraulic conductivity of unsaturated soils. *Soil Science Society of America Journal*, vol. 44. pp. 892–898.

Wang, L, Liu, S., Fu, Z., and Li, Z. 2015. Coupled hydro-mechanical analysis of slope under rainfall using modified elasto-plastic model for unsaturated soils. *Journal of Central South University*, vol. 22. pp. 1892–1900.

Appendix A – Effect of topography on dynamic wave amplification (from Damjanac *et al.*, 2013)

A.1 Two-dimensional effects

Based on typical configurations of open pit mines and natural slopes, three simplified slope geometries, shown in Figure 19, are studied using two-dimensional (2D) numerical analyses. These are (a) a single slope model that is representative of a natural slope or a wide pit, (b) a pit model representative of open pits, and (c) a hill model representative of most natural slopes. These models can be expressed in terms of following parameters:

1. Height of slope (H), assumed to be 500 m for the simplified geometry
2. Angle of slope (θ), assumed to be 45 degrees for the simplified geometry
3. Width of basin (b) or ridge crest (d), varied from 0.0 to 2.0 times the slope height.

To simulate seismic excitation, single pulses are used as input motion. The pulses are characterized by their duration T as

$$V(t)=\begin{cases}\frac{1}{2}\left(1-\cos\left(\frac{2\pi t}{T}\right)\right) & \text{if } t\le T\\ 0 & \text{if } t>T\end{cases}$$

where $V(t)$ is the particle velocity at time t.

The signal contains frequencies in the range 0 to $2/T$ Hz. Figure 20 shows the time history for two pulses with $T = 0.4$ seconds and 2.5 seconds. The motion is applied at the base of the model as a shear stress time history to simulate an incoming wave. Quiet boundaries are used at the base to avoid any reflection of outgoing waves back into the model. Appropriate forces obtained from one-dimensional site response are applied at the lateral boundaries to simulate free-field behaviour correctly. A density of 2500 kg/m^3 and shear wave velocity of 1000 m/s are assumed for the rock.

The simulations are carried out for pulse durations ranging from 0.1 to 10 seconds. The results are compared in terms of peak velocity obtained at the surface. Two parameters are recorded for each simulation, the first being the peak velocity on the slope surface, and the second being the peak velocity at the ground surface throughout the model. For short duration pulses, both parameters are the same as maximum velocity is obtained on the slope surface itself. However, for longer duration pulses, the maximum velocity is obtained behind the crest of the slope as shown in Figure 21.

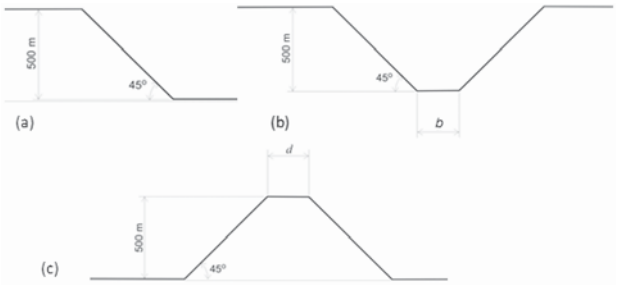

Figure 19—Idealized geometries studied: (a) slope geometry, (b) pit geometry, and (c) hill geometry

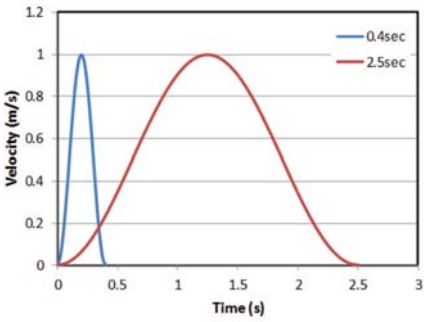

Figure 20—Two pulses of duration 0.4 and 2.5 seconds in time domain

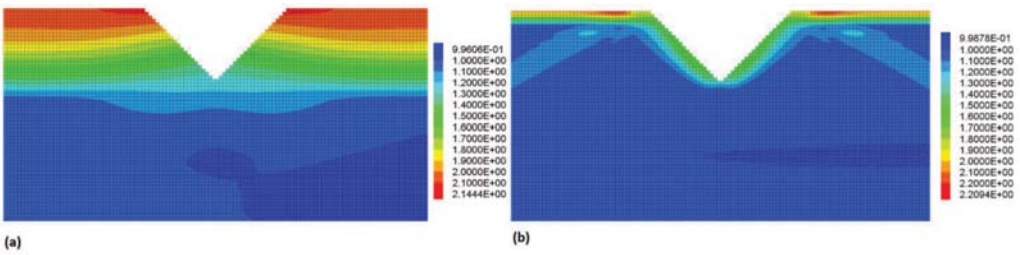

Figure 21—Peak ground velocity amplification ratio in the model for (a) 2.5 s pulse and (b) 0.4 s pulse

The results for slope and pit geometries were found to be almost identical, irrespective of the width parameter (b). This is due to the fact that incident waves travel up the slope and, given the shape of pit geometry, are reflected away from the pit. As a result, there is no interaction between the waves incident on two sides of the pit. Therefore, when comparing results, only the slope geometry results are shown and are taken to be representative of pit geometry as well.

The results are presented as the amplification factor (*i.e.*, the ratio of PGV observed to the PGV for the incoming motion). The results are plotted as a function of the inverse of pulse duration, which is indicative of the frequency content of the ground motion. The frequency can also be normalized and written in dimensionless form as H/V_sT, where V_s is the shear wave velocity of rock at surface and H is the slope height.

The results for the slope/pit geometry are shown in Figure 22. As can be seen from the results, for long duration pulses (*i.e.*, pulses containing lower frequencies), peak velocity is observed on the slope surface itself. For the limiting case of an infinitely long pulse, the amplification is 2.0, which is the same as the free surface amplification (*i.e.*, the topographic effects are negligible). As the frequency increases, the peak surface velocity also increases with the peak being observed at a frequency of 0.8 Hz ($H/V_sT = 0.4$). A further increase in frequency does not lead to any significant increase in peak ground velocity. Instead, the location of the peak velocity moves away from the slope surface to behind the crest of the slope. The maximum amplification observed for the pit geometry is around 2.24, which is not a significant increase compared to the free surface amplification factor of 2.0.

For the hill geometry, the results are a function of the width 'd'. As width increases, $\rightarrow \infty$, the amplification decreases and the amplification curve approaches the slope geometry case. Maximum amplification is observed for the case where $d = 0$. A comparison between amplification curves for peak velocity on the slope surface for the hill geometry (with $d = 0$) and slope geometry are shown in 23. The amplification curve for the hill geometry shows a similar shape as for the slope geometry with peak amplification occurring at 0.8 Hz, which corresponds to a dimensionless frequency of 0.4. However, the amplification ratio is much higher with peak amplification of 3.2. This is due to the 'focusing effect' of the hill geometry where the waves incident on the slope are directed toward the crest from both sides and result in energy from a wide base at the bottom being focused in a small area at the top. Thus, natural slopes experience much higher velocities (and acceleration) due to topographic amplification.

A.2 Three-dimensional effects

The next step was to evaluate the effect of three-dimensional pit shapes on the amplification ratio. The pit is modelled as an ellipse in plan view with an aspect ratio (AR) between the principal axes ranging from 1:1 to 8:1. The 1:1 aspect ratio corresponds to a circular pit, whereas the 8:1 case is very similar to the two-dimensional pit geometry. The results are shown in Figure 24. As the aspect ratio increases, the results tend to converge, and for an aspect ratio of 4:1 or higher, the results are nearly the same as for the 2D case. For lower aspect ratios, peak amplification occurs at a higher frequency

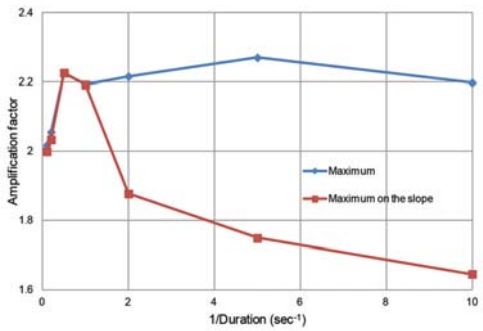

Figure 22—Amplification factors on 2D slope as functions of duration of input puls

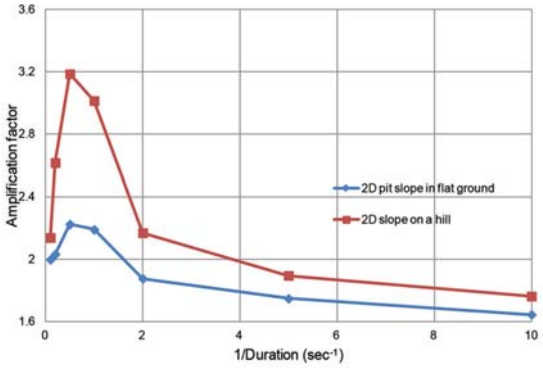

Figure 23—Amplification factors on 2D slope in flat ground and on a hill as functions of input frequency

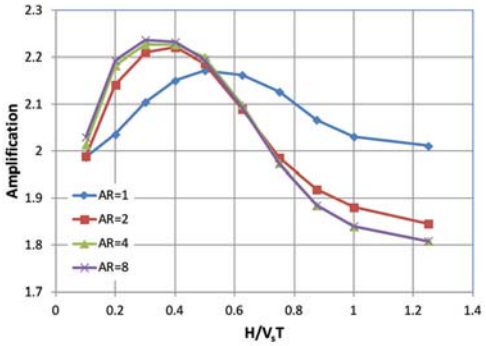

Figure 24—Maximum amplification factors on the 3D slope as a function of normalized pulse duration

and amplification ratios for higher frequencies are higher than the 2D case. However, the peak amplification ratio is still lower than the 2D case. Thus, the three-dimensional shape of pits leads to even lower amplification ratios, and hence, lesser demand.

Appendix B – Effect of heterogeneities in dynamic wave amplification (from Damjanac *et al.*, 2013)

B.1 Effect of horizontal layering

The effect of horizontal layering is examined using a 2D model. As shown in Figure 25, a softer material is assumed

to a depth of 200 m below the slope toe. Two cases are studied. In the first case, the softer material has a modulus that is 50% of the original modulus, whereas in the second case, the modulus is 10% of the original value. The results for the slope geometry are shown in Figure 26 and the results for the hill geometry are shown in Figure 27.

The presence of softer material leads to energy trapping within the narrow layer below the surface, and hence much higher amplification ratios are observed. For the slope geometry, the maximum amplification increases to about 2.7 for the 50% stiffness case, whereas an amplification ratio of 3.6 is observed for the 10% stiffness case. The frequency corresponding to peak amplification also decreases as stiffness decreases.

For the hill geometry, the effect is even more pronounced with an amplification ratio of 4.0 for the 50% stiffness ratio, and 6.0 for the 10% stiffness ratio. As the stiffness contrast increases, the amplification ratio also increases. While it is common to have a thick layer of highly weathered rock or soil above competent rock on natural slopes, open pit slopes are generally excavated in relatively good quality rock and have only a comparatively thin layer of fragmented rock that is still stiffer than highly weathered rock or soils; hence open pit slopes are less susceptible to amplification due to material heterogeneities.

B.2 Effect of vertical layering

Material heterogeneities can also be present in a horizontal direction (*e.g.*, due to the presence of the orebody). The effect of an orebody is evaluated in this section in 3D where the orebody is assumed to be vertical and intersects the pit walls 100 m above the base of pit as shown in Figure 28. The orebody is assumed to have half the stiffness of country rock. Results are shown in Figure 29.

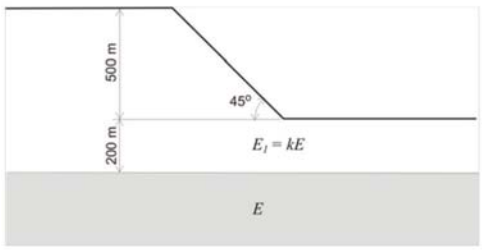

Figure 25—Geometry for stiffness contrast

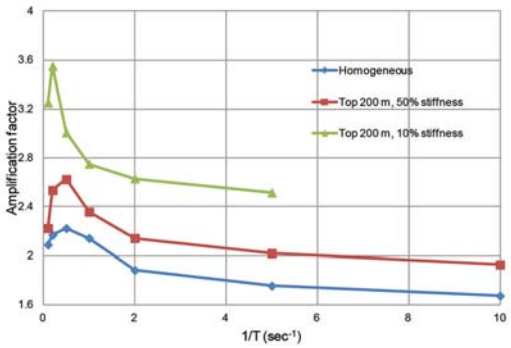

Figure 26—Effect of surface layers on amplification factors on a 2D slope as functions of input pulse duration

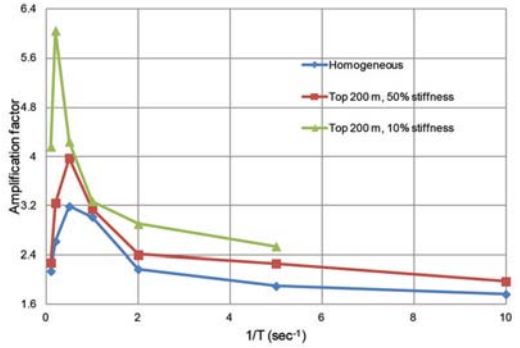

Figure 27—Effect of surface layers on amplification factors on a 2D slope on a hill as functions of input pulse duration

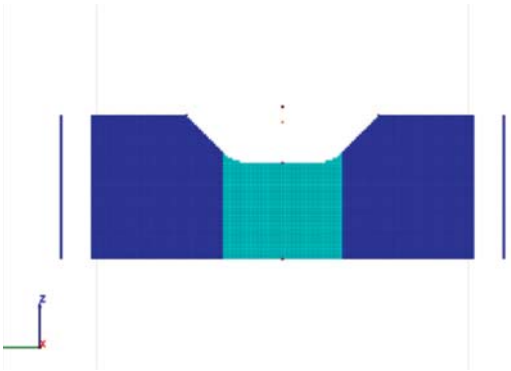

Figure 28—Orebody geometry used to study the effect of heterogeneities in horizontal direction

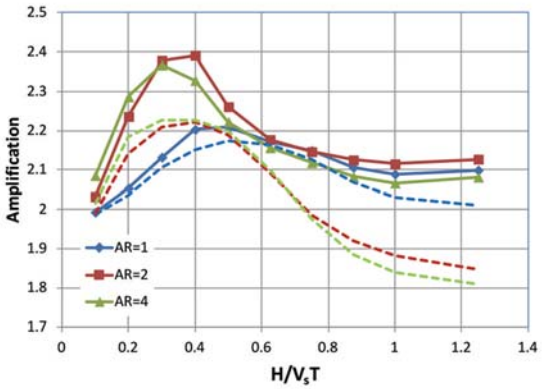

Figure 29—Maximum amplification factors on the 3D slope with an orebody (solid) and without an orebody (dotted) as a function of normalized pulse duration

As expected, the presence of the orebody leads to higher amplification ratios than for the homogenous case as energy is trapped within the orebody. One of the important observations is that the increase in amplification ratios is more pronounced for higher aspect ratios than for the circular case, where the increase is negligible. Nonetheless, the peak amplification ratio for the 4:1 case is still 2.4, which is not too high compared to the amplification ratio of 2.0 for the free field base case. ◆

http://dx.doi.org/10.17159/2411-9717/2016/v116n5a5

A comparison of slope stability analyses in two and three dimensions

by D. Wines*

Synopsis

Slope stability analyses have traditionally been undertaken in two dimensions assuming plane strain conditions. Although three-dimensional analysis techniques are widely available and used routinely for open pits, two-dimensional analyses are still more common due to the relative ease of model construction and the relatively rapid simulation times.

Two-dimensional analyses will often produce different results to three-dimensional analyses for the same slope. It is generally thought that two-dimensional analyses will produce more conservative results. The main reason for the differences is the ability of three-dimensional analyses to account for the three-dimensional nature of the various model inputs, including the slope geometry, the distribution of soil and rock mass domains, the orientation of geological structures with respect to the excavation face, the orientation of the *in situ* stresses, and the distribution of pore pressure. In some cases, for a long, straight slope in basic geological conditions, two-dimensional analyses can provide a reasonable representation of the problem. However, in many cases, the inability of a two-dimensional analysis to represent the true three-dimensional nature of the problem will lead to unrealistic analysis results.

This paper discusses the reasons, as detailed above, for the differences in two-dimensional and three-dimensional analysis results. Work by others is summarized, and additional numerical analyses are performed to provide an improved understanding of the effects of slope geometry, structural orientations, and *in situ* stresses on predicted stability. Case studies are presented for both stable and unstable slopes, and the behaviour of these slopes is related to the three-dimensional nature of the slope geometry and geology.

The previous work, the new analyses performed here, and the case studies show that it is often important to provide a realistic representation of the slope in three dimensions in order to obtain reasonable stability analysis results. This is particularly true for hard rock environments where structurally controlled failure mechanisms are most likely. The paper also highlights the fact that back-analysed properties obtained from one analysis technique are not necessarily applicable to forward analyses using another technique.

Keywords
slope stability, numerical modelling, two-dimensional, three-dimensional.

Introduction

Various methods exist to analyse the stability of natural and man-made slopes. These include limit equilibrium techniques and numerical techniques such as the finite difference and finite element methods. Both two-dimensional (2D) and three-dimensional (3D) approaches can be used when performing limit equilibrium or numerical slope stability analyses. Where 2D numerical analyses are undertaken, plane strain analyses are generally performed, whereby strains can occur only along the analysis plane (*i.e.* out-of-plane strains are not considered). Axisymmetric analyses can also be performed, whereby it is assumed that the excavation is rotationally symmetric about an axis. This allows some representation of a 3D geometry in a 2D analysis.

In the early 1980s, in the 3rd edition of their book *Rock Slope Engineering*, Hoek and Bray (1981) stated that all methods of stability analysis treated slopes two-dimensionally, whereby it is assumed that the section of slope under consideration is part of an infinitely long straight slope. 2D analysis techniques are still widely used today due to the relative ease of model construction and the relatively fast model run times.

Lorig and Varona (2007) state that 3D analyses were uncommon prior to 2003; only by 2007 had advances in personal computers allowed 3D analyses to be performed routinely. Further advances in computing and software packages since that time have significantly improved our ability to construct and run 3D models for slope stability analyses. In many cases, the time and effort required to construct and run a 3D model may be less than that required to construct and run several 2D models for the same slope.

Different analysis methods will often produce different results for the same slope. For example, a limit equilibrium analysis may produce a different result to a numerical analysis. Furthermore, a 2D analysis will often produce different results to a 3D analysis. For example, Gitirana *et al.* (2008) performed both

* *Itasca Australia Pty Ltd.*

2D and 3D back-analyses for the Lodalen Landslide in Oslo using limit equilibrium techniques, and the results were found to be different. It is often stated in the literature that 2D analyses are more conservative than 3D analyses (Cheng *et al.*, 2005; Nian *et al.*, 2012; Leong and Rahardjo, 2012). However, based on analyses of landslides in soils, Bromhead (2004) states that 3D analyses can sometimes produce lower safety factors compared to 2D analyses.

Huang and Tsai (2000) and Cala (2007) state that 2D slope stability analysis often leads to oversimplification of the problem. Nian *et al.* (2012) claim that 2D analysis may lead to incorrect evaluation of the potential failure mechanism. Zettler *et al.* (1999) state that, in many cases, a 3D problem cannot be solved with a 2D analysis. According to Lutton (1970), 3D representation is required to undertake adequate analysis of a slope.

The main reason for the differences in the results of 2D and 3D analyses is the ability of 3D analysis to provide an accurate representation of the problem, which will always be 3D in reality. In particular, a 3D analysis can accurately represent:

- The 3D slope geometry, which may be concave or convex in plan. This curvature can have a significant influence on stability (Lutton, 1970; Piteau and Jennings, 1970; Hoek and Bray; 1981; Hoek *et al.*, 2000; Bromhead, 2004; Cala, 2007; Lorig and Varona, 2007; Azocar and Hazzard, 2015)
- The 3D distribution of soil and rock mass domains (Zettler *et al.*, 1999; Bromhead 2004; Cala, 2007; Lorig and Varona, 2007; Wei *et al.*, 2009)
- The 3D orientation of geological structures with respect to the orientation of the excavation face (Lorig and Varona, 2007; Azocar and Hazzard, 2015). Lorig and Varona (2007) recommend that if the direction of the principal geological structures or material anisotropy does not strike within 20–30° of the strike of the slope, 3D analysis is required
- The *in situ* stress magnitude and orientation (Lorig and Varona, 2007; Azocar and Hazzard, 2015)
- The distribution of pore pressure (Bromhead, 2004).

It is often not possible to provide a reasonable representation of these items in a 2D model.

The main factors affecting the results of 2D and 3D analyses are discussed in more detail below. Work by others is summarized, and additional numerical analyses are performed to provide an improved understanding of the effects of concave and convex geometries and *in situ* stresses on predicted stability. Case studies are also presented.

This paper is applicable to man-made and natural slopes excavated in soil and/or rock. However, particular emphasis is placed on open pit slope stability in a hard rock environment.

Slope geometry

As discussed, performing 2D plane strain analysis requires the assumption that the slope is long and straight. However this is often not the case for actual slopes, which may be either concave or convex in plan. Open pits will always include concave slope geometries. In a long and narrow pit, the walls at each end of the pit will be concave. In a circular pit, essentially all walls will be concave. Convex geometries will also exist in natural slopes and open pits. 'Bullnose' geometries are often created in pits due to reasons such as complex orebody distribution, the existence of ramp switchbacks, and the difficulties associated with smoothly transitioning a new cutback into existing walls.

The effects of concave and convex slope geometries on slope stability are discussed separately below.

Concave slopes

Previous analyses

A review of the literature indicates general acceptance that a slope that is concave in plan will be more stable than a straight slope (assuming the same geology, stresses, *etc.*). Hoek and Bray (1981) state that the restraint provided by the material on either side of a potential failure will be greater if the slope is concave. Piteau and Jennings (1970) studied the influence of plan curvature on slope stability at five large diamond mines in South Africa. They state that steeper slopes could be created in concave walls when the radius of curvature was smaller. Armstrong and Stacey (2003) state that for a hard rock environment, the radius of curvature influences the maximum volume of wedges that can fail.

Several researchers have assessed the influence of curvature on slope stability. Lorig and Varona (2007) performed axisymmetric analyses using *FLAC* (Itasca, 2001) to assess the effects of slope curvature on the factor of safety (FoS) for a 500 m high dry slope with a face angle of 45° excavated in an isotropic homogenous material. The safety factors obtained from these analyses were greater for a concave slope than for a straight slope, and the FoS increased as the radius of curvature decreased. These results are intuitive, and are consistent with the theory that a concave geometry will provide additional lateral support.

The analyses performed by Lorig and Varona (2007) were for a circular-type failure in a homogenous material. Azocar and Hazzard (2015) also performed a series of analyses to assess the effects of curvature on rock slope stability; however, their main focus was on the effects of concave slope geometry on the stability of a jointed rock mass. Their initial analyses, which assumed no explicit jointing, produced results very similar to those reported by Lorig and Varona (2007). That is, the FoS increases with decreasing radius of curvature, and the effect of curvature decreases as the friction angle increases. The jointed rock slope analyses were performed using *3DEC* (Itasca, 2014), which allows explicit representation of a large number of joints. Analyses were performed for sliding, flexural toppling, and block toppling failure mechanisms, and as for the homogenous analyses, the FoS increased as the radius of curvature decreased for all three failure mechanisms. Also, the rate of change in FoS was highest for larger radius of curvature values, and tapered off as the radius became smaller.

Several others have performed limit equilibrium and/or numerical analyses to assess the effect of concave geometry on soil slope stability (Xing, 1988; Zettler *et al.*, 1999; Jiang *et al.*, 2003; Suarez and Gonzalez, 2003; Cheng *et al.*, 2005; Cala, 2007; Totonchi *et al.*, 2012; Zhang *et al.*, 2013). In all cases, the analyses indicated that a concave slope will be more stable than a straight slope.

Some limited work has also been performed to assess the influence of *in situ* stresses on the effects of concave slope curvature. For their base case analyses, Azocar and Hazzard (2015) assumed that the *in situ* stress was lithostatic with a *k* value of unity. One additional model was run with a *k* value of 0.5, and this produced a lower FoS compared to the model with a *k* value of unity. Based on axisymmetric limit equilibrium analyses, Xing (1988) concludes that the effect of plan curvature on stability increases as the lateral pressure coefficient increases. These results indicate that the effect of slope curvature may differ depending on the *in situ* stresses.

Additional analyses

Additional analyses for concave slopes were performed for this paper using *3DEC* based on a 60 m high slope with a 60° overall slope angle. An example model is shown in Figure 1. The analyses were performed for various radii of curvature, with the radius being measured at the toe of the pit. The slope was assumed to be made up of an isotropic, homogenous, and dry rock mass with the properties shown in Figure 1. The rock mass was represented using a linear elastic–perfectly plastic Mohr-Coulomb constitutive model with tensile strength cut-off. To assess the potential effects of *in situ* stresses on the influence of slope curvature, analyses were performed with horizontal to vertical pre-mining stress ratios of 0.5:1, 1:1, and 3:1. The safety factors for each analysis were determined using *3DEC*'s built-in FoS calculation capability, which is based on the shear strength reduction technique described by Dawson *et al.* (1999).

The results of the *3DEC* analyses for concave slopes are presented in Figure 2. To be consistent with previous work by others, the results are presented on a chart showing the relation between the normalized FoS (the FoS for a concave slope divided by the FoS for a plane strain analysis) and the ratio of slope height to radius of curvature. Therefore the actual FoS values are not shown. This is to avoid the results being used directly by practitioners for slope design. The results are unique to the assumptions made for these particular analyses, therefore it is considered unwise to use the results to develop 'rules of thumb' for actual curved slopes.

The following comments are based on these analysis results:

- In general, the results are consistent with previous work. There is a clear increase in the calculated FoS as the radius of curvature decreases. The rate of change in FoS is highest for larger radius of curvature values
- The adopted *in situ* stresses are seen to have some effect on the analyses results. The FoS is generally slightly higher as the horizontal *in situ* stress is increased. The increased horizontal stress may increase the confining effects provided by a concave slope. Despite this conclusion, the adopted stresses do not have a significant effect on the resulting safety factors. For these analyses, the difference between the safety factors produced by the analyses with different *in situ* stresses (with all other inputs the same) is always less than 0.05
- As discussed, the analysis results were normalized for presentation in Figure 2 to avoid the results being used directly by practitioners for slope design. To provide some idea of the change in FoS caused by the change in plan curvature, for these particular analyses, it is noted that the FoS increased by approximately 0.4 when comparing a straight slope to a concave slope with a radius of curvature of 60 m.

The analysis results shown here and the findings of others in relation to concave slopes are intuitive. It makes sense that the confinement provided by a concave slope will provide an increase in stability. As an extreme example, in a hard rock environment, vertical boreholes can be drilled several hundred metres deep without significant stability issues in the borehole walls. This is due to the confinement associated with the small area of the opening. If a vertical open pit wall were to be excavated in the same material to the same depth, instability is clearly more likely due to the relative lack of confinement.

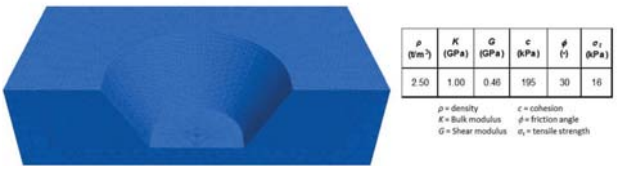

Figure 1—Example of *3DEC* model geometry for concave slope analyses, and adopted rock mass properties

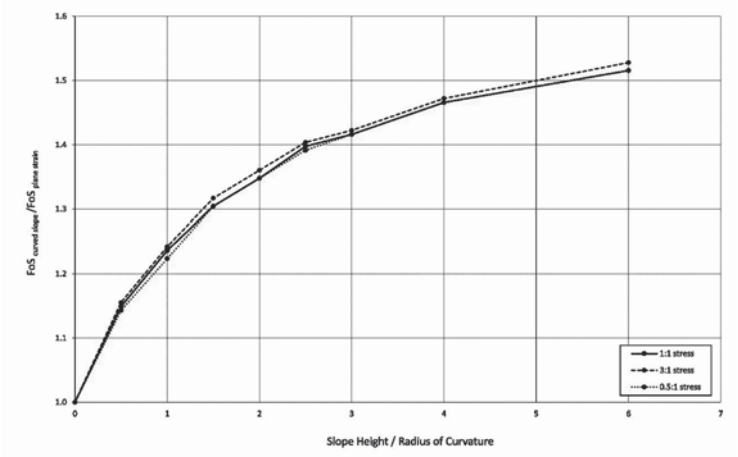

Figure 2—Results of three-dimensional *3DEC* numerical analyses for concave slopes

Convex slopes

Previous analyses

The axisymmetric analyses presented by Lorig and Varona (2007) also included analyses for convex slopes. The safety factors for convex slopes were higher than those for a straight slope. This is consistent with Cala (2007), who performed numerical analyses for a soil slope and predicted higher safety factors for a convex slope. Both Lorig and Varona (2007) and Cala (2007) found that, for a given radius, the effect of curvature is greater for a concave slope compared to a convex slope. Jiang *et al.* (2003) performed limit equilibrium analyses for soil slopes, and also found that a convex slope produced a higher FoS than a straight slope. Gomez *et al.* (2002) performed 2D, axisymmetric, and 3D numerical analyses for waste dumps at Chuquicamata mine in Chile. The axisymmetric and 3D analyses assumed a convex waste dump geometry, and these analyses produced higher safety factors than those produced by the 2D plane strain analyses.

Not all analysis findings reported in the literature are consistent with those discussed above. Based on the results of numerical analyses for soil slopes, Zettler *et al.* (1999) found that the FoS for a convex slope was slightly less than for a straight slope. Limit equilibrium analyses performed by Cheng *et al.* (2005) for a soil slope also produced lower safety factors for the convex case compared to a straight slope. Cala (2007) suggests that these results are misleading.

Anecdotal evidence suggests that convex slopes may be less stable than straight or concave slopes, particularly in a hard rock environment. Hoek and Bray (1981) state that the restraint provided by the material on either side of a potential failure will be less if the failure is situated in a 'nose' which has freedom to expand laterally. They discuss the slopes at an open pit in Tasmania, and state that two convex noses showed serious signs of instability, while the remaining slopes, which were straight or concave, were stable. Hoek *et al.* (2000) state that rock 'noses', or slopes that are convex in plan, are less stable than concave slopes due to the lack of confinement in convex slopes and the beneficial effects of confinement in concave slopes. Narendranathan *et al.* (2013) state that convex profiles or 'bullnoses' are notorious for initiating planar/wedge-type sliding instabilities. They discuss some failures in a pit in the Pilbara region of Western Australia where anisotropic rock masses are encountered. They state that, in the majority of cases, instabilities were noted to initiate on slightly convex profiles, and it was noted that the lateral extents of the instabilities were sometimes defined by the change in concavity of the slope. Kayesa (2006) discusses a multi-bench failure at the Letlhakane mine in Botswana, which occurred in a convex bullnose geometry located at the boundary between two mining areas.

The majority of analyses detailed in the literature indicate that a convex slope will be more stable than a straight slope. These results may seem counter-intuitive, given the information provided in the paragraph immediately above. For their waste dump analyses, Gomez *et al.* (2002) suggest that the increased FoS with reducing radius of curvature can be explained by a reduced volume of material being available to be mobilized as the radius decreases. They note that the depth of the failure surface determined in all analyses was similar; however, a slope with a finite radius provides less material than the equivalent infinite (plane strain) slope.

Lorig and Varona (2007) state that their results for convex slopes are not consistent with observed experience in rock slopes. They note that the analyses assume that the slope is formed in isotropic homogenous material, and the reason that noses are often less stable in reality may be related to the fact that they are more exposed to structurally-controlled failure mechanisms. Structures were not explicitly defined in their analyses, therefore structurally controlled failures were not represented.

Additional analyses

Additional analyses were performed for this paper using *3DEC* to investigate the effects of a convex geometry on slope stability. The adopted parameters are the same as those used for the concave analyses discussed above (in terms of slope height and angle, material properties, and *in situ* stresses). The analyses were performed for various radii of curvature, with the radius being measured at the crest of the slope. An example *3DEC* model is shown in Figure 3.

The results of the *3DEC* analyses for convex slopes are presented in Figure 4. The following comments are based on these analysis results:

- The FoS increases as the radius of curvature decreases
- The adopted *in situ* stresses are seen to have some effect on the analysis results. The FoS is generally slightly higher as the horizontal *in situ* stress is increased, which is consistent with the results of the concave slope analyses. Despite this conclusion, the adopted stresses do not have a significant effect on the resulting safety factors. For these analyses, the difference between the safety factors produced by the analyses with different *in situ* stresses (with all other inputs the same) is always less than 0.05
- The analyses suggest that the effect of slope curvature on stability for a convex slope is less than that for a concave slope
- As for the concave analyses, normalized values are presented for the convex slope analyses, therefore the absolute values are not shown. To provide some idea of the change in FoS, for these particular analyses, it is noted that the FoS increased by approximately 0.1 when comparing a straight slope to a convex slope with a radius of curvature of 60 m.

The results are consistent with those produced by several others, including the results of the axisymmetric analyses performed by Lorig and Varona (2007). The increased stability for a convex slope compared to a straight slope is

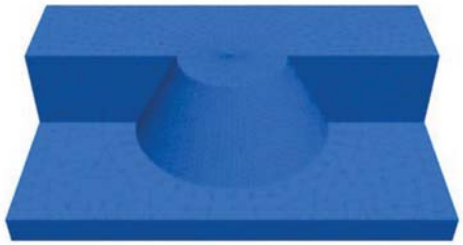

Figure 3—Example of *3DEC* model geometry for convex slope analyses

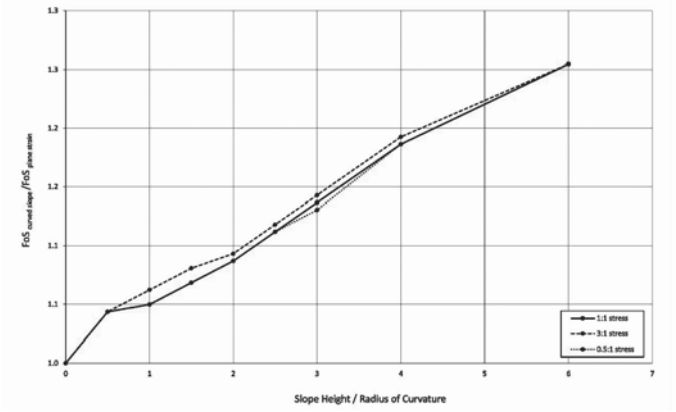

Figure 4—Results of three-dimensional *3DEC* numerical analyses for convex slopes

somewhat counter-intuitive given the lack of lateral confinement in a convex slope. A likely reason for these results is that, for a given failure shape, the failure will involve less volume for a convex slope when compared to a straight slope, and therefore the driving forces will also be less, resulting in a higher FoS. This is consistent with the hypothesis provided by Gomez *et al.* (2002) based on their waste dump analyses.

Note that the 3D isotropic, homogenous analyses performed here for both concave and convex slopes assume an idealized slope geometry, whereby the slopes are assumed to be perfectly symmetric. This is also the case for most of the previous 3D and all of the axisymmetric analyses performed by others. These idealized geometries provide a significant improvement in the predicted stability produced by the analyses. The idealized geometries would rarely occur in reality, and small perturbations to these geometries may lead to a reduction in the benefits provided by the concave and convex slopes. The effects of this difference in actual *versus* assumed slope geometries may be more important for 3D and axisymmetric analyses than for plane strain analyses.

Case study

The increase in stability indicated by the analysis results presented above is not consistent with the observed behaviour of convex slopes. As suggested by Lorig and Varona (2007), this is probably because these analyses assumed isotropic and homogenous rock mass conditions, while instability associated with convex slopes will often be structurally controlled, particularly in a hard rock environment.

An example of a failure that may have been influenced by the convex wall geometry is shown in Figure 5a. This failure occurred in an open pit gold mine in Western Australia in June 2011. The failure mechanism was a wedge controlled by two steeply-dipping structures on the sides and a flatter structure below. It can be seen in the photograph that the failure occurred within a convex 'bullnose' geometry, and it is thought that the lack of lateral confinement created by this geometry probably made instability more likely at this location. The orientation of the main controlling structures in relation to the pit face is shown in Figure 5b. The failure occurred soon after a blast was fired close below. The failure did not result in any equipment damage or injuries.

The failure was successfully back-analysed using *3DEC*. The purpose of the back-analysis was to provide an understanding of the failure mechanism, and to refine the fault and rock mass properties for use in forward analyses for other slopes at the mine. The displacement contours and vectors produced by the back-analysis model are shown in Figure 5c.

To assess the influence of slope geometry on the wall behaviour, the original *3DEC* back-analysis model was reconstructed assuming that a straight wall existed at the failure location. The model was then rerun using the same material properties that were developed as a part of the initial back-analysis, and in this case, failure was not predicted by the model. Displacements produced by the rebuilt model (with the straight wall geometry) are presented in Figure 5d. It is seen that the lateral controlling structures still daylight in the pit face. Based on strength reduction analyses, for the initial back-analysis, the FoS was slightly less than 1.0, increasing to greater than 1.5 when the wall was assumed to be straight. This indicates that the bullnose geometry may have been a significant contributing factor in this instability.

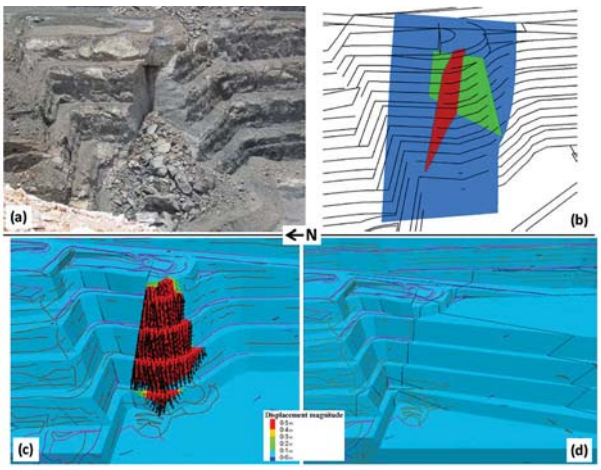

Figure 5—Plots relating to June 2011 Western Australian gold mine failure. (a) Photograph of failure, (b) surfaces showing main controlling structures in relation to design crests and toes, (c) displacement contours and vectors produced by *3DEC* back-analysis model based on actual slope geometry, and (d) displacement contours produced by *3DEC* model assuming straight slope geometry at failure location

In this particular case, the bullnose geometry made release of the unstable blocks more likely due to the reduced lateral restraint.

Orientation of geological structures

Often, the orientation of geological structures with respect to the pit wall is a very important factor in the stability of that wall. A 3D representation of the slope and the structures is generally required in order to provide a realistic representation of the problem, particularly when the strike of the structures is oblique to the excavation face. A 2D analysis running perpendicular to the slope will represent the apparent dip of the structures, which will not be the actual dip if the strike of these features is oblique to the strike of the wall. In this case, the apparent dip will always be less than the true dip. A 2D analysis will also assume that the location of the structures in relation to the excavation face is constant along strike, and this will not be the case unless the structures strike parallel to the wall.

Another case study is provided here to illustrate these effects. In October 2011, a failure occurred on the east wall of a gold mine in Western Australia, as illustrated in Figure 6a. The instability was controlled by a large structure that dips steeply to the west-northwest at the back of the failure, and a flat-lying structure that dips into the pit at the base of the failure. Lateral release occurred through the rock mass and other smaller structures at the northern end of the failure. Mining of the failure area occurred several months prior to the slip, therefore the wall stood for a considerable time before failure. Failure occurred after a very significant rainfall event. The failure did not result in any equipment damage or injuries.

The orientation of the two main controlling structures in relation to the pit face is shown in Figure 6b. This general failure mechanism is common in hard rock open pit mines. The dip of the flat-lying structure at the base of the failure (blue surface in Figure 6b) is approximately 27°. Because this is significantly less than the inter-ramp slope angle, this structure daylights in the wall. The steeper structure at the back of the failure (red surface in Figure 6b) strikes oblique to the pit face. The pit face dips to the west, while this structure dips at approximately 67° to the west-southwest. The angle between the strike of this structure and the strike of the wall is approximately 18°. Because this structure strikes obliquely to the pit face, it is further behind the wall with increasing distance to the north, therefore some 'rock mass' failure was required at the northern end of the instability for slope failure to occur.

To provide an improved understanding of the failure mechanism, and to refine fault and rock mass properties for use in forward analyses, the failure was successfully back-analysed in 3D using *3DEC*. Displacement contours and vectors produced by the back-analysis model are provided in Figure 6c. The same model was cut down to represent a 2D (plane strain) analysis for a section through the middle of the failure zone. The resulting displacement contours and vectors produced by this 2D model are shown in Figure 6d.

For the 3D back-analysis model shown in Figure 6c, the FoS was approximately 1.0. Using the same inputs, the FoS produced by the 2D analysis shown in Figure 6d was approximately 0.65. This is mainly because the 3D analysis accounts for the requirement for some breakout through the rock mass at the northern end of the failure. For the 2D analysis, based on the adopted section location, slope failure can occur in the model simply due to movement along two structures, without any requirement for lateral release to the north or south of the analysis section. The 2D analysis assumes that the location and orientation of the structures in relation to the pit face is consistent along the slope. This shows that the results of 2D and 3D analyses can differ significantly for the same slope when the same inputs are adopted. This highlights that the properties obtained from back-analyses using one analysis technique may not be applicable to another analysis technique. In this case, the resulting properties obtained from the 2D back-analysis could not be confidently used as inputs for a 3D analysis.

It is likely that different results would also be obtained if the June 2011 failure shown in Figure 5a was to be analysed in both 2D and 3D, because the geometry of wedge failures, which are very common in open pits, is clearly three-dimensional. This is why the most widely-used software for wedge analyses, such as *Swedge* (Rocscience, 2015) provide a 3D representation of the controlling structures.

Distribution of soil and rock mass domains

If soil or rock mass domains with differing strength properties exist along the strike of a slope, it may be impossible for a 2D analysis to provide a reasonable prediction of stability. If the selected section passes through the weaker materials, the resulting FoS may be too conservative, and if the section passes through the stronger materials, the FoS may be non-conservative.

Zettler *et al.* (1999) performed 2D limit equilibrium and numerical analyses, as well as 3D numerical analyses, for a slope consisting of two different materials. These were referred to as 'competent' and 'incompetent' materials. They

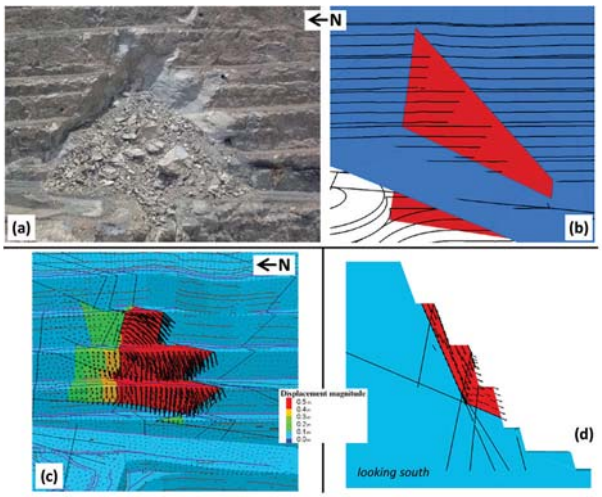

Figure 6—The October 2011 Western Australian gold mine failure. (a) Photograph of failure, (b) surfaces showing main controlling structures in relation to design crests and toes, (c) displacement contours and vectors produced by three-dimensional *3DEC* back analysis model, and (d) displacement contours and vectors produced by cut-down plane strain *3DEC* analysis through the middle of the failure zone

found that the FoS from the 3D analyses was in between the FoS produced by separate 2D analyses using the competent and the incompetent material properties. They concluded that a 3D problem cannot be solved with a 2D analysis. They stated that taking the competent material properties for the whole slope will over-estimate the FoS, while taking the incompetent properties for the entire slope will lead to conservative results.

A clear example of how the distribution of rock mass domains can affect the analysis results is provided here based on numerical analyses performed for the Porgera open pit mine in the Enga Province in the highlands of Papua New Guinea. The mine produces both gold and silver and is operated by Barrick Gold Corporation. The existing pit is approximately 500 m deep. The pit walls encounter materials of variable strength, ranging from relatively weak mudstones to significantly stronger diorites. Prior to 2012, only 2D slope stability analyses had been performed for the mine, including both limit equilibrium and numerical analyses. Since 2012, 3D numerical analyses have also been performed for all parts of the pit.

Some of the 2D analysis sections passed through the southwest corner of the pit. A photograph of the southwest wall is provided in Figure 7a. 2D analyses were performed for these sections using both limit equilibrium and numerical techniques, and all analyses identified the potential for a deep-seated global failure mechanism after final pit excavation. Note that the limit equilibrium safety factors were greater than unity, and failure occurred in the numerical analyses only when the strength properties were reduced below best-estimate values. An example of the mechanism produced by strength reduction analyses using *UDEC* (Itasca, 2011) is provided in Figure 7b, while the adopted rock mass domains for this 2D analysis are shown in Figure 7c. It can be seen that, at this particular section location, global failure is able to occur through the relatively weak brown mudstones and black sediments domains.

Three-dimensional analyses were also performed for the wall using *3DEC*, and the resulting FoS was more than 0.5 higher than that produced by the *UDEC* analyses. A north-south cut through the *3DEC* model around the location of the final pit toe, showing the exposed rock mass domains after final pit excavation, is shown in Figure 7d. The 2D section location is also shown on this figure. The figure shows that stronger materials (diorite and calcareous sediments) exist to the north and south of the 2D section, respectively. These materials are significantly stronger than the brown mudstones and black sediments. The 'bridging' effect provided by these stronger materials results in more favourable 3D modelling results. Because of the 3D distribution of the rock mass domains, the failure mechanism produced by the 2D analyses is highly unlikely. The failure produced by the *UDEC* analyses is greater than 450 m deep. As shown in Figure 7d, this would need to 'squeeze' through a zone of less than 150 m wide if it were to occur in the brown mudstones and black sediments only. The stronger materials on each side of the 2D section have no effect on the results of the 2D analyses, because they are not intersected by this section. In reality, these stronger materials probably have a significant effect on the stability of the slope. The concave geometry of the southwest wall may also have contributed to the improved FoS produced by the 3D analyses.

Conclusions

The results of 2D and 3D analyses for the same slope will often be different for several reasons. The main reason for the differences in results is the ability of 3D analyses to account for the 3D nature of the various model inputs.

Based on a review of the literature and additional analyses performed for this paper, it is shown that slope geometry can have a significant influence on wall stability. A concave slope will be more stable than a straight slope due to the additional support associated with the lateral confinement provided by the concave geometry. Assuming an idealized geometry and isotropic, homogenous soil or rock mass conditions, analyses also indicate that a convex slope will be more stable than a straight slope. However, in reality,

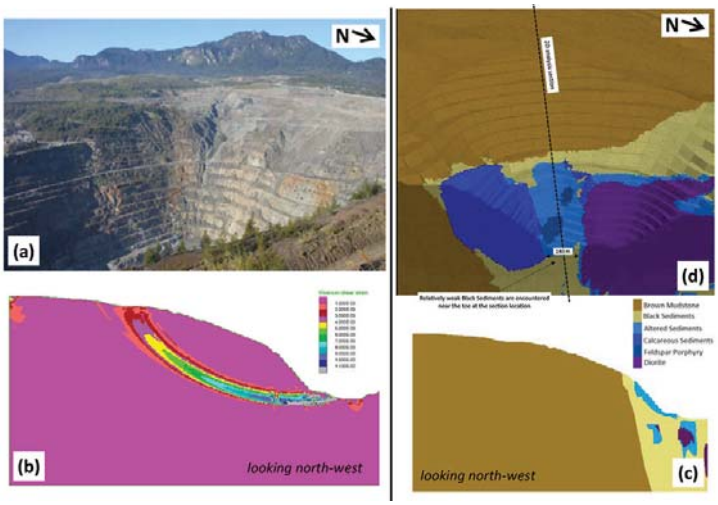

Figure 7—Analysis of the Porgera southwest wall. (a) Photograph of southwest wall, (b) deep-seated failure mechanism produced by *UDEC* strength reduction analyses, (c) rock mass domains in *UDEC* model after final pit excavation, and (d) exposed rock mass domains in *3DEC* model

particularly where potential failures are structurally controlled, convex slopes will often be less stable due to the reduced lateral restraint.

The location and orientation of geological structures in relation to a slope, and the distribution of different rock mass domains along the strike of a slope, are also important factors that can affect analysis results. In particular, in a hard rock environment, where most failure mechanisms are structurally controlled, a true representation of the 3D nature of the structures is often critical in providing realistic stability estimates.

In some cases, for a long, straight slope in basic geological conditions, 2D analyses can provide a reasonable representation of the problem. However, in many cases, the inability of a 2D analysis to represent the true 3D nature of the problem will lead to unrealistic results. In these cases, 3D analysis is required to provide confidence that the potential failure mechanisms can be represented in the model.

Acknowledgements

The author would like to thank the Porgera Joint Venture and Barrick Gold Corporation for permission to present the Porgera case study shown in this paper.

References

Armstrong, R. and Stacey, T.R. 2003. A review of information on the influence of plan curvature on rock slope stability and its effect on the volume of wedge failures. *Proceedings of the 10th International Society for Rock Mechanics Congress – Technology Roadmap for Rock Mechanics*, Johannesburg, South Africa. South African Institute of Mining and Metallurgy, Johannesburg.

Azocar, K. and Hazzard, J. 2015. The Influence of curvature on the stability of rock slopes. *The 13th International ISRM Congress 2015*, Montreal, Quebec, Canada, 10–13 May 2015. In press.

Bromhead, E.N. 2004. Landslide slip surfaces: their origins, behaviour and geometry. *Landslides: Evaluation and Stabilization*. Lacerda, W., Ehrlich, M., Fontoura, S.A.B., and Sayao, A.S.F. (eds.). Taylor & Francis, London.

Cala, M. 2007. Convex and concave slope stability analyses with numerical methods. *Archives of Mining Sciences*, vol. 52, no. 1. pp. 75–89.

Cheng, Y.M., Liu, H.T., Wei, W.B., and Au, S.K. 2005. Location of critical three-dimensional non-spherical failure surface by NURBS functions and ellipsoid with applications to highway slopes. *Computers and Geotechnics*, vol. 32. pp. 387–399.

Dawson, E.M., Roth, W.H. and Drescher, A. 1999. Slope Stability Analysis by strength reduction. *Geotechnique*, vol. 49, no. 6, pp. 83–5840.

Gitirana, G., Santos, M.A., and Fredlund, M.D. 2008. Three-dimensional analysis of the Lodalen Landslide. *GeoCongress 2008*, New Orleans, 9–12 March 2008. Reddy, K.R., Khire, M.V., and Alshawabkeh, A.N. (eds.). American Society of Civil Engineers. pp. 186–190.

Gomez, P., Diaz, M., and Lorig, L. 2002. Stability analysis of waste dumps at Chuquicamata Mine, Chile. *Felsbau Rock Mechanics Journal*, vol. 20, no. 6. pp. 61–689.

Hoek, E. and Bray, J. 1981. Rock Slope Engineering, 3rd edn. Institute of Mining and Metallurgy, London, UK.

Hoek, E., Rippere, K.H., and Stacey, P.F. 2000. Large-scale slope designs – A review of the state of the art. *Slope Stability in Surface Mining*. Hustrulid, W.A., McCarter, M.K., and Van Zyl, D.J.A. (eds.). Society for Mining, Metallurgy and Exploration, Inc., Littleton, CO. pp. 115–124.

Huang, C. and Tsai, C. 2000. New method for 3D and asymmetrical slope stability analysis. *Journal of Geotechnical and Geoenvironmental Engineering*, vol. 126, no. 10. pp. 917–927.

Itasca Consulting Group Inc. 2001. *FLAC* (Fast Lagrangian Analysis of Continua), Version 4.0. Minneapolis, MN.

Itasca Consulting Group Inc. 2011. *UDEC* (Universal Distinct Element Code), Version 5.0. Minneapolis, MN.

Itasca Consulting Group Inc. 2014. *3DEC* (3D Distinct Element Code), Version 5.0. Minneapolis, MN.

Jiang, J.C., Baker, R., and Yamagami, T. 2003. The effect of strength envelope nonlinearity on slope stability computations. *Canadian Geotechnical Journal*, vol. 40. pp. 308–325.

Kayesa, G. 2006. Prediction of slope failure at Letlhakane Mine with the GeoMoS Slope Monitoring System. *Proceedings of the International Symposium on Stability of Rock Slopes in Open Pit Mining and Civil Engineering Situations*, Cape Town, 3–6 April. *Symposium Series* S44. Southern African Institute of Mining and Metallurgy, Johannesburg. pp. 605–622.

Leong, E.C. and Rahardjo, H. 2012. Two and three-dimensional slope stability reanalysis of Bukit Batok slope. *Computers and Geotechnics*, vol. 42. pp. 81–88.

Lorig, L. and Varona, P. 2007. Numerical analysis. *Rock Slope Engineering. Civil and Mining*. 4th Edition. Wyllie, C. and Mah, C.W. (eds.). Spon Press, London and New York. pp. 218-244.

Lutton, R.J. 1970. Rock slope chart from empirical slope data. *Transactions of the Society for Mining, Metallurgy and Exploration and the American Institute of Mining, Metallurgy and Petroleum Engineers*, vol. 247, no. 2. pp. 160–162.

Narendranathan, S., Thomas, R.D.H., and Neilsen, J.M. 2013. The effect of slope curvature in rock mass shear strength derivations for stability modelling of foliated rock masses. *Slope Stability 2013*. Dight, P.M. (ed.). Australian Centre for Geomechanics, Perth.

Nian, T.K., Huang, R.Q., Wan, S.S., and Chen, G.Q. 2012. Three-dimensional strength-reduction finite element analysis of slopes: geometric effects. *Canadian Geotechnical Journal*, vol. 49. pp. 574–588.

Piteau, D.R. and Jennings, J.E. 1970. The effects of plan geometry on the stability of natural slopes in rock in the Kimberley area of South Africa. *Proceedings of the 2nd Congress of the International Society of Rock Mechanics*. Belgrade. vol. 3. Paper 7–4.

Rocscience 2015. Swedge. 3D Surface Wedge Analysis for Slopes. Toronto, Ontario.

Suarez, A.V. and Gonzalez, L.I.A. 2003. 3D slope stability analysis at Boinas East gold mine. FLAC and Numerical Modelling in Geomechanics. *Proceedings of the 3rd International FLAC Symposium*, Sudbury, Canada, 22-24 October 2003. Andrieux, P., Brummer, R., Detournay, C., and Hart, R. (eds.). A.A. Balkema, Rotterdam. pp. 117–123.

Totonchi, A., Askara, F., and Farzaneh, O. 2012. 3D Stability Analysis of concave slope in plan view using linear finite element and lower bound method. *Transactions of Civil Engineering*, vol. 36, no. C2. pp. 181–194.

Wei, W.B., Cheng, Y.M., and Li, L. 2009. Three-dimensional slope failure analysis by the strength reduction and limit equilibrium methods. *Computers and Geotechnics*, vol. 36. pp. 70–80.

Xing, Z. 1988. Three-dimensional stability analysis of concave slopes in plan view. *Journal of Geotechnical Engineering*, vol. 114. pp. 658–671.

Zettler, A.H., Poisel, R., Roth, W., and Preh, A. 1999. Slope stability analysis based on the shear strength reduction technique in 3D. *FLAC and Numerical Modeling in Geomechanics*. Detournay, C. and Hart, R. (eds.). A.A. Balkema, Rotterdam. pp. 11–16.

Zhang, Y., Chen, G., Zheng, L., Li, Y., and Zhuang, X. 2013. Effects of geometries on three-dimensional slope stability. *Canadian Geotechnical Journal*, vol. 50. pp. 233–249. ◆

http://dx.doi.org/10.17159/2411-9717/2016/v116n5a6

Reconciliation of the mining value chain — mine to design as a critical enabler for optimal and safe extraction of the mineral reserve

by M. Bester*, T. Russell*, J. van Heerden*, and R. Carey*

Synopsis

In order to reach the goal of optimal and safe extraction of the mineral reserve, the mining industry is increasingly focusing on reconciliation across the mining value chain to ensure that the mining process occurs in a progressively more predictable manner. This will consequently improve the understanding of mine plans and their associated implementation risks, ultimately leading to increased investor confidence. In terms of geotechnical engineering, mine to design performance assessment is a critical aspect of mine to plan adherence focusing on the complex aspects influencing slope performance. A mine to design reconciliation process therefore needs to systematically track implementation and geotechnical aspects in order to review or update slope design criteria and pit layouts according to the mine planning cycle as the mine is developed. This paper describes the development and implementation of a standardized mine to design reconciliation system for operations utilizing laser scanning technology, analysis tools, as well as associated key performance indicators. Performance is evaluated on final pit boundaries in terms of geometry achieved as well as blast performance evaluation of face conditions. These aspects as well as the resulting catch berm capacity should be captured in an information system, enabling longer term trend analysis and detailed root cause analysis where unsatisfactory outcomes occur. Adverse outcomes should subsequently be incorporated into the mine's risk management process informing risk mitigation measures including blast design adjustments, slope design changes, or rockfall protection measures.

Keywords
mining value chain, mine to design, reconciliation, slope management.

Introduction

In order to reach the goal of optimal and safe extraction of the mineral reserve, the mining industry is increasingly focusing on reconciliation across the mining value chain to ensure that the mining process occurs in a progressively more predictable manner. This will consequently improve the understanding of mine plans and their associated implementation risks, ultimately leading to increased investor confidence. In terms of geotechnical engineering, mine to design performance assessment is a critical aspect of mine to plan adherence focusing on the complex aspects influencing slope performance. A mine to design reconciliation process therefore needs to systematically track implementation and geotechnical aspects in order to review or update slope design criteria and pit layouts according to the mine planning cycle as the mine is developed.

The role of mine to design in mining value chain reconciliation

The mine value chain (MVC)

Most mining operations typically follow a similar process, referred to as the mine value chain (MVC). Figure 1 illustrates the MVC graphically, where the top row represents high-level processes along the value chain and the bottom row represents value.

The realization of value generated along the MVC is directly dependent on accurate planning and the controlled execution of all the different processes supporting the value chain.

An approach to MVC reconciliation

An example of a business operating model is the Business Process Framework (BPF), which essentially consists of three phases, namely planning, work management, and feedback. The feedback phase of BPF includes the measurement of performance to support analysis and improvement. It is therefore critical that the correct key performance indicators are identified and tracked to enable accurate analysis of performance and trends. Timely and correct information facilitates solid decision-making leading to optimized performance.

Table I summarizes MVC reconciliation processes in terms of mine planning/design vs execution. Both the mining and waste dumping processes can be reconciled in terms of spatial compliance to design (x, y, and z position) and temporal compliance to design (time period).

* *Anglo American Kumba Iron Ore, South Africa.*
 ISSN 2225-6253. This paper was first presented at the, International Symposium on Slope Stability in Open Pit Mining and Civil Engineering 2015, *12–14 October 2015, Cape Town Convention Centre, Cape Town.*

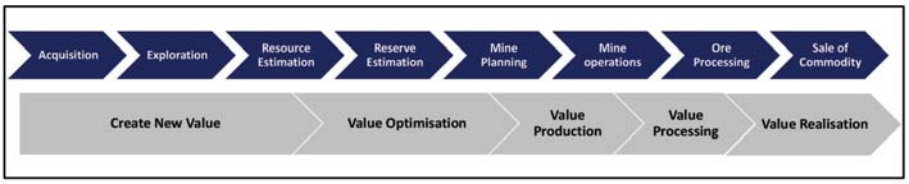

Figure 1—The mine value chain

Table I

Reconciliation processes for mine design / planning *vs* execution

	Mining reconciliation	Mine residue deposit reconciliation
Spatial	Mine to Design • Spatially according to the 12 month plan • Mine to Design accuracy • Ramp to Design accuracy	Mine Residue Deposit to Design
Temporal	Mine to Plan • In sequence to the 12-month plan • Ramp in sequence with plan	Mine Residue Deposit to Plan

Although the successful implementation of the mine plan is equally dependent on adhering to slope design as well as following the planned mining sequence, the reconciliation of mine to design as a critical aspect of slope management will be discussed further.

Development of a mine to design reconciliation process

Effective mitigation of slope failure and rockfall hazards that typify an open pit mine requires final pit slopes to be mined to design in terms of both bench width and overall design angle. Achieving design slope angles and bench widths has proven to be challenging at times, with several factors contributing to unsatisfactory compliance with the slope design and the development of poor-quality faces on final pit boundaries. In order to improve pit wall control and ultimately mine to design performance, a mine to design reconciliation system should be developed to track the performance of the mining production team on a monthly basis. This system can progressively develop into a proactive reporting tool that will measure mine to design during the mining process.

The reconciliation process discussed in this paper utilizes a laser scanning system to scan final pit boundaries that have been exposed over a given period of time. Subsequently, actual toe/crest line positions are extracted from laser scanning data to carry out a spatial analysis of the actual versus design toe/crest line positions. Maptek I-Site Studio software can automatically perform discrete minimum distance measurements between the design and actual toe/crest line positions along the length of the final pit boundary. Analysis of these individual measurements allows for the percentage of the toe/crest lines falling within distance ranges from design to be calculated. This can be compared with predefined criteria, set as key performance indicators (KPIs) for the final pit boundary compliance with design.

Data acquisition

Data acquisition for the mine to design reconciliation process initially involves the identification of final pit boundaries that have been exposed over the time period in question. Reporting on a monthly basis can be used as a starting point.

Subsequently, a plan should be sent to the survey department indicating which areas need to be scanned for the final pit boundary reconciliation in a given month. A practical consideration to enable accurate analysis is that scanning should be done from a working level that ensures line of sight of the toe and crest positions in question.

I-Site 8810 laser scanners were used for data acquisition. The scanning unit is vehicle-mounted and is operated from inside the vehicle via a wi-fi connection using a Toughbook tablet device (Figure 2). All scans can be carried out over a horizontal range of between 0 and 360 degrees with a fixed vertical range of 80 degrees. In terms of distance the scanner has ranges of 500 m, 1000 m, and 1400 m for surfaces with low reflectivity (10–40%), medium reflectivity (40–80%), and high reflectivity (>80%) respectively. In practice, scans are usually done within 200 m of the target surface, with several scans from different scanning positions making up the overall scan image for larger areas. Laser scans are taken in conjunction with a high-resolution panoramic photograph that is tied in with the laser scanning data to provide a photographic image overlay in the analysis software.

Figure 2—Vehicle-mounted laser scanner set-up

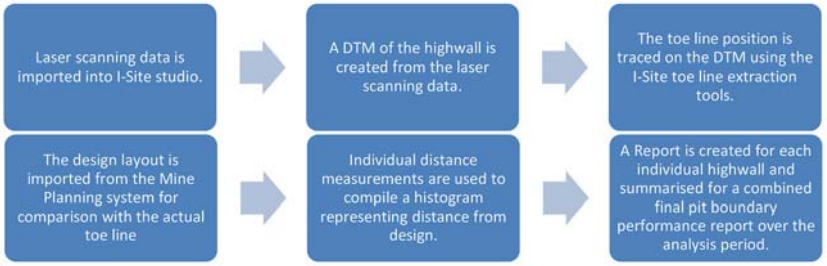

Figure 4—Scan data analysis process

The areas scanned by the mine survey department can then be imported into I-Site Studio software for analysis. An example of raw scan data of a final pit boundary is illustrated in Figure 3. Note that several scan positions are utilized to compile a single composite scan of the highwall. This is necessary for not only georeferencing the scan data, but also to reduce shadows in areas not visible to the scanner at a specific position.

Data analysis

Raw laser scanning data can be processed and analysed following the process outlined in Figure 4.

I-Site Studio software utilizes various filtering functions to process the raw scan data to allow for conversion into a digital terrain model. From the digital terrain model the toe line position can be traced using a combination of a visual assessment of the DTM surface and the in-built I-Site Studio toe/crest line assessment functions (Figure 5). Essentially, toe and crest lines can be automatically extracted using the maximum angle of curvature between the horizontal surface of the bench and the slope of the highwall.

For comparison of design to actual toe/crest line positions, the design toe/crest lines need to be imported and overlain on the trace representing the actual toe/crest line. For toe/crest line analysis, final limit block designs from the mine's planning system can be imported into I-Site Studio. Alternatively, the design pit layout can be imported and overlain over the actual toe/crest line positions.

The design *versus* actual positions can be compared using the 'Colour by Distance from Object' function in I-Site Studio. The function essentially applies a colour scheme to the extent of one surface or line based on the distance from a second 'base' object. In the case of toe line analysis the design toe line represents the base object to the actual toe line. Distance measurements are taken at discrete points along the toe line (0.2 m intervals are currently used as standard) where the absolute distance to the closest point in 3D space to the base object is measured. A colour scheme is set up to colour the actual toe line (or crest line) according to the criteria set to measure mine to design performance. For illustrative purposes, portions of a toe line falling within 3 m of design are indicated in green, portions within 4 m of design are indicated in yellow, and areas falling outside of 4 m are coloured red. Figure 6 illustrates an example of a plan view of the actual achieved pit boundary overlain on short-term planning block designs coloured according to the abovementioned criteria.

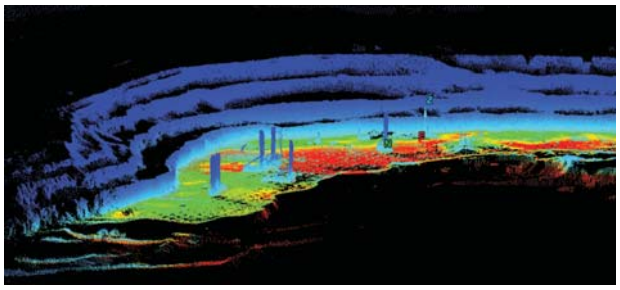

Figure 3—Raw laser scanning data

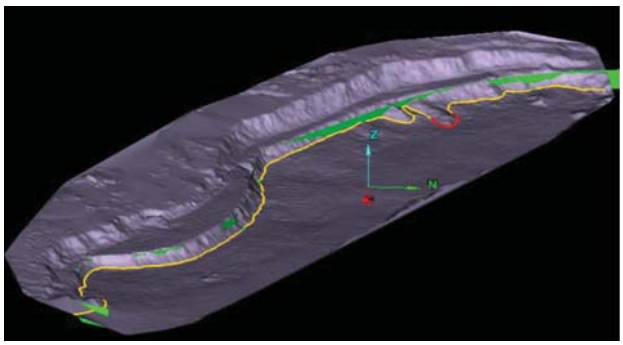

Figure 5—Example of a toe line position traced on final pit boundary DTM

Figure 6—Example of a plan view showing actual toe line overlain on planned block design

The 'Colour By Distance From Object' function in I-Site Studio allows for raw measurement data to be exported as CSV values providing the coordinates and distance measurement at each individual point along the toe line. The exported distance values are then imported into Microsoft Excel, where the following is done for reporting purposes:

- A cumulative histogram is utilized to represent the distribution of distance measurements between design and actual toe line positions (Figure 7)
- A histogram showing deviation from design elevation is produced by comparing the actual Z-elevation of each analysis point with the design elevation of the level being analysed
- Percentages of the actual toe line falling within each of the predefined limits are calculated and reported.

Following the same process, a crest line analysis can be performed to assess crest positions according to set criteria.

Each section of highwall exposed during the analysis period is assessed separately; however, data can also be combined to run an overall assessment of mine to design performance per area of responsibility or separate pits for the period under assessment. This allows for broader trends in mine to design performance to be assessed over a given period of time (Figure 8). These reporting functions can be automated utilizing current survey software applications.

Key performance indicator (KPIs)

In order to measure performance regarding final pit boundary compliance, it is essential to select KPIs that take into account industry best practice as well as practical considerations. For the purpose of explaining the process and based on acceptable results achieved (refer to Figure 9), final pit boundary compliance was measured according to the percentage of final boundary length toe positions within 3 m of design. The initial target was set at 80%.

Subsequent to implementing a mine to design reconciliation process and allowing a sufficient period of data capture, trend analysis and reporting, KPIs will need to be further developed for each individual mine taking into account practical considerations and area-specific rock mass constraints. This will typically include toe and crest performance per rock mass type as well as actual catch berm capacity.

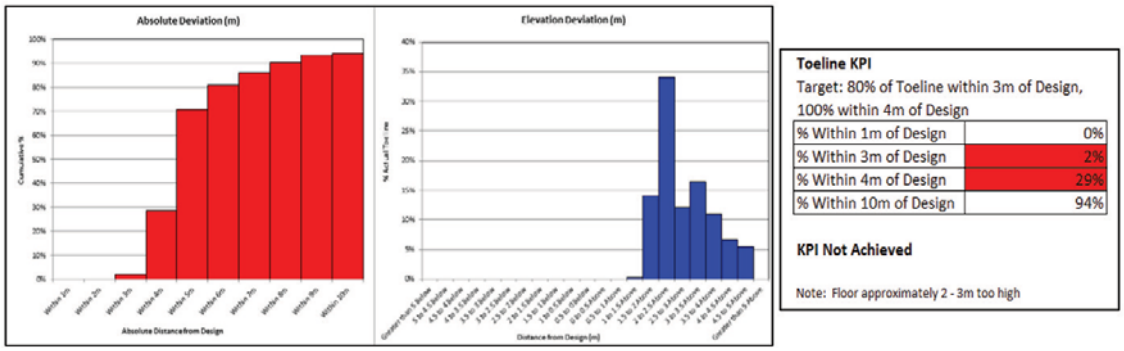

Figure 7—Example graphics showing compliance with design by percentage of linear distance

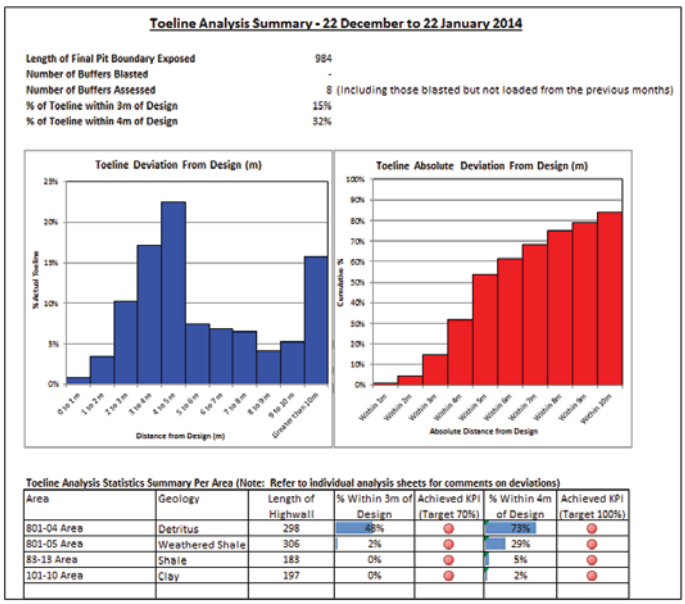

Figure 8—Example (not actual values) of a summary report of overall mine to design performance over a specific time period

Figure 9—Example of good results achieved in calcrete

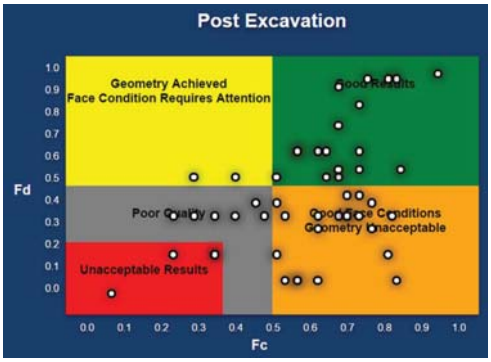

Figure 10—Example of final pit boundary block analyses in an information system

Final pit boundary performance evaluation

According to Read and Stacey (2009), several systems are available to evaluate bench design achievement. A general matrix system evaluating geometry and face conditions is discussed here.

Evaluation of geometry and catch berm capacity

The following weighted components can be evaluated based on actual geometric data obtained from laser scanners and the reporting process described above:

- Bench face angle
- Bench width
- Toe position.

Positive results according to these components ensure slope design is achieved, ultimately leading to the realization of committed value.

Evaluation of face conditions and blast performance

The following weighted components for face conditions can be evaluated by geotechnical engineers on final pit boundaries and are indicative of blast performance:

- Half barrels visible
- Intact rock breakage
- Open joints
- Loose material on face
- Face profile
- Crest conditions.

Good performance in terms of blasting in conjunction with achieving design slope geometry results in effective catch berm capacity, which is critical in successful rockfall risk management.

Data capture in an information system

As discussed earlier, the feedback phase of the Business Process Framework (a business operating model) includes the measurement of performance to support analysis and facilitate improvement. Information management systems play a key role in supporting decision-making in the slope design process through the conversion of data into information, empowering specialists with knowledge to make informed decisions, ultimately enabling improvement. It is therefore critical to implement a fit-for-purpose information system where all related data is stored. All final pit boundary blocks evaluated by geotechnical engineers according to the abovementioned parameters should be captured in a central system or database (Figure 10) that allows for the upload of photographs and any other relevant data per block.

Conclusion

The paper discussed the development of a standardized mine to design reconciliation system utilizing laser scanning technology, analysis tools, as well as associated key performance indicators. Performance is evaluated on final pit boundaries in terms of geometry achieved as well as blast performance evaluation of face conditions. These aspects, as well as the resulting catch berm capacity achieved, should be captured in an information system enabling longer term trend analysis as well as detailed root cause analysis where unsatisfactory outcomes occurred. Adverse outcomes should subsequently be incorporated into the risk management process, informing risk mitigation measures including blast design adjustments, slope design changes, or rockfall protection measures.

Acknowledgement

Our thanks to Anglo American Kumba Iron Ore for the opportunity to present this paper.

References

Dunne, A. and Laurens, P. Not dated. Obstacles in a mining operation and value chain. Department of Geology, University of the Free State.

Maptek (Pty) Ltd. 2013. Maptek I-Site 8810 Operator Manual.

Read, J, and Stacey, P. 2009. Guidelines for Open Pit Slope Design. CSIRO, Clayton, Victoria, Australia. 313 pp.

Van Heerden, J. 2014. Kumba Iron Ore technical requirement document for value chain reconciliation. Anglo American Corporation, South Africa.

Vorster, A. 2001. Planning for value in the mining value chain. *Journal of the South African Institute of Mining and Metallurgy*, vol. 100, no. 9. pp. 61–65. ◆

Photographs courtesy of
Jason Pieterse and Chris Pistorius

SCHOOL
PRODUCTION of CLEAN STEEL

25–26 July 2016

Mintek, Johannesburg

Register 4 delegates and get the fifth registration free

POSTER COMPETITION!
Abstract Submission Deadline **1 June 2016**
Prize: An overseas trip to work with Prof. Pistorius at CMU in Pittsburgh

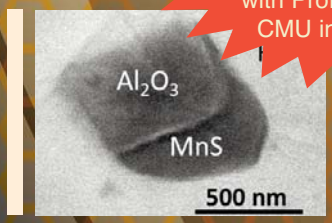

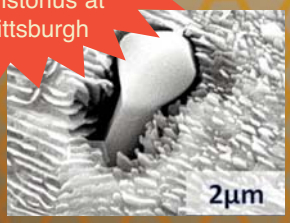

Announcement

LECTURER

Prof. C Pistorius

Chris Pistorius is the POSCO Professor of Iron and Steelmaking in the Department of Materials Science and Engineering at Carnegie Mellon University (Pittsburgh, PA, USA), where he has been since 2008. Previously he was Professor and Head of Department of Materials Science and Metallurgical Engineering at the University of Pretoria. He holds Bachelor's and Master's degrees in Metallurgical Engineering from the University of Pretoria, and a PhD from the University of Cambridge, United Kingdom. His current research interests include the fundamentals of ironmaking and steelmaking reactions, and electrochemistry of corrosion and metals production.

WHO SHOULD ATTEND

The school is aimed at delegates from steel producing companies in South Africa or those who support them, and includes:

- Senior management
- First line management
- Process/development engineers
- Researchers
- Middle management
- Plant/production engineers
- Design engineers

EXHIBITION/SPONSORSHIP

Sponsorship opportunities are available. Companies wishing to sponsor or exhibit should contact the Conference Co-ordinator.

SAIMM
THE SOUTHERN AFRICAN INSTITUTE OF MINING AND METALLURGY

For further information contact:
Conference Co-ordinator, Camielah Jardine
SAIMM, P O Box 61127, Marshalltown 2107
Tel: (011) 834-1273/7 • Fax: (011) 833-8156 or (011) 838-5923
E-mail: camielah@saimm.co.za • Website: http://www.saimm.co.za

INTRODUCTION

South Africa has a proud history in the production of both mild steel and stainless steel with production facilities in Gauteng, Kwazulu-Natal, Mpumalanga, the Eastern and Western Cape provinces. At these facilities steel is produced from scrap or from ore via ironmaking facilities.

The Center for Iron and Steelmaking Research at Carnegie Mellon University in Pittsburgh, Pennsylvania, USA has a proud history on iron and steelmaking. Collaboration between CMU and the South African iron and steel industry includes a school on steelmaking presented by Prof. Richard Fruehan in Vanderbijlpark in 1996.
At Clean Steel 2016 Prof. Chris Pistorius will continue the collaboration by addressing the following topics:

CONTROLLING DISSOLVED ELEMENTS

1. What is clean steel?
2. Relevant process conditions in blast furnace, steelmaking converter, electric arc furnace, ladle furnace and caster (temperatures, oxygen activity, slag basicity, stirring).
3. Control of dissolved elements (C, H, N, O, P, S, Cu, Sn):
   a. Sources (raw materials; environment)
   b. Thermodynamic and kinetic principles of control
   c. Practical control methods:
      i. hot metal desulfurization and dephosphorization
      ii. metal-slag reactions in blast furnace, steelmaking and ladle
      iii. clean tapping
      iv. metal-gas reactions, including nitrogen pick-up
      v. deoxidation
      vi. role of slag
      vii. mitigating the surface quality effects of Cu & Sn.

CONTROLLING MICRO-INCLUSIONS

1. Principles of control:
   a. inclusion composition evolution over time
   b. removing inclusions to slag or fluxes: gas stirring and flotation kinetics
   c. inclusion-metal-slag reactions: equilibria and kinetics (spinel formation)
   d. calcium modification.
2. Sources of micro-inclusions:
   a. deoxidation and reoxidation products
   b. ladle glaze
   c. inclusions in ferro-alloys and ferro-alloy reaction products
   d. mold flux entrainment
   e. reoxidation.
3. Assessing micro-inclusions:
   a. overall steel composition
   b. caster behavior
   c. microanalysis (polished sections; extracted inclusions)
   d. other analytical approaches.
4. Summary: general guidelines for clean-steel practice; opportunities to learn more and share information.

Sponsors:

ALS ADVANCED LABORATORY SOLUTIONS

South African Iron and Steel Institute

http://dx.doi.org/10.17159/2411-9717/2016/v116n5a7

A modified model to calculate the size of the crushed zone around a blast-hole

by W. Lu*, Z. Leng*, M. Chen*, P. Yan*, and Y. Hu*

Synopsis

After detonation of the explosive, the final blast-induced damage area around the blast-hole falls into three categories, namely crushed zone, fractured zone, and elastic deformation zone. This paper presents a modified model to calculate the size of crushed zone around a blast-hole in drill-and-blast, with the hoop compressive stress and cavity expansion effect taken into account. The material in the crushed zone was assumed to be a granular medium without cohesion, but with internal friction. On this basis, the formula for crushing zone radius was derived. The proposed approach was verified with tests reported in the literature and the simulated results from SPH-FEM coupled models. A full statistical analysis was also carried out, and the predicted values were found to be in better agreement with the test results compared with other models. A sensitivity analysis of the modified model showed that the size of the blast-induced damage area is mainly affected by the following factors: rock mass properties, *in situ* stress, and borehole pressure. In particular, the roles of borehole pressure and *in situ* stress are discussed. Finally, suggestions are made on how the size of the crushing zones can be decreased.

Keywords

drill and blast, crushed zone, modified model, hoop compressive stress, cavity expansion.

Introduction

Over the past decades, drill-and-blast has become the most commonly used technology in rock excavation. It is well known that in rock mass fragmentation with explosives, the annular rocks around the blast-hole are converted into fines. The formation of these fines consumes a significant part of the energy of the detonation, which in general is ignored in the determination of the efficiency of detonation (Glatolenkov and Ivanov, 1992; Furtney *et al.*, 2012). Many studies show that only 20–30% of the total explosive energy is effectively used in fragmenting the rock, and up to 50% of the energy generated by conventional charges is wasted in overcrushing of the crushed zone and the inner part of the fractured zone (Ouchterlony *et al.*, 2004; Sanchidrian *et al.*, 2007). How to control the crushed zone to enhance the effective utilization of explosive energy, reducing the unit explosive consumption and the engineering cost, is therefore of great significance.

One of the most important problems in the breakage of rock masses is to establish a calculation model of the crushed zone around a blast-hole. The actual process of fragmentation around the blast-hole in drilling and blasting is so complex that an exact mathematical description is almost impossible. Over the years, many scholars and engineers have researched this problem (Wang, 2005; Jimeno *et al.*,1995; Ouchterlony and Moser, 2012; Qian, 2009), and several models have been proposed for the estimation of the extent of crushed zones around a blast-hole. Table I lists the existing models for prediction of the size of crushed zone. There are notable discrepancies among these calculation models. In the model proposed by Il'yushin (1971), the material in the crushed zone is assumed to be incompressible granular medium with cohesion. However, Il'yushin's formula is applied to limestone, talc-chlorite, and concrete, and Vovk *et al.* (1973) noted that Il'yushin appeared to overestimate the size of crushed zone. On the other hand, in Il'yushin's formula derivation process, the gas adiabatic index in the process of blasting cavity expansion was taken as a constant, so the formula is not applicable to conditions of large decoupling ratios. Szuladzinski (1993) modelled the crushing and cracking around the blast-hole using transient dynamic analysis. In that model, the rocks around the blast-hole are regarded as elastic materials and the effective energy of the explosive is assumed to be roughly two-thirds that of the complete reaction, which gives no consideration to the effect of decoupling. Djordjevic (1999) developed the two-component model (TCM), with overlapping fine-coarse component distributions. Based on the Griffith failure criterion, this model is applicable only to brittle rocks.

* *Wuhan University, Wuhan, China.*

 ISSN 2225-6253. Paper received Oct. 2014; revised paper received Sep. 2015.

Table I

List of the existing models for prediction of the size of crushed zoneTable 1 List of the existing models for prediction of the size of crushed zone

Renders	Formulas	Parameter specification
Il'yushin (1971)	$\begin{cases} b_m = r_0\left(\dfrac{P_b}{-k/f+[[\sigma_c]+k/f]L^{2f/(1+f)}}\right)^{1/2\gamma}\sqrt{L} \\ L=\dfrac{E/(1+v)}{[\sigma_c]\left[1+\ln([\sigma_c]/T)\right]} \end{cases}$	b_m is the crushed zone radius (mm); r_0 is the borehole radius (mm); P_b is borehole pressure (Pa); γ is adiabatic expansion constant; k is cohesion (Pa); f is coefficient of internal friction; $[\sigma_c]$ is unconfined compressive strength (Pa): ; $[\sigma_t]$ is unconfined tensile strength (Pa); E is Young's modulus (Pa); v is Poisson's ratio; ρ_0 is the explosive density (g/mm^3); P_d is the detonation pressure (Pa); Q_{ef} is the effective energy of the explosive (Nmm/g); σ_{cd} is the confined dynamic compressive strength (Pa); K is the rock stiffness (Pa).
Szuladzinski (1993)	$b_m = r_0\sqrt{\dfrac{2\rho_0 Q_{ef}}{\sigma_{cd}}}$	
Djordjevic (1999)	$b_m = \dfrac{r_0}{\sqrt{24[\sigma_t]/P_b}}$	
Kanchibotla (1999)	$b_m = r_0\sqrt{\dfrac{P_d}{[\sigma_c]}}$	
Esen (2003)	$\begin{cases} b_m = 0.812 r_0 (CZI)^{0.219} \\ CZI = \dfrac{(P_b)^3}{K\times[\sigma_c]^2} \end{cases}$	

Kanchibotla *et al.* (1999) proposed an empirical model to determine the volume of fine material contributing to the run-of-mine blast fragmentation. Esen *et al.* (2003) reviewed different ways of calculating the size of crushed zone, introduced a dimensionless parameter called the crushing zone index (CZI), and developed their own formula particularly for smaller diameter holes and lower strength rock. Hagan and Gibson (1988) indicated that the borehole pressure will drop due to expansion of the blast-hole. The aforementioned models, except that of Il'yushin, do not consider the effect of cavity expansion on decreasing the borehole pressure. These previously proposed models have revealed some disadvantages related to the assumptions and the method used, and they cannot be applied to all types of rock masses and all charge structures. In particular, these models do not consider the effect of compressive hoop stress in the inner part of the fractured zone, as well as the *in situ* stress and the cavity expansion effect, which is of great important in the rock mass fragmentation process.

To explore the breakage mechanism of rocks around the blast-hole and to accurately predict the size of the crushed zone in drilling and blasting, a modified model for the size of the crushed zone is presented. The four-region model was established with hoop compressive stress in the inner part of fractured zone and cavity expansion effect taken into account. The material in the crushed zone is assumed to be a granular medium without cohesion, but with internal friction. The proposed approach was verified with tests reported in the literature and the simulated results from SPH-FEM coupled models. Also, the modified model is compared with a selection of existing models.

Distribution of rock fragmentation and assumptions for the modified model

Upon detonation of the explosive, the blast-hole wall is impacted by violent explosive shock waves, stress waves, and seismic waves successively, and the continuity of the rock medium changes, presenting different states of breakage and damage. The annular rock around the blast-hole will be crushed to a fine size. According to the degree of damage, the rock around the blast-hole wall can be divided into damage zones, the definition of which varies among scholars (Ghosh,1990). In previously proposed models, the final blast-induced damage area is usually divided into three categories, namely the crushed zone, radial crack zone, and elastic deformation zone (as shown in Figure 1).

The existing models hold that the region between the crushed zone and elastic deformation zone is completely destroyed by the radial cracking, as shown in Figure 1a. In order to simplify the physical process, in those models, the rock between the crushed zone and elastic deformation zone can only transmit the radial stress, and cannot support any hoop stress, which means $\sigma_\theta = 0$. However, in the actual breakage process, since the fractured zone is a constraint that connects the crushed zone and the elastic zone, it cannot be completely destroyed by radial cracks. Meanwhile, the extent of damage of the rock medium in the inner part of fractured zone will be increased due to the hoop compressive stress. Regardless of hoop compressive stress, the calculated zone of damage will be larger than the actual.

The rock in the inner part of the fractured zone, which is subject to high radial compressive stress, is restrained by the surrounding rock due to the Poisson's effect. Therefore, it is essential to take the hoop compressive stress into account in this zone when establishing the calculation model. The fractured zone is therefore divided into two parts in this four-region model: the inner part (fractured zone I) and the outer part (fractured zone II), as shown in Figure 1b. In fractured zone I, the material is subject to plastic failure, and the hoop compressive stress is not zero, while in fractured zone II there is no hoop stress as a consequence of the damage caused by radial cracks. The four-region model is established with $\sigma_\theta \neq 0$ in fractured zone I. The material in the crushed zone is assumed to be an incompressible granular medium without cohesion, and there is still internal friction among particles.

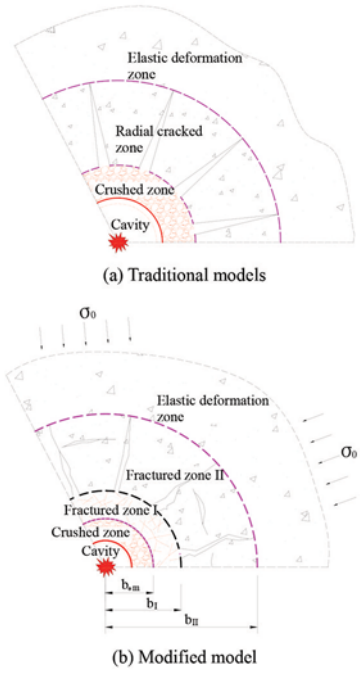

Figure 1—Schematic of the damage zones surrounding a blast-hole in traditional models and the modified model

As a result, the modified model in this paper can better reflect the actual breakage mechanism of rocks around the blast-hole.

In this four-region model, the boundaries of the drilling and blasting damage zones are determined as follows:

(1) The crushed zone $a(t) \le r \le b^*(t)$
(2) The fractured zone I $b^*(t) \le r \le b_I(t)$
(3) The fractured zone II $b_I(t) \le r \le b_{II}(t)$
(4) The elastic deformation zone $b_{II}(t) \le r \le \infty$

where $a(t)$ is the radius of the expanding cavity (mm), $b^*(t)$ is the radius of crushed zone (mm), $b_I(t)$ is the radius of fractured zone I (mm), and $b_{II}(t)$ is the radius of fractured zone II (mm).

Supposing that there is a cylindrical cavity charged with explosives in a homogeneous and isotropic rock mass. An impulsive load will be loaded on the cavity wall when the explosives are detonated. In order to simplify the problem, some assumptions are made. The cylindrical cavity extends infinitely along the axis. Thus, the problem for cylindrical charge blasting can be simplified into an axial symmetric problem and a plane strain problem. The expansion of the detonation gas is adiabatic, and the volume of the detonation gas that infiltrates the rock cracks can be ignored.

Formula derivation

The elastic deformation zone

Using a cylindrical coordinate system to describe the problem, the stress distribution in the elastic deformation zone can be written as

$$\begin{cases} \sigma_r = \sigma_0[1-(\frac{b_{II}}{r})^2]+\sigma_{r=b_{II}}(\frac{b_{II}}{r})^2 \\ \sigma_\theta = \sigma_0[1+(\frac{b_{II}}{r})^2]-\sigma_{r=b_{II}}(\frac{b_{II}}{r})^2 \end{cases} \quad [1]$$

where stresses are assumed to be positive in compression, $\sigma_{r=b_{II}}$ is the radial stress acting on the boundaries with the fractured zone II and with the elastic deformation zone, and σ_0 is the *in situ* stress in rock masses (Pa).

At the interface of the fractured zone II and the elastic deformation zone, the hoop stress reaches the tensile strength of the rock, which is $\sigma_\theta=-[\sigma_t]$, thus $\sigma_{r=b_{II}} = [\sigma_t]+2\sigma_0$ according to Equation [1].

The radial displacement in the elastic deformation zone is

$$u = \frac{1+\nu}{E}\frac{b_{II}^{\ 2}}{r}([\sigma_t]+\sigma_0) \quad [2]$$

where E is Young's modulus (Pa), and ν is Poisson's ratio.

Fractured zone II

The material in fractured zone II is destroyed by radial cracks; as a result, it cannot support any hoop stress. However, the materials in the radial direction of fractured zone II are still elastic, similar to radial column bars, which can only pass the radial stress from fractured zone I to the elastic deformation zone. So in fractured zone II the condition $\sigma_\theta = 0$ applies, then in axial symmetry, in a cylindrical system of coordinates (r, θ), the equilibrium equation reduces to:

$$\frac{d\sigma_r}{dr}+\frac{\sigma_r}{r}=0 \quad [3]$$

On the outer boundary of fractured zone II, $\sigma_r = [\sigma_t]+2\sigma_0$, and on the inter boundary $\sigma_r =[\sigma_c]$, where $[\sigma_c]$ is the unconfined compressive strength (Pa).

Integrating the two, the radial stress distribution in the fractured zone II is found to be

$$\sigma_r = \frac{([\sigma_t]+2\sigma_0)b_{II}}{r} = \frac{[\sigma_c]b_I}{r} \quad [4]$$

According to Equation [2] the displacement in the outer boundary of fractured zone II (when $r= b_{II}$) is

$$u_0(t) = \frac{1+\nu}{E}b_{II}([\sigma_t]+\sigma_0) \quad [5]$$

The displacement in the interboundary of the fractured zone II (when $r= b_I$) is

$$u_{b_I}(t) = \frac{1+\nu}{E}b_I[\sigma_c]\left(\frac{[\sigma_t]+2\sigma_0}{[\sigma_t]+\sigma_0}-(1-\nu)\ln\frac{[\sigma_t]+2\sigma_0}{[\sigma_c]}\right) \quad [6]$$

Fractured zone I

The material in fractured zone I is subject to plastic failure, which results in a large number of cracks, leading to the expansion of the volume of the medium. It is therefore necessary to consider the rock dilatancy effect in this region. In fractured zone I, according to the plastic increment constitutive theory:

$$\begin{cases} \varepsilon_r = \varepsilon_r^{\ e}+\varepsilon_r^{\ p} \\ \varepsilon_\theta = \varepsilon_\theta^{\ e}+\varepsilon_\theta^{\ p} \end{cases} \quad [7]$$

where ε_r is total radial strain, ε_θ is total tangential strain, $\varepsilon_r^{\ p}$ is radial plastic strain, $\varepsilon_r^{\ e}$ is radial elastic strain, $\varepsilon_\theta^{\ p}$ is tangential plastic strain, and $\varepsilon_\theta^{\ e}$ is tangential elastic strain.

The non-associated flow rule is used to describe the dilatancy characteristics of rock in fractured zone I.

$$h\varepsilon_r^{\ p}+\varepsilon_\theta^{\ p}=0 \quad [8]$$

where h is the dilatancy ratio of the rock mass in fractured zone I. The dilatancy ratio describes rock's propensity to expand in volume after failure, and it is used mainly to control the compensation space in blasting. The dilatancy ratio of soft rock generally is 1.20–1.30, for medium hard rock 1.30 1.50, and for hard rock 1.50 2.50.

Substituting Equation [7] with Equation [8], so that

$$h\varepsilon_r+\varepsilon_\theta=(h-1)\varepsilon_r^{\ e} \quad [9]$$

that is

$$h\frac{du}{dr}+\frac{u}{r}=(1-h)\frac{1-\nu^2}{E}[\sigma_c] \quad [10]$$

whence the displacement in the fractured zone I is given by:

$$u(t) = \frac{1+\nu}{E}[\sigma_c][\frac{(1-h)(1-\nu)}{1+h}r+b_I^{\,1+1/h}Lr^{-1/h}] \quad [11]$$

In order to describe the derivation process as simply as possible, let

$$L = \frac{[\sigma_t]+2\sigma_0}{[\sigma_t]+\sigma_0}-\frac{1-h}{1+h}(1-\nu)-(1-\nu)\ln\frac{[\sigma_t]+2\sigma_0}{[\sigma_c]} \quad [12]$$

In fractured zone I, a strength condition is fulfilled, taken in this work in the form of the Mohr-Coulomb condition

$$\sigma_r = \frac{1+\sin\phi}{1-\sin\phi}\sigma_\theta + [\sigma_c] \quad [13]$$

where ϕ is the angle of internal friction.

Substituting Equation [13] with the equilibrium Equation [14]:

$$\frac{d\sigma_r}{dr} + \frac{\sigma_r - \sigma_\theta}{r} = 0 \quad [14]$$

then the radial stress in the fractured zone I:

$$\sigma_r = \frac{1+\sin\phi}{2\sin\phi}[\sigma_c]\left(\frac{b_I}{r}\right)^{\frac{2\sin\phi}{1+\sin\phi}} - \frac{1-\sin\phi}{2\sin\phi}[\sigma_c] \quad [15]$$

The crushed zone

After the detonation of the charge, the blast-hole is filled with gaseous detonation products at a very high temperature. A thin zone is formed around the blast-hole in which the rock mass has been extensively broken and crushed by high pressure (compressive and shear stress) that is exerted immediately on the blast-hole wall. The fine crushed material cannot support any shear in the absence of pressure, thus the cohesive strength is taken to be zero. The material in the crushed zone is assumed to be an incompressible granular medium without cohesion, and there is still internal friction among particles. A Mohr-Coulomb type model without cohesive strength is employed to define the material behaviour

$$\frac{1}{2}(\sigma_\theta - \sigma_r) = -\frac{1}{2}(\sigma_r + \sigma_\theta)\sin\phi \quad [16]$$

In the outer boundary of the crushed zone $\sigma_r = \sigma_s$, where, σ_s is compressive strength of the rock under multiaxial stress (Pa) (Rakishev and Rakisheva, 2011):

$$\sigma_s = [\sigma_c]\left(\frac{\rho_m C_p^{\,2}}{[\sigma_c]}\right)^{\frac{1}{4}} \quad [17]$$

where ρ_m is the density of rock (g/mm^3) and C_p is the velocity of elastic longitudinal waves in the rock mass (m/s).

Substituting Equation [16] with the equilibrium differential (Equation [14] and integrating yields

$$\sigma_r = \sigma_s\left(\frac{b_*}{r}\right)^{\frac{2\sin\phi}{1+\sin\phi}} \quad [18]$$

Due to the continuity requirement, the radial stress acting on the boundary must be the same on both sides. From Equation [14] and Equation [18] it is apparent that $b_I = \xi b_*$, meeting the conditions

$$\xi^{\frac{2\sin\phi}{1+\sin\phi}} = \frac{2\sigma_s\sin\phi + [\sigma_c](1-\sin\phi)}{[\sigma_c](1+\sin\phi)} \quad [19]$$

The incompressible condition is fulfilled in the crushed zone:

$$\frac{du}{dr} + \frac{u}{r} = 0 \quad [20]$$

and integrating yields the radial displacement in the crushed zone:

$$u(t) = \left(\xi^{1+1/h}L + \frac{1-h}{1+h}\right)\frac{1+\nu}{E}[\sigma_c]b_*^{\,2}r^{-1} \quad [21]$$

Differentiating u(t) with respect to $b^*(t)$ yields

$$\frac{\partial u}{\partial b_*} = 2\left(\xi^{1+1/h}L + \frac{1-h}{1+h}\right)\frac{1+\nu}{E}[\sigma_c]\frac{b_*}{r} \quad [22]$$

On the condition that $\left|\frac{\partial u}{\partial r}\right| << 1$, the following approximate relationship holds:

$$v(r) = \frac{du}{dt} \approx \frac{\partial u}{\partial t} = \left(\frac{\partial u}{\partial b_*}\right)\frac{db_*}{dt} \quad [23]$$

where $v(r)$ is the velocity of particle in crushed zone (m/s).

On the expansion cavity wall ($r = a(t)$), the following equation holds:

$$ada = 2\frac{1+\nu}{E}\left(\xi^{1+1/h}L + \frac{1-h}{1+h}\right)[\sigma_c]b_*db_* \quad [24]$$

At initial time $t = 0$ the crushed zone begins generating at the cavity wall, hence $a = b^* = r_b$.

Integrating yields

$$a_m^{\,2} = 2\frac{1+\nu}{E}\left(\xi^{1+1/h}L + \frac{1-h}{1+h}\right)[\sigma_c]b_{*m}^{\,2} + \left\{1 - 2\frac{1+\nu}{E}\left(\xi^{1+1/h}L + \frac{1-h}{1+h}\right)[\sigma_c]\right\}r_b^2 \quad [25]$$

where b_{*m} is the final radius of the crushed zone (mm) and a_m is the maximum cavity radius (mm).

Letting

$$K = 2\frac{1+\nu}{E}\left(\xi^{1+1/h}L + \frac{1-h}{1+h}\right)[\sigma_c] \quad [26]$$

Equation [25] can be simplified to

$$\frac{b_{*m}}{a_m} = \sqrt{1/K + (1-1/K)\left(\frac{a_m}{r_b}\right)^{-2}} \quad [27]$$

Initially, the cavity is filled with gases with pressure P_b as a result of the explosion. There will be an increase in the blast-hole radius with an accompanying increase in the blast-hole volume and a drop in gas pressure. Gas pressure in the process of gas expansion in the explosion cavity can be calculated from the modified two-stages Jones-Miller adiabatic equation (Henrych, 1979) in the following form:

$$P_m = \begin{cases} P_b\left(\frac{a_m}{r_b}\right)^{-2\gamma_1} & (a_m \le r_k) \\ P_b\left(\frac{a_m}{r_b}\right)^{-2\gamma_2}\left(\frac{r_b}{r_k}\right)^{2(\gamma_1-\gamma_2)} & (a_m > r_k) \end{cases} \quad [28]$$

where P_b is the initial borehole pressure before expansion of the explosive (Pa), which is determined by the type of explosive and charge structure; P_m is the pressure at maximum cavity (Pa); the adiabatic isentropic exponents in two stages are γ_1=3 and γ_2=1.27, respectively; P_k is the critical pressure of explosion gases; and r_k is the critical radius of explosion cavity corresponding to P_k, P_k, $r_k = r_b\left(\frac{P_b}{P_k}\right)^{\frac{1}{2\gamma_1}}$.

According to the Chapman-Jouguet model for the detonation wave of condensed explosive, for a coupled charge, the initial explosion pressure P_b which denotes the gas pressure applied to the blast-hole wall is expressed by the widely known equation (Hustrulid 1999):

$$P_b = \frac{\rho_0 D^2}{2(\gamma_1 + 1)} \quad [29]$$

For a decoupled charge, if the decoupling coefficient is small, the initial explosion pressure P_b involved is:

$$P_b = \frac{\rho_0 D^2}{2(\gamma_1 + 1)} \left(\frac{r_e}{r_b}\right)^{2\gamma_1} \quad [30]$$

where ρ_0 is the explosive density (g/mm³), r_e is the charge radius (mm), and r_b is the blast-hole radius (mm).

If the decoupling coefficient is large, the explosion pressure decreases from > P_k above it to < P_k, where P_k is the critical gas pressure. In the calculation, the value of γ_1 is 3.0 when $P \geq P_k$, while γ_2 is 1.27 when $P < P_k$. So Equation [30] is rearranged to yield the following expression for the explosion pressure:

$$P_b = \left[\frac{\rho_0 D^2}{2(\gamma_1 + 1)}\right]^{\frac{\gamma_2}{\gamma_1}} P_k^{\frac{\gamma_1 - \gamma_2}{\gamma_1}} \left(\frac{r_e}{r_b}\right)^{2\gamma_2} \quad [31]$$

The critical pressure of explosion gases P_k is given by following equation (Henrych 1979):

$$P_k = \rho_0 D^2 (\gamma_1 + 1)^{\frac{\gamma_1 + 1}{\gamma_1 - 1}} \left\{\frac{\gamma_2 - 1}{\gamma_1}\left[\frac{Q_V}{D^2} - \frac{1}{2(\gamma_1^2 - 1)}\right]\right\}^{\frac{\gamma_1}{\gamma_1 - 1}} \quad [32]$$

where ρ_0 is the density of the explosive (g/mm³), D is the detonation velocity (m/s), and Q_v is the reaction heat of the explosive (Nmm/g).

The pressure at the wall of the maximum cavity (r=a_m) is P_m= σ_r, according to Equation [18]

$$P_m = \sigma_s \left(\frac{b_{*m}}{a_m}\right)^{\frac{2\sin\phi}{1+\sin\phi}} \quad [33]$$

Rearranging Equations [27], [28], and [33] yields

$$\sigma_s [1/K + (1 - 1/K)\left(\frac{a_m}{r_b}\right)^{-2}]^{\frac{\sin\phi}{1+\sin\phi}} = P_b \left(\frac{a_m}{r_b}\right)^{-2\gamma_1} \quad (a_m \leq r_k) \quad [34a]$$

$$\sigma_s [1/K + (1 - 1/K)\left(\frac{a_m}{r_b}\right)^{-2}]^{\frac{\sin\phi}{1+\sin\phi}} = P_b \left(\frac{a_m}{r_b}\right)^{-2\gamma_2} \left(\frac{r_b}{r_k}\right)^{2(\gamma_1 - \gamma_2)} \quad (a_m > r_k) \quad [34b]$$

From Equation [34] the ratios between maximum cavity radius and blast-hole radius (a_m/r_b) can be obtained. Substituting (a_m/r_b) into Equation [27] yields the ratios between the crushed zone radius and blast-hole radius (b_{*m}/r_b).

On the condition that the cavity expansion is noticeable, the approximate equation:

$$(1 - 1/K)\left(\frac{a_m}{r_b}\right)^{-2} \approx 0 \quad [35]$$

holds, and then Equation [27] can be simplified as:

$$b_{*m} = a_m K^{-1/2} \quad [36]$$

According to Equations [34] and [36], the radius of the crushed zone around the blast-hole in column charge blasting becomes:

$$b_{*m} = \begin{cases} r_b \left(\frac{P_b}{\sigma_s} K^{\frac{\sin\phi}{1+\sin\phi}}\right)^{\frac{1}{2\gamma_1}} K^{-1/2} & (a_m \leq r_k) \\ r_b \left(\frac{P_b}{\sigma_s} K^{\frac{\sin\phi}{1+\sin\phi}}\right)^{\frac{1}{2\gamma_2}} \left(\frac{r_k}{r_b}\right)^{\frac{\gamma_2 - \gamma_1}{\gamma_2}} K^{-1/2} & (a_m > r_k) \end{cases} \quad [37]$$

Comparison with existing models

The physical and mechanical properties of four types of rocks chosen for the calculation are summarized in Table II. Explosives used in the calculation are ANFO, emulsion explosive, Gurit explosive, and booster and ammonium nitrate explosive. The properties of the commercial explosives used in the calculation and experimental work are summarized in Table III.

Table IV shows the ratios between the crushed zone radius and the blast-hole radius in different calculation models for different rock types and different explosive types. In general, for a specific rock and charge structure, the crushed zone radius increases as the blast-hole radius increases. Similarly, the models show that the explosive with higher density and higher detonation velocity has the

Table II

Physical and mechanical properties of rock mass

Rock	$[\sigma_c]$ (MPa)	$[\sigma_t]$ (MPa)	E (GPa)	θ (°)	ρ_m (kg/m³)	v	h
Quartzite	222	18	74.6	48	2710	0.22	2.2
Granite	129.1	10.3	79.5	52	2700	0.25	2.0
Limestone	60.7	5.9	31.0	43	2600	0.24	1.4
Siltstone	36.5	4.3	24.8	39	2230	0.30	1.2

$[\sigma_c]$: Unconfined compressive strength; $[\sigma_t]$: Unconfined tensile strength; E : Young's modulus; θ : Angle of internal friction; ρ_m : Density of rock mass; v : Poisson's ratio; h: dilatancy ratio.

Table III

Specification for the explosives

Explosive	Explosive density (g/cm³)	Detonation velocity (m/s)	Heat of reaction (MJ/kg)
Emulsion	1.20	5346	3.991
ANFO	0.81	4077	3.858
Gurit	1.00	2000	3.400
TNT	1.59	6940	4.184
Booster (60% TNT and 40% PETN)	1.54	7022	4.830
Ammonium nitrate explosive	1.10	3000	3.500

Table IV

Relative comparison of the new approach with existing models

Rock	Charge structure	Explosive	b_m/r_b					
			Il'yushin	Szuladzinski	Djordjevic	Kanchibotla	Esen	Modified model
Quartzite	Full Coupled	ANFO Emulsion	5.71 6.67	1.26 1.56	1.97 3.15	3.91 6.24	1.00 1.67	1.29 1.73
Granite	Full Coupled	ANFO Emulsion	7.52 8.79	1.64 2.03	2.61 4.16	5.11 8.15	1.13 2.09	1.58 2.09
Limestone	Full Coupled	ANFO Emulsion	8.97 10.48	2.39 2.96	3.45 5.50	7.45 11.88	1.93 3.56	2.47 2.77
Siltstone	Full Coupled	ANFO Emulsion	10.58 12.37	3.08 3.82	4.04 6.45	9.60 15.33	2.55 4.72	2.85 3.26

potential to create a larger crushed zone for the same blast-hole radius and rock type. There are notable discrepancies between those calculation models. However, for a specific borehole pressure, the size of the crushed zone differs considerably between rock types; for example, the size of the crushed zone in high-strength rock types is no more than twice the radius of the blast-hole, while it can reach 3–5 times the blast-hole radius and more in low-strength rock types. The assessments of the size of crushed zone are conflicting, but most scholars hold that the size of the crushed zone does not exceed 3–5 times the blast-hole radius (Yang, 1991; Saharan *et al.*, 1995), which is in agreement with the ranges calculated in the modified model.

According to the results calculated by the modified model, the thickness of the crushed zone increases with borehole pressure and the coupling between the charge and the blast-hole wall. The size of crushed zone is normally between 1.2 and 4.0 times the blast-hole radius with a fully coupled charge. Although this area is small, it consumes a considerable part of the explosive energy. Cook (1958) and Hagan (1977) hold that this mechanism consumes no less than 27% of the available strain wave energy, but makes only a very small contribution to the actual rock fragmentation, and around 0.1% of the total volume corresponding to the normal breakage per blast-hole (Jimeno *et al.*, 1995). In addition, an increased amount of dust will be formed. Furthermore, the entry of gases into cracks can be easily hindered by the powdery materials within the crushed zone, which inhibits the 'gas wedge' effect, thus reducing the volume of rock breakage (Hagan and Gibson, 1998; Roy, 2005). Meanwhile, the high specific surface area of the particles within the crushed zone will absorb a large amount of heat from the gases, reducing the effective utilization of explosive energy.

Calculation results listed in Table IV for four types of rock indicate that there are notable discrepancies between different models. The analysis shows that the calculation results of the modified model are close to Esen's and Szuladzinski's results, while the models proposed by Il'yushin and Kanchibotla may overestimate the radius of the crushed zone. One of the reasons for the significant discrepancies is the different definitions of the crushed zone; for example, Il'yushin and Kanchibotla's models consider fractured zone I, where plastic failure occurs and fractures present mesh distribution, also as part of the crushed zone.

Comparison with experimental data

The blast-hole is fragmented and displaced after the detonation, so it is difficult to measure the radius of the crushed zone directly in a full-scale production environment. Single blast-hole blasting experiments are highly expensive and inconvenient, and related experiment data is therefore very scarce. Several drilling and blasting tests reported by other researchers have been used to validate this modified model's applicability to full-scale blasting. This paper collects four sets of data from blasting tests in limestone and concrete by Vovk (1973), one set from decoupling charge drilling blasting tests in granite by Olsson and Bergqvist, 1996 and Olsson *et al.*, 2005), three sets from blasting tests in a coal mine by Slaughter (1991), one set from blasting tests in fosroc grout by La Rosa and Onederra (2001), and two sets of data from blasting tests in hard top-coal at the No.1 Honghui Mine by Suo (2004). Detailed test parameters are given in Table V.

Two drilling and blasting experiments were conducted by La Rosa and Onederra (2001) to measure the size of the crushed zone from a decoupled charge, as shown in Figure 2. The charge configuration consisted of a 25 mm blast-hole charged with a 22 mm UEE booster composed of 60% TNT and 40% PETN (see Table III). In each test, sections of the test samples were cut to reveal the size of the crushing zone. Figure 3 shows a comparison of different models in blasting experiments under corresponding conditions. The predictions of the crushed zone radius by the modified model are compared with the experimental data, and it is found that the predicted values are in better agreement with the test results than those from other models.

According to La Rosa and Onederra (2001), the crushed zone radii for both experiments were measured as 37.5 mm, *i.e.* three times the radius of the blast-hole. As shown in Figure 3, the ratios of the crushed zone radius and the blast-hole radius (b_m/r_b) calculated by the models proposed by Il'yushin, Djordjevic, and Kanchibotla under specific conditions are 7.85 6.25, and 12.30, respectively. However, the ratio calculated by the modified model is 3.38, thus the predicted values by this modified model agree reasonably well with the experiments results of La Rosa and Onederra.

Several performance indices, including coefficient of determination R^2 and root mean square error (RMSE) were computed to evaluate the performance of the predictive models:

Table V

Test parameters

No.	Researchers	Materials	$[\sigma_c]$ (MPa)	$[\sigma_t]$ (MPa)	E (GPa)	θ (°)	ρ_m (kg/m³)	v	h	Explosive	r_b (mm)	r_e (mm)
1	Slaughter	Coal	20	1.5	8.5	28	1400	0.28	1.4	ANFO	80	80
2,3	Slaughter	Coal	20	1.5	8.5	28	1400	0.28	1.4	Emulsion	80	80
4	Olsson *et al.*	Granite	197	12	30	55	2600	0.24	2.0	Gurit	32	11
5	Olsson *et al.*	Granite	197	12	30	55	2600	0.24	2.0	Gurit	25.5	8.5
6	Vovk	Limestone	8.9	1	22	35	1900	0.30	1.1	TNT	31.0	31.0
7,8	Vovk	Limestone	8.9	1	22	35	1900	0.30	1.1	TNT	29.8	29.8
9	Vovk	Concrete	27	1.5	15	37	2070	0.25	1.5	TNT	26.2	26.2
10	La Rosa *et al.*	Fosroc Grout	58.3	4.7	14.2	45	2167	0.20	1.4	Booster	12.5	11.0
11,12	Y.L. Suo	Coal	28	1.3	3.4	31	1350	0.26	1.3	Ammonium nitrate	31	25

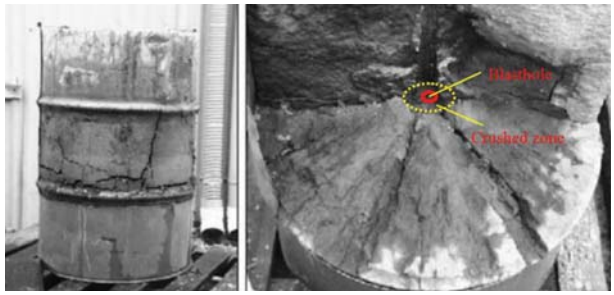

Figure 2—Crushed zone measurement tests by La Rosa and Onederra (2001)

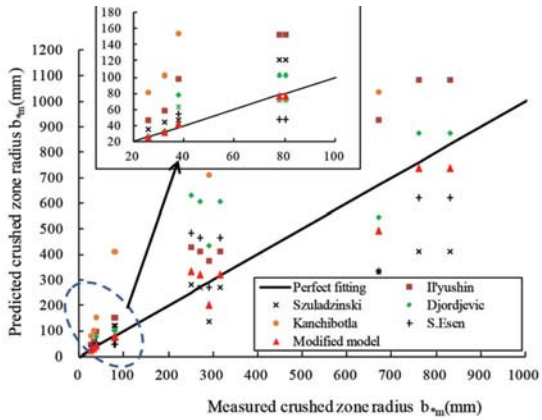

Figure 3—Comparison of different models against experimental data

$$R^2 = 1 - \frac{\sum_{i=1}^{N}(T_i - P_i)^2}{\sum_{i=1}^{N}(T_i - \bar{T})^2} \quad [38]$$

$$RMSE = \sqrt{\frac{\sum_{i=1}^{N}(T_i - P_i)^2}{N}} \quad [39]$$

where T_i, P_i and $\bar{T}$ are the measured, predicted from tests, and mean of the T_i values (mm), respectively, and N is the total number of data. Theoretically, the model will be excellent if R^2 is unity and RMSE is zero.

Results of performance indices (R^2, RMSE) for predictions and testing data-sets of different models are tabulated in Table VI. As it can be seen, the performance indices show that the modified model can predict the size of crushed zone with higher degree of accuracy compared to other models.

Since the size of the crushed zone in Szuladzinski's model is only a function of explosive density, effective energy of the explosive, and the dynamic compressive strength of the rock material, it is unsuitable for the decoupling cases. Also, the models proposed by Il'yushin and Kanchibotla seem to overestimate the size of the crushed zone under the condition of decoupling charge. The methods proposed by Esen and the modified model take an effective account of the effect of decoupling on the extent of crushing.

Comparison with numerical simulation results

A coupled numerical approach with combined smooth particle hydrodynamics (SPH) and FEM methods was also conducted to investigate the effects of single blast-hole. The SPH method, which is Lagrangian and mesh-free, it is well suited to analyse large deformation events involving failure and fragmentation (Hu *et al.*, 2015). However, the SPH method has some difficult in applying boundary conditions and its calculation efficiency becomes a bottleneck for applying this method to engineering practice. Therefore, the combination of SPH and FEM is a good solution to accurately simulate the whole process of rock blasting. The SPH technique is employed to model the explosive charge and the close-in

Table VI

Performance indices of the modified models as well as previous models

Performance indices	Predictive model					
	Il'yushin	Szuladzinski	Djordjevic	Kanchibotla	Esen	Modified model
R^2	0.66	0.38	0.58	0.54	0.77	0.91
RMSE	164.1	709.5	182.4	191.1	140.9	69.1

zones where a large amount of deformation takes place, while the normal FEM is used in the far field. One can make full use of the FEM method to apply boundary conditions for the model, thus guaranteeing the calculation accuracy as well as calculation efficiency.

A two-dimensional numerical model was developed with a combined SPH-FEM approach to simulate the blast-induced damage around a single blast-hole in granite and limestone, as illustrated in Figure 5. The RHT model, developed by Riedel, Hiermaier, and Thoma (1999), is adopted in the present study. The JWL equation of state models the pressure generated by the expansion of the detonation products of the chemical explosive (Yang *et al.*, 2015). The numerical parameters for the rock and explosive are adopted from Table II and Table III.

According the simulated results in Figure 5, the ratios of the crushed zone radius and the blast-hole radius (b_m/r_b) calculated by the numerical models are 1.75 and 3.16, while the values calculated by our modified model are 1.58 and 2.77.Although the radii of the crushed zones in both granite and limestone obtained from this modified model are a little smaller than that of numerical model, the numerical simulation results and modified model results agree well. As far as the crushed zones are concerned, it can be said that the results obtained from this modified model give a good prediction for the blast-induced crushed zone.

Factors influencing the crushed zone

The modified model shows that the crushed zone radius is affected mainly by the rock mass properties, *in situ* stress σ_0, borehole pressure P_b, and blast-hole radius r_b. In particular, the roles of borehole pressure and *in situ* stress are discussed. The sizes of the crushed zone in different types of rock under different borehole pressure and *in situ* stress are compared. The blasting load mainly induces tensile damage (the fractured zone) to the surrounding rock. Since this tensile effect is very easily inhibited by the *in situ* stress, the fractured zone is significantly reduced with increasing *in situ* stress, as shown in Figure 6. However, it has been found that the *in situ* stress apparently has a slight effect on the size of crushed zone, especially in hard rock. The size of the crushed zone increases slowly with the *in situ* stress, and such increase is more noticeable in soft rock, as shown in Figure 7. It can be predicted that for drilling and blasting in deep underground caverns, when the *in situ* stress reaches a higher level, the tension effect may be completely inhibited, and there would be a crushed area only around the blast-hole.

As shown in Figure 8, the size of the crushed zone decreases significantly as the borehole pressure falls. Reducing the borehole pressure P_b is therefore an effective way to reduce the size of the crushed zone. Borehole pressure P_b is related to explosive characteristics and charging structure, so one can reduce the crushed zone by adjusting explosive characteristics or improving charging structure, such as by using lower energy explosives, or using a decoupling or air-decked charge. When using the decoupling charging structure, the size of the crushed zone decreases quickly along with the increase in decoupling ratio, as shown in Figure 9. There is even no fine crushing if the decoupling ratio increases to a certain value.

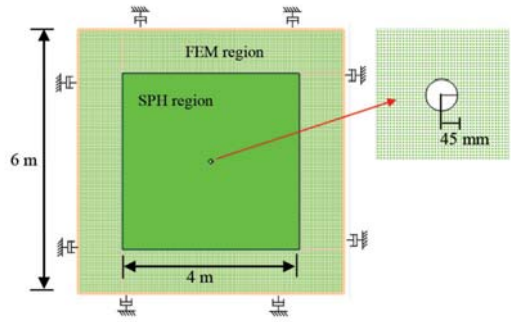

Figure 4—Overall view of the SPH-FEM coupled model

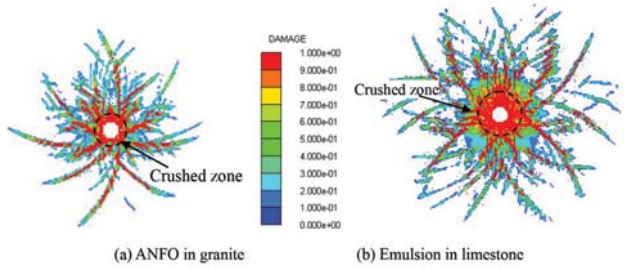

Figure 5—Numerical modelling of the size of the crushed zone around a single hole

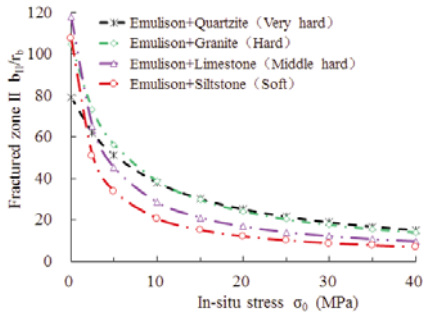

Figure 6—Effect of *in situ* stress on the size of the fractured zone

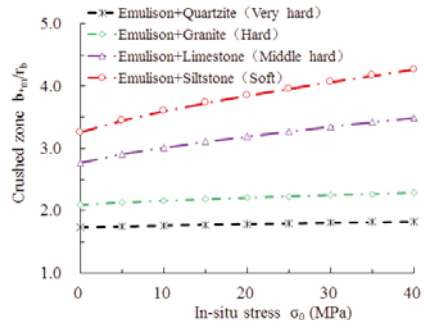

Figure 7—Effect of *in situ* stress on the size of the crushed zone

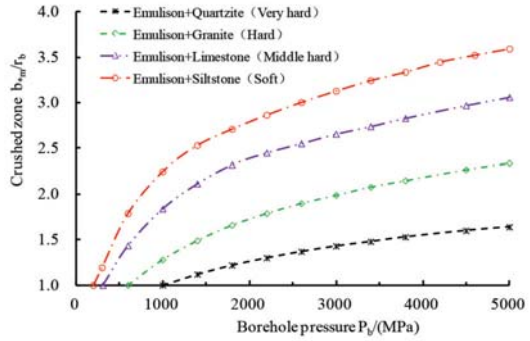

Figure 8—Effect of borehole pressure on the size of the crushed zone

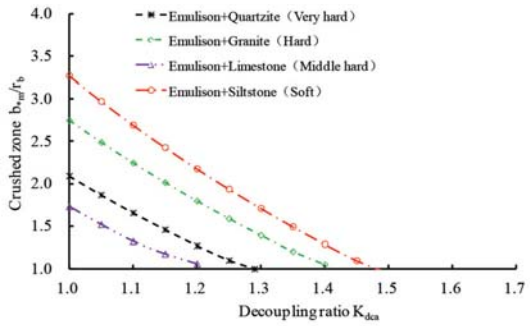

Figure 9—Effect of decoupling ratio on the size of the crushed zone

Conclusions

A modified model to calculate the size of the crushed zone around the blast-hole has been presented that takes into account the hoop compressive stress in the inner part of fractured zone and cavity expansion on decreasing the borehole pressure. As a result, the modified model can better reflect the actual breakage mechanism of rocks around the blast-hole. The proposed approach has been verified with tests reported in the literature as well as simulated results from SPH-FEM coupled models. Compared with other models, the calculation results from this model are in better agreement with the test results.

The crushed zone radius formula derived from the modified model indicates that the size of the crushed zone is related to the rock properties, the characteristics of the explosives, the charge structure, and the blast-hole radius. The analysis shows that there are notable discrepancies between rock types, and usually the size of the crushed zone ranges from 1.2 to 5.0 times the blast-hole radius.

The *in situ* stress apparently has a slight effect on the size of the crushed zone, especially in hard rock. The size of the crushed zone increases slowly with the *in situ* stress, with the increase being more noticeable in soft rock. However, the tensile fracture effect is very easily inhibited by the *in situ* stress, and the size of the fractured zone is significantly reduced with increasing *in situ* stress. One of the prime reasons for overcrushing is unacceptable levels of borehole pressure in blasting. It is found that reducing the borehole pressure P_b is an effective way to reduce the size of the crushed zone. The size of the crushed zone decreases significantly along with the increase of decoupling ratio. The crushed zone can be reduced by using a decoupling charging structure.

Acknowledgements

This work was supported by Chinese National Programs for Fundamental Research and Development (973 Program) (2011CB013501), Chinese National Natural Science Foundation (51125037 and 51279135), and the Doctoral Scientific Fund Project of the Ministry of Education of China (20110141110026). The authors wish to express their thanks to all the supporters.

References

Djordjevic, N. 1999. A two-component of blast fragmentation. *Proceedings of the Sixth International Symposium on Rock Fragmentation by Blasting (Fragblast-6)*, Johannesburg, South Africa, 8–12 August 1999. Southern African Institute of Mining and Metallurgy, Johannesburg. pp. 213–222.

Esen, S., Onederra, I., and Bilgin, H.A. 2003. Modelling the size of the crushed zone around a blasthole. *International Journal of Rock Mechanics and Mining Sciences*, vol. 40, no. 4. pp. 485–495.

Furtney, J.K., Sellers, E., and Onederra, I. 2012. Simple models for the complex process of rock blasting. *Proceedings of the 10th International Symposium on Rock Fragmentation by Blasting*, New Delhi, India. pp. 275–282.

Ghosh, A. 1990. Fractal and numerical models of explosive rock fragmentation. University of Arizona.

Glatolenkov, A.I. and Ivanov, V.I. 1992. Mechanism of breakdown of rock masses and formation of fines by blasting. *Journal of Mining Science*, vol. 27, no. 5. pp. 444–452.

Hagan, T.N. and Gibson, I.M. 1988. Lower borehole pressures: a means of reducing costs when blasting rocks of low to moderate strength. *International Journal of Mining and Geological Engineering*, vol. 6, no. 1. pp. 1–13.

Henrych, J. 1979. The Dynamics of Explosion and Its Use. Elsevier, Amsterdam.

Hu, Y.G., Lu, W.B., Chen, M., Yan, P., and Zhang, Y.Z. 2015. Numerical simulation of the complete rock blasting response by SPH–DAM–FEM approach. *Simulation Modelling Practice and Theory*, vol. 56. pp. 55–68.

Il'yushin, A.A. 1971. The mechanics of a continuous medium. Izd-vo MGU, Moscow (in Russian). Translated in: 1999. *Blasting Principles for Open Pit Blasting*, Hustrulid, W. (ed.). Balkema, Brookfield.

Jimeno, E.L., Jimino, C.L., and Carcedo, A. 1995. Drilling and Blasting of Rocks, CRC Press.

Kanchibotla, S.S., Valery, W., and Morrell, S. 1999. Modelling fines in blast fragmentation and its impact on crushing and grinding. *Proceedings of Explo'99*, Kalgoorlie, Western Australia, 7–11 November 1999. pp. 137–181.

La Rosa, D. and Onederra, I. 2001. Acceleration measurements from a small diameter explosive charge. Confidential Internal Report. JKMRC, Brisbane, Australia.

Olsson, M. and Bergqvist, I. 1996. Crack lengths from explosives in multiple hole blasting. *Proceedings of the Fifth International Symposium on Rock Fragmentation by Blasting*, Montreal, Quebec, Canada. Balkema, Rotterdam. pp. 187–191.

Olsson, M., Nie, S., Bergqvist, I., and Ouchterlony, F. 2002. What causes cracks in rock blasting? *Fragblast: International Journal for Blasting and Fragmentation*, vol. 6, no. 2. pp. 221–233.

Ouchterlony, F. and Moser, P. 2012. On the branching-merging mechanism during dynamic crack growth as a major source of fines in rock blasting. *Proceedings of the 10th International Symposium on Rock Fragmentation by Blasting*, New Delhi, India. CRC Press, Leiden, The Netherlands. pp. 65–75.

Ouchterlony, F., Nyberg, U., Olsson, M., Bergqvist, I., Granlund, L., and Grind, H. 2004. Where does the explosive energy in rock blasting rounds go?. *Science and Technology of Energetic Materials*. vol. 65, no. 2. pp. 54–63.

Qian, Q.H. 2009. Some advances in rock blasting dynamics. *Chinese Journal of Rock Mechanics and Engineering*, vol. 28, no. 10. pp. 1945–1968.

Rakishev, B. and Rakisheva, Z.B. 2011. Basic characteristics of the stages of rock mass if destruction by explosive crushing. *Proceedings of the Asia-Pacific Symposium on Blasting Techniques*, KunMing, China. pp. 65–69.

Riedel, W., Thoma, K., and Hiermaier, S. 1999. Numerical analysis using a new macroscopic concrete model for hydrocodes. *Proceedings of the 9th International Symposium on Interaction of the Effects of Munitions with Structures*, Berlin, Germany. pp. 315–322.

Roy, P.P. 2005. Rock Blasting: Effects and Operations. CRC Press.

Saharan, M.R., Mitri, H.S., and Jethwa, J.L. 2006. Rock fracturing by explosive energy: review of state-of-the-art. *Fragblast: International Journal for Blasting and Fragmentation*, vol. 10, no. 1–2. pp. 61–81.

Sanchidrian, J.A., Segarra, P., and Lopez, L.M. 2007. Energy components in rock blasting. *International Journal of Rock Mechanics and Mining Sciences*, vol. 44, no. 1. pp.130–147.

Slaughter, S. 1991. Investigation of coal fines. Internal Report, JKMRC, Australia.

Suo, Y.L. 2004. Distribution characteristic of breaking extending area of weakening-blast in hard top-coal. *Journal of China Coal Society*, vol. 29, no. 6. pp. 650–654.

Szuladzinski, G. 1993. Response of rock medium to explosive borehole pressure. *Proceedings of the Fourth International Symposium on Rock Fragmentation by Blasting (Fragblast-4)*, Vienna, Austria, 5–8 July 1993. Rossmanith, H-P. (ed.). Balkema, Rotterdam. pp. 17–23.

Vovk, A., Mikhalyuk, A., and Belinskii, I. 1973. Development of fracture zones in rocks during camouflet blasting. *Soviet Mining Science*, vol. 9, no. 4. pp. 383–392.

Yang, S.Y. 1991. Foundations of Dynamics in Rock Blasting. China Coal Industry Publishing House, Beijing.

Yang, J.H., Lu, W.B., Hu, Y.G., Chen, M., and Yan, P. 2015. Numerical simulation of rock mass damage evolution during deep-buried tunnel excavation by drill and blast. *Rock Mechanics and Rock Engineering*, vol. 48, no. 5. pp. 2045–2059.

Wang, M.Y., Deng, H.J., and Qian, Q.H. 2005. Study on problems of near cavity of penetration and explosion in rock. *Chinese Journal of Rock Mechanics and Engineering*, vol. 24, no. 16. pp. 2859–2863. ◆

http://dx.doi.org/10.17159/2411-9717/2016/v116n5a8

Multivariate geostatistical simulation of the Gole Gohar iron ore deposit, Iran

by S.A. Hosseini* and O. Asghari*

Synopsis

The quantification of mineral resources and evaluation of process performance in mining operations at Gole Gohar iron ore deposit requires a precise model of the spatial variability of three variables (Fe, P, and S) which must be determined. According to statistical analysis there are complex multivariate relationships between these variables such as stoichiometric constraints, nonlinearity, and heteroskedasticity. Due to the impact of these complexities in decision-making, they should be reproduced in geostatistical models. First of all, in order to maintain the compositional and stoichiometric constraints, additive log-ratio (alr) transformation has been applied. In the next step cosimulation, using stepwise conditional transformation (SCT) and sequential Gaussian simulation (SGS) has been used to simulate multivariate data. Through statistical and geostatistical validations it is shown that the algorithms were able to reproduce complex relationships between variables, both locally and globally.

Keywords
additive log-ratios, stepwise conditional transformation, multivariate simulation, iron ore deposit, complex relationship.

Introduction

The key steps in mining projects are the quantification of mineral resources, definition of mining reserves, and production scheduling. They rely on the construction of a block model that is used to represent basically the spatial distribution of ore grades (Montoya *et al.*, 2012). The determination of grades and tonnages affects risk assessment and economic evaluation of mining projects. Evaluation of process performance in mining operations requires geostatistical modelling of many related variables (Barnett and Deutsch, 2012). Iron ore quality is characterized by multiple variables: not only the iron grade but also the contaminants that interfere in the subsequent steel manufacturing processes. Consequently, the spatial variability of multiple variables must be determined. Key variables are frequently correlated, and such correlations must be honoured during estimation and simulation. Data from iron ore deposits constitutes compositional data; furthermore, relationships the between assay data are often heteroskedastic.

In order to capture spatial variability and to assess spatial uncertainty, conditional simulation is becoming increasingly popular in the geosciences and the minerals industry for quantifying, classifying, and reporting mineral resources and ore reserves (Journel, 1974; Snowden, 2001). Mineral deposits like iron ore contain several elements of interest with statistical and spatial dependences that require the use of joint geostatistical simulation techniques in order to generate models preserving their spatial relationships. Multivariate modelling can improve the design and planning with respect to traditional models. Additionally, it can help in the assessment of the impact of grade uncertainty on production scheduling (Montoya *et al.*, 2012).

Cosimulation approaches include methods based on the linear model of co-regionalization, or LMC (Goovaerts, 1997) that can account for the linear (or close to linear) correlations between variables, as the relationship and dimensionality of the data to be modelled may render co-simulation frameworks impractical. Relationships between variables often show complex features such as nonlinearity, heteroskedasticity, and other constraints (Leuangthong and Deutsch, 2003).

One approach is to apply a transformation to the data that removes the relationships, allowing the transformed variables to be simulated independently. Then the variable-variable relationships are restored by back-transformation of the simulated variables. A number of transformation techniques are available that remove these complex features and produce well-behaved distributions that approach Gaussianity. It is highly desirable

* *Simulation and Data Processing Laboratory, School of Mining Engineering, University College of Engineering, University of Tehran, Tehran, Iran.*

 ISSN 2225-6253. Paper received Nov. 2014; revised paper received Apr. 2015.

that the input data to the simulation are standard Gaussian for SGS. There are additional transformations for the de-correlation of variables, allowing independent simulation to proceed without the need for LMC (Barnett and Deutsch, 2012), *e.g.* principal component analysis (PCA) (Goovaerts, 1993; Hotelling, 1933) and minimum/maximum autocorrelation factors (MAF) (Desbarats and Dimitrakopoulos, 2000; Switzer and Green, 1984), UWEDGE transform (Mueller and Ferreira, 2012), the stepwise conditional transformation (SCT) (Leuangthong and Deutsch, 2003; Rosenblatt 1952) and the projection pursuit multivariate transform (PPMT) (Barnett, Manchuk, and Deutsch, 2014). A shared limitation for linear methods such as PCA and MAF transforms is the poor handling of nonlinear and heteroskedastic features (Barnett *et al.*, 2013). One of the disadvantage of stepwise conditional transformation is that in order to classify data and transform each class, there must be sufficient data to identify a conditional distribution (Leuangthong and Deutsch, 2003). As each technique possesses its own limitations, challenges may arise in choosing the appropriate transforms and the order in which they are applied. Barnett and Deutsch (2012) have proposed a workflow in which transformations are given for the removal of each complexity. No single technique addresses all of the complexities that may exist between the variables of a mineral deposit. Transformations will often be used in chains (Barnett and Deutsch, 2012). In this paper log-ratios (Aitchison, 1982; Pawlowsky-Glahn and Olea, 2004) and STC are used to overcome problems of compositional data and remove the complex features, following the work of Barnett and Deutsch (2012).

The SCT approach has been applied to the modelling of ore deposits such as multivariate simulation of the Red Dog mine (Leuangthong *et al.*, 2006), simulation of total and oxide copper grades in the Sungun copper deposit (Hosseini and Asghari, 2014), and simulation of correlated variables in Yandi Channel iron deposit (De-Vitry, 2010). De-Vitry (2010) recommended that SCT be attempted where significantly nonlinear correlations are present. Log-ratios have also been used to simulate a nickel laterite data-set (Barnett and Deutsch, 2012) and estimate grades in iron ore deposits in Brazil (Boezio *et al.*, 2011). Conditional Gaussian simulations were applied to transformed variables. Back-transformations are executed in the reverse order of which they were applied going forward.

Methodology

The methodology in the present study is the combination of additive log-ratios (alr) and stepwise conditional transformations proposed by Barnett and Deutsch (2012). Figure 1 shows the proposed order in which multivariate complexities should be addressed to form an uncorrelated multivariate Gaussian distribution. Additive log-ratios (Aitchison, 1982) are used to preserve compositional constraints, and must be applied as the first forward transformation. Then stepwise conditional transformation is used to correct for too-skewed distributions that arise after applying log-ratios and remove the complex features. The major motivation to use SCT in practice is that it is robust when dealing with complex multivariate distributions (Rossi and Deutsch, 2014). Although minimum/maximum autocorrelation factors (MAF) were used to remove correlations between variable elements before simulation, the MAF approach performs poorly with variables that do not demonstrate a linear correlation (Rondon and Tran, 2008; De-Vitry 2010). Butcher and Dimitrakopoulos (2012) have also applied the MAF method for multivariate simulation of the Yandi iron ore deposit, for which the reproduction of the coefficient of correlation between the variables was weak. This contrasts with the STC approach, which is better equipped for handling problematic correlations such nonlinearity and heteroskedasticity. Then sequential Gaussian simulation (SGS), which is efficient and widely used (Lantuejoul, 2002), was performed to simulate transformed variables. Back-transformations are executed in the reverse order to which they were applied going forward.

Additive log-ratios

The additive log-ratios transform is used to deal with this constant-sum constraint. The logarithmic transformation must be applied with care when there are zeros for head grade variables. Zeros are obviously problematic, because the logarithm of zero is undefined. The alr transform for D-part composition (Aitchison 1999) is

$$x_i = \ln\left(\frac{Z_i}{Z_D}\right), \quad i = 1,\ldots,D-1 \qquad [1]$$

where x_i is the new variable and Z_i represents each of the original variables. The back-transformation is

$$Z_i = \frac{\exp(x_i)}{\sum_{i=1}^{D-1}\exp(x_i)+1} \qquad [2]$$

where x_i is logarithmic transformed variable. Directly kriging this log-ratio-transformed data, with a direct back-transform applied results in estimates that are biased. The alternative to direct kriging of log-ratios is to apply a nonlinear approach, in which the conditional distributions of the components are modelled instead of unique values from linear kriging. It has been shown that conditional simulation, where the log-ratio values are transformed into Gaussian values, are valid techniques for dealing with compositional data (Job, 2012).

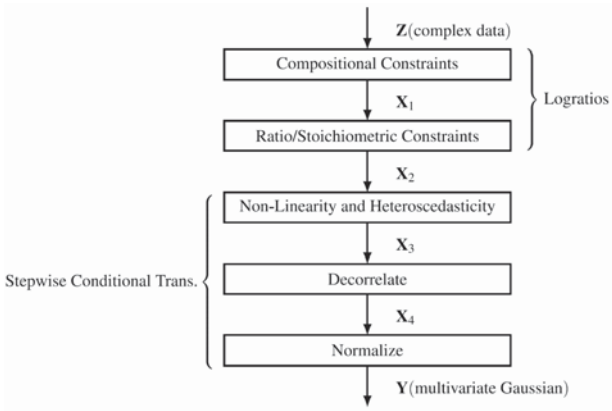

Figure 1—Techniques and order in the order they should be applied to obtain an uncorrelated distribution Y that approaches multivariate Gaussianity (Barnett and Deutsch, 2012)

Stepwise conditional transformation

The STC technique is proposed to transform multiple variables with complex relationships into univariate and multivariate Gaussian with no cross-correlation (Leuangthong and Deutsch, 2003). This method removes all correlations between variables before simulation; thus makes modelling of experimental variograms and simulation faster than conventional cosimulation because cross-variograms and cokriging are not required. The main limitation of the stepwise conditional transformation lies in the need for sufficient data, and this transformation is suitable for low dimensional data-sets (2–4 variables). This transform is identical to the normal score transform for the first variable. For multiple variables, the normal score transformation of the next variable is conditional to the probability class of the preceding variables in the following form:

$$\begin{aligned} Y_1 &= G^{-1}\left[F_1(x_1)\right] \\ Y_2 &= G^{-1}\left[F_{2|1}(x_2 \mid x_1)\right] \\ &\cdot \\ &\cdot \\ &\cdot \\ Y_n &= G^{-1}\left[F_{n|1,2,\ldots,n-1}(x_n \mid x_1, x_2, \ldots, x_{n-1})\right] \end{aligned} \quad [3]$$

where Y_i, i=1,..., n are multivariate Gaussian variables that are independent at lag distance of zero and are the new variables to be modelled. The transformation ordering for the stepwise conditional transform will affect the reproduction of the variogram from simulation. Thus, the most important variable or the most continuous variable should be chosen as the primary variable. The back-transformation enforces reproduction of the original complex features.

Application at Gole Gohar iron ore deposit, Iran

The Gole Gohar iron ore deposit is located at about 55 km southwest of Sirjan in the eastern edge of the Sanandaj-Sirjan structural zone of Iran. The Gole Gohar deposit, comprising six main anomalies and a total reserve of 1300 Mt of high-grade iron ore, is one of the most important economic mineral deposits in Iran. The host rocks include metamorphosed sedimentary and volcanic rocks of the greenschist facies, probably of Upper Proterozoic-Lower Paleozoic age. The mineralization comprises macro-, meso-, and microbanding of magnetite associated with shale, sandstone, and cherty carbonates. The presence of diamictites and phenoclasts in magnetite banding and the host rocks indicates an iron ore association similar to the Rapitan banded iron ore (Babaki and Aftabi, 2006). The Gole Gogar deposit contains 57.2% iron, 0.16% phosphorus, and 1.86% sulphur.

Study area and data

Gol-Gohar iron ore mine anomaly no. 4 is considered in this study. The host rocks are mainly metamorphic rocks, including amphibolite, mica schist, and chlorite schist. Mineralization occurs in both sulphide and oxide forms, and consists of pyrite, pyrhotite, and chalcopyrite as the sulphide minerals, accompanied by other oxide–hydroxide minerals of iron including magnetite, haematite, and limonite. A set of exploration drill-holes is available with an average sampling mesh of 50 m × 50 m. Sample data was composited to 3 m composites and extracted for geostatistical analysis and variography. The assay database comprises 3078 sample intervals from 187 boreholes assayed for iron, phosphorus, and sulphur. A 3D map of drill-hole locations is shown in Figure 2. The basic statistics for these variables are given in Table I. The block model constructed is sufficiently reliable to support mine planning and allow evaluation of the economic viability of a mining project.

Applying transformations to the Gole Gohar data-set

At Gole Gohar Fe%, P%, and S% are variable of interest. The head grades are considered compositional; that is, they are non-negative and sum to 100%. Not all elements in a sample are assayed, therefore the sum of the head grades is less than 100%. In geostatistical modelling, if this constraint is not explicitly imposed it can be violated. A logarithmic transform of four head grade variables is considered, with the fourth variable imposing the 100% constant sum:

$$Fe(\%) + P(\%) + S(\%) + Z_{filler} = 100\% \quad [4]$$

There are few zeros due to the pervasive mineralization to varying extent over the entire deposit. These values have been replaced by the analytical detection limit. The alr

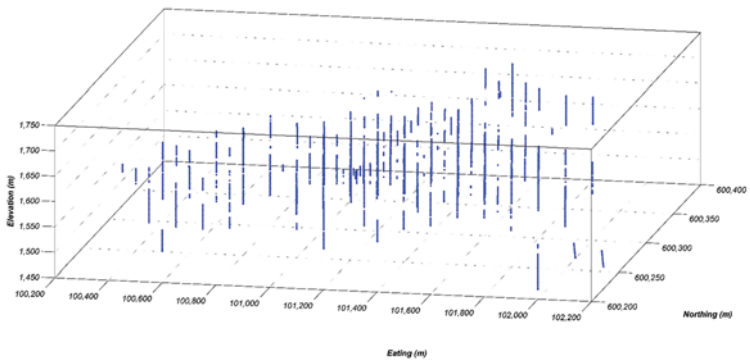

Figure 2—3D illustration of the boreholes in the fourth Gole Gohar iron ore deposit

Table I

Basic statistics of assayed grades

	Number of data	Minimum	Maximum	Median	Mean	Standard deviation
Fe(%)	3078	8.7	67.6	59.6	57.08	7.882
P(%)	3078	0.01	0.79	0.103	0.118	0.101
S(%)	3078	0.001	7.101	1.4	1.7	1.671

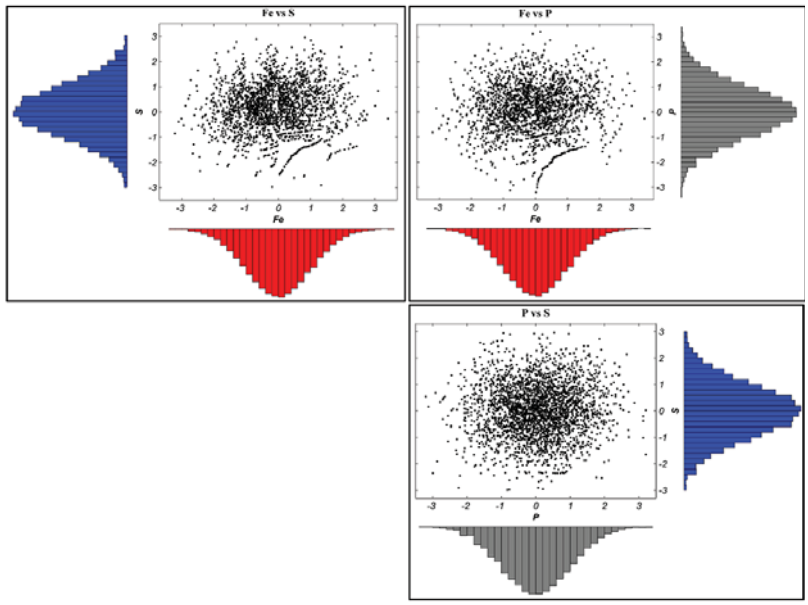

Figure 3—Cross-plot of variables after transformations. Complex features between distributions of variables have been removed following transformations

transform is used to deal with this constant sum constraint. Z_{filler} has been used as denominator in Equation [1]. There are now three logarithmic transformed variables, and STC is applied to transform them into Gaussian distributions and remove all correlations between them. For Gole Gohar, Fe is the most important variable, and so the others will be conditioned to it. Due to the spatial continuity, P and S are considered as the second and third variables respectively. Marginal histograms on the bivariate scatter plots of variables after transformations are displayed in Figure 3. The bivariate distributions again exhibit a bivariate Gaussian distribution with essentially zero correlation. Thus, Gaussian simulation techniques can be applied with no requirement for cokriging or to fit a model of co-regionalization.

Simulation of transformed variable

Geostatistical simulations generate a set of images, or 'realizations', as opposed to estimates, which output a single image. The realizations constitute a range of spatial images that are consistent with the known statistical moments (variogram and histogram) of the declustered input data, and in the case of conditional simulations, the data itself. Geostatistical simulations can be used to assess uncertainty over various scales or volumes (*e.g.* mining production intervals), and can assist in evaluating drill-hole spacing, mining selectivity and blending, and mine financial modelling (Chiles, 2012). In this study, sequential Gaussian simulation or SGS (Isaaks, 1990) has been performed for constructing the realizations. The conditioning samples are migrated to the closest grid node, and a random path is defined through all the grid nodes. Simple kriging is used to construct the conditional Gaussian distribution at each node in the path using the conditioning and previously simulated data. A simulated value is drawn from this conditional distribution and added to the grid node. The next node on the random path is then simulated until all nodes are completed. This process is then repeated to generate n realizations. Each realization contains simulated Fe, P, and S value.

Directional experimental semivariograms were produced for iron, phosphorus, and sulphur after transformations. Experimental and model semivariograms of the transformed variables are shown in Figure 4 and cross-variograms between three transformed variable are shown in Figure 5. The cross-semivariogram takes low values (almost zero). Accordingly, separate modelling of the direct variogram of these variables is undertaken. The total ranges modelled are also utilized to help define the optimum search parameter and search ellipse radii used in the simulation. Applying the two-thirds rule to the total of the variogram range in the search ellipse radius forces the interpolation to use a sample where covariance between samples exists. One joint simulation for the three elements conditional to the drill-hole data (Figure 1) is shown in Figure 6.

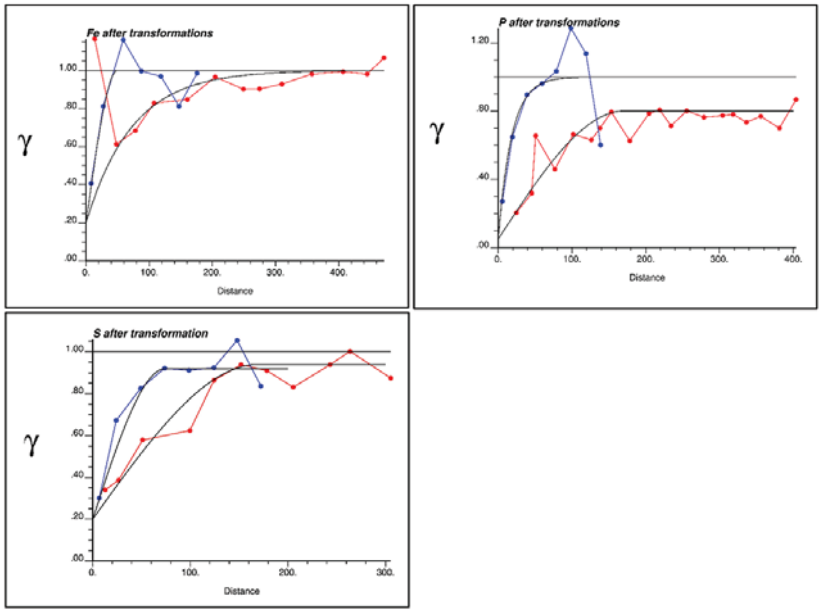

Figure 4—Experimental and model variograms of the transformed variables for horizontal (red) and vertical (blue) directions and the modelled (black)

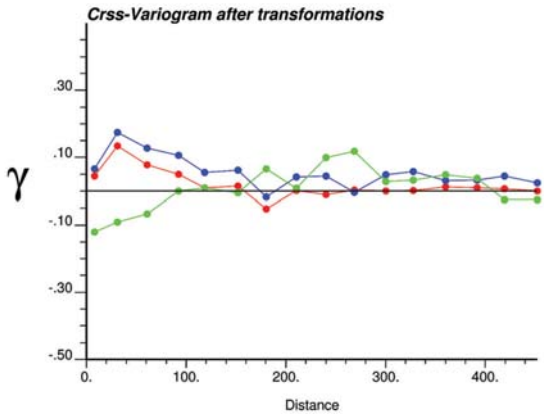

Figure 5—Cross-variograms between three transformed variable. Fe-P (blue), Fe-S (green), P-S (red)

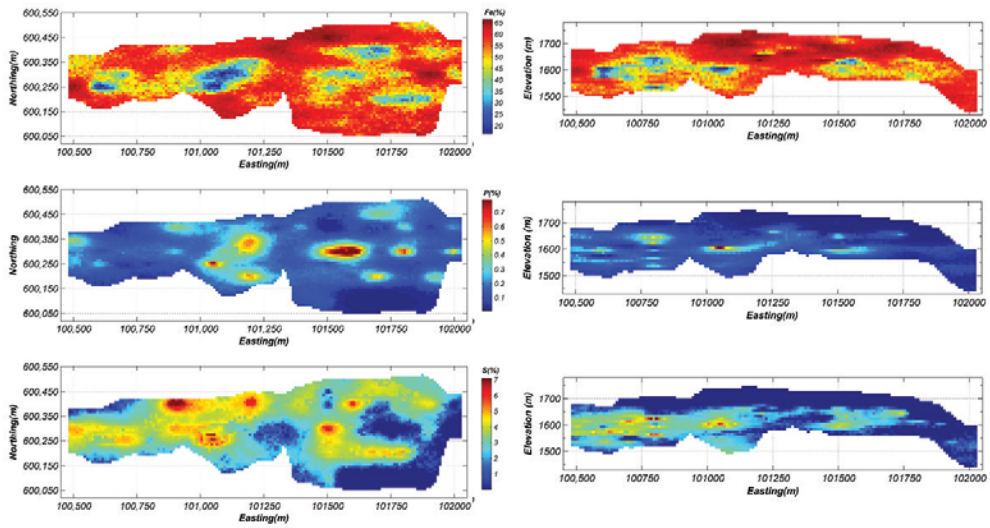

Figure 6—Representation of a joint simulation for each element. (Left) selected section at elevation of 1600 m, (right) selected section at northing of 600130 m

Checking of results

To validate the results, four steps are considered:

1. Quantile-to-quantile (Q–Q) plots between drill-hole data and simulated values
2. Comparison of drill-hole data and simulation value scatter-plots
3. Comparison of histograms of the sum of three modelled components with the original assays, and simulated values
4. Assessment of the vertical profiles of the realizations at block support level.

Figure 7 shows that the simulated results reproduce the distributions of the drill-hole data properly. A histogram correction was applied following all back-transformation steps. As a comparison, the point-scale scatter-plots between selected elements for the data, the first simulation without using transformations, and the first simulation using transformations are shown in Figure 8. When the transformations are applied, the shape of the point cloud remains substantially the same, and reproduction of the coefficient of correlation between variables is good. Figure 9 displays histograms of the sum of the three components for the experimental assays and simulated values under three different conditions: (1) without the application of alr or SCT, (2) with the application of SCT, (3) with both alr and SCT. It is observed from the descriptive statistics, especially the maximum value, that the simulated locations with the use of additive log-ratios preserved the compositional constraint explicitly. The simulated locations without the use of alr do not explicitly honour the compositional constraint. Although

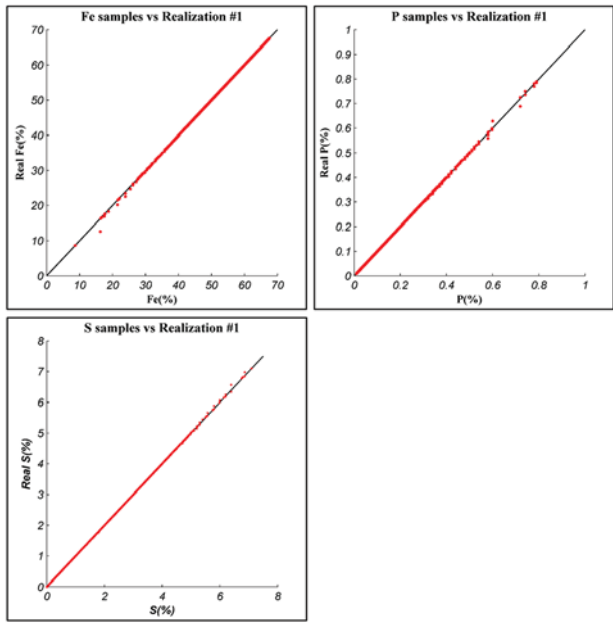

Figure 7—Q–Q plots between drill-hole data and point scale simulated values

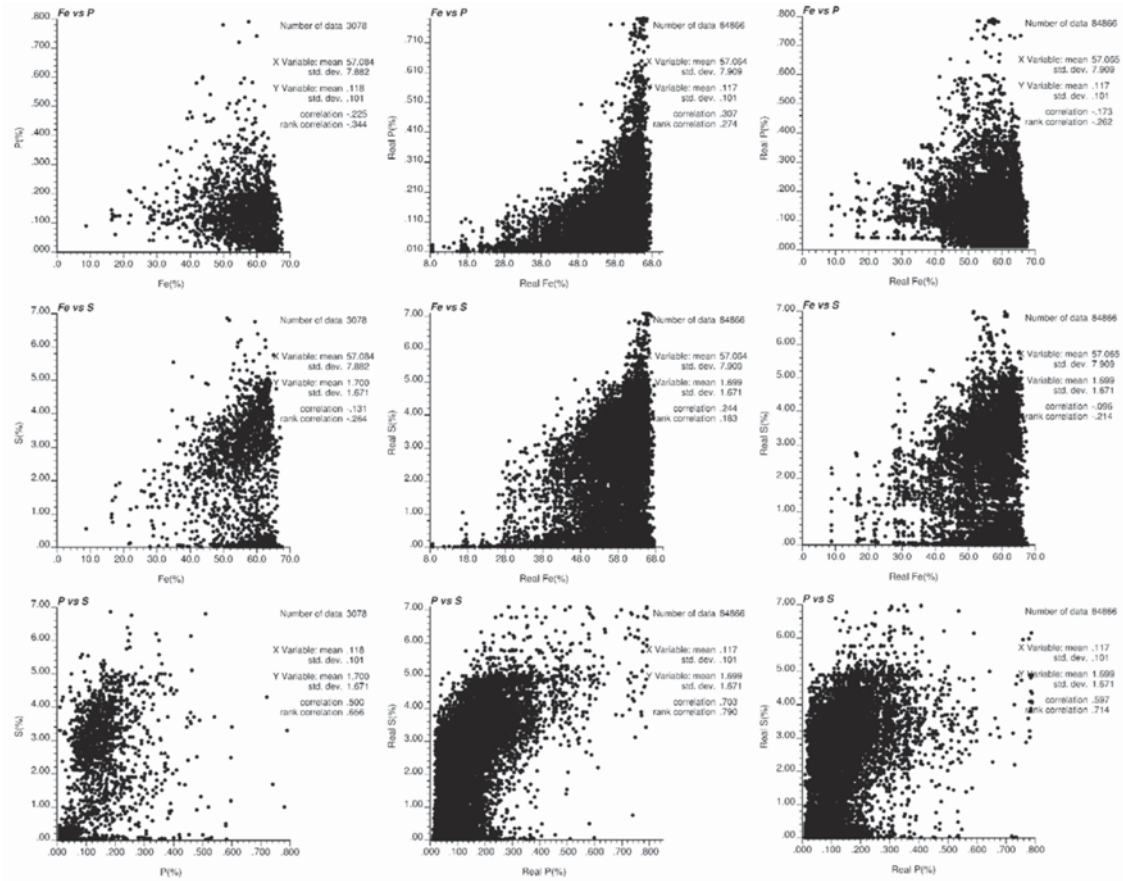

Figure 8—Point-scale scatter-plots between selected elements for the data (left), the first simulation without using alr and SCT transformations (centre), and the first simulation using transformations (right)

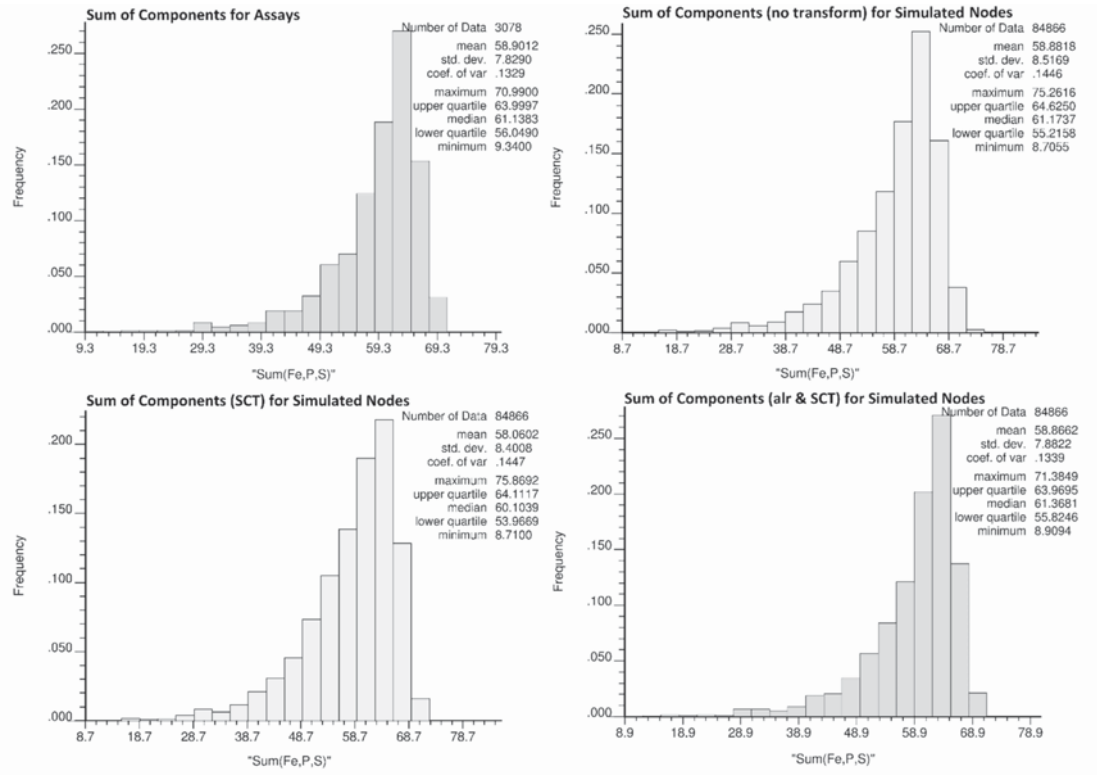

Figure 9—Histograms of the sum of three components for the original assays (top left), and simulated values: without alr and SCT (top right), with SCT (bottom right), with both alr and SCT (bottom left)

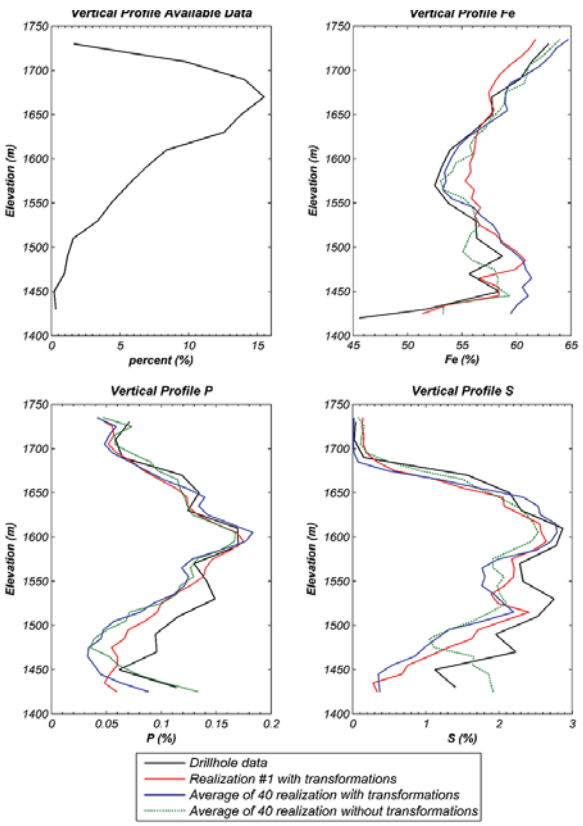

Figure 10—Vertical profiles between the point-scale drill-hole data and that of realization no. 1, average of 40 realizations with and without transformations

this issue is demonstrated with only three modelled variables, the results would be much more dramatic when considering the additional components that the mining model would require (Barnett and Deutsch, 2012). In Figure 10, the variation of three elements in the vertical direction is compared. The vertical trends of the elements are an important feature of iron ore deposits (Boucher and Dimitrakopoulos, 2012). The general shape of the profiles is well reproduced in all cases but in elevations 1430 to 1530 m, east of the deposit, there are differences between vertical profile of variables in drill-hole data and the simulation results. These differences are due to the paucity of data.

Conclusion

The quantification of mineral resources and evaluation of process performance at the Gole Gohar iron ore deposit requires consideration of three correlated variables (Fe, P, and S). Relationships between these variables show complex features. This paper has shown the practical aspects of an efficient framework for the joint simulation of correlated variables based on a combination of log-ratios and stepwise conditional transformation (proposed by Barnett and Deutsch), and directly generating point-scale realizations. Additive log-ratios were used to honour the compositional constraint, then stepwise conditional transformation was used to correct for the too-skewed distributions that log-ratios create and remove the complex features. The use of this procedure did not require fitting of a LMC for joint simulation of variables. This procedure reproduced the

relationships between the variables and histograms of variables well. The realizations are an input for the estimation of mineral resources and ore reserves, and are suitable for mine and plant optimization.

References

Aitchison, J. 1999. Logratios and natural laws in compositional data analysis. *Mathematical Geology*, vol. 31, no. 5. pp. 563–580.

Aitchison, J. 1982. The statistical analysis of compositional data. *Journal of the Royal Statistical Society, Series B (Methodological)*, vol. 44, no. 2. pp. 139–177.

Babaki, A. and Aftabi, A.J. 2006. Investigation on the model of iron mineralization at Gol Gohar iron deposit, Sirjan-Kerman. *Geosciences Scientific Quarterly Journal,* vol. 61. pp. 40–59 (in Persian with English abstract).

Barnett, R.M. and Deutsch, C.V. 2012. Practical implementation of non-linear transforms for modeling geometallurgical variables. *Proceedings of the Ninth International Geostatistics Congress*, Oslo, June 2012. Abrahamsen, P., Hauge, R., and Kolbjornsen, O. (eds). Springer, The Netherlands.

Barnett, R.M., Manchuk, J.M., and Deutsch, C.V. 2014. Projection pursuit multivariate transform. *Mathematical Geosciences*, vol. 46. pp. 337–359. DOI 10.1007/s11004-013-9497-7

Boucher, A. and Dimitrakopoulos, R. 2012. Multivariate block-support simulation of the Yandi Iron Ore Deposit, Western Australia. *Mathematical Geosciences*, vol. 44. pp. 449–468.

Chilès, J.P. and Defliner, P. 2012. Geostatistics: Modeling Spatial Uncertainty. 2nd edn. Wiley, New York. 699 pp.

Desbarats, A. and Dimitrakopoulos, R. 2000. Geostatistical simulation of regionalized pore-size distributions using min/max autocorrelation factors. *Mathematical Geology*, vol. 32. pp. 919–942.

De-Vitry, C. 2010. Simulation of correlated variables. A comparison of approaches with a case study from the Tandi Channel Irom Deposit. MSc thesis, University of Adelaide, Australia.

Goovaerts, P. 1993. Spatial orthogonality of the principal components computed from coregionalized variables. *Mathematical Geology*, vol. 25. pp. 281–302

Goovaerts, P. 1997. Geostatistics for Natural Resources Evaluation. Oxford University Press, New York.

Hosseini, S.A. and Asghari, O. 2014. Simulation of geometallurgical variables through stepwise conditional transformation in Sungun copper deposit, Iran. *Arabian Journal of Geosciences*. DOI 10.1007/s11004-012-9402-9.

Hotelling, H. 1933. Analysis of a complex of statistical variables into principal components. *Journal of Educational Psychology*, vol. 24. pp. 417–441.

Isaaks, E.H. 1990. The application of Monte Carlo methods to the analysis of spatially correlated data. PhD thesis, Stanford University.

Journel, A.G. 1974. Geostatistics for conditional simulation of orebodies. *Economic Geology*, vol. 69, no. 5. pp. 673–687.

Lantuejoul, C. 2002. Geostatistical Simulation: Models and Algorithms. Springer, New York.

Leuangthong, O. and Deutsch, C.V. 2003. Stepwise conditional transformation for simulation of multiple variables. *Mathematical Geology*, vol. 35, no. 2. pp. 155–173.

Leuangthong, O., Hodson, T., Rolley, P., and Deutsch, C.V. 2006. Multivariate simulation of Red Dog Mine, Alaska, USA, *CIM Bulletin*, May. pp. 1–26.

Job, M.R. 2012. Application of logratios for geostatistical modelling of compositional data. Master's thesis. University of Alberta.

Montoya, C., Emery, X., Rubio E., and Wiertz, J. 2012. Multivariate resource modelling for assessing uncertainty in mine design and mine planning. *Journal of the Southern African Institute of Mining and Metallurgy*, vol. 112. pp. 353–363.

Mueller, U.A. and Ferreira, J. 2012. The U-WEDGE transformation method for multivariate geostatistical simulation. *Mathematical Geosciences*, vol. 44. pp. 427–448.

Pawlowsky-Glahn, V. and Olea, R. 2004. Geostatistical Analysis of Compositional Data. Oxford University Press, New York.

Rondon, O. and Tran, T. 2008. Multivariate simulation using Min/Max autocorrelation factors: practical aspects and case studies in the mining industry. *Geostatistics 2008, Proceedings of the 8th International Geostatistical Congress*. Ortiz, J.M. and Emery, X. (eds). Springer-Verlag, Dordrecht. pp. 268–278.

Rosenblatt, M. 1952. Remarks on a multivariate transformation. *Annals of Mathematical Statistics*, vol. 23. pp. 470–472.

Rossi, M.E. and Deutsch, C.V. 2014. Mineral Resource Estimation. Springer, New York. p. 184.

Snowden, D.V. 2001. Practical interpretation of mineral resources and ore reserve classification guidelines. *Mineral Resource and Ore Reserve Estimation—the AusIMM Guide to Good Practice*. Edwards, A.C. (ed.). Australasian Institute of Mining and Metallurgy, Melbourne. pp. 643–653.

Switzer, P. and Green, A. 1984. Min/Max autocorrelation factors for multivariate spatial imaging. *Technical Report* no. 6, Department of Statistics, Stanford University. ◆

http://dx.doi.org/10.17159/2411-9717/2016/v116n5a9

Impact of thick alluvial soil on a fractured water-conducting zone: an example from Huainan coal mine, China

by D.W. Zhou*, K. Wu*, L. Li*, and J.W. Yu*

Synopsis

The presence of a fractured water-conducting zone (FWCZ) is of significant importance for the safety of underground mining under water bodies. When a coal mining area is covered with a thick layer of alluvial soil, the height, width, and distribution pattern of the FWCZ in the area shows unique features. The internal mechanism by which thick alluvial soil affects the FWCZ is still unknown. Using the Huainan coal mining area (HCMA) in China as a case study, we investigated the impact of thick alluvial soil on the height, width, and distribution pattern of the FWCZ through numerical simulation using the distinct element method, theoretical derivation, and data validation. The results indicate that a thick layer of alluvial soil inhibits the FWCZ height and increases the FWCZ lateral width. When the soil-to-rock ratio is greater than a certain value (the numerical result in this study is 15:18), the FWCZ height and width are affected by the thick alluvium significantly, and the thick alluvial soil alters the shape of the FWCZ from tall and thin to short and wide. The load exerted by the alluvial soil transfers downward to influence the FWCZ; however, this process is obstructed by the hard strata in the bedrock. Therefore, the vertical and lateral change trends show a similar step pattern. Our results can provide a basis for accurate calculation of the FWCZ height in mining areas with thick alluvial soil, to mitigate mine water hazards and increase the safety of underground mining in coal mines covered with a thick alluvium layer. Moreover, reducing the FWCZ height can help extend the upper extraction limit in coal mines covered with a thick alluvium layer, which reduces the thickness of the impermeable coal pillar and increases coal production.

Keywords

coal mining, thick alluvial soil, fractured water-conducting zone, distinct element method.

Introduction

Coal, being the primary energy source in China, supplies approximately 70% of the national energyrequirement. However, many coal mines in China are threatened by water bodies such as rivers, lakes, reservoirs, and groundwater during coal extraction. Approximately 125 rivers flow through China's coalfields, and more than 200 coal mines are confronted with problems of mining under rivers (Miao *et al.*, 2011; Peng and Zhang, 2007). According to incomplete official statistics, there are 600 major coal mines in China, approximately 285 of which are threatened by water inrushes during mining operations. The total coal reserves threatened by bodies of water are estimated at 2.5 × 10^{10} t (Miao *et al.*, 2011; Peng and Zhang, 2007; Zhang, 2005; Zhang and Shen, 2004; Zhang and Peng, 2005). During extraction from these collieries, water inrushes through fractured water-conducting zones (FWCZs) (Figure 1) into the mining area have caused water disasters (Bai *et al.*, 2013; Bureau *et al.*, 1983; Chen *et al.*, 2013; Guo *et al.*, 2008; He *et al.*, 1991; Industry, 2004; Li and Zhou, 2005; Peng and Zhang, 2007; Peng, 1992; Wang and Park, 2003; Yang *et al.*, 1994; Yuan and Wu, 2003; Yuan *et al.*, 2001; Zhang, 2005; Zhang and Shen, 2004; Zhang and Peng, 2005; Zhang *et al.*, 2002). In some cases, the consequences were catastrophic, leading to partial or even total loss of the mine (Bai *et al.*, 2013; Islam *et al.*, 2009; Li *et al.*, 2013; Peng and Zhang, 2007; Wu *et al.*, 2011, 2015; Yang *et al.*, 2007).

It is well known that, after sufficient extraction of a longwall panel, the original stress balance of the rock mass overlying the stope is disturbed and the overburden strata undergo various degrees of movement, causing subsidence and caving of the overlying rock mass. According to their movement characteristics, the fractured overburden strata can be divided into four zones from bottom to top: the caving zone, fractured zone (or fault zone), bending zone, and alluvial soil zone, as shown in Figure 1 (Brady and Brown, 2004; He *et al.*, 1991; Industry, 2004; Kratzsch, 1983; Miao *et al.*, 2011; Peng and Zhang, 2007; Peng, 1992; Qian *et al.*, 2003, 2010; Qian, 1982; Yuan and Wu, 2003):

- *Caving zone* (immediate roof)—After coal extraction, the immediate roof strata cave irregularly and fall into the void.

* *School of Environment Science and Spatial Informatics, China University of Mining and Technology, Xuzhou, China.*

 ISSN 2225-6253. Paper received Dec. 2014; revised paper received Oct. 2015.

Impact of thick alluvial soil on a fractured water-conducting zone

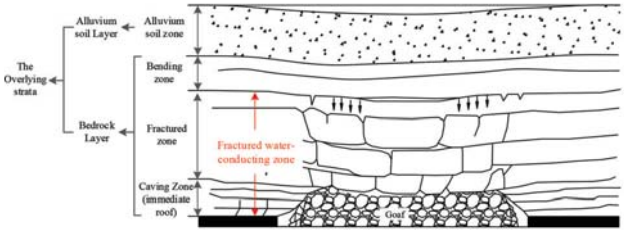

Figure 1—Cross-section of four zones of strata movement above a longwall goaf

The caved strata behave not only completely as a discontinuity, but also irregularly. The caving zone is normally 2–8 times the mining height, depending on the properties of the immediate roof strata

- *Fractured zone*—Stratum breakage and discontinuity are the basic characteristics in this zone, while the rock retains its stratified bedding. The stratum breakage gradually decreases upwards, resulting in a decrease in the fracture network development and, of course, the permeability of the stratum. The combined height of the fractured and caving zones is approximately 20–30 times the mining height in hard or strong rock, 12–15 times in medium-hard rock, and 9–11 times in soft or weak rock
- *Bending zone*—The strata above the fractured zone deflect downward without apparent breakage. The continuity of the strata and the original stratified features remain. In some cases, impermeability is temporarily lost but regained soon afterwards. Some opening fissures may appear in the tension zone but in general the strata maintain continuity
- *Alluvial soil zone*—This zone is the surface layer (also called the Quaternary alluvium layer), and its thickness depends on the location. In China, the coal-mining areas with a Quaternary alluvium layer less than 50 m thick are called thin alluvium mining areas and are the most common. Coal mining areas with an alluvium layer more than 100–300 m thick are known as thick alluvium mining areas, while areas with an alluvium layer more than 300 m thick are known as mega-thick alluvium mining areas. The areas with thick alluvium are widely distributed in China, mainly in Huaibei, Huainan, Yanzhou, Datun, Jiaozuo, Pingdingshan, Yongxia, Kailuan, Xingtai, and other mining areas of east, central, north, and northeast China (He *et al.*, 1991; Industry, 2004; Liu *et al.*, 2012; Zhou, 2014; Zhou *et al.*, 2015). Depending on the physical properties of the soils, cracks may open in the area around the working face and close again after the mining extraction face advances further. However, some cracks, especially those along the edges of the mining panel, may remain open after the mining face has moved on, but the fracture walls tend to collapse and fill in the cracks.

As shown in Figure 1, the caving zone and the fractured zone are jointly termed the FWCZ, and the bending zone and the FWCZ are jointly called the bedrock layer. The entire range of overlying strata includes the bedrock layer and the alluvial soil. When mining under water bodies, the FWCZ is critically important, providing access for water inflow into the mine workings due to the increased hydraulic conductivity in this zone.

In safe mining practice, an impermeable coal pillar is usually left in place to prevent groundwater or surface water from flowing into mining workings through the mining-induced fractured zone (He *et al.*, 1991; Industry, 2004; Peng and Zhang, 2007; Peng, 1992; Yuan and Wu, 2003; Zhang, 2005; Zhang and Shen, 2004; Zhang and Peng, 2005; Zhang *et al.*, 2002). The impermeable pillar enables successful seam extraction with neither water inrush nor excessive groundwater discharge into the mine. This practice requires that the fractured zone does not penetrate upwards into the overlying aquifers. Normally, the minimum height of the impermeable pillar must be not less than the maximum height of the fractured zone plus the height of a protective layer (He *et al.*, 1991; Industry, 2004; Peng and Zhang, 2007).

$$H_w \geq H_f + H_p \quad [1]$$

where H_w is the vertical height of the impermeable pillar, H_f is the maximum vertical height of the fractured zone, and H_p is the height of the protective layer. For example, the thickness of the impermeable coal pillar in the south mining area of the Huainan coal mining area (HCMA) under common geological conditions is 80 m (Bureau *et al.*, 1983; Wang, 1999; Yuan and Wu, 2003; Zhang *et al.*, 2002). Therefore, a large amount of coal contained in the impermeable coal pillar cannot be extracted, which represents a loss of coal resources.

Due to the importance of the FWCZ, there has been much interest in studies of the FWCZ in mining research (Bureau *et al.*, 1983; Gui *et al.*, 1997; He *et al.*, 1991; Industry, 2004; Lu and Wang, 2015; Ma *et al.*, 2013; Miao *et al.*, 2011; Peng and Zhang, 2007; Peng, 1992; Qian *et al.*, 2003, 2010; Teng, 2011; Tu, 2004; Wang *et al.*, 2003; Wu *et al.*, 2008; Xu *et al.*, 2010; Yang and Gao, 1982; Yuan and Wu, 2003; Yuan *et al.*, 2015; Zhang, 2005; Zhang and Shen, 2004; Zhang and Peng, 2005). These studies show that the main factors influencing the height and distribution pattern of the FWCZ are the lithology of the strata, the coal mining method, and the thickness of the overlying strata. According to recent data for the height of the FWCZ in thick -alluvium coal mining areas, the height, width, and distribution pattern of the mining-induced FWCZ in these areas differs from those in thin alluvium coal mining areas. Therefore, the influence of thick alluvial soil on the FWCZ must be taken into account. Based on the measured data for a longwall panel in the Yanzhou mining area, where fully mechanized mining was taking place, Teng (2011) found that the thick alluvial soil layer inhibited the height of the FWCZ. We found a similar phenomenon when analysing data from the FWCZ of the HCMA. Although this phenomenon has been recorded, the process and internal mechanism are unknown and need to be investigated. Despite recent studies on the FWCZ, a number of issues remain unresolved:

- Current research is focused more on calculation and prediction of the height than on the width of the FWCZ. However, the lateral extent of the zone is related to the inrushing of water from the old goaf adjacent to the mining area

- Research on the FWCZ in thick alluvium coal mining areas is relatively sparse, especially studies on the impact of thick alluvial soil on the FWCZ.

Using the Huainan mining areas as a case study, this paper investigates the impact of thick alluvial soil on the height, width, and distribution pattern of the FWCZ through numerical simulation, theoretical derivation, and validation with measured data, while providing a reference for an accurate calculation of the FWCZ height. Our results can be used by engineers and mining personnel to increase the safety of underground mining and to reduce the size of the impermeable coal pillars in order to increase the extraction of coal and boost production.

Geological and mining conditions of HCMA

The HCMA near the Huaihe River, China is divided into two mining areas; the 'South Area' and the 'North Area'. The layout of the mining areas is shown in Figure 2. As the two areas are part of the same coalfield, their lithologies are basically the same (Yang *et al.*, 1994; Yuan and Wu, 2003; Zhou, 2014; Zhou *et al.*, 2015). The main difference between the two areas is the thickness of the Quaternary alluvial soil layer; the thickness in the North Area is 160–500 m, while that in the South Area is only 20–40 m. This difference in the alluvial soil layer thickness provides favourable conditions for research into the impact of the layer thickness on the FWCZ.

The coal-bearing strata of the HCMA belong to the Carboniferous–Upper Permian Taiyuan Group and the Permian Lower Shanxi Group and Shihezi Group. There are 8–10 mineable coal seams in the stratum; the seams are relatively regular, and the dip is nearly flat in the North Area. The geological structure is complex; the mining depth is 500–900 m in the North Area, and the bedrock is covered with thick alluvial soil. The mining depth in the South Area is around 300 m. The lithology of the coal-seam roof and floor is mainly mudstone, sandy mudstone, and sandstone, of medium hardness (Yuan and Wu, 2003; Zhou, 2014; Zhou *et al.*, 2015).

Numerical simulation and related parameters

The Universal Distinct Element Code (UDEC) is a two-dimensional numerical program based on the distinct element method for discontinuous modeling (Cundall, 1988; ITASCA Consulting Group, 2004; Hart *et al.*, 1988; Jing, 2003) and is frequently used in rock mechanics (ITASCA Consulting Group, 2004; Moarefvand and Verdel, 2008). It is particularly suited for analysing fractured masses and large displacements along discontinuities (Cundall, 1988, 1990; ITASCA Consulting Group, 2004; Hart *et al.*, 1988; Jing, 2003; Moarefvand and Verdel, 2008; Xu and Zhang, 2002). We used UDEC4.0 for the numerical simulations in this study.

A numerical model was established for simulating a working face in HCMA with measured geological conditions. The thickness of the coal seam in the working face is 4 m on average, the average dip angle is nearly flat, and the working face is a longwall panel face with bedrock layer thickness of approximately 180 m covered by 400 m of alluvial soil (the total thickness of the overlying strata is approximately 580 m). The length of the working face is approximately 800 m and the width approximately 120 m. Fully mechanized coal-mining technology is employed, and the roof is managed with longwall full caving.

According to the geo-mining conditions, the length of the model is 1200 m; the goaf runs along the coal seam with a length of 800 m (along the length of the working face), starting at 200 m from the left edge and extending to 1000 m from the left edge of the model; and the mining height is 4 m. The interval of mining is approximately 80 m. The open-off cut is located at the left of the model and the terminal line is at the right (Figure 3).

In the model, the bedrock thickness was fixed at 180 m, and the coal seam was nearly horizontal. Ten models were constructed with alluvial soil thicknesses of 0, 50, 100, 150, 200, 250, 350, 400, and 450 m. The models are based on the Mohr-Coulomb criterion. The main physical parameters of the bedrock layers in the model are shown in Table I. These parameters were obtained by field observations in HCMA. The left and right boundaries of the model have a single constraint, the lower boundary is fully constrained, and the upper boundary is free. The horizontal observation lines are spaced at 5 m intervals in the strata above the coal seam, and the interval between the observation points on the observation lines is 10 m.

Criteria determination for the FWCZ

FWCZ height

Based on the type of damage in the overlying rock caused by the coal mining, the strata can be divided into five zones

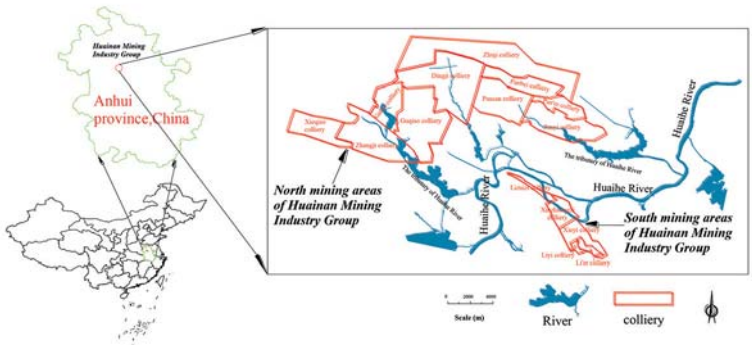

Figure 2—Layout of North Area and South Area of the HCMA

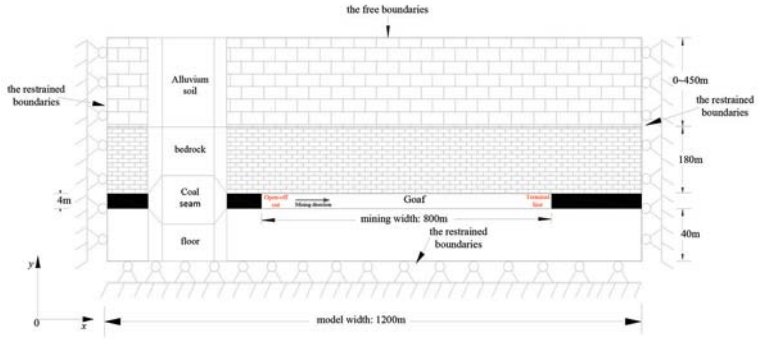

Figure 3—Schematic section of the calculation model

Table I

The main physical parameters of the bedrock layers in the model

No.	Lithology	Tensile strength (MPa)	Elasticity modulus (GPa)	Cohesion (MPa)	Internal friction angle (°)	Density (kg.m^{-3})	Poisson's ratio	Normal stiffness coefficient (GPa)	Shear stiffness coefficient (GPa)
1	Alluvial soil	0.05	1.50	0.074	24	2000	0.29	0.5	0.3
2	Siltstone	1.60	1.60	4.50	28	2570	0.25	10	8
3	Quartz sandstone	2.30	3.73	11.00	41	2730	0.24	10	8
4	Sandy mudstone	1.60	2.00	2.50	33	2530	0.22	10	8
5	Mudstone	1.26	1.80	2.32	27	2520	0.26	10	8
6	Medium sandstone	5.03	3.10	10.10	37	2600	0.23	10	8
7	Siltstone	2.02	2.60	2.80	32	2570	0.21	10	8
8	Argillaceous siltstone	1.80	2.50	5.66	30	2500	0.16	6	4
9	Silty fine sand	5.80	2.70	2.20	35	2500	0.202	6	4
10	Mudstone	1.43	1.95	1.68	27	2520	0.15	6	4
11	Sandy mudstone	2.70	2.40	2.50	32	2500	0.20	6	4
12	Coal	1.10	1.20	0.80	20	1400	0.23	0.8	0.4
13	Medium sandstone	5.14	2.20	8.50	40	2600	0.134	6	4
14	Silty fine sand rock	3.12	1.50	5.50	33	2550	0.14	6	4

(Figure 4). The characteristics of the five sections are as follows (Cui *et al.*, 2000; Gui *et al.*, 1997; Huang *et al.*, 2006; Kirsten and Stacey, 1989; Wu *et al.*, 2008):

- *Area I* (undamaged area)—the elastic zone where the rock mass is not damaged
- *Area II* (plastic deformation area)—strong rock suffers plastic deformation, and brittle rock is subject to shear failure
- *Area III* (tensile fracture zone)—tensile stress in a certain direction exceeds the tensile strength of the rock mass and generates tension cracks in this direction
- *Area IV* (tensile damage zone)—under the influence of two-way tensile stress, the stratum breaks, resulting in a large deformation, identified as the caving zone
- *Area V* (fractured zone in the local tension zone)—because the overburden rock subsides above the goaf, local fractures occur under the action of tensile stress on the edge of the subsidence basin.

Based on the analysis above, we determine the criterion for the FWCZ height as follows: the FWCZ extends vertically from the upper boundary of the tensile fracture zone to the upper boundary of the tensile damage zone.

Lateral width of FWCZ

After coal mining, the original internal stress of the rock mass is disrupted and the stress is redistributed. Stress is concentrated in the abutment rock surrounding the goaf, causing plastic deformation. Based on the stress and deformation distribution, we can identify four areas that are formed, from the goaf boundary through the surrounding rock (Liu, 2008; Qian *et al.*, 2010; Yuan and Chen, 1986): (A) the fractured zone, (B) the plastic zone, (C) the elastic zone, and (D) the original stress zone. The distribution and stress variation characteristics of the four deformation zones are shown in Figure 5. The strength of the rock mass in the fractured zone is significantly reduced, becoming lower than the original stress *rH* and leaving only a residual strength to support the external load. This leads to fracturing of the rock

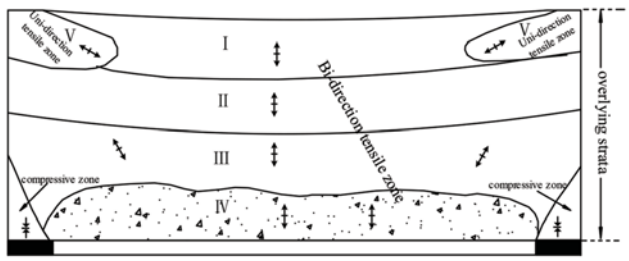

Figure 4—Principal stress distribution and destruction zones in overlying strata after mining (Gui *et al.*, 1997)

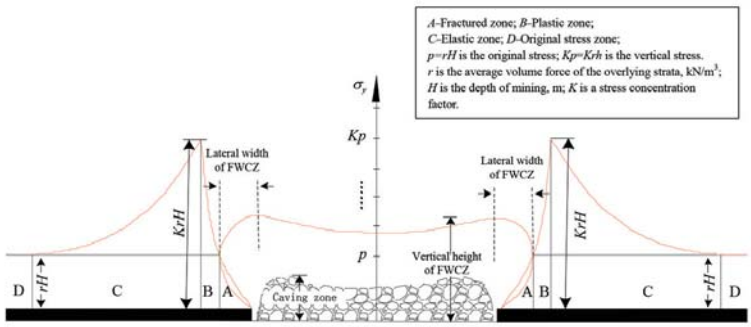

Figure 5—Vertical stress and deformation distribution of the mined-out area

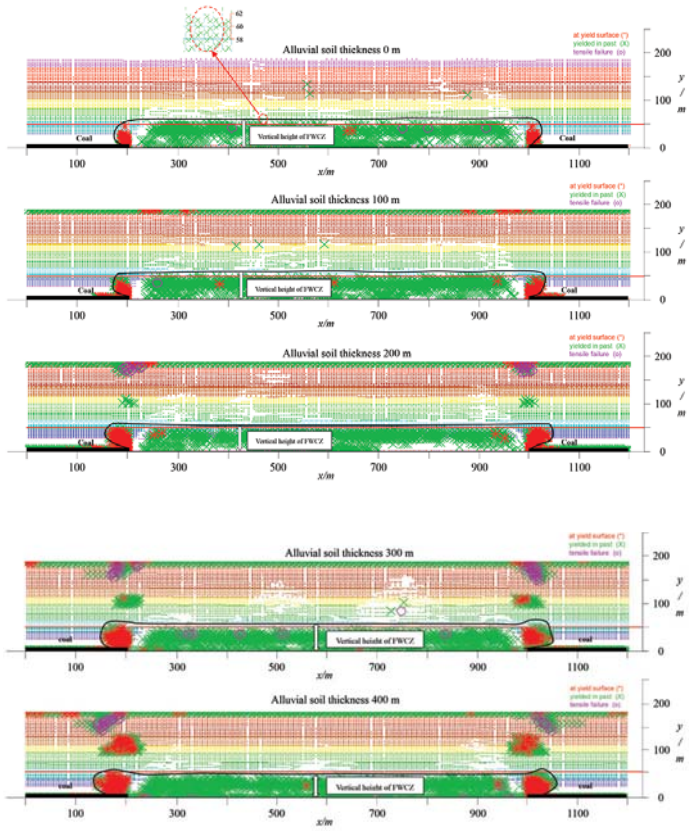

Figure 6—Diagrams of deformation distribution in the FWCZ after mining (mining scope is from 200 m to 1000 m)

mass and displacement in the 'stress-reducing area'. The internal stresses in the plastic and elastic zones are higher than the original stress; hence these zones are known as the 'increased stress area'.

Based on the analysis above, we determine the boundaries on both sides of the fracture zone as the width boundaries of the FWCZ (Figure 5).

Simulation results and discussion

Effects on the height of the FWCZ

The distribution of deformation in the FWCZ after mining with various alluvium thicknesses is shown in Figure 6. Based on the criteria for determining the FWCZ height, the heights for different alluvium thicknesses can be obtained, as shown in Table II. The vertical height in the models is measured by first determining the distribution zone of deformation, and then counting the grids, because the distance between grids is fixed.

Note: The vertical heights of the FWCZ shown in Figure 6 are quite close to each other (refer to the Table II); in order to express the results more clearly, we present the data in Figure 6 at intervals of 100 m thickness of the alluvium layer.

We define the ratio of alluvial soil thickness to the thickness of bedrock layer as the soil-to-rock ratio and use it as a standard to evaluate the effect of the alluvial soil on the FWCZ. Table II presents the FWCZ heights for different values of alluvial soil thickness. The relationship between the FWCZ height and the soil-to-rock ratio is shown in Figure 7.

From the simulation results, we can draw the following conclusions:

- From the overall trend, as the thickness of the alluvial soil layer increases, the height of the FWCZ is reduced to a certain level, which reflects the inhibition of the FWCZ height by the thick alluvium layer. According to the results of the simulations, when the soil-to-rock ratio is less than 10:18, the height of the FWCZ does not change significantly. When the ratio is greater than 15:18, the FWCZ height is considerably affected by the thick alluvium
- Through numerical simulation and theoretical analysis, we observe that when the alluvium is thick enough, it will transfer a load down to the goaf; as the alluvium thickness increases, the stress in the bedrock and goaf increases and the broken rock mass inside the caving zone in the goaf is increasingly compacted under the alluvium load. The expansion of broken rock decreases, and the fracturing and bed separation within the fracture zone become more packed, thus inhibiting the development of the FWCZ vertically
- Figure 7 and Table II show that the reduction in FWCZ height is stepped and not continuous. The main reason for this is that the process of transferring the thick alluvium load is related to the lithology of the strata, that is, it is impacted by the hard rock layer, *i.e.* the key stratum (Qian *et al.*, 2003; Qian, 1982). When the soil-to-rock ratio reaches 15:18, the effect of the first hard stratum (stratum 6 in Table I) is attenuated and the alluvium load is transmitted downward, which affects the development of the FWCZ height. When the ratio reaches 35:18, the alluvium load will break through the second hard rock stratum (stratum 9 in Table I), and the load will be transmitted down to the goaf, resulting in further reduction of the FWCZ height. However, the underground goaf space is limited (4 m goaf width) and the rock fracture and separation zone is limited; therefore the height of the FWCZ does not decrease indefinitely, but tends to gradually stabilize.

Table II

FWCZ height for different values of alluvial soil thickness

Thickness of alluvium (m)	Thickness of bedrock mass (m)	Soil-to-rock ratio	FWCZ height (m)
0	180	0:18	62
50	180	5:18	62
100	180	10:18	62
150	180	15:18	54
200	180	20:18	54
250	180	25:18	54
300	180	30:18	54
350	180	35:18	48
400	180	40:18	48
450	180	45:18	48

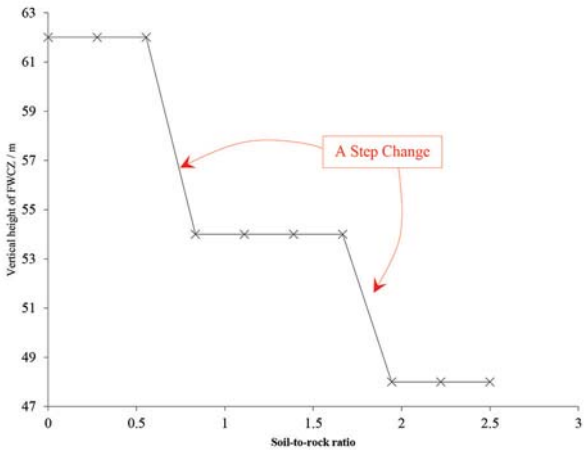

Figure 7—Relationship between the vertical height of the FWCZ and the soil-to-rock ratio

Effects on the width of the FWCZ

The vertical stresses in the roof strata and fracture zone are shown in Figure 8. Note that here, too, we present the data at 100 m intervals of the alluvium layer thickness in Figure 8; if it were drawn at 50 m intervals, Figure 8 would be too crowded be clearly understood. Table III provides statistics of the FWCZ width. The relationship between the width and the soil-to-rock ratio is shown in Figure 9.

From the simulation results, we can draw the following conclusions:

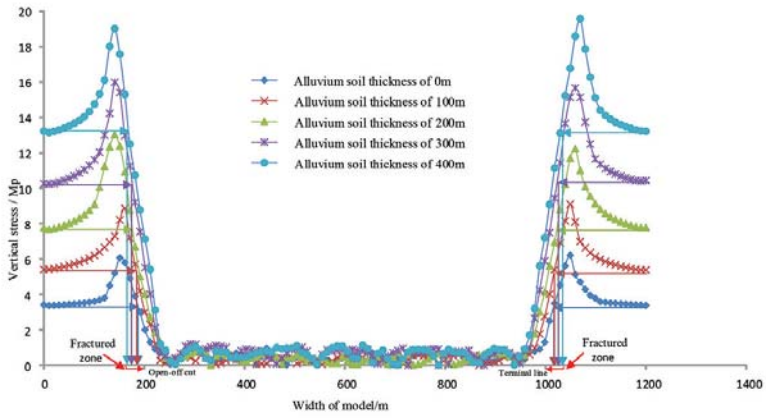

Figure 8—Roof vertical stress and coal stratum fractured zone distribution (mining scope of coal seam is 200–1000 m)

- The width of the FWCZ increases with the alluvium thickness. In the process of coal mining, the area above the goaf is the unloading area while the area above the two sides of the coal pillar is an area of stress concentration. Under the effect of compressive stress, plastic deformation occurs on both sides of the rock mass; with increased alluvial soil thickness, the compressive stress at the top of the coal pillar rises and the width of the FWCZ increases
- Since the alluvium load is affected by lithology as it spreads down through the strata, the trends for width are similar to those for height, also showing step changes. Because the bearing capacity of hard rock is quite high, the alluvium load at the initial stage (where the soil-to-rock ratio is less than 15:18) has a smaller effect on the goaf. When the soil-to-rock ratio reaches 15:18, because the rock mass has a strain-softening characteristic (Liu, 2008; Qian *et al.*, 2010; Yuan and Chen, 1986), the alluvium load reaches or becomes greater than the threshold load level of the first layer of hard rock and the strength of the rock mass itself is attenuated. The load is then transmitted down, and the FWCZ width increases from 12 m to 22 m. When the soil-to-rock ratio reaches 35:18, the strength of the second layer of hard rock is attenuated and the lateral width increases from 30 m to 32 m. Therefore, the FWCZ in thick alluvium mining areas is more likely to intersect the FWCZ in the adjacent old goaf at the lateral boundary, which can lead to water flowing from the old goaf into the mining area (Xu *et al.*, 2010).

Table III

Lateral width of the FWCZ for different alluvium thickness

Thickness of alluvium (m)	Thickness of bedrock mass (m)	Soil-to-rock ratio	Lateral width of the FWCZ (m)
0	180	0:18	12
50	180	5:18	12
100	180	10:18	13
150	180	15:18	22
200	180	20:18	22
250	180	25:18	22
300	180	30:18	22
350	180	35:18	30
400	180	40:18	32
450	180	45:18	32a

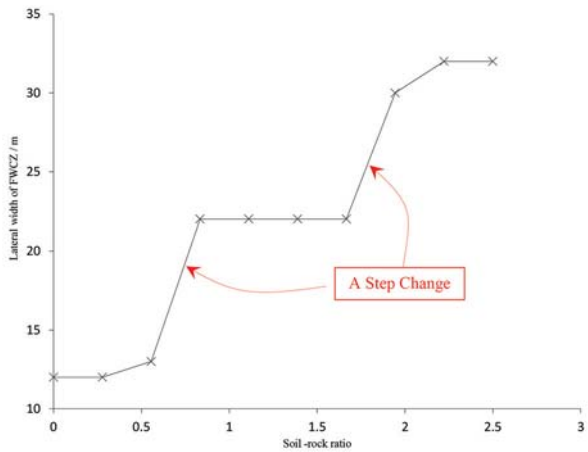

Figure 9—Relationship between the lateral width of the FWCZ and the soil-to-rock ratio

Comprehensive analysis

According to the simulation results, under the influence of a thick alluvium layer, the FWCZ height decreases and its width increases. Figure 10 shows the effect of alluvial soil thickness on the height and width of the FWCZ and its distribution pattern. The following patterns can be observed.

- When the alluvium is thick enough (soil-to-rock ratio in simulation > 15:18), the load of the thick alluvium layer is transferred to the strata below, affecting the fractured rock mass and bed separation in the goaf. This affects the height, width, and distribution pattern of the FWCZ. An alluvium layer of a certain thickness will inhibit the height and increase the width of the FWCZ, as shown in Figure 10a–c. The FWCZ changes from a tall and narrow shape (Figure 10a) to a short and wide shape (Figure 10c)
- The thick alluvial soil loads the goaf, compacting the fractured rock mass in the goaf and causing the bed separation to become more closely packed. The displaced space in the rock mass is transferred to the surface in the form of subsidence.

Validation using measured data

Borehole method for validation of FWCZ height

In the HCMA, the height of the FWCZ in the overlying strata during coal mining is ascertained mainly by drilling boreholes from the surface to the rock strata and flushing the

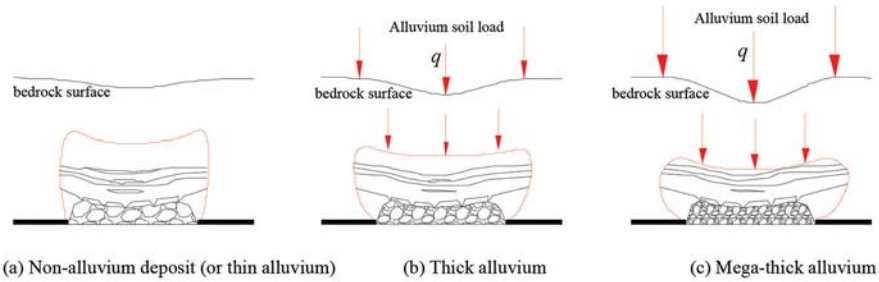

Figure 10—Effect of alluvial soil thickness on the height and width of the FWCZ and its distribution pattern

boreholes with liquid (Luo, 1982; Miao *et al.*, 2011; Yang and Gao, 1982). The permeability of the rock mass is determined mainly by the amount of absorbed liquid. Inside the FWCZ, the fracture growth increases from top to bottom and the permeability is also enhanced. The water flow leading to the fracture can be discharged by permeating through the rock mass to the goaf, but cannot be stored in this zone. The water diffuses and flows vertically inside this zone, unlike the radial flow of groundwater in aquifers. Due to this phenomenon, boreholes have the following characteristics after entering the FWCZ from the top interface of the overlying strata:

- Leakage of flushing liquid, where the amount of leakage increases with the drilling depth. After the feed stops, the water level of the borehole drops to the bottom of the hole
- Suction phenomena occur, that is, when the drill is at the bottom of the hole, the pump stops, the steel ball inside the pump bounces, and the borehole begins to draw down water. The amount of water that is drawn down is subject to the pipe impermeability, depth of drilling, and other factors
- After drilling to a certain depth, the penetration rate increases; voids and cross-holes can occur regularly.

Based on the above characteristics, we can determine when the borehole has entered the top interface of the FWCZ. Figure 11 presents the layout of observation boreholes and the development of the FWCZ.

Analysis of measured data

In this study, 15 data-points were measured for the height of FWCZs in the North Area and South Area of the HCMA. Figures 12 and 13 compare the heights of the FWCZ in the North Area and South Area with different coal mining methods.

Figure 12 shows the measured height of the FWCZ in nine boreholes in the North Area and South Area under conditions of drill-and-blast mining. The average height is 29.2 m in the North Area and 32.5 m in the South Area.

Figure 13 shows the measured height of the FWCZ in four boreholes in the North Area and South Area under conditions of fully mechanized mining. The average height is 40.6 m in the North Area and 45.6 m in South Area.

The most significant difference between the North Area and South Area is the thickness of the alluvial soil (the North Area is a thick alluvium mining area and the South Area is a thin alluvium mining area). According to the measured data, the FWCZ height in the North Area is lower than in the South Area: approximately 11.3% lower under drill-and-blast

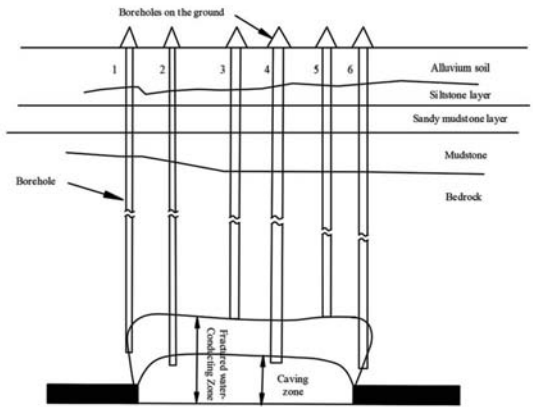

Figure 11—Layout of observation boreholes and development of the FWCZ

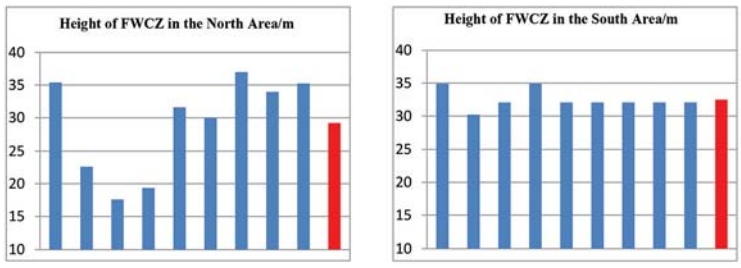

Figure 12—Comparison of measured FWCZ heights in the North Area and South Area of HCMA under longwall blasting mining. The red column represents the average of the nine data-points (soil-to-rock ratio 1.6–4.7)

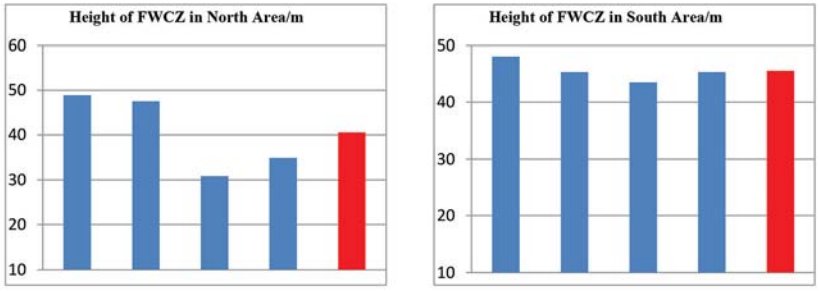

Figure 13—Comparison of measured FWCZ heights in North Area and South Area of HCMA under longwall fully-mechanized coal mining. The red column represents the average of the four data points (soil-to-rock ratio 1.6–4.7)

mining conditions and 12.3% lower under fully mechanized mining conditions. This indicates that the thick alluvium layer in the North Area has an inhibitory effect on the height of the FWCZ, which agrees with the simulation results.

The reduction in FWCZ height is helpful for extending the upper extraction limit in coal mines covered with a thick layer of alluvial soil and reducing the thickness of the impermeable coal pillar. For example, the upper extraction limit for the North Area of the HCMA can be extended up by 12.3% under fully mechanized mining conditions. As stated above, the thickness of the impermeable coal pillar in the South Area of HCMA is 80 m. Therefore, the thickness of the impermeable coal pillar in the North Area of HCMA can be reduced by 12.3%, which allows an additional 9.8 m of coal seam thickness to be extracted, greatly increasing coal production.

Conclusions

The following major conclusions can be drawn from this study.

- According to the results of the numerical simulation and measured data, a certain thickness of alluvial soil layer inhibits the height of the FWCZ. When the soil-to-rock ratio is greater than a certain value (the value in the numerical simulation of this paper is 15:18), this can significantly affect the vertical height of the FWCZ. Moreover, an alluvium layer of a certain thickness increases the width of the FWCZ. Under the influence of thick alluvium, the overall shape of the FWCZ changes from long and thin to short and wide
- The internal mechanism of the impact of thick alluvium on the FWCZ is as follows. The load from the thick alluvium spreads to the underlying rock mass, affecting the fractured rock mass above the goaf and the bed separation in the goaf. This affects the height, width, and distribution pattern of the FWCZ. When the thickness of alluvium increases, the fractured rock mass in the caving zone in the goaf is more compressed under the alluvium load, and the expansion of the broken rock decreases; the fracturing and bed separation inside the fractured zone tends to become more closely packed, thus inhibiting and reducing the height of the FWCZ. However, the space in the broken rock mass, fractured areas, and bed separation is limited. The reduction in FWCZ height is helpful for extending the upper extraction limit in coal mines covered with a thick layer of alluvial soil and reducing the thickness of the impermeable coal pillar, which greatly increases coal production.

Acknowledgements

The research was financially supported by the Priority Academic Program Development of the Jiangsu Higher Education Institutions (PAPD), Natural Science Foundation of Jiangsu Province under Grant No. BK20150187, the National Technology Support Programs of China during the Twelfth Five-Year Plan Period under Grant No. 2012BAC04B03, and The Scientific Research Foundation of the Jiangsu Key Laboratory of Resources and Environmental Information Engineering (China University of Mining and Technology), approval number JS201109. All these sources are gratefully acknowledged. We thank Professor Axel Preusse and his PhD student Markus Papst from RWTH Aachen University for improving the English of the paper. The authors are also deeply grateful to the anonymous reviewers for their very constructive criticism and suggestions, which led to the improvement of the paper.

References

Bai, H., Ma, D., and Chen, Z. 2013. Mechanical behavior of groundwater seepage in karst collapse pillars. *Engineering Geology*, vol. 164. pp. 101–-106.

Brady, B.H.G. and Brown, E.T. 2004. Rock Mechanics For Underground Mining. Springer, New York.

Bureau, H.C.M., Mine, L.T.Z.C., and Branch, T.C. 1983, Mining under the Huaihe River and its embankment. *Mine Surveying*, no. 1. pp. 26–33 (in Chinese).

Chen, L., Zhang, S., and Gui, H. 2013. Prevention of water and quicksand inrush during extracting contiguous coal seams under the lowermost aquifer in the unconsolidated Cenozoic alluvium—a case study. *Arabian Journal of Geosciences*, vol. 7, no. 6. pp. 2139–2149.

Cui, X., Miao, X., Wang, J., Yang, S., Liu, H., Song, Y., Liu, H., and Hu, X. 2000. Improved prediction of differential subsidence caused by underground mining: *International Journal of Rock Mechanics and Mining Sciences*, vol. 37. pp. 615–627.

Cundall, P.A. 1988. Formulation of a three-dimensional distinct element model Part I. A scheme to detect and represent contacts in a system composed of many polyhedral blocks. *International Journal of Rock Mechanics and Mining Sciences*, vol. 25, no. 3. pp. 107–116.

Cundall, P.A. 1990. Numerical modeling of jointed and faulted rock. *Proceedings of the International Conference on Mechanics of Jointed and Faulted Rock*, Vienna, Austria. Rossmanith, H. P. (ed.). AA Balkema, Rotterdam. pp. 11–18.

Gui, H.R., Zhou, Q.F., Liao, D.S., Kang, Q.G., and Fan, Z.Y. 1997. Prediciton of maximum height of the fractured zone by stressing method for sub-level caving mining. *Journal of China Coal Society*, vol. 22, no. 4. pp. 375–379 (in Chinese with English abstract).

Guo, H., Adhikary, D.P., and Craig, M.S. 2008. Simulation of mine water inflow and gas emission during longwall mining. *Rock Mechanics and Rock Engineering*, vol. 42, no. 1. pp. 25–51.

Hart, R., Cundall, P.A., and Lemos, J. 1988. Formulation of a three-dimensional distinct element model Part II. Mechanical calculations for motion and interaction of a system composed of many polyhedral blocks. *International Journal of Rock Mechanics and Mining Sciences*, vol. 25, no. 3. pp. 117–125.

He, G., Yang, L., Ling, G., Jia, C., and Hong, D. 1991. Mining Subsidence Science. University of Mining and Technology Press, Xuzhou, China (in Chinese).

Huang, Z.A., Tong, H.F., Zhang, Y.H., Li, S.B., Ni, W., Song, J.G., and Xing, Y. 2006. Dividing guideline and emulating determination of 'three zones' of the depressing zones overlying a goaf. *Journal of University of Science and Technology Beijing*, vol. 28, no. 7. pp. 609–612 (in Chinese with English abstract).

Industry, S.B.O.C. 2004, The regulation of leaving coal pillar and mining coal of holding under the buildings, water bodies, railways and the main roadway. Coal Industry Press, Beijing (in Chinese).

Islam, M.R., Hayashi, D., and Kamruzzaman, A.B.M. 2009. Finite element modeling of stress distributions and problems for multi-slice longwall mining in Bangladesh, with special reference to the Barapukuria coal mine: *International Journal of Coal Geology*, vol. 78, no. 2. pp. 91–109.

ITASCA Consulting Group. 2004. UDEC Manual. Minneapolis, Minnesota, USA.

Jing, L. 2003. A review of techniques, advances and outstanding issues in numerical modelling for rock mechanics and rock engineering: *International Journal of Rock Mechanics and Mining Sciences*, vol. 40, no. 3. pp. 283–353.

KIRSTEN, H.A.D. and STACEY, T.R. 1989. Stress-displacement behaviour of the fractured rock around a deep tabular stope of limited span. *Journal of the South African Institute of Mining and Metallurgy*, vol. 89, no. 2. pp. 47–58.

KRATZSCH, H. 1983. Mining Subsidence Engineering. Springer-Verlag, Berlin.

LI, G. and ZHOU, W. 2005. Impact of karst water on coal mining in North China. *Environmental Geology*, vol. 49, no. 3. pp. 449–457.

LI, T., MEI, T., SUN, X., LV, Y., SHENG, J., and CAI, M. 2013. A study on a water-inrush incident at Laohutai coalmine. *International Journal of Rock Mechanics and Mining Sciences*, vol. 59. pp. 151–159.

LIU, J.J. 2008. Analysis and calculation on parameters of stress distribution of the front coal mining face. *Journal of China Coal Society*, vol. 33, no. 8. pp. 745–747 (in Chinese with English abstract).

LIU, Y., DAI, H., and JIANG, Y. 2012. Model test for mining-induced movement law of rock and soil mass under thick unconsolidated layers. *Journal of Mining and Safety Engineering*, vol. 29, no. 5. pp. 268–272 (in Chinese with English abstract).

LU, Y. and WANG, L. 2015. Numerical simulation of mining-induced fracture evolution and water flow in coal seam floor above a confined aquifer. *Computers and Geotechnics*, vol. 67. pp. 157–171.

LUO, J. 1982. Determination of the interface of fractured water-conducting zone by drilling boreholes. *Coal Geology and Exploration*, no. 1. pp. 53–56 (in Chinese).

MA, L., ZHANG, D., SUN, G., CUI, T., and ZHOU, T. 2013. Thick alluvium full-mechanized caving mining with large mining height face roof control mechanism and practice. *Journal of China Coal Society*, vol. 38, no. 2. pp. 199–203 (in Chinese with English abstract).

MIAO, X., CUI, X., WANG, J.AA., and XU, J. 2011. The height of fractured water-conducting zone in undermined rock strata. *Engineering Geology*, vol. 120, no. 1–4. pp. 32–39.

MOAREFVAND, P. and VERDEL, T. 2008. The probabilistic distinct element method. *International Journal for Numerical and Analytical Methods in Geomechanics*, vol. 32, no. 5. pp. 559–577.

PENG, S. and ZHANG, J. 2007. Engineering Geology for Underground Rocks. Springer, New York.

PENG, S.S. 1992. Surface Subsidence Engineering. Society for Mining, Metallurgy and Exploration, Littleton, CO.

QIAN, M.G., MIAO, X.X., XU, J.L., and MAO, X.B. 2003. Study of Key Strata Theory in Ground Control. China University of Mining and Technology Press, Xuzhou (in Chinese).

QIAN, M.G. 1982. A study of the behavior of overlying strata in longwall mining and its application to strata control. *Proceedings of the Symposium on Strata Mechanics*, Newcastle-on-Tyne, 5–7 April 1982. Elsevier Scientific Publishing, New York. pp. 13–17.

QIAN, M.G., SHI, P.W., and XU, J.L. 2010. Mining Pressure and Strata Control. China University of Mining and Technology Press, Xuzhou (in Chinese).

TENG, Y.H. 2011. Development features and max height calculation of water conducted fractured zone caused by fully mechanized top coal caving mining. *Coal Science and Technology*, vol. 39, no. 4. pp. 118–120 (in Chinese with English abstract).

TU, M. 2004. Study on the growth height of separation fracture of mining rock in Panxie area. *Journal of China Coal Society*, vol. 29, no. 6. pp. 641–645 (in Chinese with English abstract).

WANG, G.C. 1999. Preliminary approach of increasing the upper limit of extraction in Pan-xie mining area. *Journal of Huainan Institute of Technology*, vol. 19, no. 1. pp. 40–44 (in Chinese).

Wang, J.A. and Park, H.D. 2003. Coal mining above a confined aquifer. *International Journal of Rock Mechanics and Mining Sciences*, vol. 40, no. 4. pp. 537-551.

WANG, Y., DENG, K., WU, K., and GUO, G. 2003. On the dynamic mechanics model of mining subsidence. *Chinese Journal of Rock Mechanics and Engineering*, vol. 22, no. 3. pp. 352–357 (in Chinese with English abstract).

WU, L., JIANG, Z., CHENG, W., ZUO, X., LV, D., and YAO, Y. 2011. Major accident analysis and prevention of coal mines in China from the year of 1949 to 2009. *Mining Science and Technology* (China), vol. 21, no. 5. pp. 693–699.

WU, Q., LIU, Y., LUO, L., LIU, S., SUN, W., and ZENG, Y. 2015. Quantitative evaluation and prediction of water inrush vulnerability from aquifers overlying coal seams in Donghuantuo Coal Mine, China. *Environmental Earth Sciences*, vol. 74, no. 2. pp. 1429–1437.

WU, X., WANG, X.G., DUAN, Q.W., YU, Q.C., YANG, J., and SUN, Y.D. 2008. Numerical modeling about developing high of water flowing fractured zone. *Journal of China Coal Society*, vol. 33, no. 6. pp. 609–612 (in Chinese with English abstract).

XU, G., XU, J.L., LU, W.Y., and FAN, D.Y. 2010. Lateral boundary prediction of water conducting fracture formed in roof and its application. Chinese *Journal of Geotechnical Engineering*, vol. 32, no. 5. pp. 724–730 (in Chinese with English abstract).

XU, Y. and ZHANG, Y. 2002. Deformation characteristics of thick unconsolidated layers due to mining by UDEC. *Journal of China Coal Society*, vol. 27, no. 3. pp. 268–272 (in Chinese with English abstract).

YANG, B. and GAO, D. 1982. Determination of top boundary of fractured water-flowing zone by drilling simple hydrogeological method. *Mine Surveying*, no. 1. pp. 53–56 (in Chinese).

YANG, T.H., LIU, J., ZHU, W.C., ELSWORTH, D., THAM, L.G., and TANG, C.A. 2007. A coupled flow-stress-damage model for groundwater outbursts from an underlying aquifer into mining excavations. *International Journal of Rock Mechanics and Mining Sciences*, vol. 44, no. 1. pp. 87–97.

YANG, Z.Z., WANG, J.C., and LU, F.W. 1994, Technical counter measures for coal mining under buildings, water-bodies and railways in Huainan coal mines. *Journal of China Coal Society*, vol. 19, no. 1. pp. 5–14.

YUAN, L. and WU, K. 2003. Theoretical Research and Technology practice on Mining under the Huaihe River Embankment. China University of Mining and Technology Press, Xuzhou (in Chinese).

YUAN, L., WU, K., DU, G., and TAN, Z. 2001. monitoring of Huaihe Dike deformation caused by mining. *Journal of China University of Mining and Technology*, vol. 11, no. 1. pp. 14–19.

YUAN, R., LI, Y., and JIAO, Z. 2015. Numerical analysis of water inrush from working face floor during mining. *Procedia Engineering*, vol. 102. pp. 1857–1866.

YUAN, W.B. and CHEN, J. 1986. Analysis of plastic zone and loose zone around opending in softening rockmass. *Journal of China Coal Society*, no. 3. pp. 78–86 (in Chinese with English abstract).

ZHANG, J. 2005. Investigations of water inrushes from aquifers under coal seams. *International Journal of Rock Mechanics and Mining Sciences*, vol. 42, no. 3. pp. 350–360.

ZHANG, J. and SHEN, B. 2004. Coal mining under aquifers in China: a case study. *International Journal of Rock Mechanics and Mining Sciences*, vol. 41, lno. 4. pp. 629–639.

ZHANG, J.C. and PENG, S.P. 2005. Water inrush and environmental impact of shallow seam mining. *Environmental Geology*, vol. 48, no. 8. pp. 1068–1076.

ZHANG, W.Y., WANG, W.G., PENG, W.D., FENG, Z.H., and SHUN, K.S. 2002. The coal mining practice of reducing waterproof coal pillars in Panxie Mining Area. *Journal of China Coal Society*, vol. 27, no. 2. pp. 128–133 (in Chinese with English abstract).

ZHOU, D.W. 2014. The synergy mechanism between rock mass and soil in mining subsidence and its prediciton. PhD thesis, China University of Mining and Technology (in Chinese with English abstract).

ZHOU, D.W., WU, K., CHENG, G.L., and LI, L. 2015. Mechanism of mining subsidence in coal mining area with thick alluvium soil in China. Arabian *Journal of Geosciences*, vol. 8, no. 4. pp. 1855–1867. ◆

http://dx.doi.org/10.17159/2411-9717/2016/v116n5a10

Engineering principles for the design of a personnel transportation system

by R.C.W. Webber-Youngman* and G.M.J. van Heerden†

Synopsis

This article describes the re-engineering principles applied in the design of a personnel transportation system for the Bafokeng Rasimone Platinum Mine in the Rustenburg area of South Africa. It incorporates conveyor belt travelling, chairlift operation, and also includes consideration of proposed changes/modifications to the existing conveyor belt infrastructure.

The purpose of the project was to identify, through a process of evaluation, the appropriate option and/or combination of transportation options that would be safe in terms of personnel transportation as well as cost-effective. Alternative measures for transporting personnel (not using belt riding) would have a significant positive spin-off, increasing the availability of the belt and thereby increasing production. This paper explores the feasibility of interventions that would improve safety through eliminating risk associated with personnel transportation as well as contributing towards improving the mine's position on the cost curve.

The design in consideration at the Bafokeng Rasimone Platinum Mine consists of two shaft systems, namely the North Shaft and South Shaft, each comprising twin decline shafts. One of the decline shafts is equipped with a conveyor belt for rock and personnel transportation, and the other with a winder for trackbound material transport. The conveyor belt has been used for personnel transportation since the commissioning of the shafts. The conveyor belt is equipped with platforms for personnel getting off and on the belt and a number of safety devices designed to ensure safety while travelling on the belt. Intensive training in the practical aspects of belt riding is given to every person, and unsupervised riding on the belt is permitted only once belt riding competence is demonstrated. Despite this, the safety results were poor, with 106 injuries between 2006 and May 2013. Fortunately, no fatalities were reported during this period.

An investigation of alternative means for personnel transportation or engineered solutions to the current conveyor belt infrastructure in the safest, most effective, and most economical way was therefore needed. There was a major risk of safety-related stoppages being imposed following another belt accident/incident. This would prevent the mine from transporting personnel underground by belt and result in major production losses. From the commissioning of the Phase 2 shaft deepening project on both shafts, dedicated chairlifts have been used for personnel transportation as opposed to the conveyor belt installed in the Phase 1 area. The chairlifts have been in operation since 2004 and no chairlift-related incidents have been recorded thus far. According to safety statistics, it is clear that the chairlift is the safer method for the transportation of people in the shaft.

To fulfil the objectives/scope of this study, it was recommended that both primary (new chairlift decline with infrastructure) and secondary options (modifications to the current conveyor belt infrastructure) be considered for implementation on both the North Shaft and South Shaft to reduce or eliminate accidents/incidents as a result of belt transportation. The associated capital expenditure would be approximately R200 million. Considering the future impact on the business as a whole, this would definitely be capital well spent.

Keywords
personnel transportation, conveyor belt, chairlift, re-engineering, evaluation.

Introduction

In any mining operation, labour is one of the most valuable resources. In order to ensure that the personnel get to the workplace safely and in time, it is important to plan and design a transportation system that also meets the required production output of the mine. The extent of the system will be determined by a number of factors. These are the mining layout, the size of the orebody, the mining method, and the number of people to be transported at any given time. This also relates to the travelling time and the actual time spent in the workplace.

During the last decade and a half, numerous declines were developed to either access deeper reserves that were inaccessible from the existing vertical infrastructure, or new declines from surface to access sub-outcrop material that was left in the past. With the change in the economic environment and the increase in demand, it became imperative to mine the available resources.

Several of these declines were planned and designed without considering the future impact of not installing a proper, effective and safe personnel transportation system. Therefore the wrong decisions and designs were adopted upfront. The Khuseleka 1 Shaft of Anglo American Platinum (AAP) is an example. When the decline was developed (September 1991), 1.1 km away from the current vertical shaft infrastructure, the decision was that the employees would either walk the horizontal distance, or be transported by means of trackbound personnel carriages. The latter option was found not to be viable and was replaced by a horizontal chairlift in July 2013.

* *University of Pretoria, Pretoria, South Africa.*
† *Anglo American Platinum, South Africa.*
 ISSN 2225-6253. Paper received May 2014; revised paper received Nov. 2015.

In some cases the existing personnel transportation system had to be altered or redesigned as it was jeopardizing the operation of the mine due to the poor safety and health statistics and risks associated with the system. The Bafokeng Rasimone Platinum Mine (BRPM), as discussed in this paper, is an example. In some instances, personnel transportation was not even taken into account. With the deepening of the operations, the travelling distances increase and actual face time is reduced, adversely affecting the productivity of employees. Alternatives have been investigated to try to minimize the damage already caused. At AAP's Bathopele Mine, for example, when the two declines (East and Central shafts) were developed in 1999, no provision was made for personnel transportation. This was not a concern during the early stages of the operation and employees easily walked in and out the shaft. When the vertical distances to the workplaces increased beyond 150 m, the mine had to provide alternative means of transport. Personnel carriers (PC) were purchased in 2006 for each section with additional for spare during maintenance cycles. Light diesel vehicles (LDVs) were also provided for supervision. The mechanized equipment was maintained by the original equipment manufacturers (OEMs).

Several design principles have to be considered when a personnel transportation system for a mine is reviewed, especially if a system is already in place. The design parameters applicable in such a case have to concurrently consider several other factors that will have a short-, medium-, and long-term impact on production. Other critical parameters such as safety, health, and environmental impacts also need to be considered. This needs to be done in the most economical way possible. The design principles considered in the re-engineering of transportation systems was done through a case study at BRPM.

Bafokeng Rasimone platinum mine (BRPM)

BRPM was established to exploit platinum group metals (PGMs) in the Merensky Reef (MR) and Upper Group 2 (UG2) reefs on the Boschkoppie, Frischgewaagd, and Styldrift farms in the Rustenburg area. BRPM is close to Boshoek in the North West Province of South Africa (RSA). (BRPM MES, 2008).

Mine layout and existing personnel transportation system

BRPM consists of two shaft systems, namely the North Shaft and South Shaft, each comprising twin decline shafts. One of the decline shafts is equipped with a conveyor belt for rock and personnel transportation and the other with a winder for trackbound material transport.

From the date of commissioning the conveyor belt was used for personnel transport. The conveyor belt is equipped with platforms for getting off and on the belt and a number of safety devices, designed to ensure the safety of personnel travelling on the belt. Despite all the approved engineering solutions, the mine continued to experience poor safety results. Mine management decided that from the commissioning of the Phase 2 shaft deepening project on both shafts, dedicated chairlifts for personnel transportation would be installed as opposed to the man-riding conveyor belt installed in the Phase 1 area. At North Shaft the Phase 1 area extends up to and including level 5, and at South Shaft up to and including level 6.

It was important to identify specific challenges related to the belt transportation system so as to be able to obtain feasible solutions in a new design, such as the mine extraction strategy (MES), safety statistics related to conveyor belt riding, and all challenges experienced with conveyor belt riding.

Mine extraction strategy (MES)

When considering the MES, it is evident that if a solution to the current method of personnel transportation is not found, the risk of injuries/incidents on the belt could persist for many years to come. BRPM was mining only the MR on the farm Boschkoppie from North Shaft and South Shaft at the time of the study. Mining the UG2 will play an important role in achieving the long-term plan (LTP) production profiles as prescribed in the MES. The LTP production profiles of the MES illustrate the duration that the proposed chairlifts will be in operation, as shown in Figure 1. North Shaft will be in operation beyond 2060 and South Shaft up to 2050. At the time of the study the focus was only the Boschkoppie area, where the current two shafts were in operation (BRPM MES, 2008).

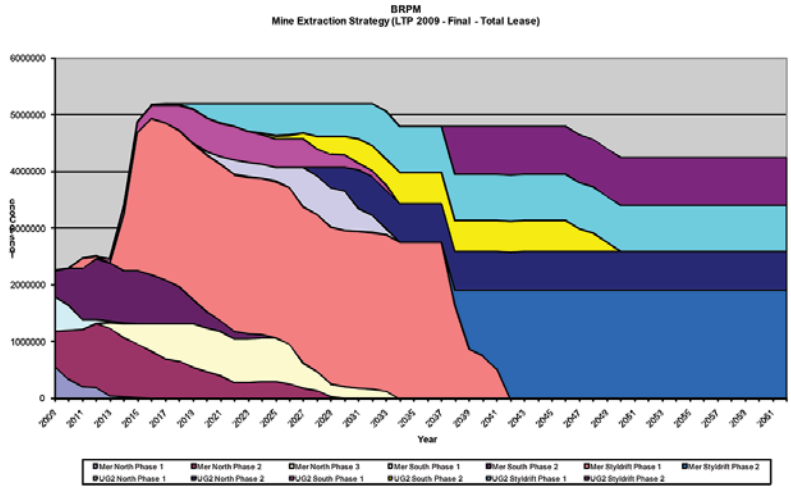

Figure 1—LTP profile for the entire BRPM lease area (both MR and UG2 reefs) (Van Heerden, 2008)

Safety-related incidents associated with conveyor belt riding

Poor safety was experienced with conveyor belt transportation of personnel, with 106 injuries reported from 2006 to May 2013. Figure 2 illustrates the classes of injuries and the number of injuries per class. During this period, 70% of the injuries were medical treatment cases (MTCs) with no shift/day lost, 20% were lost time injuries (LTIs) with less than 14 days lost, and 10% were serious injuries (SIs) resulting in more than 14 days lost. Of these 106 injuries, 98 (92.5%) were incurred while going down and coming up from underground, with the remaining 8 (7.5%) taking place during training. The training includes both practical training on the surface conveyor belt facility at North Shaft as well as applying the knowledge acquired on the actual underground conveyor belt. Since BRPM became operational in 1999, only one fatal accident has resulted from belt riding. It was assumed that a worker fell asleep while travelling on the man-riding conveyor belt from 5 level to surface. The deceased passed through the 'wake-up conveyors and chains', underneath the safety devices, and past the cap lamp transponder receiver. He was subsequently tipped into the belt transfer chute onto the overland conveyor. The deceased was not wearing a cap lamp and as a result the final safety device (the cap lamp transponder receiver) did not stop the belt (BRPM Safety Department, 2013).

Challenges experienced with conveyor belt riding

Seventy-one of the injuries that were reported happened when personnel travelled down the mine (72.5%). This is significant, as the average person travelling down the mine will get on and off the belt only once on the downward trip (at this time no rock is being transported on the belt). The same person may repeat this process up to five times on the way out of the mine due to the configuration of the level orepasses and chute infrastructure. This means that a person will have to get off the belt several times (rock is now being transported out of the mine and personnel have to get off the belt for rock to be tipped onto the belt at different levels). The personnel then walk around the chute and get back onto the belt. This is at the end of the shift, with personnel struggling with fatigue and consequently the risk of making mistakes. Despite this, most accidents happen on the way down the mine.

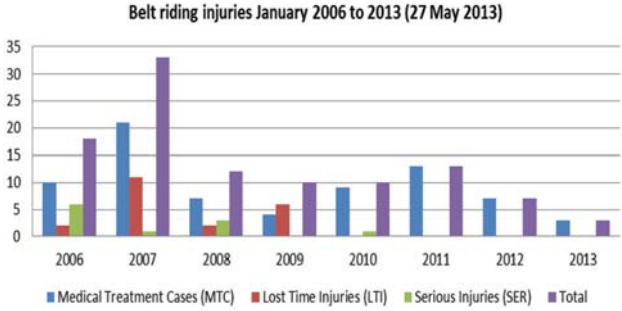

Figure 2—Classes and number of injuries per class (BRPM and Van Heerden, 2013)

Getting off the belt (going down the mine)

Of the 71 injuries recorded, 55 (77%) occurred while getting off the belt going down the mine. Sixty-five percent of the injuries related to the knees (27%), ankles (27%), feet (4%), and abdomen (7%). A breakdown of the injuries recorded is shown in Figure 3. This is definitely the most physically taxing of the tasks carried out during conveyor riding, due to the fact that the legs are forced to absorb the force imparted by the belt moving at 2.5 m/s combined with the natural acceleration due to gravity which, at an inclination of –9° amounts to 1.7 m/s^2. This combination requires a person to decelerate at the equivalent of 2.95 m/s^2 in order to stop in the required distance.

Getting off the belt (going out the mine)

Of the 27 injuries recorded, 15 (56%) occurred while getting off the belt going out the mine. An analysis indicated different types of injuries compared with those suffered when getting off the belt going down the mine. The injuries were classified as follows: head (19%) and facial (including jaw, nose, eye, and ear) 22%, which equated to 11 of the 27 (41%), followed by fingers (15%), hands (7%), and elbow (7%), 8 of the 27 (30%); and the knees, ankles. and feet, 3 of the 27 (12%). From this it was obvious that injuries occur when people fall over while getting off the belt. A breakdown of these injuries is presented in Figure 4. Getting off the belt is physically very taxing as the normally high friction coefficient between a rubber boot and rubber conveyor is

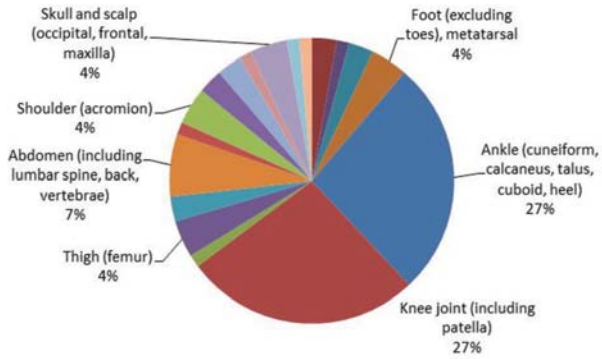

Figure 3—Breakdown of injuries – getting off the belt (going down the mine) (BRPM and Van Heerden, 2013)

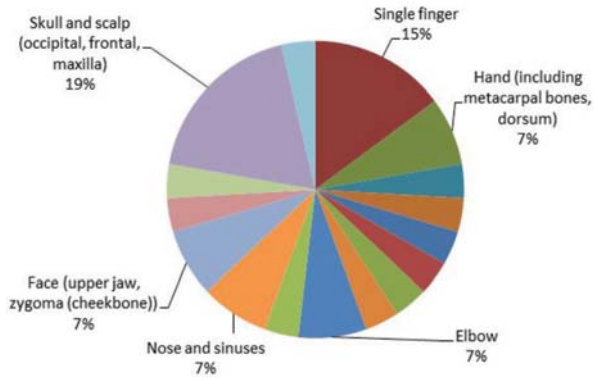

Figure 4—Breakdown of injuries – getting off the belt (going out the mine) (BRPM and Van Heerden, 2013)

reduced by the presence of small rock particles, making it very difficult to gain the necessary purchase when launching off the belt. Getting on the belt is risky for the same reasons. The presence of rock on the conveyor complicates getting on and off the belt. When comparing the number of injuries recorded going down the mine with going out the mine it is evident that the latter involves less risk due to natural deceleration imparted by gravity, which has the effect of stopping one almost as one lands on the platform, requiring almost no effort at all.

Conveyor belt training

There is a dedicated conveyor belt training facility at North Shaft. Once personnel have completed their medical examination and are proven fit for underground work (including induction and work-related training modules), belt training is done. Intensive training with regard all the practical aspects of belt riding is given to all personnel. Unsupervised riding on the belt is allowed only once competence is demonstrated. Competency is demonstrated both on the surface training belt and then on the actual underground belt at North Shaft.

In the event of belt stoppages due to accidents and/or maintenance no further travelling on the belt will be possible. This clearly indicates the vulnerability of the system in terms of personnel transportation, for which the conveyor belt is the only way of going down or getting out from underground. This will have a major production impact. Furthermore, the Mine Health and Safety Act (MHSA) also gives specific guidance with regard to the allowable vertical distance for unaided travelling.

Accordingly, and in line with BRPM's safety strategy, investigations were undertaken to identify safer engineering solutions to the current transportation system and identify alternative means of personnel transportation that could be implemented to reduce or eliminate incidents or injuries related to belt riding.

Critical items to be considered in the re-engineering investigation

It was necessary to identify through an evaluation process the appropriate option or combination of applicable transport systems that would be suitable for BRPM, taking into consideration safety as well as cost-effectiveness. Incorporation of suitable alternative personnel transportation systems could result in a significant increase in production due to an increase in belt availability. Some of the key parameters considered in the evaluation process were as follows:

- The safety and health risk involved in continued usage of the conveyor belt infrastructure for personnel transportation
- The effect of belt safety stoppages on production
- Availability of alternative personnel transportation systems
- The process of option selection and decision analysis, where no option is discarded until proven to be ineffective, unsafe, impracticable, or uneconomical
- Detail design and scheduling, costing, and effect on life of mine profile
- Involvement of relevant responsible departments such as engineering, rock engineering, geology, and ventilation that could play an important role during the selection and analysis of the various options
- Evaluating the current personnel transportation system in terms of optimizing production and reducing the risk of incidents / injuries
- Possible modifications to the current conveyor belt infrastructure while new systems are being implemented
- Benchmarking of proposed design criteria against actual achievements in terms of production, construction, and costs.

Process of option elimination

Initially, 17 different options were identified during process one (P1), which was a brainstorming workshop involving all stakeholders. Table I shows the different options considered and that were found to be most applicable for the two shafts. During this stage of the process no option was deemed impossible or discarded based on:

- Capital expenditure (CAPEX)
- Practicality in terms of implementation
- Timing in terms of the life of mine (LOM) profile, in line with the MES
- Accessibility from current infrastructure or through consideration of local communities surrounding the mine.
- Safety or impact on surface infrastructure (communities).

Following a process of elimination (P2), the decision was taken to further investigate six options at North Shaft and nine at South Shaft. Only three options were selected at North Shaft for further consideration (P3), one being a totally new chairlift decline with infrastructure (primary option) and the other two modifications to the current conveyor belt and belt infrastructure (secondary options).

Five options were selected at South Shaft during P3 for further consideration, three of which involved totally new declines with infrastructure (primary options) and two being modifications to the current conveyor belt and belt infrastructure (secondary options). At the end of P3, only one primary and one secondary option were selected. These were the new chairlift decline with new infrastructure, and safer platforms for getting on and off the conveyor belt. The secondary options were proven feasible for each of the shafts (application in the North Shaft is discussed in detail later in this article). Table II details the options selected during P3 as well as the final options selected for North Shaft.

For each of the options, the following were considered:

- Detailed design, scheduling, supply, delivery, construction, and commissioning of a chairlift system from surface to level 5 at North Shaft and level 6 at South Shaft
- Strengths, weaknesses, opportunities, and threats (SWOT) analysis for each of the options
- Project duration from start of development to commissioning, and the fit with the LOM profile
- Utilizing the current MR infrastructure
- Starting development of the chairlift decline from different positions simultaneously (various attack points)

Table I

Different options identified during process one (P1)

Option	Description	North #	South #	Comment
1	Chairlift in current belt decline	✘	✘	Sliping required – damage to belt
2a	Chairlift in zero raise – decline from surface	✘	√	N# zero raise line not straight and continuous. S# applicable for further investigation
2b	Chairlift in zero raise – vertical shaft to surface	✘	✘	Surface infrastructure / communities
3	New chairlift decline – new infrastructure	√	√	High CAPEX
4	Vertical shaft from surface to 3 level	✘	✘	Still need transport / travelling through workings to upper levels
5	Multiple chairlifts in ventilation bypass areas	✘	✘	Extensive infrastructure required with additional development
6	Slower personnel – riding speed	√	√	Applicable for further investigation
7	Single chairlift at South 40 position for both shafts	✘	✘	Logistical and infrastructure constraints (single access between shafts)
8	One-way chairlift down belt decline, up zero raise (continuous loop)	√	√	Need connection to surface, engineering challenges when considering infrastructure installation in loop configuration
9	Licence material winder for personnel transportation	✘	✘	Impact on already tight material supply schedule
10	Safer platforms for getting off the belt	√	√	Applicable for further investigation
11	1st leg chairlift in belt decline then in zero raise	✘	✘	Sliping required – damage to conveyor belt and belt infrastructure
12a	Chairlift in zero raise – incline under opencast	✘	√	N# zero raise line not straight and continuous. S# applicable for further investigation
12b	Chairlift in zero raise – portal in opencast highwall	✘	√	N# zero raise line not straight and continuous. S# applicable for further investigation
13	Vertical shaft from surface to 5 level at N# and 6 level at S#	✘	✘	Still need transport / travelling through workings to upper levels
14	Monorail system	√	√	Applicable for further investigation
15	New decline on UG2 horizon	✘	✘	Much higher CAPEX compared to MR horizon options
16	Additional belt riding conveyor in belt decline	√	√	Applicable for further investigation
17	Hector pipe	✘	✘	No personnel transport to surface, only down the mine

Table II

Different options identified during process three (P3) – North Shaft

Option	Description	North #	Comment
3	New chairlift decline – new infrastructure	√	High CAPEX. Applicable for further investigation
6	Slower personnel-riding speed	√	VSD installed. Effects of VSD to be investigated
10	Safer platforms for getting off the belt	√	Applicable for further investigationa

- Access to both MR (current operation) and UG2 (future operation)
- Increased future ventilation flow to the UG2 horizon.

Other factors considered during the selection process:

- CADSMine design and scheduling of the primary options for both shafts
- CAPEX estimation (capital development, civil engineering works, piping, electrical, mechanical, structural, instrumentation, 10% contingency, and chairlift installation)
- Financial evaluation and trade-off against major risks (*i.e.* complete belt safety stoppages resulting in total production stoppage)
- Risk analysis (from an engineering, rock engineering, geology, planning, and ventilation perspective)
- Timing in terms of the LTP and layout designs
- Access control on surface (surface transportation from lamp room to chairlift)
- Access to different levels and safety on levels when moving from one chairlift leg to another.

Other critical issues:

- Development end sizes of chairlift decline
- Lengths of different legs required and the drive stations required accommodating the layout
- Alternative travelling route for personnel when chairlift is not running due to maintenance or breakdown
- Access control at landings on different levels
- Comparison between different development and sinking methodologies – conventional, mechanized, raisebore, *etc.*

Literature study

BRPM currently uses conveyor belts for transporting personnel down and out of North and South Shafts, with the same conveyor belt being used for personnel and broken rock (reef and waste). The proposal was to either install chairlifts dedicated to personnel transport, or investigate alternative options for personnel transportation or modifications to the current conveyor belt and infrastructure and use the conveyors entirely for broken rock transportation. The updated and improved system will help to reduce safety-related injuries/incidents and provide capacity for increased tonnage output. Table III summarizes the literature study on personnel transportation systems for hard-rock decline shaft systems employed in the past, which that was conducted prior to the study of potential solutions for BRPM.

Analysis and evaluation of results

Detailed analyses and comparisons were done for both North Shaft and South Shaft. As the processes and outcomes of the two studies were similar, only the North Shaft study is discussed in this article. The results below summarize the investigations and provide a good overview of aspects considered in terms of the final re-engineering design decision for both systems investigated.

North Shaft results

Originally, three options were selected at North Shaft during P3, one of which being a totally new chairlift decline with infrastructure (primary option) and two being modifications to the current conveyor belt and belt infrastructure (secondary options). Eventually only one primary and one secondary option were found feasible for North Shaft. These are summarized below.

Primary option - new chairlift decline and infrastructure

Surface access and positioning

A portal is to be created within the shaft area. This would be the most logical approach as the entire infrastructure to support this is in place and there are no additional issues, either internal (surface infrastructure) or external (surrounding communities, either formal or informal settlements) involved.

The best position for the decline would be between the UG2 and MR horizons, as this would be in competent ground and provide easy access to both the existing MR haulages and future UG2 workings. The middling between the two horizons at North Shaft is approximately 70 m, which provides adequate space to develop the decline without impacting on the workings. The chairlift installation will begin at the exit from the existing lamp room with the first leg running to level 1. From there the decline will proceed directly to level 5 (Figure 5). Landings will be provided at each level for access to the workings (current MR and future UG2).

The outcomes of the SWOT analysis can be summarized as follows:

- Strengths
  - Access to underground workings from surface
  - Gives access to both MR and UG2 reef horizons
  - New development can be secured for LOM (50 years) – more stable ground conditions
  - Straight line – less wear and tear on moving parts
  - Six attack points for quicker development.
- Opportunities
  - Haulages to UG2 already in place
  - Two or three legs to prevent total stoppages for maintenance or breakdown
  - Additional ventilation to UG2.

The weaknesses and threats are those commonly associated with chairlift installations:

- Weaknesses
  - Cost – CAPEX and maintenance
  - Maintenance time – if only one leg (between levels 2 and 5)
  - Breakdown time – walking the only alternative to get to surface or workplaces – shift down late and blast late
  - Material cannot be taken down on chairlift.
- Threats
  - Long travelling distance in event of failure/stoppage (including safety stoppages)
  - Maintenance time
  - Workforce become negative if not running for a couple of shifts/days.

Geology and rock engineering

There are some geological features that could impact on the sinking of the chairlift decline. The major structures that could be a concern are the weathered zone (to a vertical depth of 30 m), the water-bearing shear within the initial 10 m of sinking, a fault intersection with a 4.7 m throw at a dip of 80°, the Randal and Strike dykes, and the North Shaft UG2 fault. The decline system and some footwall development have mined successfully through these features. Specific rock engineering support recommendations need to be adhered to so as to ensure successful mining through these features. Reduced mining rates are planned when features are encountered, as benchmarked from historical information.

Jointing could also be expected. At North Shaft there are four major and two minor joint sets, which provide a clear understanding of the expected ground conditions in the vicinity of the proposed chairlift decline. Mitigating the risk is similar to mining through the geological features mentioned above.

Some additional concerns include the proximity of the two portal highwalls (proposed new portal and existing portal), the large excavations in a faulted block of ground between changes over from leg one to leg two where drive units will be installed, and the possible sterilization of some UG2 reserves due to the placement of the chairlift decline. Specific rock engineering guidance and recommendations need to be adhered too to ensure the mitigation of risk.

Ventilation

There should be no holing through to the reef planes or UG2 excavations, which could result in short-circuiting of fresh air. The ventilation controls in haulages should also be correctly placed to eliminate short-circuiting of fresh air into

Table III

Literature study summary

Type of conveyance	Description	Significance	Applicability
Walking	The risks of walking are slip and fall incidents/ injuries and unauthorized riding of unapproved conveyances or cars (Frankland, 1984). 150 m is the allowable vertical distance for unaided travelling (MHSA, 1996).	In the case of BRPM, due to the configuration of the shafts and the specific requirements, walking is not the preferred option.	Not applicable for further investigation
Underground conveyor belt personnel transportation	The concept was originated as an optimized option for both rock and personnel transportation. Instead of having two separate systems as well as two separate excavations, the plan was combined to manage both the requirements of ore and waste transportation from underground as well as personnel transportation to and from the different levels in operation. This application resulted in huge savings in capital expenditure.Training and competency levels of employees are very important as the risks associated with belt transportation are very high (BRPM and Target Gold Mine, 2008–2013).	The risk of continuous usage of the conveyor belt infrastructure for personnel transportation with regards the safety and health of employees. BRPM recorded a much worse safety record (106 injuries between 2006 and May May 2013) compared to Target Gold Mine (6 injuries between 2011 and 2012). The nature of the injuries recorded at BRPM was more serious compared to Target. The effect on production associated with belt safety stoppages. Belt riding is used as the only mode of transport. It is a condition of employment that employees use belt riding as a form of transportation. Both personnel and broken rock are transported via the conveyor belt. Both BRPM and Target were forced to investigate alternative means of personnel transportation. At BRPM it was purely due to safety reasons compared to Target where they had to deal with disputes from organized labour (BRPM, 2008 - 2013), (Harmony Gold Mining Co Ltd v NUM and Others, 2012).	Not applicable for investigation: This mode of transport was not considered as an option on its own, however it was included during the consideration of proposed changes / modifcations to existing conveyor belt infrastructure
Chairlift personnel transportation	Chairlift installation has been widely, successfully applied in underground mines as a mode of transport. (Brophy, 1984). The angle of installation varies from horizontal to a maximum of 45°. The length of the installation varies, depending on the specific requirement. There are two different types of chairlifts available, namely the fixed grip and the detachable types (Frankland, 1984).	The main objectives for the installation are to increase working time at the face area, to eliminate fatigue in travelling to the workplace, and to increase production by achieving the latter (Brophy, 1984). From the commissioning of the Phase 2 shaft deepening project at BRPM, the decision was to install dedicated chairlifts opposed to the man riding conveyor belt installed in the Phase 1 area. This iinstallations were in operation since 2004 and no chairlift related incidents were recorded thus far. According to safety statistics it was clear that the chairlift installation is the safer method for the transportation of people in the shaft (BRPM, 2008 - 2013). The MHSA contains numerous sections with regards to chairlifts. The regulations stated here are the minimum requirements from the DMR. It is the mine's responsibility to have their own COP and relevant standards to ensure the compliance as well as safety of all personnel using the chairlifts as a means of transportation in and out the mine (MHSA, 1996). This is confirmed through the issuing of a licence to operate by an Inspector of Machinery from the DMR.	Applicable for further investigation
Chairlift installation in raisebore shaft	The chairlift system utilizing a raisebore shaft was investigated as a possible option or to be used in conjunction with other layout options (individually as a chairlift leg on its own or in combination with the rest of the system).	The minimum angle of inclination is 28°, this is the minimum angle required to ensure that self-cleaning occurs during the drilling of the raisebore shaft. The maintenance (preventative and routine) on the infrastructure is much higher compared to a normal chairlift installation as a result of the acute angles it has to operate in. The diameter of raisebore shaft should be clearly defined and calculated in terms of required clearance from the sidewalls (including footwall). Special permission should be granted by the DMR for application of similar type of arrangement. There should be compliance with MHSA regarding walking up and down the inclined shaft when chairlift is standing. This could be during normal maintenance or during breakdowns (Personal visit, 2008).	Applicable for further investigation
Monorail transportation system	Monorails have proven their reliability under arduous conditions. There is the option between diesel and electric driven units. The track bound monorail is easy to control and safe against derailment compared to a free-steered vehicle. It has a hoist on board and one driver can do the loading and unloading without assistance. The safety records of monorail systems are phenomenal. The on-board safety brake system will stop the train immediately when the system or human faults lead to an uncontrolled movement of the train on the rail. Low OPEX compared to LDV's and UV's (SMT by Scharf, 2010).	Able to negotiate steep gradients and sharp horizontal curves and changing gradients. Having a small cross-sectional area - minimal excavation. Includes its own load pick-up system. Being able to transport both personnel and material. Efficient delivery of men (between 60 and 75) and material (up to 15) at 2 m/s. Diesel driven (good fuel consumption - no electrical cable or connection). The mechanical controls and functions withstand humid and dusty conditions. Small cross-sectional dimensions (800 mm width) enables the train to access low and tight roadways and support the mining operations right at the face. High initial CAPEX (Personal visit, 2008).	Applicable for further investigation

Table III

Literature study summary *(continued)*

Type of conveyance	Description	Significance	Applicability
UK patent for personnel riding equipment assisting transfer to or from conveyor belt	This pending patent application discusses various modifications to the conveyor belt and belt infrastructure that could assist personnel during the process of getting on or off the conveyor belt (Gurr *et al.*, 2008).	Used during the design of proposed changes to the BRPM system as a secondary option to have an immediate impact and to reduce the risk of incidents / injuries while using the conveyor belt for personnel transportation.	Applicable for further investigation
Material and personnel transport by endless rope haulage.	This includes the design, installation, and operation of an endless rope haulage system. It includes the factors which lead to the option selection and decision analysis of the specific system as well as the advantages gained over more commonly used winding systems (Du Plessis, 2001).	This option was considered during the option selection and decision analysis process. The objective was to review the option of obtaining a license to use the material winder for the purpose of personnel transportation.	Applicable for further investigation
LDVs and personnel carriers / carriages	This included mechanized LDVs and / or personnel carriers, as well as conventional trackbound carriages	Not considered: a conventional mining method with large number of personnel, mechanized LDVs and / or personnel carriers was not practical. Not considered: Conventional trackbound carriages.	Not applicable for further investigation: Conventional trackbound carriages are applicable and very successful in horizontal transport.

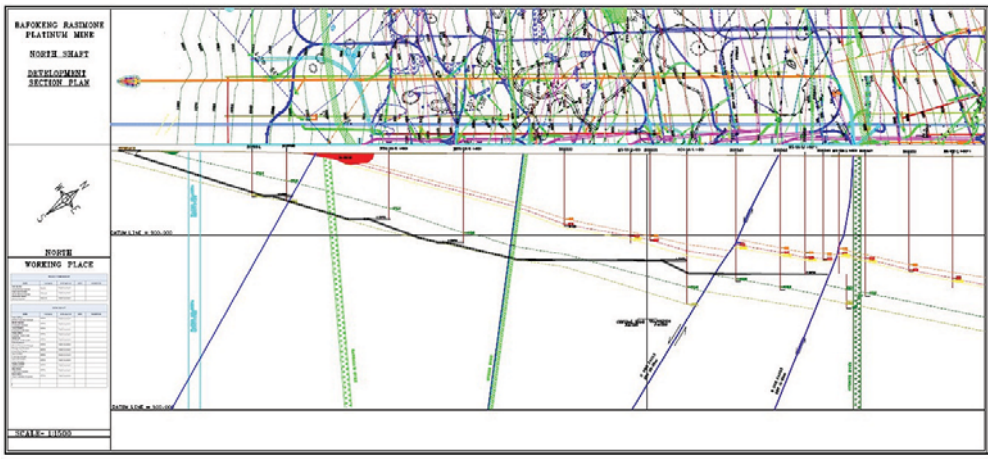

Figure 5—Plan and section view of the North Shaft chairlift decline system design (BRPM, 2013)

worked-out areas. The additional airway as a result of the chairlift decline development will entail major advantages from a ventilation perspective. These include:

- A reduction in the total shaft air resistance, leading to reduced power consumption of the main surface fans
- The additional intake can increase the overall shaft's air intake.
- Lower airflow velocities in the belt decline (less dust generation).

Development and construction schedule

Owing to the configuration of the chairlift decline and the fact that it will be developed through existing mining infrastructure, it is possible to begin development from six attack points and the schedule has been compiled as such. Figure 5 shows the various attack points from surface and underground from the different operational levels.

CADSMine design and scheduling software was used during the process. Development of the chairlift decline and associated landings and crosscuts has been scheduled at a rate of 32 m/month (instantaneous). From the scheduling it was concluded that the total duration to complete the development of the chairlift decline was 12 months. A total of 1934 m of development would be needed.

Construction will be concurrent with the development. Once a leg between two levels has been completed, it will be constructed. The only bottleneck would be the first leg from

surface to level 1, which would take two additional months to complete. Thus, the total development and construction duration would be 14 months.

Estimated CAPEX

The estimated CAPEX on the mining costs was based on 12 months for development and a total development of 1934 m. It was assumed that development would be conducted by AAP's Capital Development Services (CDS), which is currently developing the Phase 2 declines on both shafts. The development cost used, R3099 per m^3, is as per the agreed rate per cubic metre with CDS.

The chairlift costs (infrastructure and installation) were obtained from Sareco, which is installing the Phase 2 chairlifts on both shafts (refer to chairlift requirement summary in Table IV). The total estimated CAPEX for the chairlift decline at North Shaft would be R94 million.

Secondary option (safer platforms for getting on and off the belt)

Platform modifications

Having analysed the configuration, particularly of the platforms for getting off the belt, some relatively minor modifications could be made that will greatly assist with the process. The lower conveyor belt is deeply troughed, which together with the fact that the platform itself is elevated above the level of the conveyor belt, means that the rider has to take a step up of approximately 400 mm to get off the conveyor belt. The platform is also broad, being 1200 mm from the side of the conveyor belt to the grab rail, and hence the grab rail currently installed is ineffective when getting onto or off the belt.

Getting off the belt while going down the mine is the most challenging action required considering the past safety performance at BRPM. This platform requires the most attention. Figure 6 shows a section of the current configuration of the platform.

One interim solution to improve the safety of the conveyor belt for the purpose of personnel transportation is to change the idlers at platforms going down, replacing troughing idlers with flat idlers for a distance equal to the length of the platform plus one idler at either end of the platform. Two transition idlers either side of the platform would be added to assist the belt in changing from troughing idlers to flat idlers and back again

Replacing the troughed idlers with flat idlers will immediately create a flatter transition surface between the belt and the platform and remove the height differential between the two. This is illustrated conceptually in Figure 7.

Table IV

Chairlift requirements

	North Shaft	South Shaft
Personnel capacity	900 per hour	900 per hour
Chairlift decline average inclination	10.0°	17.9°
Chairlift decline maximum inclination	17.6°	19.0°
Chairlift decline minimum inclination (excluding the landing areas, which are flat)	8.5°	10.0°
Length of decline	1934 m	1727 m
Rope speed	1.5 m/s	1.5 m/s
Deceleration limits (as per SANS 273)	1.5–0.375 m/s²	1.5–0.375 m/s²

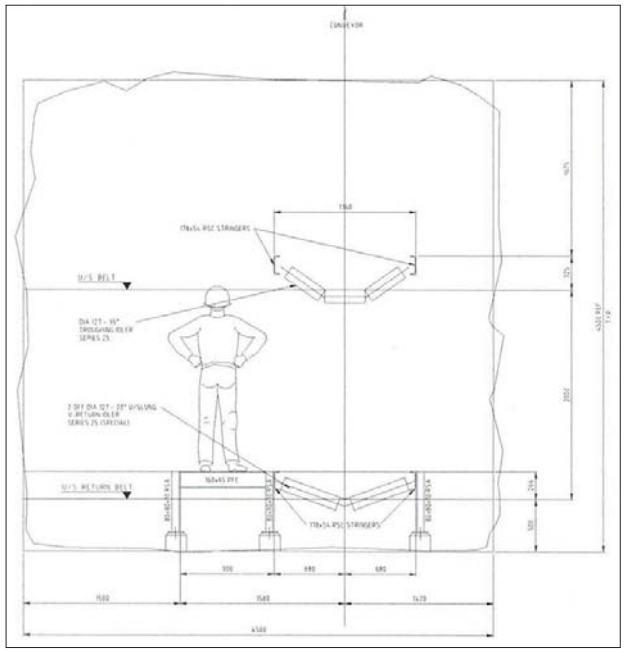

Figure 6—Getting off the belt (going down the mine) – section through platform (bottom belt – existing) (BRPM, 2008)

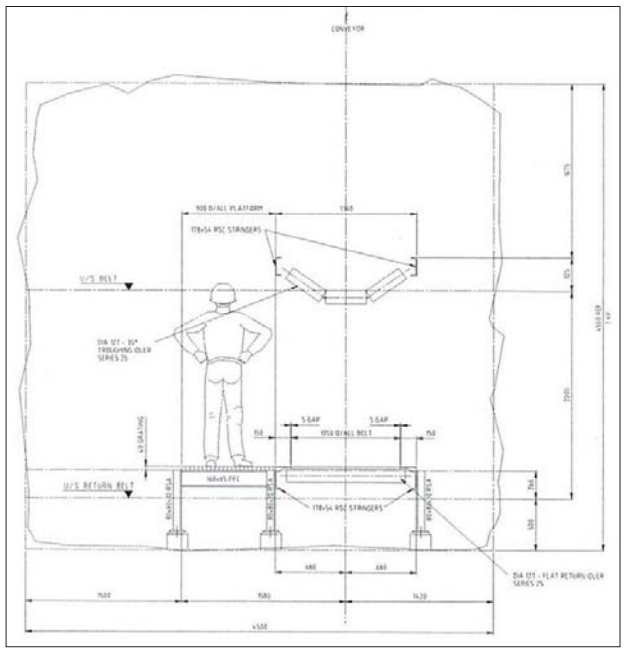

Figure 7—Getting off the belt (going down the mine) – section through platform (bottom belt – modifications) (BRPM, 2008)

Reducing the width of the platform from 1200 mm to no more than 900 mm will also allow personnel to utilize the grab rail to steady themselves if in need. As there is no broken rock on the bottom belt there is no reason why this cannot be implemented. It is also recommended that the current grating used for the floor of the platform be replaced by the non-slip variety to prevent people slipping while attempting to brake rapidly.

Although getting off the belt when going out the mine does not carry the same risk as when going down the mine, it would still be of assistance to improve the ergonomics of the platform, particularly when personnel alight off broken rock. This could be done by lowering the platform by approximately 50 mm to reduce the height differential.

Adjustable trough idlers are proposed for the platform areas used when going up. Flat idlers cannot be used for the ascending conveyor belt as this section of belt carries broken rock and there is a possibility of rock rolling off should flat idlers be incorporated here. Instead, adjustable idlers can be installed, giving the potential for trying various angles of trough to keep broken rock on the belt and provide a flatter belt at platform areas when going out the mine. Adjustable idlers would replace the existing troughing idlers for the length of the platforms. The first option is to install adjustable idlers, which could be tuned to reduce the trough as much as possible without causing spillage from the conveyor belt. The other option is narrowing the platform to 900 mm so as to allow personnel to utilize the grab rail. These existing platforms as well as the proposed modifications are illustrated in Figure 8 and 9. The estimated CAPEX for the modifications is approximately R1.0 million, as shown in Table V.

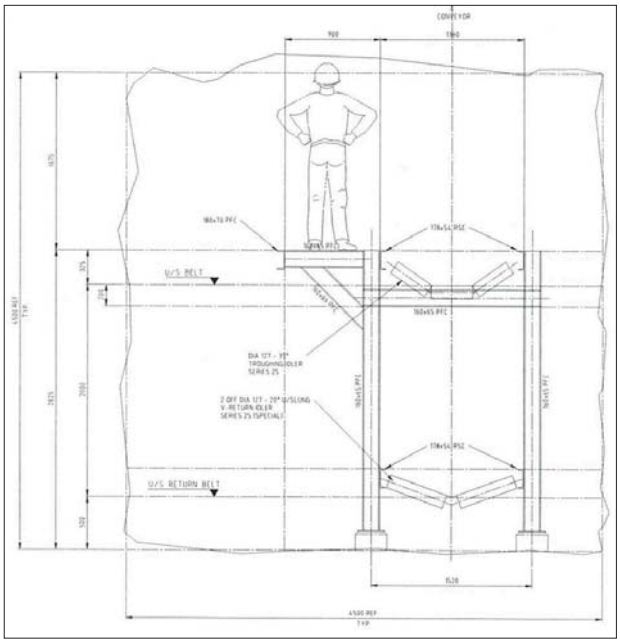

Figure 8—Getting off the belt (going out the mine) – section through platform (top belt – existing) (BRPM, 2008)

Addition of an intermediate conveyor belt for assistance when getting off the belt

Installation of an intermediate conveyor belt for assisting personnel getting off the belt going down the mine is recommended. The speed will be 1.5 m/s and the belt can be installed in place of the existing platforms. A 4 kW variable-speed drive (VSD) and 4 kW motor driving through a bevel helical gearbox will power the conveyor. A multiply medium-duty conveyor belt has been selected, running on 127 mm flat idlers and with a skid plate with 324 mm diameter drive and return pulleys, unlagged. The VSD will allow an optimum speed to be selected should the initial estimate of 1.5 m/s not be ideal. A trial-and-error procedure will be run to determine the best speed on the intermediate belt. The estimated CAPEX

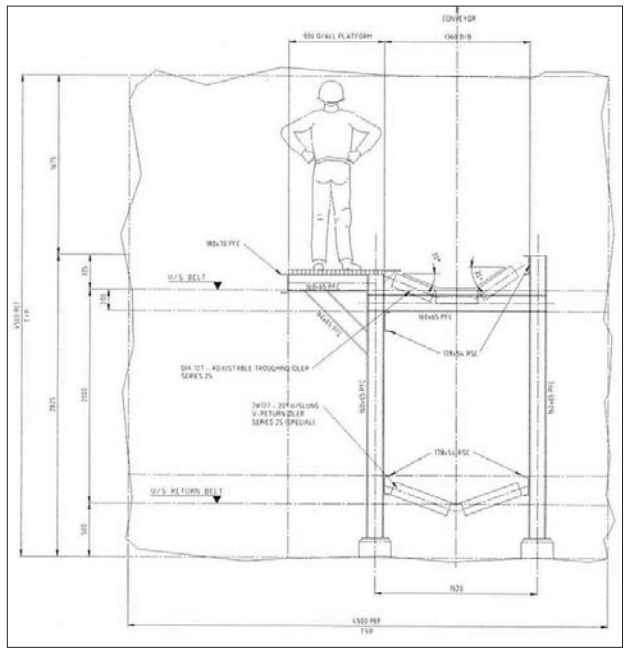

Figure 9—Getting off the belt (going out the mine) – section through platform (top belt – modifications) (BRPM, 2008)

Table V

Total estimated CAPEX – North Shaft

Item	Quantity	Price per unit (R)	Total (R)
Primary option			
New chairlift decline			
North Shaft total	1934 m	48 374	93 555 572
Secondary options			
Modifications to platform areas			
North Shaft total	5 levels	205 085	1 025 423
Intermediate conveyor			
North Shaft total	5 levels	180 ,368	926 842
Endless rope arrangement			
North Shaft total	5 levels	106 022	530 109
Grand total			96 037 947

for the modifications is approximately R0.9 million, as shown in Table V.

Addition of overhead endless ropeway for assistance when getting off the belt

To assist personnel to get off from the conveyor belt when going down the mine, the installation of an overhead endless rope running across the conveyor belt to the platform is proposed. The system is driven by a 3 kW VSD with 400 mm diameter pulleys and a 16 mm plastic-coated steel rope running at 1.5 m/s. The idea is for personnel to grab hold of the rope to steady themselves when getting off from the belt to the platform. Since the belt is running at 2.5 m/s and the rope at 1.5 m/s, the effect is that the rope is travelling towards the person. It would be mandatory for all personnel to wear gloves when going down to help prevent possible rope burn. Again, a process of trial and error is required to determine the best speed for the rope and the VSD will allow a suitable speed to be selected. Table V shows the estimated CAPEX for this installation. Figure 10 illustrates rope assistance at a typical elevation. The estimated CAPEX for the modifications is approximately R0.5 million.

Completed platform modifications

Figure 11 illustrates a platform complete with all safety enhancements, namely flat idlers, ropeway assistance, and an intermediate belt. These modifications are seen only as a short-term solution to the current problem experienced with personnel transportation at BRPM, and could be done rapidly resulting in an immediate improvement in safety. They will

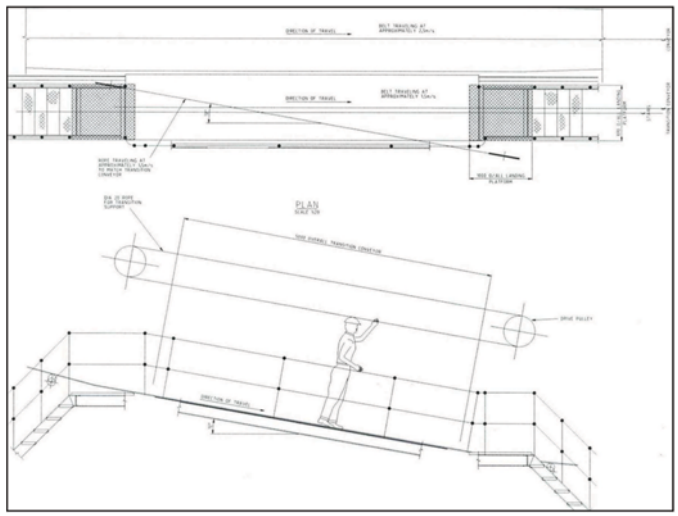

Figure 10 – Rope assistance – typical elevation (BRPM, 2008)

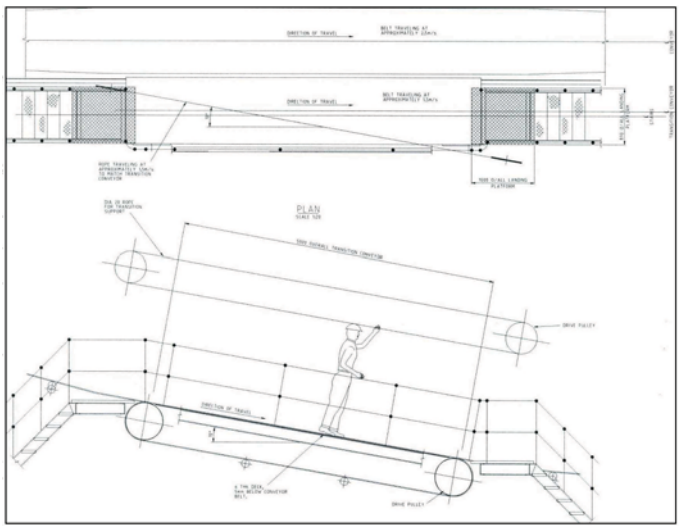

Figure 11 – Completely modified platform, including intermediate belt and rope assistance (BRPM, 2008)

also come with a limited CAPEX (Table V) should all modifications prove viable. The reason why emphasis is placed on these modifications is that developing a new decline system at North Shaft and South Shaft would take approximately 12 and 15 months respectively. Two months could be added for installation of the infrastructure.

It is also assumed that approval of the feasibility study for capital funding would take an additional 18 months. Thus it would take approximately 32 and 35 months before the new chairlift declines on North Shaft and South Shaft could be utilized, respectively. In the interim, there would be a continuing risk of injuries/incidents as a result of personnel transportation on the conveyor belt, which could lead to stoppages.

Summary of North Shaft estimated CAPEX

The total estimated CAPEX for the complete North Shaft installation (primary and secondary options) is approximately R96 million (Table V). This is based on the assumption that the secondary options would be implemented while the development of the chairlift decline is in progress. This would have an immediate impact on safety. The secondary options could be implemented quickly compared to the 32-month project duration for the chairlift decline.

Analysis and evaluation of results

In an attempt to reduce injuries on the conveyor belt, VSDs were installed at both shafts at the end of 2008 at a cost of R7.8 million. The intention was to reduce the belt speed to 1.5 m/s when personnel are riding. A reduced production of 47% was simulated by Anglo Technical Division (Jele, 2008). The calculated financial impact at that stage would have been R52.4 million per month if a belt speed of 1.5 m/s was maintained.

The decision was taken by mine management to increase the belt speed to 2.0 m/s when personnel are travelling on the belt. However, the impact on production persisted, with possible losses of R26.2 million per month. A very tight shaft schedule would have to be implemented to ensure that personnel travel on the belt only when the speed is reduced. VSDs as a stand-alone are not the solution for BRPM. However, in conjunction with the reduction in belt speed, belt training was also reviewed. Sirens were implemented as early warning devices to notify personnel to get off at each level. Cushions were also installed against the rails at each of the landing areas. A soft start and stop mechanism was also installed.

All these initiatives have had a definite impact on safety since their introduction towards the end of 2008 (Figure 2), but accidents/incidents have not been eliminated entirely. Other options will have to be implemented to ensure the belt is running at design capacity, delivering the planned tonnages with no impact on the safety and health of employees.

The primary and secondary options considered would not only reduce the risks of accidents/incidents, but would also allow the mine to utilize the design capacity of the belt 24 hours a day. The total estimated CAPEX for both primary and secondary options at BRPM is approximately R200 million. This amount is relatively small compared to that resulting from possible safety stoppages. It should also be emphasized that these options would play a vital role during the remaining 40 to 50 years of the estimated LOM.

When considering chairlifts as an option compared to conveyor belt riding, some productivity sacrifices were required to ensure the safety of personnel. The simulation conducted by Simulation Engineering Technologies (Nichol, 2009) proved this. Travel time is expected to increase by 33% as a result of severe queuing, hence personnel would spend less time in the working areas. The only viable option for reducing the impact is to have a pre-determined shaft schedule (per level – beginning of shift and end of shift) to reduce queuing times.

After completion of the study, application for CAPEX was submitted to continue with the primary options (new chairlift decline with infrastructure) at both North and South shafts. The North Shaft CAPEX application was approved and sinking of the chairlift decline at North Shaft is currently in progress.

It is the authors' opinion that with the delay in the new South Shaft chairlift decline, BRPM will continue facing the risk of safety stoppages as a result of accidents/incidents due to conveyor belt riding. The opportunity of utilizing the design capacity of the belt through increased productivity will remain lost.

Additional recommendations

The mine should start immediately with the secondary options, which will reduce the accident/incident risks while the belt continues to be used for personnel transportation. This will also reduce the risk of safety stoppages, which will minimize unnecessary losses. The total estimated CAPEX for these secondary options was calculated as approximately R5.5 million. These options could be implemented very quickly compared to the 32 and 35 months that would be required for funding approval, development, and construction of the primary options at North Shaft and South Shaft respectively. This will buy the mine some time to complete the formal approval processes. Once the funds are available, the shafts could start immediately with the development of the chairlift declines.

Development of the chairlift declines should start on available MR levels concurrently. The construction of infrastructure and the development of the chairlift declines should take place concurrently. As soon as a leg between two levels is completed, it should be constructed. This will ensure that the project schedule is adhered to.

Once the chairlift decline has been commissioned, the ultimate design speed of the conveyor needs to be determined through adjustment of the installed VSDs. This could have a significant positive spin-off by increasing the tonnage output from the shafts. The belt maintenance schedule needs to be reviewed as unnecessary personnel-detecting safety devices could be removed. This will reduce the maintenance duration and intervals required.

Conclusions

Despite all the initiatives incorporated to mitigate the risk, BRPM has a very bad safety record with regard to conveyor belt transportation of personnel. 106 injuries were recorded

between 2006 and May 2013. The existing conveyor belts utilized for personnel transportation, installed in the Phase 1 areas of both shafts, were equipped with platforms for getting on and off the belt as well as an array of safety devices, which were designed to ensure the safety of personnel travelling on the belt.

Since the introduction of chairlifts in the Phase 2 areas of both shafts in 2004, BRPM has not recorded a single chairlift accident/incident. The safety statistics clearly show that the chairlift is the safer method for transportation of people into and out of the mine. There is a specific belt training facility on the mine but even with this intensive training programme, accidents/incidents continue to occur. Should there be another belt accident/incident, a safety stoppage could be imposed, which would have a major impact on the mine in terms of production and financial performance. There was therefore the need to identify appropriate option(s) for safe and cost-effective personnel transportation.

The literature study identified several options and combination of options for further investigation during the next phase of the study. These included chairlift installations (in a normal decline or with the variation of utilizing a raisebore shaft for access between levels/connections), a monorail transportation system, modifications to the current belt infrastructure, and utilizing an endless rope haulage system whereby the material winder would be used for material/equipment and personnel transportation.

Further options were identified, including walking, utilizing the current underground conveyor belt system for both broken rock and personnel transportation), LDVs, and personnel carriers, but these were discarded based on the configuration of the decline shafts, BRPM's specific requirements (historical safety performance and mining methods dictating the number of personnel), and compliance with the MHSA.

The options for further investigation were identified followed a process of selection and decision analysis. No option was discarded until proven to be ineffective, unsafe, impractical, and uneconomical. Initially 17 different options were identified during P1. After a process of elimination, the decision was taken to further investigate six options at North Shaft and nine at South Shaft during P2.

Finally, only three options were selected at North Shaft during P3, one of which was a total new chairlift decline with infrastructure and two being modifications to the current conveyor belt infrastructure. Five options were selected at South Shaft during P3, three of which comprised total new declines with infrastructure and two being modifications to the current conveyor belt and belt infrastructure. At the end of P3, only one primary and one secondary option were proven feasible for each of the shafts. Throughout the different stages of the investigation, all relevant responsible departments were involved in the selection and analysis of the various options. The final primary options on both shafts were designed and scheduled using the CADSMine design and scheduling software packages. The proposed design criterion was benchmarked against actual achievements in terms of production, construction, and costs.

Development and construction of the chairlift declines would take 14 months for North Shaft (1934 m development) and 17 months for South Shaft (1727 m development) at a cost pf R3099 per m^3 and R3452 per m^3 respectively. The total estimated CAPEX would be approximately R93.6 million for North Shaft and 100.9 million for South Shaft. The secondary options included modifications to the current conveyor belt infrastructure. The total estimated CAPEX for these modifications were calculated as approximately R2.5 million at North Shaft and R3 million at South Shaft.

The total estimated CAPEX to implement both the primary and secondary options at North Shaft and South Shaft was calculated as approximately R96 million and R104 million respectively. The total CAPEX spend of R200 million will have a direct impact in terms of improved safety by eliminating accidents/incidents related to personnel transportation. This is proved by the fact that since the introduction of chairlifts in the Phase 2 areas of both shafts in 2004, BRPM has not recorded a single chairlift-related accident/incident.

It is clear that the chairlift installation is the safer method for personnel transportation at BRPM. The VSDs installed on the current personnel transportation belts are not in themselves a solution. The reduction in conveyor belt speed to 2.0 m/s towards end of 2008 definitely improved safety, but the risk of safety stoppages and associated losses remained. Reducing the belt speed to 1.5 m/s (refer to Target mine in the literature study), which could have further reduced the number of accidents/incidents, was considered not economical viable for BRPM.

Other options will have to be implemented to ensure that the belt is running at design capacity and safety of personnel is improved. The implementation of chairlifts will result in a 33% increase in travelling time, since the speed of the chairlift and the spacing of the seats will result in severe queuing. An appropriate shaft schedule will resolve this problem.

To fulfil the objectives and scope of this investigation, it is recommended that both the primary and the secondary options be considered for implementation on North Shaft and South Shaft to reduce or eliminate accidents resulting from belt transportation.

Suggestions for further work

During the final design and scheduling of the chairlift declines, the following aspects should be considered and incorporated:

- An appropriate portal design in the weathered zone
- The sizes of excavations should be minimized and important excavations should not be sited in areas where geological features exist
- Excavations should be placed so as to avoid sterilization of the UG2 reserves
- Development rates should be slower through known features such as the weathered zone, shear zone, and UG2 fault. A robust support design as per rock engineering recommendations will also be required when mining through these features and when intersecting sills.

Consideration of the above would require re-evaluation of the project duration and the CAPEX required.

The future planning for North Shaft indicates that the shaft will be developed to level 13, with production from the UG2 stopes in the upper levels of the mine taking place concurrently with MR stoping in the lower levels. Although the total output from the shaft will remain constant, the geographic spread of the operations is likely to put additional strain on the materials handling system. For this reason it is suggested that developing a decline of sufficient width (6 m) to accommodate both a chairlift and a winder system for materials transport be investigated. This would have the effect of almost doubling the CAPEX of the decline and raise several safety issues with regard to transporting men and material in the same excavation. A detailed simulation of the logistics should be carried out in order to ascertain the risk to production before a decision is taken in this regard.

The installation of the secondary options/modifications to the current belt infrastructure may require additional OPEX with regard to increased electricity consumption, additional engineering requirements (maintenance and breakdowns), and labour, and this should be investigated.

The additional OPEX requirements as a result of the chairlift installations on both shafts will have to be considered. This will include the following:

- Normal running of the chairlift and costs associated with increased electricity consumption and maintenance (preventative maintenance and breakdowns)
- Labour requirements in terms of chairlift attendants and engineering personnel responsible for maintenance. Training requirements should also be considered.

The trade-off between the abovementioned factors and the possible savings once the chairlifts are commissioned should be determined. Once the conveyor belt is utilized only for broken rock transportation, huge savings could result due to reduced maintenance, with specific reference to safety devices, as well as a possible reduction in labour requirements (belt attendants and engineering personnel).

The increase in available belt time as well as the increase in conveyor belt speed will have to be determined. These will lead to an increase in belt capacity and overall potential increase in tonnage output from the shafts. The business planning process will have to be revisited to utilize this potential. This could have a definite financial benefit for BRPM and its stakeholders.

Acknowledgements

- To BRPM and AAP, Rustenburg (RSA) for permission to publish this article.
- To colleagues at BRPM and AAP, Rustenburg for their contributions to and assistance towards submitting this article.

References

Anglo Gold Ashanti Kopanong Mine. 2008. Personal communication, 14 April.

Anglo American Platinum Union Section Mine. 2008. Personal communication, 18 August.

Brophy, G J. 1984. Chairlift Installations at No. 1 Shaft Western Holdings – Holdings Division. *Proceedings of the Underground Transport Symposium*, 1986 Edgar, R.C.R. (ed.). Special Publication no. 1. South African Institute of Mining and Metallurgy, Johannesburg. pp. 167–185.

BRPM. 2007–2013. Personal communication.

BRPM Safety Department, 2013. Personal communication, 27 August.

Du Plessis, G.L. 2001. Material and personnel transport by endless rope haulage – the 21st century approach. *Proceedings of the 6th International Symposium on Mine Mechanisation and Automation*, Sandton Convention Centre, South Africa, 25-28 September, 2001. Willis, R.P.H. (ed.). South African Institute of Mining and Metallurgy, Johannesburg.

Frankland, J.R. 1984. Chairlifts for the South African mining industry. *Underground Transport Symposium*, 1986. Edgar, R.C.R. (ed.) South African Institute of Mining and Metallurgy, Johannesburg. pp. 153–166.

Gurr, M.E. and Jenkins, P. 2008. Man-riding conveyor equipment assisting transfer to or from conveyor. British Patent 2059376A.

Harmony Gold Mining Co Ltd v National Union of Mineworkers (NUM) and Others (J367/12). 2012. ZALCJHB 32; (2012) 33 ILJ 2609 (LC) (14 March 2012), Johannesburg Labour Court, Johannesburg, South Africa.. http://www. SAFLII/Databases/South Africa: Johannesburg Labour Court, Johannesburg/2012/[2012] ZALCJHB 32 [Accessed 23 August 2013].

Jele, Z. 2008. Anglo Platinum Bafokeng Rasimone Platinum Mine Conveyor Simulation Report. March 2008.

South Africa. 1996. Mine Health and Safety Act, Act 29 of 1996. http://www.acts.co.za/mine-health-and-safety-act-1996/index.html

Nichol, S. 2009. Anglo Platinum Bafokeng Rasimone platinum mine personnel transportation simulation report (Third draft, 5 October 2009).

Scharf. 2010. Solutions for Mining Transport (SMT). http://www.smtscharf.com [Accessed 20 August 2010] .

Target Gold Mine. 2013. Mining Technology, 2013. http://www.mining–technology.com/projects/target/ [Accessed 23 August 2013].

Van Heerden, G.M.J. 2008. BRPM chairlift investigation presentation. Anglo American Platinum, Johannesburg.

Van Heerden, G.M.J. 2008. BRPM 2009 Budget presentation. Anglo American Platinum, Johannesburg.

Van Heerden, G.M.J. 2008. BRPM MES 2009 presentation. Anglo American Platinum, Johannesburg.

Van Heerden, G.M.J. 2014. Engineering principles for the design of a new / existing mine's personnel transportation system. MEng thesis, University of Pretoria. ◆

http://dx.doi.org/10.17159/2411-9717/2016/v116n5a11

Interpretation of transformation—perspectives from mining executives in South Africa

by N.V. Moraka*

Synopsis

In dealing with transformational aspects, the South African Constitution aspires for a balance between attempts to broadly represent the country's demographics in the way in which organizations are structured and the need to maintain the necessary skills to ensure continual retention of skills for optimum and efficient organizational performance. Through the Mining Charter, government aimed to redress gender and racial imbalances in the mining industry as part of transforming the demographic representation of mining companies to include black people, women, and people living with disabilities in all job levels up to top management. While the Constitution calls for an appropriate balance between demographic representation and competency, this aspiration for mining poses challenges for companies due to the proficient and competent skills needed in this industry. To this end, the South African mining industry has been subjected to substantial criticism from government regarding the slow progress of transformation. The mining industry justifies its slow pace of transformation by pointing at inconsistent, varying legislation and definitions governing transformation, limited skills available from historically disadvantaged groups, and cautioning not to compromise the sustainability of mining companies by marginalizing white males and white youth with the objective of addressing racial imbalances. This lack of understanding between industry and the government has led to considerable confusion regarding the accountability of stakeholders in transforming the industry. This article presents the perspectives of ten mining executives on transformation in the South African mining industry. The theoretical description of transformation, as well as other mining stakeholders' interpretations of transformation. is presented. Qualitative data from interviews with mining executives demonstrates their understanding of transformation through rich descriptions, interpretations, and implications in their contexts. The findings demonstrate that transformation in the mining industry is not simply about race and gender, but about cultural change, a change in mind-sets, embracing diversity, equalizing rights and opportunities, and attaining social justice. Moreover, transformation is clearly a gradual process. The article concludes with a recommendation for the definition of transformation to be corroborated with the views of mining executives and that of the Constitution of South Africa. This will create an overarching, simplified definition of transformation that can be accepted and interpreted by all stakeholders.

Keywords

transformation, constitution, Mining Charter, mining executives.

Introduction

During the 2014 mining Lekgotlha, the newly appointed Minister of Mineral Resources, Ngoako Ramatlhodi, emphasized that the increasing labour unrest in mining companies demonstrated that there is an urgent need for transformation in the mining industry. In his statement Ramatlhodi said, '[We] shall regain their [the mineworkers'] confidence only when they feel improvement in their material conditions. This and only this can guarantee the long term stability and sustainability of the mining industry. The author must salute those companies that have not just embraced transformation as a compliance matter but recognise it as a tool for reconciliation. These companies have understood that transformation delivers good business results' (Ramatlhodi, 2014). The term 'transformation' is often used to define some radical change that should take place in order to improve the employment and living conditions of workers, the distribution of wealth, and the facilitation of black economic empowerment (BEE) in the mining industry. If implemented correctly, transformation would confront South Africa's three main challenges, namely inequality, poverty, and unemployment among (mainly) black people, women, the youth, and people living with disabilities, in the realization of the African National Congress (ANC) strategy of 'a better life for all' (Mbeki, 2007). The historically disadvantaged South Africans (HDSAs) and companies would be the main beneficiaries of transformation strategies.

The South African mining industry continues to be perceived as possessing untapped resources which, after mining and processing have taken place, could be worth hundreds of billions of dollars in value (Sergeant, 2013). It is against this background that this industry's long-term importance, as well as its history, is being monitored closely for progress towards transformation. Since 1994 the government has promulgated policies, programmes, and initiatives to facilitate transformation in the mining industry. Mining is governed by transfor-

* *Department of Business Management, University of South Africa, South Africa.*

 ISSN 2225-6253. Paper received Mar. 2015; revised paper received Nov. 2015.

mation legislation such as the Constitution of South Africa, the Mining Charter (revised in 2010), the Broad-based Black Economic Empowerment Act of 2003 (BBBEE), the Employment Equity Act of 1998 (EE Act), and the Minerals and Petroleum Development Act–amended in 2013 (MPRDA). However, a series of studies to measure the status of transformation in the South African mining industry continuously reported on the slow pace of transformation. In their defence, mining companies have justified their noncompliance and slow transformation by pointing at inconsistent, broad, and varying definitions in Acts applicable to mining transformation (Rungan, Cawood, and Minnitt, 2005).

The meaning of the term 'transformation' is still being debated and there is no consistency in its definitions. Transformation is a 'buzzword' often meaning different things to different people and can be taken out of context if not defined correctly (Levy and Merry, 1986). What have been defined in the Mining Charter, though, are solid transformation guidelines by means of scorecards in which companies will be evaluated by the first quarter of 2015. Until such time as all stakeholders agree to a common definition of 'Ttansformation', efforts to transform will be hampered by this deficiency. Also, the question remains, does meeting the scorecard targets and ticking each box of the mining scorecard demonstrate transformation? It is evident that the term 'transformation' needs to be clearly defined. Without a clear definition the industry will take longer to transform and will always justify its slow transformation as being a result of the different definitions of transformation. The mining industry seems to have its own interpretations and government have their own expectations and set guidelines for transformation. Moreover, the Chamber of Mines, as well as the unions, has documented how they would like to see the mining sector transforming.

The purpose of this paper is to provide insight into the perspective of transformation from executives in the mining industry. A literature review on transformation, including stakeholder definitions, expectations, and guidelines, is provided. After the literature review the methodology used to explore the understanding of transformation is described, followed by a discussion of the results. Rich descriptions are presented in the results section to provide a deeper understanding of the meaning of transformation by executives in the mining industry. This paper concludes with a definitive and simplified description of transformation.

Theoretical understanding of transformation

In the literature on the topic, the term 'transformation' has several connotations. Levy and Merry (1986) define transformation as a drastic reshuffling in the change process, which requires radical action for change. Esterhuyse (2003) explains transformation as a moral obligation to remove the legacies of *apartheid*. Transformation has a further political association expressed as a 'political, social, and economic change process, with the aim of redressing historical imbalances' (Robertshaw, 2006, p. 8). It is a government strategy to restructure and to bring about culture change by instilling new core values, equitable access to resources and opportunities and skills (Engdahl and Hauki, 2001; Selby and Sutherland, 2006). Engdahl and Hauki (2001) state that transformation depends on how people successfully attain mind-set changes to embrace diversity in organizations. Schoeman (2010) defines transformation as a change process that transforms institutions into achieving employment equity and diversity and creating opportunities for previously disadvantaged groups. According to Schoeman (2010), diversity and equal opportunities ensure that institutions include the mixture of individuals that reflects the demographics of South Africa. For the mining industry, it is often difficult to interpret the concept as transformation is guided by several pieces of legislatione (Rungan *et al.*, 2005), which include the Constitution of South Africa, the Mining Charter (revised in 2010), the Broad-based Black Economic Empowerment Act of 2003 (BBBEE), the Employment Equity Act of 1998 (EE Act), and the Minerals and Petroleum Development Act – amended in 2013 (MPRDA). For the purposes of this article only the Constitution and the scorecard are discussed as these other Acts are already incorporated within the scorecard.

The Constitution of South Africa – perspective on transformation

The Constitution of the Republic of South Africa is an extraction from the Freedom Charter's objectives in order to achieve the promise of a non-racial, democratic, and unitary country (Esterhuyse and Nel, 1990). The Constitution is considered the highest law detailing some transformative guidelines (Cawood, 2004). It is the commitment of the Constitution (Section 25 Act 108, 1996) to transform the mining industry through its provisions of primary pillars of the mineral policy (Cawood, 2004). In particular, the mines have to consider the constitutional aspects regarding transformation and practice common law in their business activities in order to care for human rights (Cawood, 2004; Swart, 2003). The Constitution contains provisions for improving the quality of life for all South Africans and promoting equality (Booyens, 2006). The Constitution also requires a balance between race and gender representivity so as to broadly represent the country's demographics in the way in which organizations are structured. Organizations also need to maintain the necessary skills in these structures to ensure sustainability through the retention of skills and optimum functioning and performance (Republic of South Africa, 1996).

Scorecard perspective on transformation in the South African mining industry

The scorecard for transformation in the South African mining industry is derived from the broad-based transformation charter of the South African mining industry, namely the Mining Charter. The main objective of the Mining Charter is to accelerate BEE by requiring mining companies to reach targets set out in a scorecard. Specific goals and targets are stated in each area of the scorecard (see Table I), namely human resources development, employment equity, mine community development, procurement and enterprise development, ownership, beneficiation, and reporting (Mitchell, 2013). It is important to note that the specific goals and targets should not contradict and lead to the introduction of inappropriate discrimination. The targets of each area of the scorecard are discussed below:

Table I

Scorecard for the South African mining industry

Element	Description	Measure	Compliance target by 2014	Progress achieved by 2010	2011	2012	2013	2014	Weighting
Reporting	Has the company reported the level of compliance with the Charter for the Calendar year	Documentary proof of receipt from the department	Annually	March 2011	March 2012	March 2013	March 2014	March 2015	Y/N
Ownership	Minimum target for effective HDSA ownership	Meaningful economic participation	26%	15%	→			26%	Y/N
		Full shareholder rights	26%	15%	→			26%	
Housing and living conditions	Conversion and upgrading of hostels to attain the occupancy rate of one person per room	Percentage reduction of occupancy rate towards 2014 target	Occupancy rate of one person per room	Base-line	25%	50%	75%	100%	Y/N
	Conversion and upgrading of hostels into family units	Percentage conversion of hostels into family units	Family units established	Base-line	25%	50%	75%	100%	
Procurement and Enterprise Development	Procurement spent from BEE entity	Capital goods	40%	5%	10%	20%	30%	40%	5%
		Services	70%	30%	40%	50%	60%	70%	5%
		Consumable goods	50%	10%	15%	25%	40%	50%	2%
	Multinational suppliers contribution to the social fund	Annual spend on procurement from multinational suppliers	0.5% of procurement value	0.50%	0.50%	0.50%	0.50%	0.50%	3%
Employment Equity	Diversification of the workplace to reflect the country's demographics to attain competitiveness	Top Management (Board)	40%	20%	25%	30%	35%	40%	3%
		Senior Management (Exco)	40%	20%	25%	30%	35%	40%	4%
		Middle Management	40%	30%	35%	40%	40%	40%	3%
		Junior Management	40%	40%	40%	40%	40%	40%	1%
		Core skills	40%	15%	20%	30%	35%	40%	5
Human Resource Development	Development of requisite skills, including support for South African based research and development initiatives intended to develop solutions in exploration, mining, processing, technology efficiency (energy and water use in mining), beneficiation as well as environmental conservation and rehabilitation	HRD expenditure as percentage of total annual payroll (excluding mandatory skills development levy)	5%	3%	3.5%	4.0%	4.5%	5.0%	25%

Scorecard for the broad-based socio-economic empowerment charter for the South African mining industy

Element	Description	Measure	Compliance target by 2014	Progress achieved by 2010	2011	2012	2013	2014	Weighting
Mine community development	Conduct ethnographic community consultative and collaborative processes to delineate community needs analysis	Implement approved community projects	Up-to-date project implementation	Implementation of projects will serve to enhance relationships amongst stakeholders leading to communities owing patronage to projects					15%
Sustainable development and growth	Improvement of the industry's environment management	Implementation of the approved EMPs	100%	Annual progress achieved against approved EMPs					12%
	Improvement of the industry's mine health and safety performance	Implementation of tripartite action plan on health and safety	100%	Annual progress achieved against commitments in the tripartite action plan on health and safety					12%
	Utilisation of South African based research facilities for analysis of samples across the mining value chain	Percentage of samples in South African facilities	100%	Establish	25% baseline	50%	75%	100%	5%
Beneficiation	Contribution of a mining company towards beneficiation (this measure is effective from 2012)	Additional production volume contributory to local value addition beyond the base-line	Section 26 of the MPRDA (percentage above baseline)	The beneficiation strategy and its modalities of implementation outline the beneficiation requirements per commodity extracted in South Africa.					
Total score									100%

Human resources development scorecard

The mining industry was expected to achieve a 5% target in the specific objectives by 2014. These objectives entail that mining companies are expected to:

- Apply and provide a certain percentage of the annual payroll (as per applicable legislation) in required skills development activities that take demographics into consideration (excluding compulsory skills levy)
- Offer support for the national research that is based on development initiatives and recommendations or solutions in exploration, mining, processing technology, efficient use of energy and water in mining, beneficiation, and environmental conservation and rehabilitation (DMR, 2010, p. 3).

The mining industry is required to present a skills audit in which a skills development plan with short-term and long-term goals is featured. Some of the long-term goal requirements are to grant scholarships and bursaries that support mining education. For the immediate goals, the mining industry is required to provide entrepreneurship programmes and provide literacy and numeracy as part of adult education (Cawood, 2004).

Employment equity scorecard

A 40% HDSA participation in each management category and core and critical skills by 2014 was expected (DMR, 2010, p. 3). Critical and core skills include those possessed by artisans, engineers, professionals, and specialists (*e.g.* surveyors, safety specialists, geologists, metallurgists, winding engine drivers, environmentalists, technologists, technicians, and persons with mining-specific qualifications or licences). Mining companies should identify and fast-track their current employees into talent pools to give them experience of high-quality exposure. A key focus is on women in mining, and mining companies were expected to establish a plan to achieve a set target of 10% participation of women in mining by 2014.

Mine community development scorecard

Mining companies were expected to review global best practices in terms of policies, principles, and guidelines in their dealings with other mining companies. The principles require mining companies to be devoted to ethnographic discussions and consultations through concerted efforts before becoming engaged in mining projects, development, and implementation. Mining companies are furthermore expected to perform a needs assessment within the community to establish developmental focus areas. As part of their projects, mining companies should establish initatives to match the needs for community development, and these details should be incorporated in their integrated development plans.

Housing and living conditions scorecard

It was expected that mining companies would put in place development plans to improve the housing and living conditions of mineworkers by converting or upgrading hostels into family units, attaining an occupancy rate of one person per room, and facilitating home ownership options for all mine employees in consultation with organized labour.

Procurement and enterprise development scorecard

Procurement opportunities from mining companies with BEE entities should bee in agreement with the following criteria: the procurement of at least 40% of capital goods from BEE entities by 2014, and ensuring that multinational suppliers of capital goods contribute at least 0.5% of the annual income generated from local mining companies into a social development fund towards the socio-economic development of local communities. Procurement of 70% of services and 50% of consumer goods should be from BEE entities by 2014 (DMR, 2010, p. 2).

Ownership mining scorecard

HDSAs should obtain meaningful economic participation in the mining sector by way of shareholder participation.

Beneficiation scorecard

Mining companies were required to ensure local beneficiation of mineral products by submitting to the requirements of the MPRDA Section 26 mineral beneficiation strategy. Mining companies may set off the value of the level of beneficiation achieved by the company against a portion of its HDSA ownership requirements not exceeding 11% (DMR, 2010).

Reporting mining scorecard

The mining industry was obliged to report on its transformation status in terms of the Mining Charter on a yearly basis with reference to the MPRDA Section 28(2) (c). Reports will be evaluated by the DMR on an annual basis and formal assessments will be performed every five years (DMR, 2010).

In addition to the scorecard perspective on transformation, mining stakeholders have expectations for the realization of a transformed mining industry. These perspectives are discussed below.

Department of Mineral Resources transformation perspective

The DMR, formerly known as the Department of Minerals and Energy (DME), as a government department has as one of its main responsibilities the enactment of policy for the sustainable use of mineral resources (DMR, 2010). The vision of the DMR is 'to enable a globally competitive, sustainable and meaningfully transformed minerals and mining sector to ensure that all South Africans derive sustainable benefit from the country's mineral wealth' (Shabangu, 2014). The DMR views transformation as a measure to 'redress historical imbalances engendered by *apartheid* so that the industry is consistent with the changes in South Africa's overall transformation of its social, political and economic landscape' (Shabangu, 2014).

The Chamber of Mines transformation perspective

The Chamber of Mines acts as an advocacy body with the goal of creating an environment in which the mining industry will be able to deliver, timeously and cost-effectively, sufficient appropriately skilled employees, who are trainable for advancement and deployment (Chamber of Mines, 2010). It also monitors the industry's adherence to the Minerals and Petroleum Resources Development Act of 2002 and the Mining Charter (Shabangu, 2010). The vision of the Chamber of Mines is to 'achieve a policy, legislative and governance

framework, which is widely supported and will allow the mining industry to convert as great part as possible of the country's abundant mineral resources into wealth for the benefit of South Africa' (Chamber of Mines, 2014). In its advocacy role, the Chamber is required to act as a custodian of the monitoring of transformation and sustainability progress on an annual basis as one of its key objectives.

The National Union of Mineworkers perspective on transformation

The National Union of Mineworkers (NUM) was the dominant representative of mineworkers in South Africa. It was founded in 1982 and was affiliated to the Congress of the South African Trade Unions (COSATU). NUM defines itself in terms of the concept of social-movement trade unionism (Fafuli, 2012). This union has the overall aim of improving the lives of mineworkers and has been instrumental in transforming the mining industry with regard to the conversion of hostels into family units and single units. The mandate of organized labour is to defend the rights of employees at the workplace, drive and monitor training and skills development, take up grievances, protect employees against unfair labour practices, and bargain to improve salaries and working conditions (NUM, 2013). NUM supports affirmative action strategies that seek to empower black people into senior positions, and contribute to the struggle for non-racialism and against racial inequality and gender domination in the mining, energy, and construction industries (NUM, 2013).

The South African Mining Development Association perspective on transformation

The South African Mining Development Association (SAMDA) is a non-profit organization that was established in 2000 to represent the interests of junior and BEE mining companies. SAMDA advocates for transformation and compliance with national transformation objectives in the mining sector (SAMDA, 2011). It is insistent on transformation and continues to lobby for developmental policy objectives in the sector through the existing channels (SAMDA, 2011). SAMDA has been involved in the draft of the Minerals Bill and participated in the drawing up of the charter on empowerment of HDSAs. This commission drafted the agreement between the government and the mining sector on time frames and quotas to allow the objectives of the Mining Charter to be met. Amongst other things, SAMDA also takes responsibility for developing capital markets for junior companies.

The mining industry has a task to attempt to meet each stakeholder's expectation. Thus this research offers views on how such expectations are interpreted by mining executives.

Population sampling

A non-probability purposive sampling technique was used to sample the participants from the population comprising mining companies listed on the Johannesburg Stock Exchange, ranging from micro- to mega-companies. This technique allowed the researcher flexibility to make judgements regarding the selection of specific participants to partake in the research. Participants who monitor and oversee transformation in mining companies were invited to share their understanding and interpretation of transformation. The 10 participants selected had different job titles but all were executives and members of senior management responsible for overseeing transformation, sustainability, human resources, people management, or employment equity in their respective organizations.

Data collection method

This study was exploratory and was conducted within an interpretivist paradigm. The data collection involved in-depth interviews with 10 participants. A structured interview guide was used to pose open-ended questions which allowed the interviewees to elaborate, to explain their answers, and to offer additional information which was not part of the solution. This method offered the interviewer the flexibility to probe for further information, clarify issues, and seek explanations to assist in the reporting of results. The purpose of the study was explained to the participants and informed consent was obtained for participation. Participants voluntarily participated in the research and anonymity and confidentiality of their responses were ensured. The interviews ranged from 45 minutes to one-and-a-half hours, and were held at a place convenient for each participant. The majority of interviews were conducted at the participants' offices. All the interviews were recorded and were later transcribed into primary documents ready for qualitative content analysis.

Data analysis strategy

Primary documents were loaded onto the Atlas.ti software, which is a qualitative data analysis software package that offers support involving the interpretation of text through coding, theme identification, and making sense of data. Atlas.ti 'has the capacity to deal with large amounts of text, as well as the management of annotations, concepts and complex structures, including conceptual relationships that emerge in the process of interpretation' (Muhr, 1991, p. 349).

Qualitative content analysis was used to analyse the transcribed verbatim data. A summative approach was used, which started with the coding of text into quotations, counting and comparing quotations, keywords, or paragraphs, followed by the interpretation of the codes to form categories or themes (Rosengren, 1981). Results are presented verbatim using direct quotation.

Results and key findings

The results of the study indicated that six common themes emerged to explain stakeholders' perspectives of transformation as interpreted during the analysis. It was found that the participants interpreted transformation as a cultural change but not a race issue. Transformation was seen as a mind-set change, embracing diversity, equalizing rights, and creating opportunities; about doing what is right for organizations; and being a long-term process.

Transformation is about cultural change, not about race and gender

Three participants (30%) considered transformation as not being about racial issues and meeting the scorecard targets. They explained that appointing black candidates for key

positions was not a reflection of transformation; rather, transformation was seen as a complete cultural change and a way of transforming the way things are done in the business:

'*Transformation is not getting black managers on top of the organizational structure. Transformation is [a] complete culture change, doing things differently, in order to make sure that you sustain the organization. People think that when you have got two or three black managers sitting in the board or at the top of the organization, then you are transformed*' *(Participant 1)*.

'*Transformation is also determined by the nature of your business and how much are you prepared to develop talent and balance it out. That is why we have to be big and make sure about it, look at the demographics of the country. Not [to] build negative dynamics within the company for yourself by trying to push a particular agenda because of colour. So we are not going to use colour that much. But at the same time, you need to look into it to say, you can't just have 100% Africans*' *(Participant 5)*.

'*White people are feeling so disenfranchised now. They are feeling so reversed apartheid. [They] feel like second-class citizens at the moment. [They] feel they have got something, but at any moment [they] can lose it and it is actually very depressing for white people' (Participant 2)*.

Transformation was regarded as a complete and cohesive practice of doing things differently in an organization. This implies removing old ways of doing things and adopting new ways to meet transformation targets:

'*We go along and say African, African, African, before we know it we have marginalized the youth of another colour [white youth]. What are we turning them into, because now we are complicating the social problems' (Participant 6)*.

'*Because if [refers to a stakeholder] understanding of transformation is getting more blacks and getting more women, then we have got a serious challenge there, because you cannot put a black individual in a position who hasn't got the competencies' (Participant 1)*.

Participant 1 quoted above was weary of the racial connotation attached to transformation by strongly disregarding the numbers (achieving demographic statistics as per scorecard) as evidence of transformation.

Transformation is about a change of mind-set

The transition to changing the way business is done perpetuates the change of mind-set which had a strong connotation to transformation, supported by the views of six participants. The majority of the participants stated that their understanding of transformation meant a mental shift towards transformation and accepting that the imbalances of the past need to be addressed:

'*Transformation in the mining industry means addressing the imbalances of the past, simply put. Addressing of the imbalances of the past does not mean you still compromise quality. You don't say, for instance, let me go if you talk appointments, let me go an appoint a black woman because we need figures. It's not about that. It's about the right people for the right positions with the right skills, okay, number one. It's also about in my opinion the mind-set change' (Participant 10)*.

'*We all now understand that we had these imbalances, it's a question of now changing our minds instead of us being pushed by the Act to make these changes, by now we should be making these changes ourselves without waiting for the Act*' *(Participant 10)*.

'*Transformation means doing things differently than you used to do them before … now what we need to do, we need to make sure that we transform the way we do things*' *(Participant 1)*.

Transformation is about the creation of opportunities and equalizing rights

The results further indicated that transformation was interpreted as creating opportunities, equalizing rights, and ensuring fair representation for all, as described by two participants. Equal and fair presentation of opportunities should be afforded to all, and this will equalize society:

'*That is quite an overloaded word. We have got different meanings to attach to these things and I think for me transformation or any other thing; for example with us, we had to come together and say, how we define transformation for ourselves … Amongst others it would mean affording every person who is in the system an opportunity to be developed in the areas of their future careers, career aspirations*' *(Participant 5)*.

'*Transformation means that there has to be fair representation and distribution of everything. Then coming back to the work context, fair distribution of wealth, possessions, there must be just equity and fairness in the workplace' (Participant 4)*.

In equalizing rights, Participant 4 (quoted above) referred to a fair distribution of wealth and possessions and was adamant on the need for equity and fairness in the workplace:

'*Transformation in South Africa is … first and foremost about equalizing the rights, it's about equalizing society … and giving an opportunity to those that didn't have an opportunity before. I think transformation in South Africa is an opportunity. It's an opportunity of saying if I was a white manager and I'm running [name of company], it will be an opportunity, I would see that the growth of my business is in my people in my country, whether they're black, green, yellow, blue, understanding my business and what I do about my business*' *(Participant 8)*.

Participant 8 strongly argued that transformation was about opportunity creation for all, regardless of one's race. She believed that holding this transformation perspective would be a long-term and sustainable objective rather than numbers objectives:

'*We all now understand that we had these imbalances, it's a question of now changing our minds instead of us being pushed by the Act to make these changes, by now we should be making these changes ourselves without waiting for the Act. I think that 18 years into democracy a lot of companies have made progress at this moment. We shouldn't be talking about employment equity at all now, I think we should now be talking about we are now*

equal in terms of qualifications and the colour should not be an issue and the issue should now be who is the best. But because a lot of companies started a bit late, they are still sitting in my opinion, the Act is still breathing in their necks because they are, they have been very slow' (Participant 10).

'*Transformation is a very huge and broad thing. It is primarily a social, people thing. So it is dealing with the disparities, the economic divide. It is dealing with these different barriers, dealing with the poverty barrier, the skills barrier, the business barrier, the opportunity barrier, and the equitable economic opportunities barrier, between our different race groups in South Africa' (Participant 3).*

Transformation is about valuing diversity

The majority of participants (90%) revealed that transformation meant valuing and embracing diversity. In the response below, Participant 3 reflected on the tension that exists when people of different races work together as a team:

'*Because people fundamentally don't understand what diversity means and the fact that the more different we are, the better we can be ... because typically we try to gravitate towards the sameness. If I am an African female, maybe I will work better with a fellow African female. Now [when] a white woman comes in, all of a sudden there is tension, maybe we don't understand why, but we don't leverage off the difference' (Participant 3).*

There is a strong correlation between the responses of Participants 3 and 4. Participants 4 advocated for a sense of belonging to be created for new entrants in mining companies. According to this participant, a sense of belonging should be fostered to create an industry that employees belong to:

'*You know, you can't bring people into an organization and still make them feel like they don't belong' (Participant 4).*

Participant 8 added that even though transformation implies creating a sense of belonging in an accommodative environment, *Ubuntu* should be promoted and preserved. This participant stated that the African culture should be preserved without compromising on profits and sacrificing the standards of the business by including HDSAs who do not integrate well with how the business operates:

'*Transformation, what it means for this country going forward is that we have to embrace the African culture, the South African culture, the indigenous of South African culture into business. And making it work and make money out of it. Nowhere does it say you must lower your standards because the world will eat you alive. Nowhere [transformation] says you must compromise your profits' (Participant 8).*

The majority of participants showed that they accepted diversity but they were concerned that it was not embraced in mining companies. They emphasized that people who enter the mining industry need to have a sense of belonging and feel accommodated.

Transformation is doing what is right

Doing what is right was positively correlated with transformation by responses from two participants. These participants highlighted the nobleness in the quest for transformation by stating that transformation was not about achieving the targets of the scorecard, but associated with doing right:

'*Our view is not necessarily to tick the box in the scorecard, our view is to do the right things and the numbers will come ... so we are not really fixated about ticking the scorecard. We are more fixated about doing what is right for the business' (Participant 6).*

'*[Transformation] is not about ticking box number 1. It is not just about meeting the compliance requirements. But [transformation] is also about what is it that we would like to see the industry, starting with our own organization, look like at a particular point in time, because transformation assumes a particular journey now knowing and understanding the history of mining in South Africa within the context of the history of the country. You can't transform the country and have the [mining] industry stay where it was' (Participant 3).*

The responses of the participants reveal that for them transformation means more than just a tick on a scorecard: it is a process of social justice and of transforming this industry which historically had an enormous impact on the country as a whole.

Transformation is a process

Lastly, the results showed that the participants agreed that transformation is a long-term process that cannot be fast-tracked. The view was that change, embracing the whole culture, must first take place before real and solid transformation can happen:

'*Today must obviously be better than yesterday and tomorrow must always be better than today etc., as you move forward in transformation, it is a gradual process. [Transformation] is a process, but it must be a process that indicates a difference as you move' (Participant 3).*

'*[Transformation] is not a process that you can just plug in, then wow, the organization has transformed' (Participant 1).*

'*[Transformation]is actually moving the different segments of society at least up one or two notches [so that], the next generation can be better off ... so it is a long-term transformation' (Participant 2).*

Participant 3 argued that the process of transformation is lengthy because the mining industry started to transform from a zero base. Therefore, rapid transformation cannot be expected, although the industry is gradually embracing the need for transformation:

'*There was a point in time where women were not allowed to be involved in mining. So really, [it's] an industry [where] you come from a zero base where there were no women that could work underground. There were certain jobs ... ground that could be done by women; limited, but ja, not even talking African women. I am talking about there would have been white women*

at that time because black women were not allowed. So the kind of progress that has been made is a progress from zero' (Participant 3).

Conclusions

This paper aimed to explore mining executives' understanding of transformation and to understand how this understanding supports or differs from existing definitions and expectations in the literature, relevant legislation, and industry guidelines. The results of the study show that the interpretation of transformation varies in mining companies but can be consolidated to feature in a definition for transformation.

- Firstly, Participant 1 interpreted transformation as *culture change*, and not related to race or gender. It cannot be regarded as entailing that a white individual is replaced by a black individual. This implies that companies should create a culture of embracing change, regarding new values and providing equitable resources and opportunities by accepting the agenda of transformation, which will be reflected in their new and innovative ways in their business dealings. This view supports the interpretation of transformation by Schoeman (2010), Selby and Sutherland (2006), Engdahl and Hauki (2001), and the Constitution, that transformation aims to inspire new fundamental values, equitable access to resources, and opportunities and skills development
- Secondly, transformation is regarded as a change of mind-set whereby individuals in organizations acknowledge that historical imbalances need to be addressed, and innovative ways should be sought to accept policies that encourage transformation. This finding supports the meaning of transformation according to Engdahl and Hauki (2001), as well as the Constitution, in that transformation is about embracing diversity and equal opportunities and ensuring that institutions include the mixture of individuals reflecting the demographics of of South Africa
- Thirdly, transformation is interpreted as the creation of opportunities and safeguarding equity, and fairness for employees in the workplace. This finding was discussed by Schoeman (2010) and Levy and Merry (1986), that structural, but radical change was needed for the creation of opportunities for all. This endeavour requires that mining companies accept legislative, regulatory, and statutory frameworks that seek to facilitate transformation. Examples of such policies are the EE Act, MPRDA, and the Mining Charter. These frameworks should be consulted to ensure fair and equitable hiring procedures, with fair and equitable treatment of all employees. However, the change in organizational demographics should be subject to the maintenance of competency
- Fourthly, transformation is explained as the embracement and valuing of diversity. Diversity is valued when mining companies' employee demographics reflect the demographics of the country. This finding implies that all occupational levels within mining companies should reflect diversity in terms of race, age, and gender. In relation to embracing diversity, the findings revealed that transformation is about creating a sense of belonging for mining industry entrants. It is nonsensical to recruit people for the sake of achieving the scorecard targets, but making them feel as if they do not belong. This finding confirms a perspective described by Schoeman (2010), discussed in the literature review, namely that diversity in institutions should be encouraged
- Fifthly, it was found that transformation is associated with justice – doing the right thing. Given past injustices and inequalities, transformation is seen as a corrective measure to redress past equalities. Comments made by Participants 3 and 6 suggest that transformation is seen as a vehicle to make things right and achieve social justice, given the inequalities of the country. This finding concurs with Esterhuyse's (2003) claim that transformation is a moral obligation
- Lastly, transformation is seen as a long-term process, as indicated by Participants 2 and 3, because the mining industry started transforming from a zero base. Given the need for cultural change, it was found that the industry will transform gradually; thus, transformation is regarded as a journey and a process that will not happen overnight. It can be concluded that systems should allow a cultural change process to take place. This finding is in line with the recommendation by Rungan *et al.* (2005) that there should be realistic expectations from mining companies. It is clear, therefore, that transformation is interpreted differently by other stakeholders in comparison to mining executives as stakeholders. However, the interpretation in the literature does not deviate from the perspectives of mining executives. This shows that mining executives and government, as well as other stakeholders, need to align their interpretations of transformation.

Recommendations

- It is imperative for all industry stakeholders, mining companies, and government to agree on a common definition of transformation
- The study recommends that the regulator define transformation as suggested by Esterhuyse (2003) and Rungan *et al.* (2005). This definition should be corroborated with the views from mining executives and that of the Constitution. This definition should include a reference to cultural change that involves a mind-set change to create equal opportunities, equalize rights, and embrace diversity. Cultural change is about the creation of a sense of belonging for all employees. Transformation ensures social justice by doing the right things to correct past imbalances and ensure fair and equitable opportunities to all. Transformation is a process that will take place gradually and for it to successfully happen, a culture change is needed first
- It is also recommended that the regulator integrates applicable policy documents in the mining environment; namely, the Mining Charter, the BBBEE, and the MPRDA of 2002 as recommended by Rungan

et al. (2005). New and realistic transformational targets need to be set for the period 2018–2030, and these should be in accordance with the National Development Plan. Once the new targets have been set, an awareness regarding the new targets should be created and the implications and consequences of noncompliance should be communicated

- It is further suggested that the transformation targets be monitored and evaluated on an annual basis to ensure substantive progress. Moreover, strict and legal enforcement must be put in place so that mining companies will adhere to the targets, and operational consequences for noncompliance should be imposed. For example, the licence to operate should not be renewed for companies showing a lack of transformation. The results of the study are not generalizable, but are limited to the South African mining industry. However, future research can be extended to compare the interpretation of transformation by other industries.

Limitations of the study

Transformation is a sensitive issue in South Africa, and most participants who were contacted for interviews showed a reluctance to participate. The researcher is aware that the participants' views may not necessarily represent the views of the overall population in the mining industry. Also, this study presents views by mining executives at a particular point in time, in the prevailing circumstances; it is possible that the results would differ if the research were to be repeated at another time or by a different researcher.

References

Booyens, S.A. 2006. The scorecard for the broad-based socio-economic empowerment charter for the South African mining industry: a performance measuring instrument. Master's thesis, North-West University.

Cawood, F.T. 2004. The Mineral and Petroleum Resources Development Act of 2002: a paradigm shift in mineral policy in South Africa. *Journal of the South African Institute of Mining and Metallurgy*, Jan/Feb. pp. 53–64.

Chamber of Mines of South Africa. 2010. What is the Chamber? http://www.bullion.org.za [Accessed 10 May 2010].

Chamber of Mines 2007. The South African mining industry transformation and sustainability report 2007. [http://www.bullion.org.za/Departments/SafetySusDevl/Downloads/SDRtext07.pdf [Accessed 28 June 2010].

Chamber of Mines of South Africa. 2014. Vision. http://chamberofmines.org.za/about/mission-statement [Accessed 14 October 2014].

Dansereau, S. 2010. Comparing duelling approaches to the transformation of South African mining: corporate social responsibility of labour restructuring? *Labour. Capital and Society*, vol. 43, no. 1. pp. 63–98.

DMR (Department of Mineral Resources). 2010. Mineral policy development. Pretoria.

Engdahl, C. and Hauki, H. 2001. Black Economic Empowerment: an introduction for non-South African business. Master's thesis. Gothenburg University, Sweden.

Esterhuyse, W.P. 2003. The challenge of transformation: breaking the barriers. *South African Journal of Business Management*, vol. 3, no. 42. pp. 1–8.

Esterhuyse, W.P. and Nell, P. 1990. Die ANC. Tafelberg, Cape Town.

Fafuli, M. 2012. The role of NUM in transforming the mining industry. *International Mining History Conference*, Gold Reef City, Johannesburg, 17–20 April, 2012.

Levy, A. and Merry, U. 1986. Organizational transformation: Approaches, strategies, theories. Praeger, New York.

Mbeki, T. 2007. Address by President Thabo Mbeki to the National Council of Provinces (NCOP). http://www.anc.org.za/show.php?id=4245 [Accessed: 10 August 2014].

Mitchell, G. 2013. Making sense of transformation claims in the South African mining industry. *Journal of the Southern African Institute of Mining and Metallurgy*, vol. 113, no. 1. pp. 39–43.

Muhr, T. 1991. ATLAS/ti--A prototype for the support of text interpretation. *Qualitative Sociology*, vol. 14, no. 4. pp. 341–371.

Num (National Union of Mineworkers). 2013. NUM History. http://www.num.org.za/AboutUs/History.aspx [Accessed: 29 June 2013].

Ramatlhodi, N. 2014. Mining Lekgotlha 2014 Annual Address. http://www.polity.org.za/article/sa-ngoako-ramatlhodi-address-by-the-minister-of-mineral-resources-at-t-the-2014-annual-mining-lekgotla-gallagher-convention-center-midrand-13082014-2014-08-13 [Accessed 26 August 2014].

Robertshaw, A.M. 2006. Transformation of the civil engineering sector: a review of the response of established civil engineering consultancies to this challenge. Master's thesis. University of KwaZulu-Natal, Pietermaritzburg.

Rosengren, K.E. 1981. Advances in Scandinavia content analysis: an introduction. *Advances in Content Analysis*. Rosengren, K.E. (d.). Sage, Beverly Hills, CA. pp. 9-19.

Rungan, S.V., Cawood, F.T., and Minnitt, R.C.A. 2005. Incorporating BEE into the new mineral law framework for the South African mining industry. *Journal of the South African Institute of Mining and Metallurgy*, vol. 105. pp. 735–744.

SAMDA (South African Mining Development Association). 2011. History. http://www.samda.co.za/History.aspx [Accessed 13 August 2013].

Schoeman, N. 2010. The drivers and restraining factors for achieving employment equity at management level in gold mining companies. MBA thesis, Gordon Institute of Business Science, Johannesburg.

Selby, K. and Sutherland, M. 2006. 'Space creation': a strategy for achieving employment equity at senior management level. *South African Journal of Labour Relations*, vol. 30, no. 2. pp. 42–65.

Sergeant, B. 2013. Nationalisation: an analysis of the competing interest of capital, labour, and government. *Journal of the Southern African Institute of Mining and Metallurgy*, vol. 113. pp. 21–30.

Shabangu, S. 2010. Mining charter aims not met. http://www.news24.com/SouthAfrica/Politics/Mining-charter-hasnt-achieved-aims-Shabangu-20100913 [Accessed 23 September 2010].

Shabangu, S. 2014. Department of Mineral Resources: Protecting the nation's interests and assets. http://thesa-mag.com/features/mining/department-mineral-resources-protecting-nations-interests-assets/ [Accessed 14 October 2014].

Republic of South Africa. 1996. The Constitution of the RSA, Act 108 of 1996 as amended. Government Printing Works, Pretoria.

Swart, E. 2003. The South African legislative framework for mine closure, *Proceedings of the Colloquium on Mine Closure for Sustainable Development*. South African Institute of Mining and Metallurgy. Johannesburg. ◆

Conference Announcement

The Southern African Institute of Mining and Metallurgy

in collaboration with the SAIMM Western Cape Branch is hosting the

Hydrometallurgy Conference 2016

Sustainable Hydrometallurgical Extraction of Metals

31 July 2016—Workshop • 1–3 August 2016—Conference

Belmont Mount Nelson Hotel, Cape Town

KEYNOTE SPEAKERS
F. Crundwell
M. Nicol
K. Osseo-Asare
M. Reuter
S. Bhargava

- Register 4 delegates and get the **fifth registration free**
- Book and pay full conference by **1 July 2016** and attend the **workshop for free**

(limited to the first 50 registrations)

Metals play a significant role in industrialisation and technological advancements. Do you ever wonder then what life would be like without metal resources?

The depletion of natural rich ore deposits coupled with a fall in grade, a decline in productivity, rising operational and energy costs, concerns on sustainability and environmental impact of mining and metal related activities have been affecting the mining and metals industry in the recent past. Unless innovative methods that look at the smart use and recovery of metals from metal resources are developed, the world will be faced by a metal supply risk that will impact on future economic growth and technological development.

The SAIMM Hydrometallurgy Conference, 2016, will bring together internationally and locally recognized experts, industries, R&D establishments, academia as well as students to explore how future metal demands can be met through modern hydrometallurgical technologies that can:

- Assist in sustainable metal extraction
- Lower energy costs
- Minimise the impact on the environment

WHO SHOULD ATTEND

The conference will be of value to:

- Hydrometallurgical plant managers and metallurgists
- Equipment and reagent suppliers to the hydrometallurgical industry
- Hydrometallurgical technology development companies
- Mining industry consultants
- Research and academic personnel

SPONSORSHIP/EXHIBITIONS

Companies wishing to sponsor or exhibit should contact the Conference Co-ordinator

Funding Sponsor

science & technology
Department: Science and Technology
REPUBLIC OF SOUTH AFRICA

NRF National Research Foundation

Sponsors

CiDRA Minerals Processing

Outotec

CYTEC SOLVAY GROUP

FLSmidth

TOTAL COMMITTED TO BETTER ENERGY

WorleyParsons resources & energy

For further information contact:

Head of Conferencing, Raymond van der Berg
Saimm, P O Box 61127, Marshalltown 2107
Tel: +27 (0) 11 834-1273/7 · E-mail: raymond@saimm.co.za
Website: http://www.saimm.co.za

SAIMM THE SOUTHERN AFRICAN INSTITUTE OF MINING AND METALLURGY

http://dx.doi.org/10.17159/2411-9717/2016/v116n5a12

The tap-hole – key to furnace performance

by L.R. Nelson* and R.J. Hundermark†

Synopsis

The critical importance of tap-hole design and management for furnace performance and longevity is explored through examining some of the specific matte, metal, and slag tapping requirements of non-ferrous copper blister and matte converting and smelting, ferroalloy smelting, and ironmaking systems. Process conditions and productivity requirements and their influence on tapping are reviewed for these different pyrometallurgical systems. Some critical aspects of the evolution of tap-hole design to meet the diverging process and tapping duties are examined. Differences and similarities in tapping practices and tap-hole management are reviewed. Finally, core aspects of tap-hole equipment and maintenance are identified – aspects that are considered important for securing improved tap-hole performance and life, so pivotal to superior furnace smelting performance.

Keywords
tapping, tap-hole, ironmaking, ferroalloy, non-ferrous, matte, slag, blister, smelting.

Introduction

The sheer diversity of tapping configurations used on industrial pyrometallurgical operations is at first bewildering. They range from historical tilting furnaces without tap-holes to modern eccentric bottom tapping (EBT) tilting and/or bottom slide-gate electric arc furnaces; to classical single tap-hole multiphase tapping (*e.g.* metal/matte and slag); to dedicated phase tap-holes (*e.g.* dedicated metal/matte-only and slag-only); to dedicated phase multiple tap-hole configurations (up to eight metal/matte-only tap-holes and six slag-only tap-holes); to more esoteric metal/matte-only siphons and slag overflow skimming, *e.g.* Mitsubishi Continuous Process (Matsutani, n.d.). This can be further complicated by periodic batch tapping; consecutive tapping on a given tap-hole; alternating tap-hole tapping practice; near-continuous slag-only tapping, with discrete batch matte/metal tapping on higher productivity, but low metal/matte fall (<20% by mass feed) Co and Ni ferroalloy and platinum group metal (PGM) matte furnaces; near-continuous tapping through batch tapping of individual tap-holes that are opened consecutively (Tanzil *et al.*, 2001; Post *et al.*, 2003); to fully continuous tapping on coupled multi-furnace cascades (Matsutani, n.d.).

This is largely a consequence of differing processing conditions (process temperature, superheat (ΔT), Prandtl number, $Pr = \mu C_P/k$, where μ = dynamic viscosity, C_P = specific heat capacity and k = thermal conductivity, and resulting heat flux). But this can also be influenced strongly by industrial operating philosophy in terms of furnace design for campaign life longevity (*i.e.* greater capital expenditure for longer, say 20–30 years' life) *versus* furnace productivity (*i.e.* number of heats/campaigns to provide the greatest possible dilution of fixed costs per unit of commodity produced). And this may not even be consistent within a given commodity; all ironmakers (blast furnace (BF) campaign life–based) supply downstream steelmakers (who use heat/campaign-based converters and/or electric arc furnaces).

However, regardless of the specific tap-hole configuration or operating philosophy, owing to the addition of dynamic (often periodic) and more intense process conditions (exposure to higher temperatures leading to accelerated corrosion, greater turbulence, and elevated rates of mass and heat transfer) and higher concomitant thermomechanical forces (from thermal or flow shear stresses), furnace performance and longevity is intimately linked to tap-hole performance. For good reason Van Laar (2001) titled his paper '*The taphole: the heart of the blast furnace*' at the 2001 symposium entitled *The taphole – the blast furnace lifeline* (Irons, 2001), while the title of the 2010 Coetzee and Sylven (2010) contribution '*No taphole – no furnace*' and the staging of the SAIMM Furnace Tapping conference in 2014 suggest continued criticality and relevance.

* *Anglo American Platinum Ltd.*
† *Anglo American plc.*

 This paper was first presented at the, Furnace Tapping Conference 2014, *27–28 May 2014, Misty Hills Country Hotel, Muldersdrift, South Africa.*

The tap-hole – key to furnace performance

By first comparing and contrasting some of the process conditions and resulting tap-hole and tapping requirements of different commodities, we make an attempt at identifying key elements of tap-hole design, physical tapping practices, equipment, and monitoring and maintenance practices characteristic of superior tap-hole management and required to secure increased tap-hole performance and prolonged life.

Commodity-specific process and operating conditions

To provide some context to the range of tap-hole designs, and operating and maintenance practices adopted for different commodities, it is instructive to compare some key process physicochemical and operating conditions prevailing. Notable features include:

- Sheer metal fall and productivity of ironmaking BFs >10 000 t/day hot metal (HM), achieved through near-continuous tapping at more than double the rate and velocity of, but through tap-hole diameters not too dissimilar to, other commodities
- High pressure of tapping liquids of ironmaking BFs (up to 5 bar blast pressure at tuyeres, to add to already high hydrostatic pressure of comparatively thick slag and thick and dense metal)
- More limited accessibility of smaller circular blast and electric furnaces (EFs) (up to 22 m diameter) to multiple tap-holes, than larger rectangular six-in-line (6iL) furnaces (up to 36 × 12 m)
- Low comparative temperatures and superheats of (often near-autogenous) copper smelting

Table I

Indicative[1] process limits, properties and operating conditions for specific commodities

	Iron making	Cr ferroalloy	Mn ferroalloy	Ni ferroalloy	Cu blister/matte	Ni Matte	PGM matte
Furnace	BF	SAF/DC–arc	BF/SAF	Circ/6iL EF	FF/TSL	6iL/TSL/FF	6iL/Circ/TSL
M + S tap–holes	1–4	1–3, 1–2+1–2	1–2, 2+2	2+4–6	2–8+2–6	2+2	2–3+2–3
$T_{metal/matte}$, °C	1480–1530	1500–1650	1300–1450	1430–1550	~1170–1320	1150–1300	1300–1500
$\Delta T_{metal/matte}$, °C	~350	50–100	50–150	20–350	100–250	50–300	400–650
T_{slag}, °C	1480–1530	1600–1750	1350–1550	1550–1630	1170–1350	1200–1400	1450–1600
ΔT_{slag}, °C	~200	<50	50–100	50–150	50–100	50–150	50–200
$q_{average}$, kW/m^2	25	5	5	50–100	20–100	20–50	30–100
$q_{peak\ tap–hole}$, kW/m^2	>200	>15	>15	>200	>300	>200	>300
$\rho_{metal/matte}$, t/m^3	7	~6.7	~5.5	~7.5	~5–7.5	~4.5	~4.2
ρ_{slag}, t/m^3	2.8–3.1	2.7–3.2	2.7–3.3	2.8–3.2	3.5–4	2.8–3.2[&]	2.8–3.2
$\mu_{metal/matte}$, Pa.s	~0.007	~0.007	0.005	~0.006	0.002–0.005	0.003(0.05[&])	0.0025
μ_{slag}, Pa.s	0.1	~0.5	0.7–1.5	~0.5	0.03–0.07	0.3	0.3
$k_{metal/matte}$,◆W/m°C	50	~20	~14	~30	~5–160	17[&]	17[&]
k_{slag},◆W/m°C	~0.5	~0.2	~0.2	~0.7	~2–8	0.8 (8[&])	~0.8
$C_{p,metal/matte}$, MJ/t°C	0.8	~0.9	~0.9	~0.5	~0.5	~0.7	~0.8
$C_{p,slag}$, MJ/t°C	~1	~1.7	~1	~1.2	~1	1.25[&]	~1.3
$\beta_{metal/matte}$, /°C	8 x10^{-5}	7 x10^{-5}	–	8 x10^{-5}	1 x10^{-5}	1 x10^{-4}	1 x10^{-4}
β_{slag}, /°C	–	–	–	–	–	3 x10^{-4}[&]	3 x10^{-4}
$Pr_{metal/matte}$	0.1	0.3	0.5	0.2	0.01	0.13 (2.1[&])	0.12
Pr_{slag}	50	–	–	–	–	470 (47[&])	~450
$H_{metal/matte > MTH}$, m	~2	0.3–0.6	0.3–0.6	0.15–0.3	0.25–0.4	0.25	~0.3
$H_{metal/matte–STH+Top}$, m	~2	(0.3+) ~1	(0.3+) ~1	0.6–1+0.4–1	0.2–0.4+0.2–0.4	0.2–0.4+0.2–0.6	0.5+0.6–0.9
$P_{top\ of\ liquid\ level}$, bar	5	>1[$]	>1[$]	>1[$]	~1	~1	>1[$]
$d_{metal/matte\ tap–hole}$, m[#]	~0.07	0.07–0.2	0.04–0.1	0.04–0.1	~0.05	~0.07	0.04–0.07
$v_{tapping}$, m/s	5 (to 8)	~4	~2–4	~2–4	~2–4	~2–4	~2–4
$\dot{m}_{metal/matte}$, t/min[*]	7	~1–4	1–2.5[§]	~1.5–3	1–3	~2.5	0.5–1.5[§]
Metal/matte fall	60–75%	35–50%	35–60%	5–20%	~40%	30–40%	10–25%
Tap–hole repair, w	4	>12	>26	1–2/8	4	3–9/26	1–4/12
Tap–hole life, y	10 (12)	2–6	2–6	1–4	1–4	1–3	1–2
Furnace life, y	15–20	12	20	20	6–12	30	12

[#]Non-HM tap-holes often start ~40 mm diameter
◆At process temperature; Mn solid at 727°C
[*]FA and non-ferrous instantaneous batch mass tapping rate
[§]Higher value also typical $\dot{m}_{slag}$
[&](Sheng *et al.*, 1998).
[$]Operate with significant charge burden

[1]Some operations may operate quite far from these generically indicative values. Mills and Keene, (1987) and Sundström *et al.* (2008) provide much of the slag and matte properties data, respectively

- Relatively low superheats of ferroalloys (FA) in DC arc and submerged-arc furnaces (SAFs)
- Higher viscosity (and *Pr*), but lower thermal conductivity and density of slag than metal/matte
- High thermal conductivity (*k*) of liquid blister Cu
- Extreme superheat (ΔT) of PGM matte (Shaw *et al.*, 2012; Hundermark *et al.*, 2014).

Slag freeze lining *versus* matte/blister copper 'hit' potentials

A striking industrial observation is the ease with which slag freeze linings can be formed and maintained (almost 'self–healing') from even superheated slag, provided cooling is adequate. It is also quite remarkable how effectively just a thin accretion layer of slag (a couple of millimetres thick) can provide a sufficient thermal resistance to appreciably lower critical lining and copper hot-face temperatures.

In stark contrast, especially in PGM matte and blister Cu processing, equivalent matte/metal accretion formation often seems near impossible to achieve, to the extent that the operation of copper coolers on blister Cu requires 'demonstrated ability to maintain a protective accretion coating' (George, 2002). Or stated in another way in the PGM matte industry: the operation of copper coolers unprotected from direct contact with superheated liquid matte is simply not tolerated.

Considering the heat transfer conditions applicable to the successful implementation of a water-cooled composite copper lining, four key criteria can be defined when considering the influence of process heat flux, $q = h_b \Delta T$ (where $\Delta T = T_B - T_f$ and h_b = convective heat transfer coefficient from bulk process liquid of temperature T_B, to accretion freeze lining[2] of temperature T_f), into and out through the composite cooling system. The latter is described for the simplest one-dimensional case by

$$q_C = (T_f - T_C)/(x_f/k_f + x_R/k_R + 1/h_I + x_C/k_C + 1/h_C)$$

where q_C = composite cooler heat flux; T_f = effective accretion freeze lining temperature in contact with process liquid (whether matte or slag); T_C = bulk temperature of cooling fluid; x_f and k_f are, respectively, thickness and thermal conductivity of the accretion freeze lining; x_R and k_R are thickness and thermal conductivity of the residual refractory; h_I = convective heat transfer coefficient at the cooler hot-face; x_C and k_C are thickness and thermal conductivity of residual refractory; and h_C = convective heat transfer coefficient of the cooling medium (*e.g.* air or water).

Following the example of Robertson and Kang (1999), we describe some relevant limiting conditions for such a heat transfer system:

(1) For an accretion to freeze (sustainably), q must be less than q_C
(2) The cooling system hot-face temperature (be it refractory or copper) must be less than T_f of the specific accretion in question (be it metal/matte or slag)
(3) The copper hot-face temperature must not exceed copper's melting point (or copper's long-term service limit of < 461°C)
(4) Usually, unless specifically designed for, the boiling point of the cooling medium should not be exceeded (as defined by the prevailing coolant operating pressure).

Somewhat paradoxically, when the thermal conductivity of matte is accounted for (k_{matte} approximately 20 times that of k_{slag}), estimates of h_{matte} remain approximately 20 times that of h_{slag}. This is despite the significantly higher *Pr* number of slag (Robertson and Kang, 1999; Table I) and its positive contribution to both natural and forced convection heat transfer Nusselt numbers through correlations:[3] $Nu = hL/k \propto (GrPr)^{1/4}$ and $(Re^{1/2}Pr^{1/3})$, respectively.

So, considering the first condition, compared to slag, superheated matte of potentially four times greater superheat (ΔT_{matte} up to 650°C) and approximately 20 times the convective heat transfer coefficient delivers far greater incident heat flux than slag ($q_{matte} = h_{matte}\Delta T_{matte}$ = approx. $80q_{slag}$) and so is capable of up to a couple of orders of magnitude greater thermal 'hit' of the cooling system (condition 1 above). This higher heat flux of matte compared to slag leads to higher temperatures of critical lining hot-faces (*e.g.* refractory and copper cooler – conditions 2 and 3), which then (condition 2) all too easily exceed the unusually low T_f of matte, due to its unusually low solidus (850°C) and even liquidus (950°C) temperatures.

In such a situation a copper cooler unprotected by any alternative thermal barrier (*e.g.* refractory/slag) is at significant risk from any superheated matte/blister Cu 'hit' that can rapidly lead to hot-face temperatures rising to where the cooler copper simply melts (1085°C). Yet for most slag systems these conditions are rarely violated; stable slag accretion freeze linings prevail, supported additionally by a high-viscosity slag 'mushy zone' adjacent to T_f (Guevara and Irons, 2007) to protect the composite cooling system.

Comparing k_{matte}, k_{FA}, k_{HM}, and $k_{blister\ Cu}$ of 17, 10, 50, and 160 W/m°C and resulting Pr_{matte}, Pr_{FA}, Pr_{HM}, and $Pr_{blister\ Cu}$ values of approximately 0.2, 0.2–0.5, 0.1, and 0.01, respectively (Table I), one can estimate ratios of convective heat transfer relative to PGM matte as h_{matte}:h_{FA}:h_{HM}:$h_{blister\ Cu}$ = 1:~1.5:~2:~5, respectively. Relative to matte, convective heat transfer coefficients of HM and blister Cu are greater. Maximum superheats $\Delta T_{PGM\ matte}$, ΔT_{FA}, ΔT_{HM}, $\Delta T_{blister\ Cu}$ of 650, 150–350, 350, and 350°C, respectively, will tend somewhat to help balance the resulting process heat fluxes, $q = h\Delta T$. So it would appear that it is low T_f (listed here at its solidus lowest extreme) of T_{matte}, T_{FA}, T_{HM}, $T_{blister\ Cu}$ of 850, >1250, 1130, and 1065°C that most limit the ability to form a protective accretion freeze lining, and so render copper coolers ultimately more prone to thermal 'hit' by (PGM) matte/blister Cu.

[2] $T_{liquidus}$ commonly used to describe the real freeze-lining temperature T_f. Recently, Fallah-Mehrjardi and co-authors (2014) proposed a mechanism that supports the temperature of the interface of stationary steady-state freeze-lining deposit (T_f) being lower than the liquidus temperature (but no lower than $T_{solidus}$), which potentially facilitates operations with freeze linings at temperatures below the liquiduss.

[3] Grashof number, $Gr = g\beta\Delta TL^3/(\mu/\ )^2$, Reynolds number, $Re = \ \nu L/\mu$, g = gravitational acceleration, β = volume expansion coefficient, ΔT = surface to bulk liquid temperature difference, L = characteristic length, μ = dynamic viscosity, = density, υ = fluid velocity, h = convective heat transfer coefficient, and k = thermal conductivity.

Integrated tap-hole and tapping system management

Key aspects of tap-hole design and tapping operation, maintenance, and monitoring will be presented separately for convenience. However, it should be emphasized that all aspects need to be considered as part of an integral system, which must be managed as such for success. Overly focusing on one component at the expense of another (*e.g.* tap-hole clay optimization, without due consideration for mudgun and drill capabilities) is unlikely to yield optimal results. A 'chain being only as strong as its weakest link' adequately describes the role of integration of all aspects of the tap-hole and tapping into a comprehensive system for sound management.

Types of tapping systems

Tapping systems can be conveniently categorized according to the product phases being tapped and the process conditions prevailing: primarily temperature, ΔT (*versus* solidus or liquidus), k, and Pr.

Slag-only tapping

With its high Pr number and elevated melting properties (Table I), slag – provided it is kept free of metal/matte/bullion – is potentially the simplest liquid for which to design an effective tap-hole system, comprising merely a high-intensity water-cooled copper slag tap-block protected by an accretion freeze lining of product slag. A significant advantage of slag-only tapping is that it facilitates direct downstream treatment of slag by either traditional water granulation (Atland and Grabietz, 2001; Szymkowski and Bultitude-Paull, 1992), or, increasingly, 'dry' air atomization (sometimes with energy recovery) to obtain useful slag products amenable to handling and sale in ironmaking, steelmaking, and Ni and SiMn ferroalloy applications (Andō, 1985; Rodd *et al.*, 2010).

Dedication of the tap-hole to slag is particularly effective for handling corrosive slags (especially acidic slags >50% SiO_2 that are fundamentally incompatible with basic and some other refractory oxides), because there is no chemical potential for reaction with a frozen slag of essentially the same composition. Thus retention of a protective freeze lining reverts to a more predictable issue of designing for thermal equilibrium thickness, and adoption of suitable safety factors to provide some protection against deviations therefrom.

On many industrial furnaces, a combination of level measurement and phase separation is more than adequate to tap slag free of metal/matte. Nishi (2007) reports on the importance of designing the height of the slag tap-hole to avoid Mn ferroalloy discharge through it. This is also a typical requirement of more quiescent EF or slag cleaning furnace (SCF) processes of low (< 20%) metal/matte fall (effectively 'slag-making' processes, that may even be subject to near-continuous slag tapping, such as Co and Ni ferroalloy and base metal and PGM matte smelting). On other matte flash furnace (FF) to TSL converting processes (*e.g.* blister Cu to PGM matte, respectively), it is typically necessary to equip them with downstream FF settling and/or SCF processes for further recovery of pay metals from slag, especially oxidic losses that require recovery through reductive processes.

Theoretically, the critical height for entrainment (h_e) of a two-layer liquid through an orifice of diameter (d) is related to $\alpha d Fr^{0.4}$, where α depends on the density difference and which phase is being withdrawn (typically $\alpha < 0.625$ when lower viscosity phase is withdrawn; $\alpha \geq 0.8$ when uppermost viscous layer is withdrawn), $Fr = \upsilon/(dg\Delta\rho/\rho)$ and υ is the discharge velocity, $\Delta\rho$ is the density difference between heavier and lighter liquid, and ρ is the density of the lighter liquid (Liow *et al.*, 2001, 2003). Using assumed physicochemical properties and tap-hole conditions (Table I), one can predict h_e of the order of 0.12 m for copper FF settler and PGM EF smelting (and theoretically even ironmaking BF conditions). Not too surprisingly, therefore, the dedicated slag tap-holes located up to 1 m above the metal/matte tap-holes, coupled with tight metal/matte level control (to a maximum height of 0.25–0.4 m above matte tap-holes on blister Cu and PGM matte furnaces – Table I), permit slag tapping substantially free of metal/matte from the interface with the bulk slag, and entrained specifically through tapping (ignoring the presence by other sources of entrained and unsettled metal/matte droplets).

Similar two-phase liquid entrainment and an initial declination of the slag interface towards the tap-hole as tapping commences followed by a switch to initial inclination and even 'pumping' out of the tap-hole later in the tap has been modelled on BFs by CFD (Shao, 2013; Shao and Saxen, 2011, 2013a, 2013b). However, in the modelling of BF tapping, He and co-authors (2012) caution that the metal should not be maintained at a depth too low above the tap-hole, as one runs a risk of entraining process gas by 'viscous fingering' during tapping, especially (1) when the slag viscosity is high, or (2) in the presence of a permeable bed of solids through tapping occurs (*e.g.* coke bed).

The efficacy of intense copper cooling (predominantly in a circular slag tap-block configuration) is clear (Figure 1 and Figure 2). These coolers directly impart a thicker protective freeze lining than the alternatives of just top lintel copper blocks, or 'inverted-U' square copper blocks and circular block water-cooled copper pin designs (Marx *et al.*, 2005; Henning *et al.*, 2010) (the latter choosing rather to try to moderate freeze lining thickness). These latter designs all avoid the presence of water below the tap-hole. It is a moot point whether this is indeed universally a safer situation, especially if control of furnace operating levels is adequate, simply because of the less desirable trade-off of imparting an inherently thinner protective freeze lining with less cooling.

Concerns frequently articulated of overly cooling copper coolers (Trapani *et al.*, 2003; Marx *et al.*, 2005; Henning *et al.*, 2010) are extravagant costs, fear of preventing easy tap-

Figure 1—All three slag tap-holes open with near-continuous slag tapping on a PGM matte furnace. Notice hood extraction

Figure 2—High-intensity water-cooled slag tap-block with solidified slag freeze lining core through which slag is tapping at 1659°C

hole opening, or freezing of a tapping stream. Even with the least intense top lintel or shallow-cooled (*i.e.* water circuits outside the furnace) copper and refractory-lined slag tap-blocks, problems associated with the latter two operational aspects can occur, and are generally coupled with undesirable increased copper slag tap-block wear rates. Szekely and DiNovo (1974), in a modelling study of the critical factors for tap-hole blockage of a molten stream (*e.g.* during tapping), determined that nozzle diameter was most critical, followed by metal superheat, with the extent of preheating (or in this case cooling) of the nozzle walls being less significant. Effectively, this implies that the tapping channel diameter should be enlarged if the slag tapping stream is freezing.

So again it is a moot point if reduced cooling intensity, including the removal of water circuits from beneath the tapping channel, indeed universally represents the safer option, if the consequent (sometimes inadequate) protective freeze lining thickness results in increased copper hot-face temperatures that will reduce the long-term integrity of the copper block itself (*i.e.* requires sustained temperatures below 461°C [Robertson and Kang, 1999]). Furthermore, if the tap-hole is still prone to 'slow tapping' even with less intense cooling, it may suggest that an alternative operational tapping strategy is appropriate.

Some of the larger ferroalloy furnaces for Mn and DC Cr alloy production also operate separate slag tap-holes, which assist greatly in separating post-tap-hole metal- and slag-handling logistics. In many instances the separate slag tap-holes are merely refractory graphite/microporous carbon/carbon tap-blocks (usually the former two owing to improved resistance to wetting and lower corrosion by slag). Increasingly, deep-cooled (*i.e.* water-cooled copper extending inside the furnace) copper lintel, or 'inverted-U' blocks are used to promote cooling of such refractory slag tap-holes.

Combined metal/matte and slag tapping

This is decidedly the norm, but it also often presents the greatest design challenge because of the different natures of slag and metal and their chemical incompatibility with linings selected as suitable for the other phase. Traditionally, refractory tap-blocks (refractory oxide or carbon-based) were adopted for combined metal/matte and slag tapping. With few exceptions, the refractory oxides are relatively resilient to metal- and matte-only tapping. Carbon-based tap-blocks risk carbon dissolution and/or oxidation (*e.g.* by dissolved oxygen) in service with carbon-unsaturated metal/matte. Corrosion of both carbon-based and oxide refractories is invariably accelerated by slag, even to the extent that corrosion becomes catastrophic, *e.g.* if acidic slags make contact with basic refractories (such as magnesia). Depending on the specific slag system, amphoteric (alumina) refractories can also be susceptible to both acidic (*e.g.* high-silica) or basic (*e.g.* high-lime) slags.

Refractory-lined overflow launders are used in continuous tapping of copper matte and slag from the Mitsubishi Continuous Process smelting furnace, and certain corrosion challenges are presented (addressed largely by fused cast magnesia-chrome). Somewhat remarkably, unlined water-cooled copper tap-plates are routinely fitted on to the furnace exterior for combined matte-slag tapping elsewhere in the copper industry, such as TSL furnaces. This presumably is only possible owing to the comparatively low temperature (< 1200°C, Table I) and relatively low copper matte superheat in combination, critically, with slag that has the potential to freeze (even if only as a thin layer a couple of millimetres thick) as a protective accretion on copper tapping surfaces.

Most combined metal-slag tap-hole processes are characterized by lower slag-metal ratios of about 0.4–1.5 t slag per ton metal (metal fall is approximately 35–60% in the case of Cr and Mn ferroalloys, Table I), or significantly lower 0.2–0.4 t slag per ton HM in ironmaking BFs (metal fall is approximately 65%, Table I), to near-slagless tapping in Si (and Si alloy) processes. A striking feature of the ironmaking BF is its sheer productivity (>10 000 t/day) coupled with complex internal process structures ('deadman' and tap-hole 'mushrooms'). Even with multiple tap-holes, these process structures would complicate attempts to control hot metal and slag levels adequately and to the extent necessary to permit effective dedicated metal- and slag-only tapping. Therefore, as with the majority of older ferroalloy SAFs and BFs, deep cooling is generally not contemplated, with limited water-cooled elements being applied more judiciously.

Dedicated metal/matte tapping

Provided that metal/matte can be tapped substantially slag-free, a configuration for dedicated metal/matte tapping is possible. Theoretically, it can be calculated that the separation of slag to at least 0.07 m above the metal/matte tap-hole should facilitate matte tapping without slag entrainment (α drops to 0.625 for tapping of the denser, less-viscous phase [Liow *et al.*, 2003]). Efficient separation of metal/matte from slag already in the furnace decidedly simplifies post-tap-hole handling and associated logistics.

Emergency/drain tap-hole

Some furnaces are equipped with emergency/drain tap-holes (Newman and Weaver, 2002) that are used when the furnace does not drain from operating tap-holes (Cassini, 2001), or to effect bath drainage to a lower level than normal operating tap-holes for safer repairs. Some operators prefer to avoid such tap-holes for fear that they potentially increase risk by tempting non-emergency/non-drain use, and present another weakened region of furnace lining (at a higher pressure head) for unplanned drainage.

The tap-hole – key to furnace performance

Tap-hole design

Tap-hole and tapping-channel heat transfer

On a large furnace crucible wall, bath heat transfer can reasonably be approximated as one-dimensional. In the simplest configuration of a long circular tap-hole, heat transfer from a fast-flowing hot tapped liquid is dominated by radial heat loss in the passage down the tapping channel. Even with a reasonably fast water cooling flow rate of 6 m³/h, it can readily be estimated using $q = Q/A = (mC_P)\Delta T$ that for just a 1°C rise in water temperature, the equivalent tapping channel (tap-block or faceplate) heat flux (q) exceeds 0.5 MW/m².

In a real tapping channel, in addition to the tapping channel heat transfer, heat transfer from the contained furnace bath also exists, which results in a three-dimensional heat transfer situation that is more extreme than in almost any other region of the furnace crucible. The tap-hole specifically is invariably subjected to the most arduous of conditions (Van Laar *et al.*, 2003; Van Ikelen *et al.*, 2000): the highest liquid (metal/matte and slag) velocities, affected by the degree of radial or peripheral flow and total flow that converge on the tap-hole to achieve the productivity set-point; the highest turbulence (increased by gas entrainment and even blowing under pressure, and associated enhanced mass and heat transfer from both stream tapping and through the action of any tap-hole clay flash devolatilization and subsequent 'boiling' at the back of the channel); wildly fluctuating and periodic thermal loads (from cool, dormant conditions, heating rapidly when the tap-hole is opened with oxygen, or hot liquid tapping, and with tap-hole clays 'boiling' and gas bubble-driven circulation upon tap-hole closure); and high dynamic loads (the action of opening and closing a tap-hole). Tap-holes are also prone to gas leakage, especially when operated under pressure in a BF, which may result (particularly in the case of ironmaking or ferroalloy processes adopting carbon-based refractories) in a continuous threat of exposure to, and reaction by, CO (the risk of carbon deposition), oxidation by injected oxygen, air, or steam (especially if water leaks), slag and maybe even SiO(g), and reaction with volatile gas species such as alkalis and zinc (which leads to refractory attack) (Van Laar, 2001; Van Laar *et al.*, 2003; Spreij *et al.*, 1995; Iiyama *et al.*, 1998; Tomala and Basista, 2007).

Tap-hole 'refractory' design

Clearly, to be successful, tap-hole designs need to cater not only for average, but peak, process heat flux conditions. Van Laar (2014) suggests that in BF tap-holes, peak heat fluxes exceeding 1 MW/m² have been detected, which is considerably in excess of the normal average heat fluxes measured (25 kW/m², Table I). This would not be inconsistent with a 1.4 MW/m² event involving metal encroaching on the lower zone of a copper waffle cooler recorded in Co ferroalloy production (Nelson *et al.*, 2004).

Nearly all tap-holes are designed with a length that exceeds the adjacent sidewall thickness. Unfortunately, this provides only short-term protection against liquid breakout in the tap-hole area, because the tap-hole length will at best rapidly recede to its thermal equilibrium dimension.

Several refractory types (Figure 3) are used in BF tapholes and their environs (Stokman *et al.*, 2004; Jameson *et al.*, 1999; Irons, 2001; Van Laar, 2001; Van Laar *et al.*, 2003; Brunnbauer *et al.*, 2001; Atland and Grabietz, 2001). They include:

- 100% alumina (the most 'insulating': k = 1–5 W/m°C)
- Pitch-impregnated carbon/alumina (Black and Bobek, 2001)
- Large carbon blocks (k approx. 14 W/m°C)
- Hot-pressed small carbon or semi-graphite bricks (a lower iron content of the latter, to reduce CO disintegration [Stokman *et al.*, 2004; Spreij *et al.*, 1995])
- Microporous (potential advantages of less metal infiltration if the maximum pore size is less than 1 μm [Stokman *et al.*, 2004; Piel *et al.*, 1998; Spreij *et al.*, 1995; Tomala and Basista, 2007]), large carbon or semi-graphite blocks
- Thermally conductive graphite (k approx. 140 W/m°C, frequently applied as 'safety' tiles glued to the steel wall in the immediate tap-block vicinity [Van Laar *et al.*, 2003; Edwards and Hutchinson, 2001; Atland and Grabietz, 2001])
- Sometimes graphite with high-alumina silicon carbide castable in the centre (favoured for reasons of improved tapping stream dissolution and erosion resistance over graphite in the event of the latter's loss of freeze lining or protective baked tap-hole clay inner annulus, somewhat improved tolerance to oxygen lancing over graphite, provision of some heat storage for tap-hole clay baking, and possibly some improved tolerance to microcracking induced through mudgun and drill impact forces)
- The use of higher conductivity silicon carbide (Brown and Steele, 1988) in conjunction with a carbon surround and alumina tapping channel hot-face bricks has also been reported (Yamashita *et al.*, 1995). In some instances, heat removal is further enhanced by the addition of water-cooled iron or copper tap-hole notch channels, or even water-cooled copper inserts/plate coolers (Irons, 2001; Van Laar, 2001).

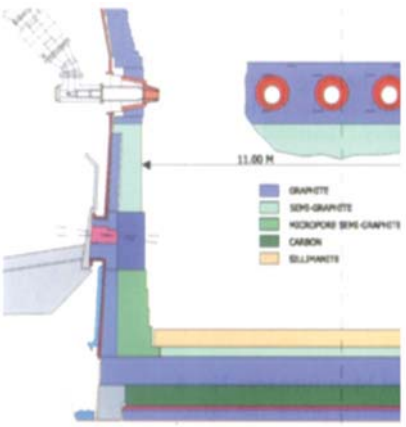

Figure 3—Tap-hole and environs equipped with refractory of various thermal conductivities and integration into BF lining (after Stokman *et al.*, 2004)

Table II

Carbon-based refractory and onset of key wear and attack mechanisms (Van Laar *et al.*, 2003; Spreij *et al.*, 1995; Tomala and Basista, 2007)

Thermomechanical and chemical attack mechanisms	Onset temperature* °C
Alkali and zinc#	400
CO deposition	450
Stress cracking	500
Oxidation (enriched, or air)#	600
Steam oxidation	700
CO_2 oxidation	1050
Liquid penetration, corrosion (*e.g.*, by carbon dissolution, or by slag) and ensuing erosion#	1150

*Depending on specific refractory type; oxide- or carbon-based, calcined anthracite or graphite aggregate, or binder-derived (Spreij *et al.*, 1995) (binder more prone to attack than aggregate) and associated trace impurity catalysts (*e.g.* Fe)
#Especially in tap-hole region (Piel *et al.*, 1988)

In all instances involving the use of composite refractory types (Figure 3), especially when water-cooled components are included, a critical design requirement is to cater for differential thermal expansion properties that can easily differ by an order of magnitude, with the potential to cause gaps, stresses, and strains, so raising the potential for liquid infiltration (Van Laar, 2014). An experience reported (Duncanson and Sylven, 2011) of furnace campaign life reduced from 14 to just 3 years when switching from a design where 'the original furnace had forced air cooling in the bottom, but no additional (water) cooling for the furnace walls' (and, by inference, attempt at freeze lining in, or at least near, the tap-block) may well illustrate this. Moreover, the additional requirement for effective freeze linings around thermal equilibrium has led Singh and co-authors (2007) to state: 'but in the present Indian scenario with process parameters not stable … it is difficult to maintain the conditions inside the furnace desirable for a true freeze lining,' so failing to 'give the expected lifetime of over 25 years'.

For the adoption of any freeze lining concept, half measures are entirely unacceptable. The achievement of just a partial and/or periodic freeze lining will prove unsuccessful and present a considerably more dangerous operating condition than a traditional insulating tap-hole design concept.

The first technique crucial to tap-hole refractory longevity is the ability to create and retain a protective accretion freeze lining or skull (Eden *et al.*, 2001), as tap-hole performance is greatly compromised by operating in the partial or substantial absence of a stable accretion freeze- lining, which is described as a 'no-skull' condition (Stokman *et al.*, 2004). Accretion freeze lining thickness has already been shown to be enhanced by placing refractories of higher conductivity in actively cooled furnace-lining systems, with the resulting colder refractory presenting fundamentally more resistance to attack by a number of wear mechanisms, depending on the temperature of onset of thermomechanical or chemical attack by a given mechanism (Table II).

Role of the tap-hole clay 'mushroom'

The second crucial feature, specific to ironmaking BF tap-hole design, is the active development and continuous renewal of a tap-hole clay (also described as mud) 'mushroom' to provide some hot-face protection on the back of the tapping channel (Figure 4) (Uenaka *et al.*, 1989; Jameson *et al.*, 1999; Eden *et al.*, 2001; Nightingale *et al.*, 2001, 2006; Tanzil *et al.*, 2001; Atland and Grabietz, 2001; Cassini, 2001; Wells, 2002; Horita and Hara, 2005; Kageyama *et al.*, 2005, 2007; Nakamura *et al.*, 2007; Niiya *et al.*, 2012; Kitamura, 2014). The 'mushroom' requires tap-hole clay for its development and consists additionally of incorporated slag, iron, and coke. Tsuchiya and co-workers (1998) hypothesize that a necessary condition for the development of a 'mushroom' is that the tap-hole length can be extended only when the holding space for the injected tap-hole clay is effectively realized, so that the major part of the tap-hole clay surface is covered by the coke column (Figure 5). Niiya and co-authors (2012) hypothesized further that the tap-hole clay is 'extruded in the furnace like strings' and that these 'strings accumulate in the coke-free spaces by folding together with solidified iron and/or slag'. Other conditions required for

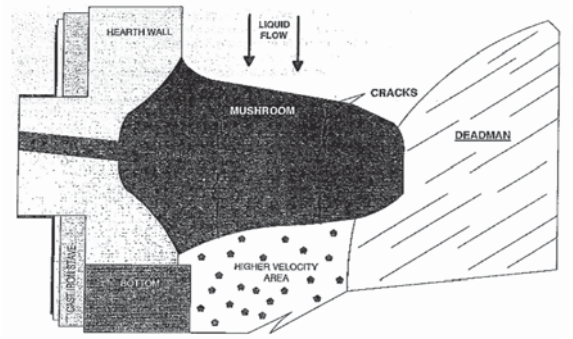

Figure 4—'Mushroom' connection of tap-hole hot-face and 'deadman'. Diversion of descending liquid around the 'mushroom' is depicted. In tapping, this combines with peripheral liquid flow around the 'deadman' to increase the velocity of the liquid flow below the tap-hole and lining hot-face, with the potential for hotter flow conditions and enhanced wear (after Van Laar, 2001)

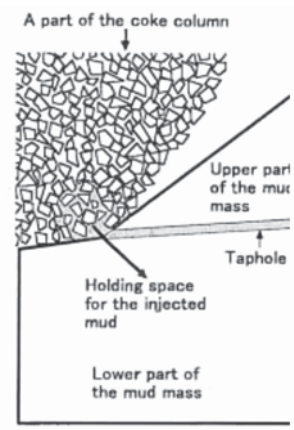

Figure 5—Schematic drawing of the holding space for injected mud into the BF (after Tsuchiya *et al.*, 1998)

increasing the tap-hole length to develop the 'mushroom' then include there being sufficient tap-hole clay sintering time in the holding space and the specific characteristics of the clay during and after heating and sintering. 'Mushroom' stability can be adversely affected by the 'floating' of an ironmaking BF 'deadman', especially if it is physically connected to the back of the 'mushroom' (Van Laar, 2001). Water leaks are also reported to cause a 'mushroom', a frozen skull, and lining damage (Van Laar *et al.*, 2003; Van Laar, 2001).

The necessary condition of a 'holding space covered by a coke column' may well explain why a protective tap-hole clay 'mushroom' is routinely reported only for ironmaking BFs. In non-ferrous processing coke is absent (or substantially absent), so the necessary requirement of a coke column to cover tap-hole clay in the holding space is missing. Moreover, as we describe later, certainly in electric smelting of PGM mattes, matte superheat is so high (as much as 650°C, Table I) that tap-hole clay injected into matte appears to react near-instantaneously, with the release of gas and extreme turbulence, so that a tap-hole clay-based 'mushroom' cannot be stabilized.

While a coke bed is a well-reported feature of ferroalloy smelting (Nelson, 2014), it remains local to the electrode tips. The extension of the coke bed to the furnace tap-hole – a necessary condition of the proposed mechanism of 'mushroom' development – would almost certainly result in a condition too conductive for effective electrical power input. A genuine 'mushroom', at least in the equivalent sense to that of an ironmaking BF, therefore seems improbable. At best, some extent of tap-hole clay 'self-lining', but not a 'mushroom', is depicted in ferroalloy electric SAFs (Ishitobi *et al.*, 2010).

Ferroalloy tap-hole design

The ironmaking BF tap-hole refractory list fairly represents the experience in Cr, Mn, and Si ferroalloys, one of an increasing general trend towards the use of materials of higher thermal conductivity, and to what is colloquially known in the industry as 'freeze linings'. For traditional insulating (especially large) furnace designs, just 2–6 years of furnace lining life on Cr and Mn ferroalloys are commonly reported (De Kievit *et al.*, 2004; Van der Walt, 1986; Coetzee and Sylven, 2010; Coetzee *et al.*, 2010), with one slag tap-hole life reported to be as short as 2 months (Van der Walt, 1986). However, longer furnace lifetimes of 10–15 year have been achieved on traditional insulating linings in Japan. Generally, Cr and Mn ferroalloy SAFs have made use of only refractory alumina tap-blocks, silicon carbide tap-blocks surrounded by alumina, carbon, or microporous carbon blocks.

This supports a progression from more insulating refractories (refractory oxide castable and brick, carbon-based ram or Söderberg paste), to carbon blocks of intermediate thermal conductivity and even more thermally conductive semi-graphites and graphites. The latter designs have delivered in excess of 20 years' lining life on some large Mn ferroalloys furnaces (Van der Walt, 1986; Hearn *et al.*, 1998).

An emerging trend is of an additional composite refractory variant involving use of a thermally conductive graphite sleeve inside an insulating carbon tap-block (Figure 6). This concept, intriguingly, is the converse of placing insulating refractory oxide inside graphite, reported as a preferred option for ironmaking BFs.

Hearn and co-workers (1998) describe the reasons for this as follows: the end hot-face of the graphite insert is protected by a carbon tap-block, while the cold-face is protected by a removable carbon 'mickey' block, which can be replaced if damaged by either drilling or oxygen lancing, to secure a flat mating surface against which the mudgun can more effectively close without excessive tap-hole clay bypass. During tapping the graphite absorbs the tap heat, which the outer annulus carbon tap-block of lower thermal conductivity cannot transmit as effectively, so ensuring a hot tap-hole with improved flow rates. The heat retained in the graphite sleeve after tapping and immediately following tap-hole closure by the mudgun aids tap-hole clay baking. At the next tap, a 45 mm diameter hole is drilled through the baked taphole clay core to create a tap-hole clay annulus inside the graphite sleeve that affords some protection against its coming into direct contact with the molten tap stream. Obviously, the tap-hole clay can erode with time. With the removal of the front 'mickey' carbon block, the graphite sleeve can be core-drilled out and both items replaced to effect a taphole repair. An additional tap-hole repair design feature involves splitting in two and gluing the carbon tap-block (which contains the graphite sleeve) with carbon paste rammed to close the gap between it and the adjacent furnace sidewall lining, a measure that allows for easier removal with less peripheral lining damage during replacement in planned maintenance (Duncanson and Sylven, 2011; Coetzee and Sylven, 2010; Coetzee *et al.*, 2010).

Some Mn (Ishitobi *et al.*, 2010) and DC arc Cr (Sager *et al.*, 2010) ferroalloy furnaces make use of inserted water-cooled copper components on both metal and slag tap-blocks, components that range from top lintel to 'inverted-U' designs, to cool the graphite (advantage of less wetting by slag) or microporous carbon (if dissolution and erosion of graphite by the metal tapping stream prove too aggressive) tap-blocks.

High-intensity water-cooled tap-block design

Quite different, though, are the more intensely cooled tap-block designs on blister Cu (Henning *et al.*, 2011; Marx *et al.*, 2005; George-Kennedy *et al.*, 2005; George, 2002; Zhou and Sun 2013; Newman and Weaver, 2002; pers. comm. 1999, 2003) and non-autogenous processes requiring electric

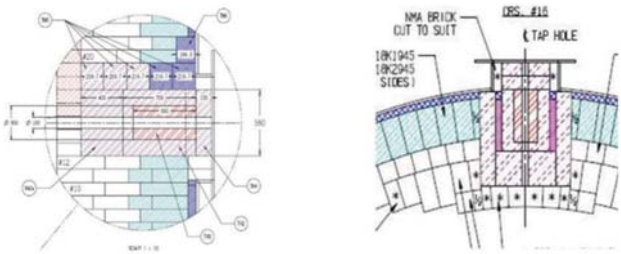

Figure 6—Latest ferroalloy tap-hole design to be incorporated into SAF freeze lining, incorporating replaceable carbon 'mickey' brick on cold face, replaceable graphite sleeve inside two-piece carbon tap-block, carbon rammed against side carbon tap-blocks, with carbon block hot-face at the back of the tap-hole (after Duncanson and Sylven, 2011)

smelting, such as Ni and Co ferroalloy (Henning *et al.*, 2010; Nelson *et al.*, 2004, 2007; Walker *et al.*, 2009; And , 1985; Voermann *et al.*, 2010; pers. comm. 1999, 2003), base metal, and PGM matte furnaces (Cameron *et al.*, 1995; Shaw *et al.*, 2012; Hundermark *et al.*, 2014; Nolet, 2014; pers. comm. 1999, 2003, 2010). These almost universally adopt water-cooled copper tap-blocks of rectangular shape: three-sided (inverted U-shape, so there is no water-cooled copper below the tapping channel), four-sided 'dogbox' (Figure 14; Nelson *et al.*, 2007), or high-intensity one-piece waffle cooler copper tap-block designs (Figure 7 and Figure 8). Some are equipped with pin cooling (with inverted-U water passages [Henning *et al.*, 2010]—Figure 9).

These copper coolers are lined internally with a square configuration of surround bricks, usually made of magnesia (graphite was apparently also trialed successfully in nickel matte smelting [Cameron *et al.*, 1995], but was reported to have been discontinued), containing internal tapping module refractory bricks through which the tapping channel runs (Figure 7, Figure 8, Figure 12 and Figure 14). The latter comprises refractories that vary with commodity: almost exclusively pitch-impregnated magnesia in Ni ferroalloys (Nelson *et al.*, 2007; pers. comm. 1999, 2003), magnesia-chrome in blister Cu or matte (Cameron *et al.*, 1995; Nolet, 2014; George- Kennedy *et al.*, 2005; pers. comm. 1999, 2003), or alumina-chrome in PGM mattes (Nolet, 2014; pers. comm. 1999, 2003). Both graphite and silicon carbide have been trialed in matte smelting (Cameron *et al.*, 1995; pers. comm. 1999, 2003).

For Pb bullion (temperatures of 800–1100°C tapping, with 700°C drossing) (Veenstra *et al.*, 1997; pers. comm. 1999, 2003) and PGM matte processes (Shaw *et al.*, 2012; Hundermark *et al.*, 2014; Nolet, 2014; pers. comm. 1999, 2003), process superheats are high (Table I). Specifically for the latter, process temperatures are elevated to the extent that the potential for corrosion of magnesia chrome refractory by PGM matte above 1500°C has recently been investigated (Lange *et al.*, 2014). Good evidence of expected significant matte penetration and signs of FeO and MgO corrosion products have been found, but not as yet a CrS product suggested by any proposed mechanism. This suggests a potential for high refractory wear rates with exceptionally high matte superheats (approaching 650°C, Table I).

In Pb bullion smelting (Veenstra *et al.*, 1997; pers. comm. 1999, 2003), blister copper (Henning *et al.*, 2011; pers. comm. 1999), and PGM matte ACP top submerged-lance converting (Nelson *et al.*, 2006; pers. comm. 2003), circular copper tap-blocks have also been used, with both annular graphite and silicon carbide inserts, or silicon carbide, high alumina, or graphite tapping module bricks.

So whereas ironmaking BF superheats of 350°C may seem challenging to copper-cooled operations, they are only half the matte superheats experienced on the highest intensity non-ferrous operations. Consider also the significantly lower melting temperatures of many mattes (<950°C, Table I) and this effectively makes it impossible to develop any protective matte freeze lining, even when using higher cooling water flow rates (but still short of those legislated for designation as pressure vessels). Notwithstanding this limitation, Ni and PGM mattes also have a greater solubility for copper than do iron and steel, blister copper, and copper mattes; so additionally they have a greater driving force for the chemical dissolution, not merely melting, of copper.

As we have described earlier, in such a harsh pyrometallurgical processing environment the consequence of a superheated matte/blister Cu 'hit', or lancing a water-cooled tap-block (George-Kennedy *et al.*, 2005) and tap-hole failure is extreme. It can occur rapidly with a near-identical sequence

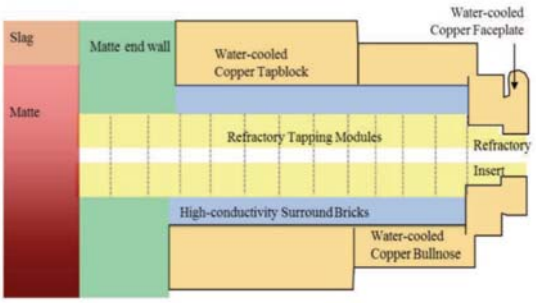

Figure 8—Schematic of a high-intensity water-cooled copper matte tap-block system, with water-cooled copper bullnose extension and water-cooled copper faceplate, both outside furnace. Only the copper faceplate has 'inverted-U' water passages, where water is absent on the underside of the tapping channel

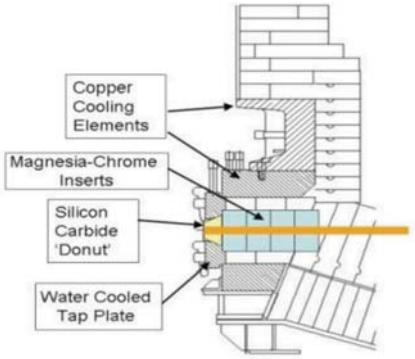

Figure 7—High-intensity composite water-cooled and refractories tap-block for blister copper (after George-Kennedy *et al.*, 2005)

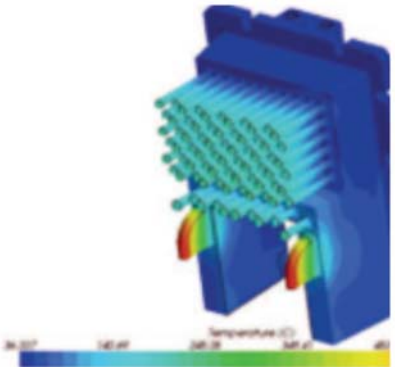

Figure 9—Water-cooled copper pin and 'inverted-U' metal tap-block design (after Henning *et al.*, 2010)

of events, regardless of furnace size (Nelson *et al.*, 2006). The potential for catastrophic cooler failure and/or furnace refractory breakout (Zhou and Sun, 2013; Newman and Weaver, 2002) within, most commonly, a few minutes of mudgun closure, is high (Hundermark *et al.*, 2014). A breakout following mudgun closure has even prompted one PGM producer to resort to drilling and lancing, but to closing tap-holes with clay manually using stopper rods rather than mudguns (Coetzee, 2006).

Faceplate and refractory insert design

External faceplates are important for providing a 'perfectly' flat vertical mating face for the mudgun to engage the tapping channel (for accuracy of tap-hole clay quantity injected into the tapping channel, so ensuring minimal bypass), coupled with the refractory insert, for providing a mechanism to help secure tight joints along the length of the tapping channel to minimize infiltration and gas leakage (Eden *et al.*, 2001), and to help prevent the entire tapping channel lining from dislodging and 'tapping' out of the furnace lining owing to internal furnace pressure (comprising both internal operating pressure and any blast pressure and hydrostatic head). The last of these incidents has apparently been experienced in the past on a Ni matte EF.

Thermal fatigue cracking or direct matte attack of water-cooled copper faceplates, typically associated with matte splashing during tap-hole plugging, presents a risk of water leaks. Sacrificial refractory or metallic cover plates have been used to address this risk (Cameron *et al.*, 1995), with the introduction of inverted-U water-cooled pipe arrangements to secure the absence of water-cooling directly below the tapping channel, a measure that better mitigates the risk of matte making contact with water.

Tap-hole inclination and active hearth sump design

Tap-holes are normally designed with a horizontal or vertical (*e.g.* EBT) orientation. The notable exception is the near-universal implementation of inclined tap-holes (approx. 10°) on ironmaking BFs. Modelling has shown that inclined tap-holes, coupled with longer tapping channels and deeper hearth sumps (the minimum sump depth is 20% of the hearth diameter [Jameson *et al.*, 1999; Gudenau *et al.*, 1988]) that drain liquid deeper in the furnace (further from the sidewalls), lower liquid velocities (and resultant wall shear stress and wear) both below the tap-hole and at the wall periphery (that otherwise lead to undercutting and so-called 'elephant's foot' wear) (Stokman *et al.*, 2004; Eden *et al.*, 2001; Smith *et al.*, 2005; Dash *et al.*, 2004; Jameson *et al.*, 1999; Post *et al.*, 2003). The localized higher velocities below the tap-hole are attributed to the draining of liquid down past the 'mushroom' (Figure 4, Van Laar, 2001). The higher peripheral velocities at the wall periphery are more a function of draining through and around a 'deadman' (Dash *et al.*, 2004; Jameson *et al.*, 1999; Tanzil *et al.*, 2001). Optimum tap-hole inclination was modelled as 15° (Dash *et al.*, 2004). Tapping conditions are further noted to distort fluid flow to the extent that, towards the end of tapping, the slag is lowest in the vicinity of the draining tap-hole, inclined to its highest at the opposite side of the BF (Post *et al.*, 2003; Tanzil *et al.*, 2001). We are aware of at least one high-carbon (HC) Cr ferroalloy furnace equipped with a declined tap-hole.

Modelling has similarly motivated the deepening of the metal bath of a circular HC Mn ferroalloy SAF (but still with a horizontal tapping channel, presumably in part because of the absence of anything equivalent to a 'sitting deadman') by removing a full course of carbon blocks to reduce the peripheral liquid flow velocity along the wall to a draining tap-hole (Ishitobi *et al.*, 2010). The reduced peripheral flow induced by the deepening of the hearth reduced metal tapping temperatures by an average of 40°C (to 1350°C), despite the uprating of the transformer capacity to permit a simultaneous increase of the electrode current by 25 kA to raise the average power load at night by 2.3 MW, combined with operation at a higher coke loading to allow approach to metal carbon saturation (so limiting wear by dissolution of the carbon lining). Deepening of another Japanese HC Mn ferroalloy furnace gave benefits of marginally increased power input, faster tapping, and increased productivity (Nishi, 2007). On Si ferroalloy SAFs (Kadkhodabeigi *et al.*, 2011), where metal drains through a porous bed of solids to the tap-hole, crater pressure and bed permeability significantly influence the rate of drainage of metals to and through the tap-hole.

In the largest rectangular six-in-line PGM matte smelting furnace, the matte inventory can exceed 600 t, with contained metal value exceeding US$50 million. Furnace deepening will come at a greater cost. Fortunately, with a combination of periodic and low-volume matte tapping (< 20% matte fall) through an end-wall of an inverted arch hearth design, in a rectangular furnace configuration, tap-hole wear has recently been predictable even at operations exceeding 60 MW power input (Hundermark *et al.*, 2014). With a circular furnace configuration more conducive to the development of circumferential flow along the sidewall to a draining matte tap-hole, especially when the matte tap-hole is located almost on the top of the skew line of the hearth invert, it is not inconceivable that conditions for accelerated matte tap-hole wear could develop, even at far lower inputs of power.

Tap sequencing

A variety of strategies are adopted, depending largely on productivity requirements, number and layout of tap-holes, and process conditions. For single tap-holes processing dual metal-slag mixtures, total reliance is placed on the availability of the sole tap-hole. Such tapping systems are especially common in Cr and Mn ferroalloy SAFs, which may emphasize the importance of the tapping stream superheat (average-to-maximum heat flux 1–10 kW/m^2 [De Kievit *et al.*, 2004; Table I]) over absolute temperature in describing an onerous process condition.

That said, a still impressive 5 700 t/d HM in a campaign life of 13 years at the time of reporting was achieved from a single taphole BF operation (Ballewski *et al.*, 2001). Similarly the Mitsubishi Continuous Process for copper relies on continuous liquid flow down heated launders from smelting, to slag cleaning, to converting, and to anode refining furnaces, this being effected through a combination of furnace overflow, skimming, and siphon tapping arrangements, at overall availabilities exceeding 92% (Matsutani, n.d.). These examples illustrate what is possible with superior tap-hole management and tapping practices.

Consecutive individual tapping practice

Consecutive tapping on an individual tap-hole is a common traditional practice on several ironmaking BFs (Rüther, 1988; Cassini, 2001), ferroalloy, and matte-smelting operations. Even on two-tap-hole BFs, tapping campaigns of 4 days to 3 weeks are reported (Rüther, 1988). Matte tap-hole temperature trends in Ni matte smelting clearly demonstrate the accumulation of heat in the tap-hole refractory when taps are in close succession (Cameron *et al.*, 1995; Figure 10). Similar rising temperature trends with tapping have been observed in PGM matte smelting (Gerritsen *et al.*, 2009; Figure 11). With an ironmaking BF interpretation this could possibly be considered desirable for promoting tap-hole clay baking and sintering. However, in the more intensely superheated matte-only tap-hole environment this is rather interpreted to imply that a resting or recovery period of no tapping is called for, to help lower refractory temperatures and re-establish improved accretion, as evidently occurred on the tap-hole on the furnace in Figure 10.

Alternating tap-hole practice

This variant, also described as 'side-to-side' casting (Petruccelli *et al.*, 2003), is certainly the norm for achieving the highest of productivities through optimal tap-hole condition, consistent operability, and reliable availabilities; it also best supports preventative tap-hole maintenance. This is true of two tap-holes (Petruccelli *et al.*, 2003) and tap-hole pairs on four-tap-hole ironmaking BFs (Rüther, 1988; Steigauf and Storm, 2001); 2–8 metal-only and 2–6 slag-only tap-holes on blister Cu and ferroalloy furnaces (George, 2002; Zhou and Sun, 2003; Newman and Weaver, 2002; George- Kennedy *et al.*, 2005; Nelson *et al.*, 2004, 2007; Walker *et al.*, 2009; pers. comm. 1999, 2003); and up to three matte- and three slag-only tap-holes on base metal and PGM matte EFs (Nolet, 2014; Nelson *et al.*, 2006; pers. comm. 1999, 2003). It includes ironmaking BF variants described as 'back-to-back' or 'mother-daughter' tapping (Irons, 2001; Cassini, 2001), where a pair of taps is made before alternating tap-holes. In the case of the ironmaking BF, this practice of a pair of taps is usually in response to suboptimal conditions, such as inadequate draining or persistent taps of short duration.

A detrimental feature reported for alternating tapping on BFs, where a zone of low permeability exists between tap-holes, is the potential for the slag level to rise due to excessive pressure loss, which disrupts bosh gas flow (Iida *et al.*, 2009; Shao, 2013; Shao and Saxen, 2011, 2013a, 2013b). Slag levels could conceivably fluctuate on SAFs similarly, owing to the presence of less permeable zones. Iida and co-workers (2009) recommend enlarging the tap-hole diameter (by approx. 10%) as the best remedy to alleviating this issue.

While operating at a still impressive HM superheat, ΔT approx. 350°C, the focus on the BF is largely HM productivity-driven, with up to 75% metal fall and daily targets exceeding 10 000 t HM, thus demanding the most effective and efficient tapping with reliable operability. Most operators appear to seek to operate somewhere close to a 'dry' hearth condition (De Pagter and Molenaar, 2001), in which hot metal and slag levels in the hearth are kept as low as possible (Van Laar *et al.*, 2003), but without escape of hot gas (Nightingale *et al.*, 2001; Tanzil *et al.*, 2001). In contrast, the requirement on the multiple tap-hole, lower metal/matte fall (<20%) Ni ferroalloy and matte furnaces is primarily to secure maximum tap-hole and furnace reliability. This is especially true of high-intensity PGM matte furnaces, with their onerous matte superheat, ΔT approx. 650°C, that imposes integrity challenges on even the most intensely water-cooled, refractory-lined copper tap-hole.

On the highest intensity of these operations, even with less frequent matte tapping events, the practice generally is to alternate tapping between the available tap-holes in order to give the tap-holes maximum 'recovery' time to lower tap-hole temperatures between taps. This is reported (Eden *et al.*, 2001; Mitsui *et al.*, 1988; Entwistle, 2001; Cameron *et al.*, 1995; Gerritsen *et al.*, 2009) and has been modelled in the BF (Ko *et al.*, 2008). The merits of such an approach, originally diagnosed from scrutinizing well-instrumented copper tap-block and cooling water temperature tapping trends, are presented using the latest fibre-optic temperature measurement trends available in PGM matte smelting (see section on *Advanced tap-hole monitoring*).

At first glance an alternating tap-hole practice would appear to complicate the timing of minor routine, monthly planned tap-hole maintenance activities (Nolet, 2014). However, it should be appreciated that, despite such diligent monthly repairs and essentially slag-free tapping, process conditions remain so onerous that all but the hot-face matte tapping module bricks have to be replaced roughly every quarter to secure incident-free tapping, good tap-hole

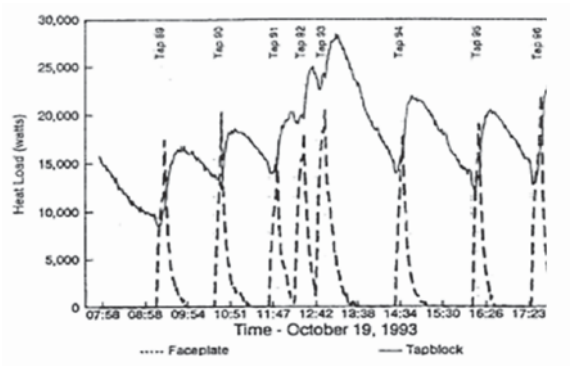

Figure 10—Typical heat load and accumulation of heat with taps in close succession (after Cameron *et al.*, 1995)

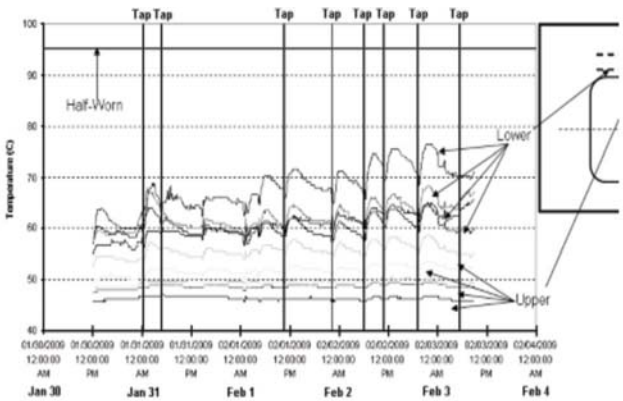

Figure 11—Trend of tap-hole temperature rise with consecutive tapping on a tap-hole (after Gerritsen *et al.*, 2009)

condition, and ultimately furnace integrity and longevity. To undertake such a deep tap-hole repair, tap-hole temperatures and safety dictate that the furnace power needs to be lowered for the duration of the repair. So in fact a simultaneous repair of all matte tap-holes by a team of masons on a furnace at lowered furnace power actually minimizes the impact on overall furnace utilization.

Also, it should be clarified that in high-intensity PGM matte smelting the 'as-low-as-possible' liquid matte and slag levels of the BF 'dry hearth' operation are definitely not sought, nor considered desirable. Considering first the overall liquid level, one finds that generally too high a pressure head is not sought, because it promotes an increased rate of tapping and increases the potential for matte infiltration of the furnace lining. Specifically, one also does not seek too high a matte level, for fear of exposing the effective slag-line, water-cooled copper waffle coolers to a greater risk of making contact with superheated matte. While the waffle cooler design reportedly (Trapani *et al.*, 2002; Merry *et al.*, 2000) caters for metal contact of copper waffle coolers in Ni (Nelson *et al.*, 2007) and Co (Nelson *et al.*, 2004) ferroalloy processing, contact by matte, especially superheated matte, can rapidly lead to catastrophic failure.

However, this still does not warrant seeking the lowest possible matte level. This is because the matte-only tap-hole is especially configured to be refractory oxide-lined, with generally good corrosion resistance to matte, but with decidedly poor corrosion resistance to acidic slags (> 50% SiO_2 content). Indiscriminate lowering of the matte level would therefore not only expose the tap-hole to the risk of 'slagging' by the hotter slag, but would accelerate corrosion, and ultimately wear, of the refractory lining. A target minimum matte level is therefore simultaneously sought with matte operated below the maximum matte level permissible.

In respect of the slag level, the absolute minimum furnace slag level is controlled by its interface with matte. Operation around the slag tap-hole, located typically approximately 1 m above the matte tap-hole (Table I), represents the lowest overall pressure head condition on the matte, which is beneficial. However, at the highest smelting rates with < 20% matte fall, slag make becomes significant, which requires near-continuous tapping in contrast to periodic batch matte tapping. With the slag level only at the level of the slag tap-hole, the pressure head is simply inadequate for slag tapping rates to be acceptable. So a practical minimum operating slag level exists, above which slag tapping rates are adequate for achieving an efficient rate of slag drainage (even if multiple slag tap-holes are open).

Finally, the maximum permissible top of slag level is designed relative to the slag tap-hole. This measure primarily ensures that superheated slag does not rise above the zone of sound crucible containment below the top of the copper coolers, but also limits excess pressure head at both the slag tap-hole and the underlying matte tap-hole.

Slag tapping

Where consecutive tapping practice has indeed found nonferrous application is during 'slow' slag tapping on both Ni ferroalloy and PGM matte smelters. The slag tap-hole has a tendency to open fast and then the tapping rate declines with time. In situations where the number of slag tap-holes available is limited (*e.g.* owing to planned maintenance), an effective solution involves closing on lazy-flowing slag with the mudgun, and shortly thereafter re-drilling the slag tap-hole open again (exposure of drill bits to slag only is far less aggressive than exposure to metal or matte). This can easily double the initial tapping rate on a 'slow' slag tap-hole.

Closure on flowing slag is crucial to this operation, because it ensures easy re-drilling of tap-hole clay only to open the slag-tapping channel. In the event where the flow from a slag tap-hole has been allowed to stop, even with an attempted mudgun closure, an adequate plug of tap-hole clay to the inner hot-face cannot be secured. When re-drilling is attempted, solidified slag is quickly encountered, which impedes the drill and can cause skew drilling – potentially towards a water-cooled copper cooler! So somewhat paradoxically, to be safer, oxygen lancing with its ability to 'cut' open, and so straighten, the solidified slag tapping channel then becomes necessary to re-open the slag tap-hole.

Tap-hole opening

It is essential to be able to 'quickly and certainly open the tap-hole whenever required' (Tanzil *et al.*, 2001).

Discounting the most primitive past practices of 'pricking' or 'excavating' the tap-hole open, a wide range of tap-hole opening methods are adopted (Ballewski *et al.*, 2001), including:

- Manual oxygen lancing, suggested near universally to be minimized to < 1% of taps (Jameson *et al.*, 1999), or for 'emergency only' on ironmaking BFs (Ballewski *et al.*, 2001). This practice has led directly to a reported blister tap-hole failure and resulting explosion on at least one site (George-Kennedy *et al.*, 2005), and yet is still adopted as the primary means of tap-hole opening on 36% of PGM matte furnaces (Nolet, 2014)
- Automated or robotic oxygen lancing (pers. comm., 2010)[4]
- A soaking bar technique[5]
- Conventional pneumatic drilling (air)
- Improved pneumatic drilling (nitrogen and/or water-mist-bit cooling)
- Hydraulic drilling (nitrogen and/or water-mist-bit cooling)

[4]See also http://www.mirs.cl/img/video/punzado_descarga_escoria_hornos.wmv

[5]The soaking bar practice found favour in iron BF tapping as an emerging development to replace tap-hole drilling in the 1980s. It involved pushing/hammering a 50 mm bar through the mud in the tapping channel. The bar promised to provide improved thermal conductivity from the inner hearth up the tapping channel, which helped bake and sinter the tap-hole clay better. To open the tap-hole, the bar was reverse-hammered out of the tapping channel, now of well-defined dimension, and with the promise of no risk of skew drilling or oxygen lancing damage. This practice, however, had fallen out of favour by the 1990s, because it required (1) time-consuming predrilling to assist with the soaking-bar insertion and (2) an assessment of the all-critical drill depth. Furthermore, matching this depth to an optimal tap-hole-clay addition was difficult, shorter tap-hole-clay curing times increased the risk of a tap-hole re-opening, and hammering in and removing the bar damaged the tap-hole and 'mushroom' in other ways (Jameson *et al.*, 1999; Van Ikelen *et al.*, 2000; Steigauf and Storm, 2001; Ballewski *et al.*, 2001; Entwistle, 2001; Östlund, 2001)

- Combination pneumatic drilling (without opening) and deliberate lancing of the last remaining metal/matte plug.

It is worth noting that to avoid contamination by iron or other elements, metallurgical-grade silicon tapping requires a variety of alternative tools to open a tap-hole and maintain the flow of metal. These alternatives include an electric stinger (connected to a busbar system from the furnace transformers), a kiln gun (Guthrie, 1992)[6], steel and graphite lances, wooden poles, and graphite bott tools (Szymkowski and Bultitude-Paull, 1992).

Tapping rate

A primary requirement of tapping is to reliably secure the desired rate of furnace products. Thus, it is important to establish the factors influencing tapping rate. Guthrie (1992), applying Bernoulli's equation, provides a useful estimate of tapping rate, $\dot{m} = \rho C_D(\pi d^2/4)(2gH)^{½}$, through a tap-hole of diameter d, where, C_D is a discharge coefficient (approx. 0.9), g is the gravitational acceleration constant, and H is the effective liquid head of the phase being tapped, with a phase of density ρ.

Mitsui and co-workers (1988), combining Bernoulli's and Darcy- Weisbach's equations, estimated the iron BF tapping rates as $\dot{m} = \rho(\pi d^2/4)(2[P/\rho + gH]/[1 + \lambda l/d])^{½}$, thereby including a correction for the tapping-channel length (l). This yields typical iron BF tapping rates of 7 t/min (approx. 10 000 t/day on a near-continuous tapping basis) and liquid tapping velocities of 5 m/s in tap-holes of 70 mm diameter by 3.5 m length. Both approaches show that tap-hole geometry strongly influences tapping rate (with velocities of up to 8 m/s recorded [He *et al.*, 2001; Atland and Grabietz, 2001]), primarily through the tap-hole diameter. The second equation suggests tap-hole length as the next most significant influence.

In the case of Si ferroalloy SAFs (Kadkhodabeigi *et al.*, 2011), where metal must drain through a permeable bed of solids to the tap-hole, the height of liquid metal influences the onset of gas breakthrough to the tap-hole and the concomitant sudden drop in tapping rate, but exerts less influence than crater pressure and bed permeability on the initial tapping flow rate.

Tap-hole wear mechanisms

Given a dominant influence of tap-hole dimensions on tapping rate, it is instructive to consider factors contributing to tap-hole wear (Figure 12), which are elegantly summarized by three sequential steps: penetration, corrosion, and erosion (Figure 13; Campbell *et al.*, 2002).

The first step in refractory wear involves the penetration of refractory, the rate of which, u_{pen}, can be described by a capillary-force-driven flow according to $r\gamma\cos\theta/4\mu l_p$, where r is the capillary (pore) radius, γ is surface tension, θ is the contact angle, l_p is penetration depth, and μ is liquid viscosity. The last property (viscosity) is related inversely to process temperature.

Once a liquid has penetrated a refractory, corrosion by the infiltrating liquid becomes possible. Campbell and co-workers (2002) describe corrosion as a 'cooking time' to illustrate that its rate relates to how long a penetrated refractory has been at a temperature that supports reaction. Furthermore, as corrosion rate conforms to Arrhenius's Law, an exponential (as opposed to linear) scale of temperature is required to predict the increase in the rate of corrosion with temperature.

Once a refractory has been penetrated and further weakened by corrosion, erosion becomes possible if the shear stress, $\tau = \mu(dv/dy)$ induced by the liquid flow through the tap-hole is sufficient to remove refractory. Once again, temperature affects liquid viscosity, whereas the rate of tapping affects the velocity gradient (dv/dy). Estimated tapping velocities of 1–5 m/s suggest that the applied shear force is a few orders of magnitude lower than the hot modulus of rupture of most refractories. So it is well-argued that tap-hole refractory erosion cannot occur until the refractory structure has somehow first been weakened by liquid penetration and corrosion (Campbell *et al.*, 2002).

In PGM matte tap-holes an annulus of tap-hole clay does not appear to persist in lining the tapping module refractories (Figure 12). However, the same (low) velocities may possibly provide a shear force that is in excess of the hot modulus of rupture of poorly baked/sintered tap-hole clay. So in operations that critically depend on a 'maintainable' baked and sintered annulus of tap-hole clay to line the tapping channel to protect the tap-hole refractory (*e.g.* especially when combined tapping of more corrosive slag, as in ironmaking BFs), far more attention should be paid to the issue of tap-hole clay sintering and erosion-resistance properties (Mitsui *et al.*, 1988).

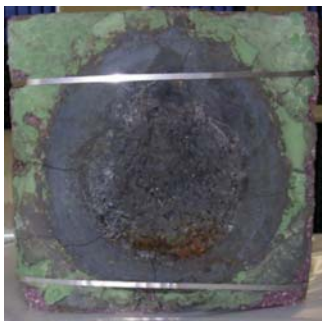

Figure 12—Matte tapping module brick with matte core; no evidence of a tap-hole clay annulus; penetrated dense brittle-zone annulus inside brick

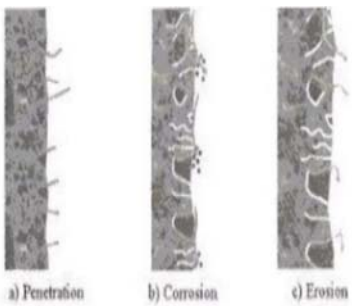

Figure 13—Representation of refractory wear mechanisms (after Campbell *et al.*, 2002)

[6]See also http://www.youtube.com/watch?v=u_4cEWTzQnI

Generally, the potential adverse influences of suboptimal tapping velocities are:

- *Too slow tapping*—limits tapped production; delays liquid drainage, which may potentially be unsafe if critical furnace levels are threatened (*e.g.* matte encroachment to near the vicinity of copper coolers, or slag overflow over the design maximum crucible containment height)
- *Too fast tapping*—induces loss of control, thereby creating unsafe tapping and post-tap-hole conditions; in the extreme, and only then, promotes tapping channel and furnace lining erosion.

These influences may have more adverse consequences than erosion does.

Drilling practices

Owing to the potential for oxygen-induced lancing damage to tap-holes, the vast majority of operations seek to practise drilling the tap-hole open. This typically includes sacrificing the drill bit and, potentially, the drill rod. In at least one Japanese Mn ferroalloy operation, to conserve costly drill bits, the operator withdraws the drill as soon as metal is expected to be encountered, places a sacrificial crimped steel pipe over the drill bit, and then drills the hole open. This protects the drill bit enough to permit re-use.

Combination drilling and 'plug' oxygen lancing practice

On most alloy-only and matte-only tap-holes operated in the substantial absence of any tap-hole hot-face 'mushroom', a combination of deep drilling followed by 'plug' oxygen lancing is practised deliberately. The aim is to drill through the tap-hole clay as (consistently) deep as possible (700–1200 mm, depending on tap-hole design length), until the drill encounters resistance from a 'plug' of metal/matte/residual entrained slag. Experience indicates that attempts to drill further through this 'plug' often lead to unintended skew drilling. This measure is particularly hazardous in a water-cooled copper tap-block configuration, and often results in the drill simply getting stuck in the tapping channel. Even with reverse percussion hammering (Bell *et al.*, 2004), it may become impossible to free a stuck drill bit and rod, an outcome that requires the tapper to resort to oxygen lancing to remove the obstruction.

In combination practice, the drill is then withdrawn, and the drill length measured accurately (but manually) with a gradated drill-T, which simultaneously verifies that the drilling was not off-centre. Once the drill-hole is confirmed as being straight, oxygen lancing of the short remaining tapping channel 'plug' is then undertaken to open the tap-hole. This usually requires a minimum of lancing (less than one lance pipe). In this way there is also a lower risk of tappers losing the skill of using oxygen lances safely owing to infrequent practice.

The rationale behind this practice is driven by a decided requirement not to overfill tap-hole clay, through the addition of a metered amount of tap-hole clay, which permits operation with a consistent short (as possible) tapping-channel 'plug' to lance.

Tap-hole drilling requirements

The requirements to control and optimize the rate of drainage to the tap-hole (to reduce liquid velocities and wear of the furnace lining) and the associated tapping rate through it (a controlled liquid tap with stable post-tap-hole conditions) impose a need to maintain a constant and optimal tap-hole length and smooth shape (Van Ikelen *et al.*, 2000). The length is usually as long as is practicably achievable, while one maintains a near-cylindrical channel shape of defined diameter. In reality, some extent of fluting towards the hot-face (conveniently modelled as a cone [Van Ikelen *et al.*, 2000; Nightingale *et al.*, 2001]) with erosion at the hot-face (conveniently modelled as a paraboloid to represent a zone for 'mushroom' development [Van Ikelen *et al.*, 2000; Nightingale *et al.*, 2001]) has been inferred from tapping channel temperatures, drill depths, and their distributions (Mitsui *et al.* 1988; Van Ikelen *et al.*, 2000; Nightingale *et al.* 2001).

In ironmaking operations with lower metal fall (a high slag ratio of lower density) it is argued that 'the decision for diameter and tapping practice must be focused on slag' (Brunnbauer *et al.*, 2001). This highlights the role of reliable drilling, as it represents the primary means for controlling tap-hole diameter.

Tap-hole drilling equipment and control

Owing to the excessive risk of skew drilling (directly contributing to similarly skew oxygen lancing in combination drilling and 'plug'-lancing practice), especially to operations with water-cooled copper tap-blocks, practice typically requires that the accurate alignment (to surveyed tap-hole centre/s [Estrabillo, 2001]) of mudgun/s and drill/s be checked and, if necessary, recalibrated at the start of each shift (Irons, 2001). Tap-hole-centering notches are also reported; they locate and indent the tap-hole clay to help keep the drill from 'walking off' from the centre of the tap-hole (Estrabillo, 2001).

In addition, guided and stiff drill rods are essential to reducing excessive drill flex and securing a straight, centred tap-hole. Guide systems include automatic travel to within limits, followed by a hydraulic pin, sometimes colloquially called 'antlers' (Black and Bobek, 2001), being physically positioned down into latch hooks. For drilling 4 m long ironmaking BF tap-holes (requiring 6 m drill rods), additional hydraulic rod devices are fixed to the drills to prevent bending of the drill rods and drilling off the tap-hole axis (Ballewski *et al.*, 2001). The undesirable consequence of using a less precise suspended rock drill for tap-hole drilling has been reported previously in a four-piece, water-cooled copper Ni ferroalloy tap-block operation (Nelson *et al.*, 2007; Figure 14 and Figure 15).

An encoder that measures the drill position can be correlated with drill torque (in hydraulic systems – Jameson *et al.*, 1999; Atland and Grabietz, 2001) or drill air-pressure forward drive (in pneumatic systems – Van Ikelen *et al.*, 2000) and drill speed to determine automatically the start and end of the tapping channel and hence the all-important tap-hole length (Jameson *et al.*, 1999; Van Ikelen *et al.*, 2000; Eden *et al.*, 2001; Tanzil *et al.*, 2001; Edwards and Hutchinson, 2001; Smith *et al.*, 2005). Drill-time sigma

Figure 14—Water-cooled 'dogbox' with minor cracks in surround bricks around tapping module brick with '+-shaped' crack and off-centre drill-hole (Nelson *et al.*, 2007)

Figure 15—Tapping module brick 4 after 219 taps. Multiple drillings of the tap-hole are off-centre, and are coupled with skew lancing (Nelson *et al.*, 2007)

(Black and Bobek, 2001) and tap-hole length (Jameson *et al.*, 1999) are regarded as benchmark statistics and, with the application of statistical process control (SPC), measures with which to quantify and effect tap-hole improvements.

Drill rod and bits

Drill-bit shape and material – carbide (Black and Bobek, 2001; Tanzil *et al.*, 2001; Entwistle, 2001) or heat-resistant Cr-Ni alloy (Atland and Grabietz, 2001) tips are preferred – has been the subject of intense investigation, especially in the ironmaking BF application (Van Ikelen *et al.*, 2000; Ballewski *et al.*, 2001; Black and Bobek, 2001; Brunnbauer *et al.*, 2001; Estrabillo, 2001; Entwistle, 2001; Atland and Grabietz, 2001). The ability to retain a sharp cutting edge so as to cut, rather than hammer, through the tap-hole clay 'plug', with the bit cutting face presented to a debris- and dust-free face to drill, is essential (Estrabillo, 2001). Drill-bit diameter is controlled usually within the range of 33 mm (Tanzil *et al.*, 2001) to 45–65 mm (Steigauf and Storm, 2001; Atland and Grabietz, 2001). Where hammering is considered important, an inside bit face that is totally flat (to maximize transmission of impact energy) is reported (Tanzil *et al.*, 2001), coupled with transition from spherical to semi-spherical carbide shapes.

Air scavenging is typically used to clear the hole, providing additionally some cooling of the drill bit to help prolong its life (Van Ikelen *et al.*, 2000). Further improvement has involved progressively improving drill-bit cooling (from air, to nitrogen, to water mist) on ironmaking BFs (Eden *et al.*, 2001; Petruccelli *et al.*, 2003; Van Ikelen *et al.*, 2000; Smith *et al.*, 2005; Irons, 2001; Steigauf and Storm, 2001; Ballewski *et al.*, 2001; De Pagter and Molenaar, 2001; Black and Bobek, 2001; Edwards and Hutchinson, 2001), where water-mist cooling rates are in the range of 2–5 L/min and typically 4 L/min (Tanzil *et al.*, 2001). Water-mist cooling systems are reported to have undergone still further development to overcome disadvantages of increased risk of drill equipment corrosion (Van Ikelen *et al.*, 2000).

In ferroalloy and matte operations, especially those equipped with any potentially hydratable magnesia-based refractory, use of any water would be taboo (in fact even to the extent that dew-point condensation associated with liquid-nitrogen cooling to accelerate tapping channel repair is sometimes a concern). The short drill-bit life is largely overcome when drilling only tap-hole clay (*i.e.* deliberately not drilling metal/matte/slag) in both metal/matte-only combination drilling and slag-only drilling open tapping practices.

Two opposing effects of drilling on the control of tapping channel diameter are reported. With premature bit wear, negative fluting of the tapping channel (diameter decreasing evenly down to the drill rod diameter towards the hot-face) has been reported (Van Ikelen *et al.*, 2000). Side-cutting designs capable of cutting during both forward and reverse drilling have been developed to limit the influence of drill-bit wear on the resulting drilled diameter (Van Ikelen *et al.*, 2000). More frequently, though, a bit that fails to retain its cutting edge tends to wander, which causes positive fluting to the hot-face (Nightingale *et al.*, 2001; Mitsui *et al.*, 1988; Tanzil *et al.*, 2001), or a 'mushrooming' effect (Estrabillo, 2001; Edwards and Hutchinson, 2001). Traditional rock drill-bit designs provide some increased resistance to this, and are often preferred (Estrabillo, 2001), despite still requiring drill-bit replacement every tap on an ironmaking BF. This warrants further clarification: on ironmaking BF tap-holes the ability to open with 'one drill-bit for every attempt' is regarded as an achievement (Estrabillo, 2001), with only a 50% success rate reported at one site (Nakamura *et al.*, 2007), or an average of 1.2 drill bits per tap reported (Atland and Grabietz, 2001). Progression from threaded to bayonet drill-rod couplings is reported (Estrabillo, 2001) to limit the incidence of drill rods jammed tightly in couplings.

The direct consequence of a smooth, straight tapping channel is a consistent smooth tapping stream and controlled post-tap-hole logistics. In contrast, a tapping channel that has an inner corkscrew shape is reported to induce a rotating and spraying tapping stream (Van Ikelen *et al.*, 2000), an outcome exacerbated by any gas-tracking on a pressurized BF operation. 'Softer drilling' (feed-forward pressure < 3 bar) together with instructions to the operator to 'let the drill do the work' and so not try to force the tap-hole open using maximum force, which can bend the drill rod and promote a corkscrew channel, is reported to lower the incidence of rotating and spraying tapping streams (Van Ikelen *et al.*, 2000).

This is remarkably akin to the requirements of successful oxygen lancing: a good tapper tends to use the hot burning lance tip (> 2000°C) to progressively cut the tap-hole open in a series of small precessing actions to guide the lance ever deeper to make a straight tapping channel. An inexperienced tapper, on the other hand, tends to try to force-burn the tap-hole open by pushing hard on the thin, long and flexible lance pipe, which readily causes it to deflect off-course and cause damage.

Finally, it is said that 'a rotating drilling method for opening the tap-hole, without hammering … is expected to give an improvement of the tapping process' (Van Ikelen *et al.*, 2000). Similarly, many local ferroalloy and PGM matte tap-holes are indeed opened by drill rotating action alone without hammer action, despite the latter's usual availability. Even on ironmaking BFs it is suggested that 'future advancements will be directed toward drilling the tap-hole without the need for hammering' (Estrabillo, 2001).

Tap-hole closure

It is essential to be able to 'close the tap-hole with a high degree of certainty that the desired volume of tap-hole clay has in fact been installed' (Tanzil *et al.*, 2001), and additionally ensure that mudgun retraction does not result in an unplanned tap-hole re-opening. Total elimination of reopening events remains important, even given reported improvement from 10 to just one such event per annum by 2000 on one site (Black and Bobek, 2001).

Especially on slag-only closure, stopper bars, water-cooled 'rosebuds', and manual stopper tap-hole clay 'plugs' remain common in the ferroalloy and non-ferrous industry. Slightly more sophisticated variants are used on some of the lower temperature and lower superheat mattes and blister Cu operations, *e.g.* 'Polish plug', comprising ceramic surrounding a cone-shaped tap-hole clay 'plug' (George-Kennedy *et al.*, 2005). Over 25% of PGM and local Ni matte operations still practise manual plugging of tap-holes (Nolet, 2014; Coetzee, 2006).

However, by far the majority of ferroalloy furnaces, 70% of PGM and local Ni matte operations (Nolet, 2014), and all ironmaking BFs have increasingly adopted sophisticated and powerful mudguns to effect tap-hole closure. Again, the importance of considering mudgun, tap-hole clay, and tap-hole operating practice holistically as a fully integrated system cannot be understated – coupling a hard new-generation tap-hole clay with an old weak mudgun incapable of properly delivering the clay into the tap-hole is bound to fail. Smith, Franklin, and Fonseca (2005) describe this well: the 'design of tap-hole clay is usually a compromise between "equipment capability" and "process" requirements.'

Mudgun equipment and operation

Manual plugging may at first glance seem extremely simplistic, requiring a direct interface of the operator with a hot tapping stream. However, if the operation is not correctly controlled, excessive tap-hole clay addition – which is possible with the use of automated mudguns – can potentially have a destructive, but often hidden, action on a tap-hole and lining environs. It was not that long ago that one of the authors witnessed a large furnace, about 30 m in length, 'disappear from view' due to excessive gas release and a concentrate blowback when a tap-hole was closed with a full 25 L mudgun load of wet clay recently 'dug from the veld'. Other observations include both metal and matte 'boils' at the back of tap-holes, tap-hole 'blows', and even gas eruption from tar binder (Mitsui *et al.*, 1988) caused by mudgun closure involving use of excessive tap-hole clay with high loss-on-ignition content. Water flashes with a 1500-times volume increase at bath temperatures, and hydroxides, carbonates, and hydrocarbons can react almost instantaneously and decompose, devolatilize, and crack (Cassini, 2001) to release CO, CO_2, H_2, and/or H_2O gases. In high-duty applications, tap-hole clay of low gassing potential is therefore a prerequisite, and almost all operators seek an anhydrous clay (Abramowitz *et al.*, 1983) or 'water-free plastic mass' (Smith *et al.*, 2005).

A perfectly cylindrical 1 m long tapping channel 50 mm in diameter requires theoretically only 2 L of tap-hole clay to completely fill it. This increases to 5 L if the tap-hole is worn on average to 80 mm diameter, by either positive fluting (exacerbated by any oxygen lancing and/or enlargement by bath wear of the tap-hole hot-face) or negative fluting down the tapping channel. Iida and co-authors (2009) even suggest that tap-hole enlargement occurs typically at a rate of 5.6×10^{-4} mm/s during tapping (1×10^{-3} mm/s when using 'poorer durability tap-hole mix' [Iida *et al.* 2009], a practice also modelled by others [Shao, 2013; Shao and Saxen, 2013b]). It is quite staggering to compare this addition with the range reported for ironmaking BFs – admittedly with tap-hole lengths of 1.8–2 m (Edwards and Hutchinson, 2001; Atland and Grabietz, 2001), or more usually 2.5–4 m (Irons, 2001) – from as little as 10–20 L (Irons, 2001) to 50–120 L (Irons, 2001; Atland and Grabietz, 2001; Van Laar, 2014; Nightingale *et al.*, 2001; Jameson *et al.*, 1999; Cassini, 2001) or even 200–300 L of tap-hole clay per closure when trying to stabilize a 'mushroom' (Eden *et al.*, 2001; Irons, 2001).

In an ironmaking BF, where tap-hole clay 'mushroom' operation is feasible, several operators report stable (consistently deep) tap-hole length and reduced tap-hole clay consumption, *i.e.* 'not excessive addition' (Nightingale *et al.*, 2001; Tanzil *et al.*, 2001; Cassini, 2001), and reduction by as much as 50% to 100–120 L on a 3 m tap-hole length (Nightingale *et al.*, 2001), which led to generally improved overall practice (Smith *et al.*, 2005; Jameson *et al.*, 1999; Black and Bobek, 2001; Tanzil *et al.*, 2001; Estrabillo, 2001; Nightingale and Rooney, 2001; Bell *et al.*, 2004; Cassini, 2001). This is particularly the case when the tap-hole-clay injection rates – rapid to assist with clean plugging of tap-hole clay down the tapping channel, yet with sufficient time for densification and crack sealing of the protective annular tap-hole-clay tapping-channel core (Andou *et al.*, 1989; Smith *et al.*, 2005) – and quantities added are controlled predictively, based on prior tapping and drilling metrics.

Again, this can involve SPC to control tap-hole length (*e.g.* to 3.1 m; Jameson *et al.*, 1999) by varying the tap-hole clay volume (around a 100 L setpoint; Jameson *et al.*, 1999); or by advising the operator of the recommended tap-hole clay volume after 1.5 hours of tapping, basing the advice on automatically measured tap-hole lengths and tap-hole diameter (the latter automatically inferred from measured blast pressure, liquid level, and mass tapping rates (Nightingale *et al.*, 2001; Tanzil *et al.*, 2001). Continuous weighing using load cells and microwave radar level detection are used to determine hot metal torpedo and/or slag-ladle filling rates, and thus related mass tapping rates (Tanzil *et al.*, 2001; Cassini, 2001; Shao, 2013). Operation usually involves increased tap-hole clay injection when the tap-hole length decreases, and decreased clay injection when the length increases. In consecutive individual tapping practice in particular, a common additional practice advocated on the other resting tap-holes is for occasional tap-hole clay injection to maintain the 'mushroom' condition on those tap-holes, which otherwise are subject to progressive dissolution

(if metal is marginally carbon-unsaturated) and wear in contact with hearth liquid (Jameson *et al.*, 1999; Nightingale and Rooney, 2001).

Ironmaking BF experience suggests that less than one-third of tap-hole clay purchased is pushed through the gun. This wastage is ascribed to combinations of (1) incorrect storage under uncontrolled conditions of temperature; (2) the tap-hole clay getting wet; or (3) situations where the tap-hole clay is allowed to go beyond its useful shelf life. Of the remaining tap-hole clay, only 24% is estimated to be delivered into the tapping channel (Smith, Franklin, and Fonseca, 2005) (Figure 16). Nozzle cleaning, push-out waste (used to ensure that tap-hole clay is compressed in the mudgun barrel), clay leakage between the nozzle and tap-hole face (Figure 17 and Figure 18), mudgun clean-out, and 20% for 'mushroom' replacement constitute the remaining portion of tap-hole clay usage.

Sacrificial wooden or ceramic nozzle covers – known locally as 'dinner plates' (Ndlovu *et al.*, 2005; Figure 19) – are commonly used to limit tap-hole clay losses associated with mudgun push-out waste (full nozzle cover) and nozzle-face/faceplate leakage (full or annular nozzle cover [Ndlovu *et al.*, 2005; Eden *et al.* 2001; Jameson *et al.*, 1999; De Pagter and Molenaar, 2001; Brunnbauer *et al.*, 2001; Estrabillo, 2001; Bell *et al.*, 2004]). A 25% reduction in mudgun-nozzle tap-hole clay leakage events, from a somewhat poor norm of 50%, has been reported for this practice (Estrabillo, 2001).

Well-designed faceplates normally further improve mating with a flat nozzle face – common on Co and Ni ferroalloy and matte-smelting operations. However, where faceplates are absent, some ironmaking BF operations have adopted tapered nozzle tips, for which better sealing against the tap-hole socket is claimed (Steigauf and Storm, 2001). Upgrading to high-nitride mudgun barrels is also cited as a factor preventing wear (Petruccelli *et al.*, 2003; Bell *et al.*, 2004).

On modern mudguns, rapid and automated pressure-regulated mudgun slew is applied to minimize damage to the mudgun nozzle, and to lower the risk of heavy impact on the tapping channel face and/or channel, a risk that might otherwise crack or even dislodge tap-hole refractory and the ironmaking BF 'mushroom' (Smith *et al.*, 2005; Jameson *et al.*, 1999). Slew pressure is usually set slightly higher than the mudgun barrel pressure (200–315 bar tap-hole clay pressure, which results in a pushing force of > 60 t on the tap-hole face/faceplate, particularly to push higher-strength tap-hole clays [Van Ikelen *et al.*, 2000; Smith *et al.*, 2005; Black and Bobek, 2001; Atland and Grabietz, 2001; Cassini, 2001]) – a measure that tends to limit the potential for bypass of clay between the nozzle and tap-hole face/faceplate (Eden *et al.*, 2001; Cámpora *et al.*, 1998; Jameson *et al.*, 1999; Entwistle, 2001). Automatic control of the mudgun contact force is also preferred in order to limit the risk of undue mechanical damage to the tap-hole refractory, a control that one site achieved by a variable-machine, minimum-pressure setpoint of 150 bar plus a variable proportion of 0.3 times the plugging pressure (Ballewski *et al.*, 2001). In the absence of rigid faceplates, tap-hole face wear can be estimated from a relationship to cylinder stroke measured by LVDT (Black and Bobek, 2001; Entwistle, 2001).

In the extreme practice of combination drill and 'plug' oxygen lance, which aims to avoid excessive tap-hole clay delivery beyond the tapping channel hot-face (for fear

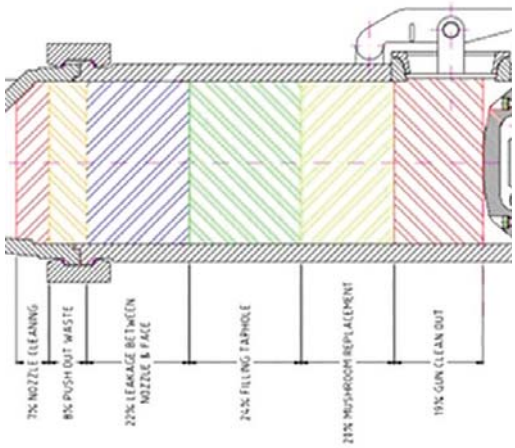

Figure 16—Estimation of tap-hole clay consumption and waste (after Smith *et al.*, 2005)

Figure 17—Excessive tap-hole clay bypass (Ndlovu *et al.*, 2005)

Figure 18—Controlled dosage of tap-hole clay (Ndlovu *et al.*, 2005)

Figure 19—Sacrificial mudgun nozzle 'dinner plate' (Ndlovu *et al.*, 2005)

otherwise of the tap-hole clay boiling and ensuing damage to the tap-hole hot-face), precise control of tap-hole clay input is imperative. This often involves measurement and automated control of the injected tap-hole clay volume. Indeed, in several instances when tap-hole clay addition has been excessive (Hundermark *et al.*, 2014; Ndlovu *et al.*, 2005) it has been demonstrated that controlled reduction of tap-hole clay additions (closer to the volume predicted theoretically for 'normal' tap-hole dimensions) has even resulted in increased drilling depths, further enhanced by improved furnace operating control of allowable upper matte temperature (Figure 20).

On ironmaking BF operations (Smith et al, 2005; Ballewski *et al.*, 2001; Tanzil *et al.*, 2001; Bell *et al.*, 2004), staggered, multi-stage mudgun injection at different speeds can be practised to achieve optimal tap-hole conditions. This may involve (Bell *et al.*, 2004) (1) a first fast push of 45 kg tap-hole clay to displace any other material from the tapping channel, followed by a slower push of another 45 kg clay to build the 'mushroom', and a final very slow push of variable clay mass to build the 'mushroom' still further and compact the tap-hole clay in the tap-hole, and (2) a second very slow push 5 minutes after the first push, with < 5 kg tap-hole clay added to compact the tap-hole clay still further and close voids. To diminish the risk of tap-hole breakout, the mudgun then remains in position for 5 minutes to allow adequate tap-hole clay curing before the mudgun is removed from the tap-hole face. On another operation, with a constant ram hydraulic pressure of 275 bar, a rate of tap-hole clay injection of 14 kg/s was sought (Black and Bobek, 2001).

Tap-hole clay

Tap-hole clay requirements

Typical requirements cited for tap-hole clay include the following (Abramowitz *et al.*, 1983; Andou *et al.*, 1989; Uenaka *et al.*, 1989; Hubert *et al.*, 1995; Ballewski *et al.*, 2001; Cassini, 2001; Wells, 2002; Smith *et al.*, 2005; Horita and Hara, 2005; Kageyama *et al.*, 2005, 2007; Nightingale *et al.*, 2006; Nakamura *et al.*, 2007; Pan and Shao, 2009; Niiya *et al.*, 2012; Kitamura, 2014):

- It should be soft and plastic enough to inject when pushed by the mudgun, but 'hard' enough to displace tapping liquid effectively and deliver a 'plug' of tap-hole clay only to the required depth in the tapping channel

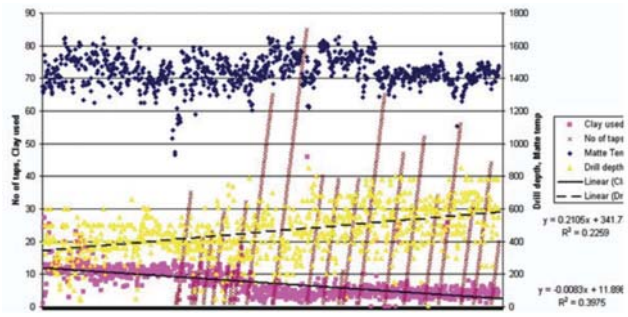

Figure 20—Reduced tap-hole clay injection (by 60%) leading to increased drilling depth, even before tighter matte-temperature control (Ndlovu *et al.*, 2005)

- After curing, it should attain the required strength (often described as 'sinterability' [Abramowitz *et al.*, 1983]) without shrinkage to ensure a tight seal within the tap-hole (and not prematurely in the mudgun), do so in the required mudgun dwell time, and plug the hole until the next tapping time
- It should effect safe tap-hole closure (*i.e.* without subsequent re-opening) without damage to the tap-hole and furnace lining (*e.g.* through limited gas evolution and associated turbulence), yet with the 'mushroom' remaining stable where required, *e.g.* in an ironmaking BF. This requires consideration of both effective tap-hole clay displacement in the injection direction (Uenaka *et al.*, 1989; Nakamura *et al.*, 2007; Kitamura, 2014) and a 'good spreading ability in the direction perpendicular to the injection direction' to maintain a stable 'sedimentary deposit that is gradually and stably grown' (Kitamura, 2014) and exhibiting good high-temperature adhesion to the constituents already present in the tapping channel (Niiya *et al.*, 2012)
- It should be soft enough to be readily drilled straight down the middle of the tapping channel without deviation and in an acceptable time (this is especially important where productivity constraints exist, as in an ironmaking BF)
- It should allow a stable, controlled tapping stream flow without surging or splash (often associated in ironmaking with blast gas tracking [He *et al.*, 2001; Pan and Shao, 2009] and gas entrained with 'viscous fingering' to above the critical value that induces a deleterious splashing casting stream [He *et al.*, 2002; 2012], even to the extent of slug flows [Shao, 2013; Stevenson and He, 2005; Shao and Saxen 2011, 2013b])
- It should be ideally 'hard' and durable (Abramowitz *et al.*, 1983) enough to withstand penetration, corrosion, and erosion by the tapped metal/matte and/or slag and so preserve a protective annulus between the tap stream and tap-block refractory (without additional corrosive reaction to the tap-hole refractory), thereby extending the useful life of the tapping channel with an acceptable, controlled diameter, shape (*i.e.* minimal long-term fluting), and length.

To ensure optimal tap-hole clay quality, additional measures for tap-hole clay preparation are recommended (Black and Bobek, 2001; Delabre *et al.*, 1991; Hubert *et al.*, 1991). These measures may include a stand-alone tap-hole clay storage building, maintaining a 10-day supply of tap-hole clay, and controlling the temperature in the building and the in-process temperature for storing tap-hole clay at the tap floor to 25–30°C (Abramowitz *et al.*, 1983). Maturation of the clay as a function of the binder quantity and type for two months is reported (Delabre *et al.*, 1991) to permit one clay to attain desired plasticity properties, these properties also being dependent on storage conditions. On the other hand, prolonged storage of resin-bonded tap-hole clay, especially at temperatures exceeding 40°C, is reported specifically as being detrimental to its performance (Wells, 2002). However, especially for tar-bonded tap-hole clays, a minimum of 15 days' ageing is reported as essential to secure adequate tap-

hole clay loss in plasticity and increased hardness (Hubert *et al.*, 1995). A tap-hole clay producer even reports forced cooling of tap-hole clay to avoid any risk of continued undue temperature rise before final packaging of product (Nakamura *et al.*, 2007).

Tap-hole clay aggregate

Most technical developments of tap-hole clay originate from the ironmaking BF industry, where the high productivity (10 000 t/d HM), combined metal and slag duty, high pressure (approx. 10 bar at tap-hole - Van Laar, 2014), and long tap-hole length (2.5–4 m – Table I) make high demands on tap-hole clay quality. Mitsui and co-workers (1998) use lowering of specific tap-hole clay consumption (kg/t HM) to outline early developments from the 1970s to 1988. These include a progression from coke, to alumina, to silica, and back to pitch-impregnated alumina (Niiya *et al.*, 2012) and high-alumina clays comprising a fine matrix (< 45 μm and > 50% by mass [Kageyama *et al.*, 2007; Horita and Hara, 2005]) and/or coarser aggregates (1–3 mm and approx. 20% by mass [Horita and Hara, 2005]). These clays include variously additions of zirconia, kyanite (Andou *et al.*, 1989), SiC, and metals or nitrides of silicon, aluminium, and ferrosilicon. These elements and compounds are added as fine powders to the matrix to lower porosity, reduce shrinkage, decrease volatiles, increase antioxidant action, lower wettability by slag, and improve extrudability, sintering, and resistance to corrosion and erosion (Abramowitz *et al.*, 1983; Andou *et al.*, 1989; Uenaka *et al.*, 1989; Black and Bobek, 2001; Wells, 2002; Smith *et al.*, 2005; Kageyama *et al.*, 2007; Nakamura *et al.*, 2007; Pan and Shao, 2009; Niiya *et al.*, 2012; Kitamura, 2014). Mention is also made of a trend to smaller particle size for improved compaction (Black and Bobek, 2001) and better sealing of the tapping channel against gas egress (Pan and Shao, 2009). Some sources even claim that ultrafines (< 10 m [Kageyama *et al.*, 2007]) improve strength, resistance to corrosion and abrasion, and an 'ability to go straight during gun-up instead of extending transversely inside the furnace' (Nakamura *et al.*, 2007). Improved corrosion resistance and higher positive residual expansion coefficients of pure silica and pure alumina sources compared with aluminosilicates are also reported (Mitsui *et al.*, 1998). Such a 'swelling' characteristic (Mitsui *et al.*, 1998; Cassini, 2001; Nightingale *et al.*, 2006) is important for helping to seal a tap-hole subject to temperature fluctuation from the extreme of superheated tapping temperatures to cold closure conditions in water-cooled tap-blocks. Additives are also beneficial in instances where the clay has not fully baked before the next tap, and provide strength at lower clay temperatures (Delabre *et al.*, 1991). A somewhat more empirical approach has similarly led to convergence on the use of tap-hole clays of high alumina content for high-intensity operations in the local pyrometallurgical industry.

Tap-hole-clay binder

Traditionally, coal tar pitch was used as a binder (approx. 20% by mass [Kageyama *et al.*, 2005]) in tap-hole clay. This was followed by a period in the 1990s where phenolic resin found favour. By 2001 it was reported that 90% of Japanese ironmaking BFs (Irons, 2001) and a Canadian producer (Bell *et al.*, 2004) had reverted to tar-bonded tap-hole clay, while in Europe tar, resin, and resin-tar binder combinations all continued to find favour (Irons, 2001). By 2005 one supplier of tap-hole clay reported that only two ironmaking plants in Japan were using resin-bonded tap-hole clay (Horita and Hara, 2005).

Tar-bonded tap-hole clays are generally thermoplastic, hard (often requiring pre-heating of the tap-hole clay in the mudgun barrel by gas heaters, hot water, or steam to become pliable [Ballewski *et al.*, 2001], especially for operation in colder climates), and slower curing (a cast time of 2 hours is deemed insufficient for full curing and sintering [Black and Bobek, 2001], although only 20–30 minutes is frequently encountered as being available for curing in practice [Uenaka *et al.*, 1989; Shao and Saxen, 2011, 2013a; Shao, 2013]). Slow curing necessitates the mudgun remaining in position for an extended time after plugging to avoid the tap-hole re-opening unintentionally. Unlike resin binders, tar-bonded tap-hole clay is reported to have the advantage of forming a transition-free union with a carbon-based refractory, which results in a monolithic tap-hole lining (Ballewski *et al.*, 2001) and improved adhesiveness at high temperatures (Niiya *et al.*, 2012). Radiant heating from the tapping launder may necessitate protection of the barrel by metal or ceramic insulating shields (Bell *et al.*, 2004), or even water-cooling. Mudguns with a partial or full circumferential water jacket and dual heating/cooling systems are quite common in ironmaking BFs and some Cr and Mn ferroalloy operations. These systems are often automated to operate at a fixed temperature setpoint, *e.g.*, a constant 50–65°C (De Pagter and Molenaar, 2001; Ballewski *et al.*, 2001; Bell *et al.*, 2004; Atland and Grabietz, 2001); or for maximum flexibility an adjustable, controlled temperature range, *e.g.*, 25–90°C (Black and Bobek, 2001) is provided for and tailored specifically to a given tap-hole clay type in use (Cámpora *et al.*, 1998). A reduction in tap-hole clay consumption by wastage of between 10 and 30% is reported in uses of water-cooled mudguns (Ballewski *et al.*, 2001; Atland and Grabietz, 2001).

Resin-bonded tap-hole clays are faster curing (Uenaka *et al.*, 1989; Wells, 2002; Kageyama *et al.*, 2005), a property promoting shorter mudgun dwell time and quicker tap-hole turnaround (of importance in a high-productivity operation such as an ironmaking BF). Occasionally, though, the tap-hole clays can cure too quickly, which leads, in hotter tap-holes, to the clay curing before injection is complete (Jameson *et al.*, 1999; Nakamura *et al.*, 2007); or, in the extreme, to its blocking prematurely in an excessively hot mudgun barrel and possibly delaying an effective tap-hole closure. Resin-bonded tap-hole clay can be prone to greater volatility upon heating (Kageyama *et al.*, 2005), to more undesirable gas evolution (observed in local industry), and is generally softer (to the extent of being found incapable of effecting tap-hole closure on some high-temperature and superheated Cr metal-only and PGM matte-only tap-holes). Some resin-bonded tap-hole clays have also been reported to cure too hard for acceptable drill times (< 15 minutes), a development requiring binder reformulation (Nakamura *et al.*, 2007). In high-intensity PGM matte operations, the risk of failing to close timeously a 'vicious' superheated tap is considered so extreme that procedures further dictate that no matte tap-hole

be opened without the availability of two fully prepared mudguns loaded with tar-bonded tap-hole clay to close the matte tap-hole.

Ballewski and co-workers (2001) observe that generally 'the lower the temperature, the more difficult the correct choice of a binder system for mud becomes . . . otherwise the front tap-hole area would extend negatively on the cold side'. Ostensibly for other reasons, just such a tap-hole extension outside the furnace (colloquially described as a bullnose, Figure 8) is precisely what has tended to happen with intensely cooled copper tap-blocks.

Abramowitz and co-workers (1983) reported that 'small changes (< 5%)' in either light oil loss (260°C for 6 hours) or loss on ignition (defined by them at a temperature of 1204°C, rather than a more common 900°C, or 1000°C [Hubert *et al.*, 1995]) can 'change many dimensional and strength properties (as high as 119%)' of tap-hole clays. This emphasizes the need for close control of conditions in the manufacture of all tap-hole clays, if one is to yield a product of consistent quality. Using cold crushing strength (> 7.6 MPa) and workability (18–28%) as quality criteria in the early 1980s, tap-hole clay manufacturers found that tap-hole clay rejection rates of up to 40%, sometimes more, were not uncommon. Rejection rates below 15% were suggested as acceptable.

In the local industry, variable supply and quality of coal tar pitch has at times led to suboptimal 'cutting' additions of oils to overly viscous pitch, with additions of resin to try to restore curing times. With binder additions of typically 20% by mass (Kageyama *et al.*, 2007), this has often led to tap-hole clays being prone to excessive gas evolution and having suboptimal handling and plugging characteristics, properties that make the clay possibly suitable for less onerous slag tap-hole closure, but unsuitable for high-duty, superheated Cr metal-only and PGM matte-only applications.

Tap-hole clay health issues

While imposing a minimum 45-minute tap-hole clay curing time before re-drilling and tapping is reported to result in less emission of fumes (Estrabillo, 2001), tar binders pose health risks through the release of polycyclic aromatic compounds such as benzopyrene, which are carcinogenic (Perez *et al.*, 2001; Hershey *et al.*, 2013; Irons, 2001). The release of similarly undesirable formaldehydes and phenols is associated with resin binders. Molenaar (Irons, 2001) argues that benzopyrene particles in the air condense on dust, and hence some protection is afforded by wearing a mask, which is ineffectual for protection against formaldehyde and phenol gases.

Non-polluting tap-hole clay is therefore desirable, provided that it can adequately meet the arduous duty and requirements of tap-hole clay without introducing further risk (*e.g.* tap-hole liquid breakout). Tarless tap-hole clays have been available since the 1970s (Hubert *et al.*, 1991), as well as tap-hole clay utilizing commercial tar binder of 'one thirtieth of the benzopyrene' content of ordinary coal tar for binders (Kitamura, 2014). More recently clays which do not contain any polycyclic aromatic hydrocarbons have also become available (Lungmuß Feuerfest, 2014). However, it was reported (Perez *et al.*, 2001) that non-polluting single-phase binders have proved unsuccessful, but that a single-phase binder A plus binder B (made of several mixtures) manifested comparable plasticity, high-temperature adhesivity, high thermal expansion, and low erosion properties to existing tap-hole clays.

Industry's adoption of non-polluting tap-hole clays has not been universal. This is possibly owing to concerns regarding some perceived deficiencies in their performance in tap-hole duty for certain commodities compared to more traditional tar-based clay products.

Tapping and tap-hole environment

Tap-hole opening, the act of tapping metal/matte/slag, and tap-hole closure all lead to increased environmental emissions around the furnace. That is, emissions associated with drilling uncured tap-hole clay, or fumes released in oxygen lancing; release of process gases such as CO or H_2 under pressure, especially in ironmaking BFs, or SO_2, possibly even H_2S, by release or reaction, especially in matte smelting, but also other trace gases, *e.g.*, Cl and F, or contained volatile heavy metal impurities, *e.g.* Pb, As, Cd, and Zn, depending on specific composition; and volatile emissions from injecting tap-hole clay. Extraction systems on tap-hole, launder, and ladle hoods (Figure 1), and even on entire tapping aisles, are increasingly required to achieve the necessary and acceptable workplace hygiene and environmental abatement.

Tap-hole maintenance and life

Preventative maintenance

Ironmaking BFs incorporate robust designs that usually last for more than 10 years with little maintenance reported (Steigauf and Storm, 2001) of the castable at the front cold-face (and without 'mickey' bricks). An original four-tap-hole construction that lasted 12 years is also reported. Other BF sites report a 28-day cycle of casting tap-hole pairs (Steigauf and Storm, 2001), or recasting of tap-hole faces in planned maintenance scheduled every 18 weeks (Tanzil *et al.*, 2001). Tap-block graphite block inspection every 4 years is also reported (Black and Bobek, 2001).

Longer time-frames and operation to tap-hole breakout (usually within 3–4 years) are also practised on many local ferroalloy furnaces, but usually with the consequence of far more severe furnace lining damage and shortened cycle times to the next breakout. A notable exception is a campaign life of 9–12 years before a first small tap-hole repair, reported on combined metal-slag tap-holes of freeze lining design on a Cr ferroalloy furnace (Duncanson and Sylven, 2011). On Cr ferroalloy furnaces with water-cooled copper tap-block elements, other periodic planned maintenance may present ideal opportunities to effect annual slag tap-block and/or biannual metal tap-block repairs.

Most typically in Mn ferroalloys, total furnace (and by inference tap-hole) life is reported as being only 6–10 years (De Kievit *et al.*, 2004; Van der Walt, 1986; Hearn *et al.*, 1998), with some early freeze lining furnace designs giving over 20 years of life being the exception (Van der Walt, 1986; Hearn *et al.*, 1998). On many Mn ferroalloy furnaces, periodic 'mickey' block replacement may be planned and performed as often as every 6 months, with a tap-block campaign life of three years being typical. With the freeze

lining tap-hole design, life in excess of 18 months for the annular replaceable carbon block and graphite sleeve design has been reported in SiMn production (Hearn *et al.*, 1998), and 400 mm (out of 870 mm) wear of tap-block hot-face in just over three years of service is reported in HC FeMn production (O'Shaughnessy *et al.*, 2013). Apparently this wear is not attributed to erosion by tapping practices alone (which involve drilling and minimal use of oxygen lancing); rather, it is suspected that standard furnace thermal equilibrium conditions do not always permit the tap-holes to remain at their design length (O'Shaughnessy *et al.*, 2013). On Mn ferroalloy furnaces with water-cooled copper tap-block elements, planned maintenance activities are understandably more aggressive, with 'mickey' repairs being carried out as frequently as every 4 months.

Blister tap-holes were reported to operate for 8 000 t between inner change, while flash converting furnaces were projected to deliver more than 4 years of life (George, 2002). The latest furnace life estimate is now in excess of 5 years (George-Kennedy *et al.*, 2005).

On Ni ferroalloy and Ni and PGM matte furnaces, preventative maintenance may be time-based on lower intensity furnaces, but is more usually based on number of taps (Nolet, 2014; Jastrzebski *et al.*, 2012) rather than on mass tapped, with the assumption that a 'tapping event' (comprising tap-hole opening, tapping, and tap-hole closing) is a more significant determinant of tap-hole wear than the mere act of tapping. As previously intimated, especially on higher-intensity superheated PGM matte operations, excessive tapping rates can also be used to trigger tap-hole maintenance.

Typical tap-hole maintenance cycles that result are 1–4 weeks between faceplate refractory insert and shallow tapping module brick replacement; quarterly for deep tapping module and/or surround brick replacement; 1–2 years for full tapping channel repair and potentially water-cooled copper tap-block replacement (Nolet, 2014).

In addition, condition-based maintenance can be triggered immediately by any of the following: suspicion of any water leak; overly skew drilling; overly skew lancing (less easy to diagnose); excessive oxygen lance consumption; undue difficulty in tap-hole closure by tap-hole clay; damaged faceplate refractory insert; damaged faceplate (the flat, vertical, mating surface presented to the mudgun nozzle is compromised); the insert tapping channel diameter is greater than a prescribed limit (practice requires the oversize diameter to be followed down the tapping channel, replacing adjacent tapping module bricks until the diameter is deemed within a prescribed limit); and tap-hole temperature spikes reaching above alarm limits.

Special maintenance

Online repair techniques to improve the tap-hole condition on ironmaking BFs include (Yamashita *et al.*, 1995; Jameson *et al.*, 1999; Ballewski *et al.*, 2001) the following: use of higher plasticity tap-hole clays to help seal gaps and reconstruct 'mushrooms'; use of an emergency 'nozzle can' (Estrabillo, 2001); injection of resin down a partially drilled (blind) tap-hole to seal cracks and reduce gas tracking; and grouting through injection under pressure of tar-bonded carbon mortars to fill voids more generally and so re-establish thermal contact and reduce gas tracking (Edwards, and Hutchinson, 2001). Details of several grouting and zoned-plug (blind) repairs and basic procedures in ironmaking BFs are described by Cámpora and co-workers (1998), Yamashita and co-workers (1995), and Ballewski and co-workers (2001). A caution is sounded: great care should be exercised in grouting, using a sufficient number of open grouting points in the repair vicinity, to avoid the risk of grouting leading to excessive build-up of pressure and so leading inadvertently to refractory movement and even to lining failure.

A comprehensive mudgun and drill inspection programme, with weekly, monthly, quarterly, and annual activities to ensure equipment reliability, and early detection and prevention of possible failures, is described by Petruccelli (2003). Reliability of air supply on pneumatic drills is quoted fairly frequently as a cause of poor drilling, with air accumulators and new compressors being installed to address the problem (Petruccelli, 2003).

Tap-hole monitoring

Standard tap-hole monitoring

Three general levels of tap-hole monitoring are identified:

- Limited use of single thermocouples inserted into the lining, some around the tap-hole, often associated with a furnace campaign (let alone tap-hole) life of under 6 years on both (historically) ironmaking BFs (Eden *et al.*, 2001; Jameson *et al.*, 1999) and ferroalloy furnaces (Van der Walt, 1986; Hearn *et al.*, 1998; De Kievit *et al.*, 2004; Coetzee and Sylven, 2010; Coetzee *et al.*, 2010; Duncanson, and Sylven, 2011)
- Progression to more thermocouples (15–50), predominantly duplex in configuration, to permit heat flux calculations and monitoring on ironmaking BFs (Stokman *et al.*, 2004; Jameson *et al.*, 1999; Irons, 2001; Entwistle, 2001) and ferroalloy furnaces (De Kievit *et al.*, 2004). Furnace campaign life now ranges more typically between 10 and 20 years on both ironmaking BFs (Van Laar *et al.*, 2003; Eden *et al.*, 2001; Jameson *et al.*, 1999) and ferroalloy furnaces (Van der Walt, 1986; Hearn *et al.*, 1998; De Kievit *et al.*, 2004; Duncanson and Sylven, 2011)
- Dedicated multiple thermocouples for in-tap-hole temperature measurement (Estrabillo, 2001), heat flux probes (equipped with thermocouples) (Atland and Grabietz, 2001), and, in the extreme, up to 30 copper thermocouples and water circuit RTDs (to determine temperatures, and water temperature rises and associated local heat fluxes) to monitor water-cooled copper tap-blocks (let alone the adjacent furnace lining), practices that are adopted on some high-intensity non-ferrous operations.

Advanced tap-hole monitoring

Conditions inside the tap-hole during tap-hole clay curing can be determined by drilling a pilot hole and

- Inserting temporary thermocouples down the tapping channel to determine tap-hole temperature profiles with depth, *e.g.* on ironmaking BFs temperatures rise on

average from 200 to 800°C (maximum 550 to 1200°C) from 0.25 to 1.75 m down the tap-hole (Abramowitz *et al.*, 1983; Delabre *et al.*, 1991; Cámpora *et al.*, 1998; Ballewski *et al.* 2001; Nightingale *et al.*, 2006; Niiya *et al.*, 2012), thereafter reaching a plateau down the 3 m long tap-hole (Ballewski *et al.* 2001) and with time (700– 900°C within 30 minutes of injection (Entwistle, 2001), and applicable to establishing tap-hole-clay set-up times (Abramowitz *et al.*, 1983; Mitsui *et al.*, 1988; Delabre *et al.*, 1991; Cámpora *et al.*, 1998; Ballewski *et al.*, 2001; Bell *et al.*, 2004; Niiya *et al.*, 2012)

- Measuring with a contact thermocouple at 20 cm intervals, even reported apparently in normal opening of the tap-hole (Ballewski *et al.* 2001)
- Inserting nitrogen-cooled (Entwistle, 2001) or water-cooled (Ballewski *et al.*, 2001) fibre-optic cameras to view internal tapping channel conditions
- Core drilling the curing/cured tap-hole clay samples for chemical and mineralogical/petrographic analysis and physical testing (Andou *et al.*, 1989; Van Laar *et al.*, 2003; Shao, 2013), sometimes on a two-year planned maintenance cycle (Bell *et al.*, 2004).

In some BF stacks ceramic rods are integrated into the lining to permit wear to be determined by the ultrasonic measurement of rod length (here one assumes ceramic wear is coincident with lining wear [Stokman *et al.*, 2004]). What is uncertain is the status of the application and the efficacy of this or any alternative, external, nondestructive testing (NDT), acoustic emission (AE) technique (Sadri *et al.*, 2008; pers. comm. 2010, 2011) in more intensely cooled tap-hole regions, frequently with the presence of composite refractory materials and/or water-cooled copper coolers.

A more recent development has been the use of electrical resistance-based sensors (continuous along the length of the sensor, but for peak temperature only [Hopf and Rossouw, 2006]) and fibre-optic temperature sensors (either continuous sensor length maximum temperature, or discrete [about 25 per sensor] temperature measurements [Gerritsen *et al.*, 2009; Hopf, 2014; pers. comm. 2010]) to record more accurately and better map matte (and slag) tap-block temperatures in Ni and PGM matte smelting.

This development is an attempt to avoid a 'porcupine' copper tap-block containing more conventional copper thermocouples and water RTDs than available for labelling by the alphabet! This recognizes the limited range (akin to 'fishing with a rod' [Wasmund, 2003], so raising the chance of missing vital information) of only local temperature detection by thermocouples in an intensely water-cooled copper tap-block environment. Tap-blocks are often equipped with yet a third redundant cooling circuit recessed towards the cold-face. This circuit has been successfully used on at least one occasion as a backup water circuit that permitted the safe shutdown of the furnace under controlled conditions following a cooler 'hit' and the loss of the primary hot-face cooling water circuit and/or furnace refractory breakout. This further recognizes the more global monitoring capability, but poorer temperature resolution, of a rise in cooling water temperature on intensely cooled copper tap-blocks (akin to 'fishing with a net' [Wasmund, 2003], so being better at capturing key thermal events).

Although conventional duplex thermocouples are capable of detecting the accumulation of thermal energy in tap-hole refractories when tapping in close succession on one matte tap-hole (Figure 10 and Figure 21), fibre optics provide more detailed local mapping of the distributions and rises in temperature associated with consecutive tapping. Alternatively, the beneficial effects of resting a tap-hole to lower temperatures, as practised in alternating tapping procedures, may require less exhaustive monitoring (Figure 11).

Preliminary results seem to confirm a distinct temperature rise following tap-hole closure, consistent with the previously observed heat load rise following tap-hole closure (Cameron *et al.*, 1995). Cooling during tapping was also reported (Figure 22). The former was plausibly ascribed to the significantly increased heat flux associated with tap-hole clay coming into contact with superheated matte and the associated turbulence of gas bubbles and concomitant enhanced heat transfer. The cause of the latter is unknown.

Depending on whether temperatures are measured at the chamfer or in the tapping channel during tapping on another matte tap-hole (Figure 21), recent fibre-optic measurements seem to show some trends of rising temperatures (and only sometimes falling) already during tapping. Temperatures continue at best on a similar trajectory, rather than with any distinct rise as may be expected for tap-hole clay closure (tapping events being determined from pyrometer temperature data). Moreover, while it may be tempting to ascribe apparent minor temperature dips around some tap-hole closure events to a theoretically plausible effect of tap-

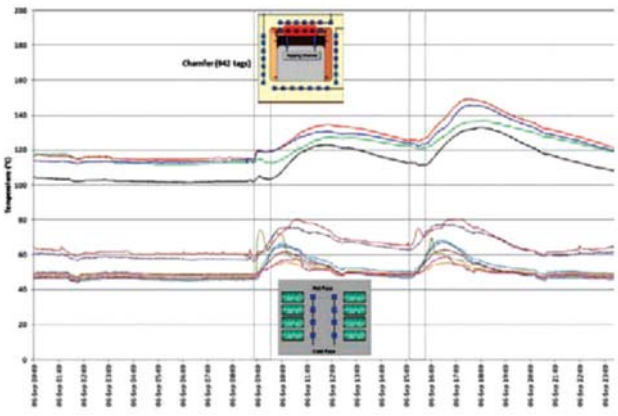

Figure 21—Recent tapping period close-up of fibre-optic temperatures on another matte tap-block (open-close shown as lines)

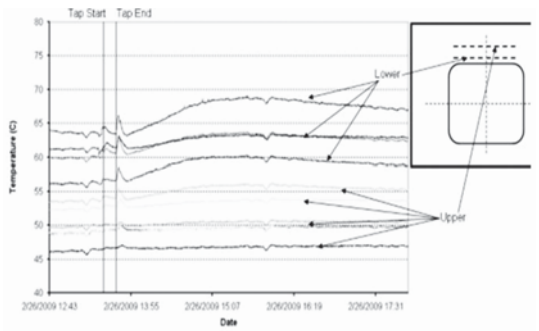

Figure 22—Close-up of tapping period showing fibre-optic temperature drop during tap (after Gerritsen *et al.*, 2009)

hole cooling by the injection of tap-hole clay (modelled in SiMn ferroalloy tapping [Muller and Steenkamp, 2013]), closer analysis suggests that the apparent dips are more likely to be an artefact of cooling induced periodically by the coarse temperature control of the copper tap-block water-cooling heat-exchanger circuit.

Clearly, still more work is required to understand and explain fully the tap-block fibre-optic temperature trends. This is a fundamental requirement prior to attempting more complex projections of possible tap-hole brick wear trends by thermal modelling – projections in support of advanced condition monitoring.

In response to difficulties and risks in the timeous detection of a significant tap-block temperature rise (see *Dedicated metal/matte tapping* section), other more advanced monitoring and diagnostic systems have been pursued, including principal component analysis (PCA), to try to provide some advanced view of the development of some abnormal tap-hole conditions (Gerritsen *et al.*, 2009; Plikas *et al.*, 2005; pers. comm., 2010), and tap-hole acoustic monitoring (TAM), which has the potential to identify the development of off-centre lancing (Sadri *et al.*, 2008; Wasmund, 2003; pers. comm., 2010, 2011).

Tapping system water hazards

Given the sheer rapidity, often with very limited warning, and consequences of a matte/blister Cu 'hit' of a water-cooled furnace component, it is quite simply deemed that refractory or accretion freeze lining must always persist to prevent such direct matte/blister Cu contact with the copper tap-blocks, a condition somewhat analogous to protection against the physical cause of loss of the space shuttle Columbia, being a '*breach in the Thermal Protection system*' (Gehman *et al.*, 2003). This disaster involved the loss of thermal protection tiles; the analogy to protective refractory layers in a composite copper cooling system is patent. A final critical warning served on all furnace operating and maintenance personnel is a learning outcome from the Columbia disaster: avoid falling into the trap of complacency by analogously 'deeming damage to the Thermal Protection System an "accepted flight risk"' (Gehman *et al.*, 2003). Any decision not to investigate thoroughly a suspected matte/blister Cu 'hit', or breach of protective refractory and/or accretion freeze lining, should always be challenged with vigour!

Alternative coolants are suggested as a means to mitigate some of the risks associated with linings that use water cooling in high-temperature molten-bath systems (Kennedy *et al.*, 2013). Certainly until such cooling media achieve common commercial application, effective water leak detection is a vital safety requirement of designs that incorporate water-cooled linings. Monitoring of abnormal drops in temperature in tap-holes or linings through cooling by water (Jameson *et al.*, 1999; Nelson *et al.*, 2004) or of abnormal rises in temperature, either through conversion to steam and its subsequent transport and heating effect in the nearby environs, or through the loss of the freeze lining skull (Entwistle, 2001), is another procedure adopted to identify water leaks. Other methods involve off-gas analysis for increased hydrogen content (in reducing ironmaking BF and ferroalloy processes) or, directly, for water vapour using hygrometers.

Systems that require closed-circuit water cooling need to take the following into account: monitoring frequency, the rate of change of make-up water, and the standpipe level to detect leaks (Jameson *et al.*, 1999; pers. comm. 2010); differential flow (MacRosty *et al.*, 2007; pers. comm. 2010) and multi-tier sensors that involve the monitoring of copper and water temperatures, water flow, and (periodically) water pressure (Valentas and Thierney, 2010; Shaw *et al.*, 2013; Bussell *et al.*, 2013). Such automated pressure testing of individual cooler-water circuits (at operator-selected scan rates) has proved capable of detecting even the smallest of 'drip' leaks on commercial furnaces (Shaw *et al.*, 2013). These systems are most direct and effective, but more expensive and, for safety, dependent on coolers equipped with redundant water-cooling circuits and/or process and cooler design conditions in which the termination of a cooler water circuit supply for a brief period of pressure testing carries no risk of converting water so entrapped to steam.

Conclusions

The critical importance of tap-hole design and management to furnace performance and longevity on a variety of ferrous and non-ferrous smelting processes has been demonstrated. Process conditions and productivity requirements dictate specific differences and similarities in tapping equipment and practices, and in managing tap-hole operations and maintenance. Operators are challenged to benchmark continually against other established best tapping practices and tap-hole management systems in order to seek further incremental improvements in safety and performance.

Molenaar's vision (Irons, 2001) of the tap-hole of the future, now well over a decade old, was of a fully automated and remote-controlled environment. This effectively describes operating with personnel safely removed to the maximum extent possible from direct interface with hot liquids, their containment systems (hot lining and environmental), and tapping systems. While progress has indeed been made in this direction, further effort is required to realize such an ideal, consistent with still further improvements in tap-hole performance and life, improvements that are pivotal to ensuring the safest and highest productivity furnace tapping operation possible.

Acknowledgments

Permission by Anglo American Platinum Ltd. to publish, technical discussions and contributions by Reinoud van Laar, Paul den Hoed, Bart Pieterse, Alpheus Moshokwa, Phillimon Mukumbe, Joalet Steenkamp, Paul van Manen, and Whitey Seyanund, and assistance with manuscript preparation by Emerelda Kieser are gratefully acknowledged.

References

Abramowitz, H., Goffney, L.J., and Ziegert, W.L. 1983. Taphole mix properties and performance for the first year of operation on Inland's No. 7 blast furnace. *Proceedings of the 42nd Ironmaking Conference*, Atlanta, GA, 17–20 April. Iron and Steel Society of AIME, Warrendale, PA. pp. 681–694.

Andō, J. 1985. Development of slag blast granulating plant characterised by innovation of the slag treatment method, heat recovery and recovery of slag as resources. *Mitsubishi Heavy Industries*, Ltd., *Technical Review*, June. p. 7.

Andou, T., Nagahara, M., Tsutsui, N., Ikeda, M., Nomura, M., and Suetaki, T. 1989. Wear mechanism of taphole mix. *Nippon Steel Technical Report*, no. 41. pp. 7–11.

Atland, R. and Grabietz, G. 2001. Tap-hole design and experience. *Proceedings of the McMaster Symposium on Iron and Steelmaking*. pp. 211–230.

Ballewski, T., Peters, M., Ruther, P., and Schmole, P. 2001. New improvements of the tap-hole area at Thyssen Krupp Stahl AG. *Proceedings of the McMaster Symposium on Iron and Steelmaking*. pp. 48–56.

Bell, C., Boettcher, B.D., Hribljan, F., Kinsman, B.M., and Van Laar, F. 2004. Tap-hole maintenance improvements at Dofasco. *AISTech*, vol. 1. pp. 303–321.

Black, B. and Bobek, J. 2001. Improvement in tap-hole life and casting performance at Ispat Inland's no. 7 BF. *Proceedings of the McMaster Symposium on Iron and Steelmaking*. pp. 156–176.

Brown, R.W. and Steele, D.F. 1988. Bond developments in silicon carbide blast furnace refractories during the 1980's. *Aachen Proceedings*. pp. 41–46.

Brunnbauer, G., Mauhart, J., Ferstl, A., Nogratnig, N., and Rummer, B. 2001. Tapping practice at Voest Alpine Stahl Linz. *Proceedings of the McMaster Symposium on Iron and Steelmaking*. pp. 178–182.

Bussell, B., Janzen, J., St. Amant, M., Miron, R., Emond, M., Braun, W., and Gerritsen, T. 2013. Improved furnace cooling water pressure leak detection system at VALE. *Proceedings of INFACON 13*, Almaty, Kazakhstan. pp. 377–384.

Cameron, I.A., Sriram, R., and Ham, F. 1995. Electric furnace matte tap hole developments at Falconbridge Limited. *CIM Bulletin*, vol. 88, no. 991. pp. 102–108.

Campbell, A.P., Pericleous, K.A., and Cross, M. 2002. Modeling of freeze layers and refractory wear in direct smelting processes. *Iron and Steelmaker*, vol. 29, no. 9. pp. 41–45.

Cámpora, S., Doro, E., Giandomenico, F., and Gonzalez, J.M. 1998. Improvements on the cast house operation at Siderar's blast furnace #2 since the blow-in. *Proceedings of the 57th Ironmaking Conference*, Toronto, 22–25 March 1998. pp. 203–217.

Cassini, C. 2001. Tap-holes operating and face repair practices at Sollac-Méditerranée FOS Plant. *Proceedings of the McMaster Symposium on Iron and Steelmaking*. pp. 68–80.

Coetzee, C. and Sylven, P. 2010. No tap-hole – no furnace. *Proceedings of Refractories 2010*. Southern African Institute of Mining and Metallurgy, Johannesburg. pp. 55–66.

Coetzee, C., Duncanson, P., and Sylven, P. 2010. Campaign extension for ferroalloy furnaces with improved tap hole repair system. *Proceedings of INFACON XII*, Helsinki. pp. 857–865.

Coetzee, V. 2006. Common-sense improvements to electric smelting at Impala Platinum. *Journal of the Southern African Institute of Mining and Metallurgy*, vol. 106, no. 3. pp. 155–164.

Dash, S.K., Jha, D.N.S., Ajmani, K., and Upadhyaya, A. 2004. Optimisation of tap-hole angle to minimise flow induced wall shear stress on the hearth. *Iron and Steelmaker*, vol. 31, no.3. p. 207–215.

De Kievit, A., Ganguly, S., and Dennis, P. 2004. Monitoring and control of furnace 1 freeze lining at Tasmanian electro-metallurgical company. *Proceedings of INFACON X*, Cape Town. pp. 477–487.

De Pagter, J. and Molenaar, R. 2001. Tap-hole experience at BF6 and BF7 of Corus strip products Ijmuiden. *Proceedings of the McMaster Symposium on Iron and Steelmaking*. pp. 107–125.

Delabre, Ph., Dufour, A., Guenard, C., Hitier, B., Hubert, P., Le Runigo, I., and Venturini, M.J. 1991. Taphole mud: a refractory key control of blast furnace casting conditions. *Proceedings of the Unite CR Congress*. pp. 299–305.

Duncanson, P.L and Sylven, P. 2011. New refractory lining direction at Jindal stainless – first Indian FeCr producer to install UCAR Chillkote® linings. *GrafTech International*. pp. 2–10.

Eden, M.G., Ferstl, A., and Doel, P. 2001. The tap-hole zone of a blast furnace – the critical region for a long campaign life. *Proceedings of the Third IAS Ironmaking Seminar*, Buenos Aires, Argentina. pp. 123–130.

Edwards, B. and Hutchinson, S. 2001. Emergency tap-hole repair No. 4 Blast Furnace at STELCO Hilton Works. *Proceedings of the McMaster Symposium on Iron and Steelmaking*. pp. 273–290.

Entwistle, J.W. 2001. The tap-hole: A unique system. *Proceedings of the McMaster Symposium on Iron and Steelmaking*. pp. 243–258.

Estrabillo, L.S. 2001.Tap-hole management practices at Lake Erie steel company. *Proceedings of the McMaster Symposium on Iron and Steelmaking*. pp. 233–241

Fallah-Mehrjardi, A., Hayes, P., and Jak, E. 2014. From phase equilibrium and thermodynamic modeling to freeze linings – the development of techniques for the analysis of complex slag systems. *Celebrating the Megascale: Proceedings of the EPD Symposium on Pyrometallurgy in Honor of David G.C. Robertson*. TMS, Warrendale, PA. pp. 259–266.

Gehman, H.W., Barry, J.L., Del, D.W., Hallock, J.N., Hess, K.W., Hubbard, G.S., Logsdon, J.M., Osheroff, D.D., Ride, S.K., Tetrault, R.E., Turcotte, S.A., Wallace, S.B., and Widnall, S.E. 2003. Report of Columbia Accident Investigation Board. National Aeronautics and Space Administration, Washington, DC. http://s3.amazonaws.com/akamai.netstorage/ anon.nasaglobal/ CAIB/CAIB_lowres_full.pdf

George, D.B. 2002. Continuous copper converting – A perspective and view of the future. *Sulfide Smelting 2002, Proceedings of a Symposium held during the TMS Annual Meeting*, 17–21 February. pp. 3–13. TMS, Warrendale, PA.

George-Kennedy, D., Walton R., George, D.B., and Nexhip, C. 2005. Flash converting after 10 years. *Proceedings of the 11th International Flash Smelting Congress*, Bulgaria/Spain. pp. 79–97.

Gerritsen, T., Shadlyn, P., Macrosty, R., Zhang, J., and Van Beek, B. 2009. Tapblock fibre-optic temperature system. *Proceedings of Pyrometallurgy of Nickel & Cobalt 2009*. pp. 627–639.

Gudenau, H.W., Krönert, W., and Fusenig, R. 1988. Wear profiles in blast furnace hearth, giving particular consideration to the formation of blast furnace salamander. *Aachen Proceedings*. pp. 28–31.

Guevara, F.J. and Irons, G.A. 2007. Slag freeze layer formation in an electric smelting furnace. *Proceedings of Cu2007. Carlos Díaz Symposium on Pyrometallurgy*, Toronto. vol. 3 (book 2). pp. 481–493.

Guthrie, R.I.L. 1992. Engineering in Process Metallurgy. Oxford Science Publications.

He, Q., Zulli, P., Tanzil, F., Lee, B., and Evans, G. 2001. An insight into flow behaviour of blast furnace taphole streams. *Proceedings of the McMaster Symposium on Iron and Steelmaking*, no. 29. pp. 149–153.

He, Q., Zulli, P., Tanzil, F., Lee, B., Dunning, J., and Evans, G. 2002. Flow characteristics of a blast furnace taphole stream and its effects on trough refractory wear. *ISIJ International*, vol. 42, no. 3. pp. 235–242.

He, Q., Evans, G., Zulli, P., and Tanzil, F. 2012. Cold model study of blast gas discharge from the tap-hole during the blast furnace hearth drainage. *ISIJ International*, vol. 52, no. 5. pp. 774–778.

Hearn, A.M., Dzermejko, A.J., and Lamont, P.H. 1998. 'Freeze' lining concepts for improving submerged arc furnace lining life and performance. *Proceedings of INFACON VIII*, Beijing. pp. 401–426.

Henning, B., Shapiro, M., Marx, F., Pienaar, D., and Nel, H. 2010. Evaluating AC and DC furnace water-cooling systems using CFD analysis. *Proceedings of INFACON XII*, Helsinki. pp. 849–856.

Henning, B., Marx, F., Hartzenberg, D., Fowler, N., and Shapiro, M. 2011. Simulating the blister tap hole concept design using conjugate heat transfer capabilities in STAR-CCM+ V5.02.009. *Proceedings of the STAR European Conference*, Noordwijk, The Netherlands, 22–23 March.

Hershey, R.A., Stendera, J.W., and Biever, G.G. 2013. Sorting out the hazards of anhydrous taphole clays. *AISTech Conference Proceedings*, Pittsburgh, May 2013. pp. 169–174.

Hopf, M. 2014. Monitoring the wear of water-cooled tap-hole blocks by the fibre-optic method Optisave. *Proceedings of the Furnace Tapping Conference 2014*, Misty Hills, Cradle of Humankind, Johannesburg, South Africa. South African Institute of Mining and Metallurgy, Johannesburg. pp. 33–49.

Hopf, M. and Rossouw, E. 2006. New opportunities – Exhaustive monitored copper coolers for submerged arc furnaces. *Proceedings of Southern African Pyrometallurgy 2006*. Jones, R.T. (ed.). Southern African Institute of Mining and Metallurgy, Johannesburg. pp. 89–100.

Horita, S. and Hara, S. 2005. Excellent performance taphole mix. *Shinagawa Technical Report*, no. 48. pp. 47–50.

Hubert, P., Farda, H., Cadilhon, P., and Poirson, G. 1991. The total quality control installation: Improvement factor for tap hole clays. *Proceedings of the Unified International Technical Conference on Refractories*, 2 edn. Aachen, FDR, 23–26 September. pp. 397–402.

Hubert, P., Philippon, B., Ruer, C., and Lambert, F. 1995. Evolution of taphole clays properties during ageing. *Proceedings of the Unified International Technical Conference on Refractories*, Kyoto, Japan, 19–22 November. pp. 129–136.

Hundermark, R.J., Nelson, L.R., De Villiers, B., Ndlovu, J., Mokwena, D., Mukumbe, P., Pieterse, B., Seyanund, W., and Van Manen, P. 2014. Redoubling platinum group metal smelting intensity – operational challenges and solutions. *Proceedings of the EPD Symposium on Pyrometallurgy in Honor of David G.C. Robertson*. TMS, Warrendale, PA. pp. 189–196.

Iida, M., Oguru, K., and Hakone, T. 2009. Numerical study on metal/slag drainage rate deviation during blast furnace tapping. *ISIJ International*, vol. 49, no. 8. pp. 1123–1132.

Iiyama, M., Numata, N., Imabeppu, M., and Miwa, T. 1998. Microcracks caused by thermal stress in blast furnace carbon blocks. *Aachen Proceedings*. pp. 19–21.

Irons, G. (ed.). 2001. The tap-hole – the blast furnace lifeline: design / maintenance / operating practices. *Proceedings of the McMaster Symposium on Iron and Steelmaking*. pp. 1–352.

Ishitobi, T., Ichihara, K., and Homma, T. 2010. Operational improvements of submerged arc furnace in Kashima works KF-1 relined in 2006. *Proceedings of INFACON XII*, Helsinki. pp. 509–515.

Jameson, D., Eden, M.G., and Gordon, R. 1999. The tap-hole zone – The critical factor in long campaign life. *Proceedings of the 58th Ironmaking Conference.* Iron and Steel Society of AIME, Warrendale, PA. pp. 625–631.

Jastrzebski, M., Koehler, T., Wallace, K., Novikov, N.V., Novikov, N., Zaporozhets, B., Shevchenko, D., Kryzhanovskaya, N., and Kapran, I. 2012. Redesign of furnace no. 1 at the Pobuzhsky Ferronickel Combine. *Proceedings of COM 2012*, Niagara Falls. pp. 29-41.

Kadkhodabeigi, M., Tveit, H., and Johansen, S.T. 2011. Modelling the tapping process in submerged arc furnaces used in high silicon alloys production. *ISIJ International*, vol. 51, no. 2. pp. 193–202.

Kageyama, T., Kitamura, M., and Tanaka, D. 2005. Eco-friendly high performance taphole mix. *Shinagawa Technical Report*, no. 48. pp. 41–46.

Kageyama, T., Kitamura, M., and Tanaka, D. 2007. Effects of ultra fine powder additions on taphole mix. *Shinagawa Technical Report*, vol. 50. pp. 41–48.

Kennedy, M.W., Nos, P., Bratt, M., and Weaver, M. 2013. Alternative coolants and cooling system designs for safer freeze lined furnace operation. *Proceedings of Ni-Co 2013*, San Antonio, TX, 3–7 March 2013. pp. 299–314.

Kitamura, M. 2014. Optimising taphole clay technology. *Shinagawa Technical Report*, vol. 57. pp. 1–6.

Ko, Y.C., Ho, C.K., and Kuo, H.T. 2008. The thermal behaviour analysis in taphole area. *China Steel Technical Report*. no. 21. pp. 13-20.

Lange, M., Garbers-Craig, A.M., and Cromarty, R. 2014. Wear of magnesia chrome bricks as a function of matte temperature. *Journal of the Southern African Institute of Mining and Metallurgy*, vol. 114, no. 4. pp. 341–346.

Liow, J-L., Juusela, M., and Gray, N.B. 2001. Viscosity effects in the discharge of a two-layer liquid through an orifice. *14th Australasian Fluid Mechanics Conference*, Adelaide University, Adelaide, Australia, 10–14 December 2001. pp. 853–856

Liow, J.L., Juusela, M., Gray, N.B., and Šutalo, I.D. 2003. Entrainment of a two-layer liquid through a tap-hole. *Metallurgical and Materials. Transactions*, vol. 34B. pp. 821–832.

Lungmuss Feuerfest. 2014. Lungmuß taphole clays for submerged arc & shaft furnaces (company brochure). http://www.envicomab.com/wp-content/uploads/2014/08/Lungmuss-Taphole-Clays-for-SAF-May-2014.pdf

Macrosty, R., Nitschke, S., Gerritsen, T., and Karges, A. 2007. Advances in furnace monitoring: instrumentation. COM 2007. *Proceedings of the 6th International Copper-Cobre Conference*, Toronto, Ontario, 25–30 August 2007. Vol. VII. pp. 203–216.

Marx, F., Shapiro, M., and Henning, B. 2005. Application of high intensity refractory cooling systems in pyrometallurgical vessel design. *Proceedings of INFACON XII*, Helsinki. pp. 769–778.

Matsutani, T. Not dated. The Mitsubishi Process – Copper smelting for the 21st century. http://www.scribd.com/doc/127397992/The-Mitsubishi-Process-Copper-Smelting-for-the-21st-Century-Manuscript

Merry, J., Sarvinis, J., and Voermann, N. 2000. Modern furnace cooling design. *JOM*, vol. 52, no. 2. pp. 62–64.

Mills, K.C. and Keene, B.J. 1987. Physical properties of BOS slags. *International Materials Reviews*, vol. 32, no. 1–2. pp. 1–44.

Mitsui, H., Toritani, T., Yamane, S., Oguchi, Y., and Kawakami, T. 1988. Recent developments in tap hole mud for blast furnaces. *Aachen Proceedings*. pp. 98–107.

Muller, J. and Steenkamp, J.D. 2013. Evaluation of HCFeMN and SiMn slag taphole performance using CFD and thermochemical property modelling for CaO-MnO-SiO_2-Al_2O_3-MgO slag. *Proceedings of INFACON XIII*, Almaty, Kazakhstan. pp. 385–392.

Nakamura, R., Sumimura, H., and Kitamura, M. 2007. Development of a new resin-bonded taphole mix for high productivity blast furnaces. *Shinagawa Technical Report*, vol. 50. pp. 71–76.

Ndlovu, J., Amadi-Echendu, J.E., Nelson, L.R., and Stober, F. 2005. Operational readiness – a value proposition. *Proceedings of Nickel and Cobalt 2005. Challenges in Extraction and Production. 44th Annual Conference of Metallurgists of CIM*, Calgary, Canada. pp. 389–404.

Nelson, L.R. 2014. Evolution of the mega-scale in ferroalloy electric furnace smelting. Celebrating the Megascale: *Proceedings of the EPD Symposium on Pyrometallurgy in Honor of David G.C. Robertson*. TMS, Warrendale, PA. pp. 39–68.

Nelson, L.R., Geldenhuis, J.M.A., Emery, B., De Vries, M., Joiner, K., and Ma, T. 2006. Hatch development in furnace design in conjunction with smelting plants in Africa. *Proceedings of Southern African Pyrometallurgy 2006*. Jones, R.T. (ed.). Southern African Institute of Mining and Metallurgy, Johannesburg. pp. 417–435.

Nelson, L.R., Geldenhuis, J.M.A., Miraza, T., Badrujaman, T., Taofic Hidyat, A., Jauhari, I., Stober, F.A., Voermann, N., Wasmund, B.O., and Jahnsen, E.J.M. 2007. Role of operational support in ramp-up of the FeNi-II furnace at PT Antam in Pomalaa. *Proceedings of INFACON XI*, New Delhi. pp. 798–813.

Nelson, L.R., Sullivan, R., Jacobs, P., Munnik, E., Lewarne, P., Roos, E., Uys, M.J.N., Salt, B., De Vries, M., Mckenna, K., Voermann, N., and Wasmund, B.O. 2004. Application of a high intensity cooling system to dc-arc furnace production of ferrocobalt at Chambishi. *Journal of the South African Institute of Mining and Metallurgy*, vol. 104. pp. 551–561.

Newman, C.J. and Weaver, M.M. 2002. Kennecott flash converting furnace design improvements – 2001. *Proceedings of Sulfide Smelting 2002*. TMS, Warrenadale, PA. pp. 317–328.

Nightingale, R.J. and Rooney, B.J. 2001. Damage to tap-hole and sidewalls of Port Kembla no. 5 blast furnace – causes and remedies. No.3 tap-hole spool breakout. *Proceedings of the McMaster Symposium on Iron and Steelmaking*. pp. 302–307.

Nightingale, R.J., Tanzil, F.W.B.U., Beck, A.J.G., and Price, K. 2001. Blast furnace hearth condition monitoring and tap-hole management techniques. *La Revue de Mètallurgie*. pp. 533–540.

Nightingale, S.A., Wells, L., Tanzil, F., Cummins, J., Monaghan, B.J., and Price, K. 2006. Assessment of the structural development of resin bonded taphole clay. *ICSTI 06, International Conference on the Science and Technology of Ironmaking.* Osaka, Japan. ISIJ. pp. 251–255.

Niiya, Y., Kitamura, M., and Kajitani, A. 2012. Study on the adhesion properties of taphole mixes. *Shinagawa Technical Report*, no. 55, pp. 1–10.

Nishi, T. 2007. The buildup of additional HC FeMn production capacity by the deepening of a furnace. *Proceedings of INFACON XI*, New Delhi. pp. 183–190.

Nolet, I. 2014. Tapping of PGM-Ni mattes: an industry survey. *Proceedings of the Furnace Tapping Conference*, Misty Hills, Cradle of Humankind, Johannesburg, South Africa. Southern African Institute of Mining and Metallurgy, Johannesburg. pp. 12.

O'shaughnessy, P., Wei, D., Guoxhu, K., and Sylven, O. 2013. Improved furnace lining performance at Yiwang Ferroalloys. *Proceedings of INFACON XIII*, Almaty, Kazakhstan. pp. 401–406.

Östlund, P. 2001. Developments in tap-hole design, tapping methods and refractory repair over the last twenty years at SSÅB Oxselösund. *Proceedings of the McMaster Symposium on Iron and Steelmaking*. pp. 322–322.

Pan, C.-N. and Shao, C.-H. 2009. Development of anti-splashing taphole mud. *China Steel Technical Report*, no. 22. pp. 48–52.

Perez, J.L., Takeda, K., Shiraishi, K., Inoue, F., and Honda, N. 2001. Development of non-polluting tap-hole mixture. *Proceedings of the Unified International Technical Conference on Refractories*, Cancun, Mexico, 4–7 November. pp. 200–207.

Petruccelli, A., Van Laar, F., and Hriblj, F. 2003. Alternating tap-hole practice with a two-tap-hole blast furnace. *Proceedings of the ISS Technical Conference 2003*. pp. 457–468.

Piel, K.-Th , Wilkening, S., Lechthaler, K., and Santowski, K. 1988. Improved carbon blocks for blast furnaces. *Aachen Proceedings*. pp. 22–25.

Plikas, T., Gunnewiek, L., Gerritsen, T., Brothers, M., and Karges, A. 2005. The predictive control of furnace tapblock operation using CFD and PCA modelling. *JOM*, Oct. 2005. p. 37–43.

Post, J.R., Teeters, T., Yang, Y., and Reuter, M.A. 2003. Hot metal flow in the blast furnace hearth: Thermal and carbon dissolution effects on buoyancy, flow and refractory wear. *Proceedings of the 3rd International Conference on CFD in the Minerals and Process Industries*, 10–12 December 2003. CSIRO, Melbourne, Australia. pp. 433–440.

Personal Communication. 1999. Mississauga, 29–30 March 1999.

Personal Communication. 2003. Rustenburg, 8–9 April 2003.

Personal Communication. 2010. Johannesburg, 27–29 April 2010.

Personal Communication. 2011. Victoria Falls, 2–8 October 2011.

Robertson, D.G.C. and Kang, S. 1999. Model studies of heat transfer and flow in slag-cleaning furnaces. *Fluid-Flow Phenomena in Metals Processing*. El-Kaddah, N. (ed.). The Metallurgical Society, Warrendale, PA. pp. 1–20.

Rodd, L., Koehler, T., Walker, C., and Voermann, N. 2010. Economics of slag heat recovery from ferronickel slags. *Proceedings of Sustainability for Profit, COM2010*, Vancouver. pp. 3–17.

Rüther, H.P. 1988. Refractory technology and operational experience with tapholes and troughs of blast furnaces in the Federal Republic of Germany. *Aachen Proceedings*. pp. 60–66.

Sadri, A., Gebski, P., and George-Kennedy, D. 2008. Development of the taphole acoustic monitoring (TAM) system for water-cooled copper tapblocks. *Proceedings of COM 2008*, Winnipeg. pp. 7–19.

Sager, D., Grant, D., Stadle, R., and Schreiter, T. 2010. Low cost ferroalloy extraction in DC-arc furnace at Middleburg Ferrochrome. *Journal of the Southern African Institute of Mining and Metallurgy*, vol. 110. pp. 717–724.

Shao, L. 2013. Model-based estimation of liquid flows in the blast furnace hearth and taphole. Doctor of Technology thesis, Abo Akademi University, Turku/Abo, Finland. (ISBN 978-952-12-2941-1).

Shao, L. and Saxen, H. 2011. A simulation study of blast furnace hearth drainage using a two-phase flow model of the tap-hole. *ISIJ International*, vol. 51, no. 2. pp. 228–235

Shao, L. and Saxen, H. 2013a. A simulation study of two-liquid flow in the taphole of the blast furnace. *ISIJ International*, vol. 53, no. 6. pp. 988–994.

Shao, L. and Saxen, H. 2013b. Flow patterns of iron and slag in the blast furnace taphole. *ISIJ International*, vol. 53, no. 10. pp. 1756–1767.

Shaw, A., De Villiers, L.P.Vs., Hundermark, R.J., Ndlovu, J., Nelson, L.R., Pieterse, B., Sullivan, R., Voermann, N., Walker, C., Stober, F., and Mckenzie, A.D. 2012. Challenges and solutions in PGM furnace operation: High matte temperature and copper cooler corrosion. *Journal of the Southern African Institute of Mining and Metallurgy*, vol. 113. pp. 251–261.

Sheng, Y.Y., Irons, G.A., and Tisdale, D.G. 1998. Transport phenomena in electric smelting of nickel matte: Part II. Mathematical modelling. *Metallurgical and Materials Transactions B*, vol. 29B. February. pp. 85–94.

Singh, B.B, Suresh Kumar, P.G., and Mahata, S.K. 2007. Modern practices of post tap-hole operation in ferro chrome production and its advantages. *Proceedings of INFACON XI*, New Delhi. pp. 530–538.

Smith, M., Franklin, S., and Fonseca, F. 2005. Improving blast furnace operations by co-ordinated improvements in tap-hole clay, guns and drills. *Proceedings of the 5th AIS Ironmaking Conference*. Instituto Argentino de Siderurgia, pp. 197–202.

Spreij, M., Tijhuis, G.J., Trow, J., and Franken, M.C. 1995. A quantitative selection of blast furnace hearth refractories. *Proceedings of the Unite CR Congress*. pp. 167–175.

Steigauf, C. and Storm, L. 2001. Optimization of tap-hole construction, maintenance, and casting practice for high productivity, high reliability, and long campaign life. *Proceedings of the McMaster Symposium on Iron and Steelmaking*. pp. 37–47.

Stevenson, P. and He, Q. 2005. Slug flow in blast furnace taphole. *Chemical Engineering and Processing*, vol. 44. pp. 1094–1097.

Stokman, R., Van Stein Callenfels, E., and Van Laar, R. 2004. Blast furnace lining and cooling technology: experience at Corus IJmuiden. Association for Iron & Steel Technology, Warrendale, PA. pp. 21–29.

Sundström, A.W., Eksteen, J.J., and Georgalli, G.A. 2008. A review of the physical properties of base metal mattes. *Journal of the Southern African Institute of Mining and Metallurgy*, vol. 108, Aug. 2008. pp. 431–449.

Szekely, J. and Dinovo, S.T. 1974. Thermal criteria for tundish nozzle or taphole blockage. *Metallurgical Transactions*, vol. 5. pp. 747–754.

Szymkowski, S.J. and Bultitude-Paull, J.M. 1992. The production of high quality silicon metal and Simcoa. *Proceedings of INFACON VI*, Cape Town. pp. 185–191.

Tanzil, F.W.B.U., Nightingale, R.J., Lee, R.C., Dunning, J.P., and Ratter, J. 2001. The application of novel techniques and new sensors to tap-hole management practice at Port Kembla no. 6 blast furnace. *Proceedings of the McMaster Symposium on Iron and Steelmaking*. pp. 193–207.

Tomala, J. and Basista, S. 2007. Micropore carbon furnace lining. *Proceedings of INFACON XI*, New Delhi. pp. 722–727.

Trapani, M.L., Kyllo, A.K., and Gray, N.B. 2002. Improvements to tap-hole design. *Proceedings of the 3rd International Sulfide Smelting Symposium (Sulfide Smelting '02)*, Seattle, Washington, 17–21 February 2002. pp. 339–348.

Tsuchiya, N., Fukutake, Y., Yamauchi, Y., and Matsumoto, T. 1998. In-furnace conditions as prerequisites for proper use and design of mud to control blast furnace tap-hole length. *ISIJ International*, vol. 38. pp. 116–125.

Uenaka, T., Yulubo, Y., Shimomura, K., Yorita, E., Ohara, K., and Omori, H. 1989. An evaluation method of taphole mud for blast furnace. *Shinagawa Technical Report*, no. 32. pp. 29–44.

Valentas, L.S. and Thierney, E.P. 2010. Furnace panel leak detection system. US patent 7,832,367 B2. 16 Nov. 2010.

Van Der Walt, N.J. 1986. The design and development of furnace linings for manganese alloys smelting. *Proceedings of INFACON IV*, Rio de Janeiro. pp. 17–30.

Van Ikelen, J.P., De Pagter, J.J., and Belleman, G.T.J. 2000. Experience with tap-hole drilling technology. *Proceedings of the 4th European Coke and Ironmaking Congress*, Paris, 19–21 June. vol. 2. pp. 610–616.

Van Laar, K. 2001. The tap-hole: the heart of the blast furnace. *Proceedings of the McMaster Symposium on Iron and Steelmaking*. pp. 1–21.

Van Laar, R. 2014. Personal communication.

Van Laar, R.J., Höll, H., Dzermejko, A.J., Risi, J., and Malan, J. 2001. Improving profitability by analysing ferroalloys furnace lining performance to improve lifetime. *Proceedings of INFACON IX*, Quebec City. pp. 475–485.

Van Laar, R., Van Stein Callenfels, E., and Geerdes, M. 2003. Blast furnace hearth management for safe and long campaigns. *ISSTech 2003 Conference Proceedings*. pp. 1079-1090.

Veenstra, R., Voermann, N., and Wasmund, B. 1997. Prototype metal tap block design. *Proceedings of Nickel-Cobalt 97*, Montreal. vol. 3. pp. 595–607.

Voermann, N., Gerritsen, T., Candy, I., Stober, F., and Matyas, A. 2010. Developments in furnace technology for ferro-nickel production. *Proceedings of INFACON X*, Cape Town. pp. 455–465.

Walker, C., Kashani-Nejad, S., Dalvi, A.D., Voermann, N., Candy, I.M., and Wasmund, B. 2009. Nickel laterite rotary kiln-electric furnace plant of the future. *Proceedings of COM 2009*, Sudbury. pp. 19.

Wasmund, B.O. 2003. Personal Communication.

Wells, L.J. 2002. The rheology of a composite polymer ceramic plastic refractory. PhD thesis, University of Wollongong, Australia.

Yamashita, M., Kashiwada, M., and Shibuta, H. 1995. Improvement of tap holes at Wakayama no. 5 blast furnace. *Proceedings of the 54th Ironmaking Conference*, Nashville, TN. Iron and Steel Society, Warrendale, PA. pp. 177–182.

Zhou, J. and Sun, L. 2013. Flash smelting and flash converting process and start-up at Jinguan Copper. *Proceedings of Copper 2013*, Santiago. pp. 199–212. ◆

The Southern African Institute of Mining and Metallurgy

in collaboration with The Zululand Branch are organising

The Tenth International

HEAVY MINERALS CONFERENCE

'Expanding the horizon'

HMC 2016 HEAVY MINERALS 2016

16–17 August 2016—Conference
18 August 2016—Technical Visit

Sun City, South Africa

KEYNOTE SPEAKERS

J. Beukes, *Tronox*
J. Elder, *Hatch*
V. Hugo, *Iluka*
M. Rossouw, *Eskom*
C. Steenkamp, *Samancor*

CONFERENCE THEME

The series of heavy minerals conferences has traditionally focused on the industries associated with ilmenite, rutile and zircon. There are many other economic minerals which have specific gravities such that they may also be classed as 'heavy minerals'. The physical and chemical properties of these other minerals results in them being processed by similar technologies and sharing similar markets to the more traditional heavy minerals. In this conference we continue to examine the mining, processing and usage of the traditional heavy minerals but also 'expand our horizons' to include other valuable minerals.

CONFERENCE OBJECTIVE

This Conference series was started in 1997 and has run every second year since that date. The Conference alternates between South Africa and other heavy mineral producing countries. It will provide a forum for an exchange of knowledge in all aspects from exploration through processing and product applications.

This is a strictly technical conference and efforts by the organizing committee are aimed at preserving this technical nature. The benefit of this focus is that it allows the operators of businesses within this sector to discuss topics not normally covered in such forums. The focus on heavy minerals includes the more obvious minerals such as ilmenite, rutile and zircon; and in addition also covers other heavy minerals such as garnet, andalucite, sillimanite, and chromite.

ABOUT THE VENUE

Nestled in the rolling hills of the Pilanesberg, one of South Africa's most scenic locations, Sun City is a world unto itself and has earned its reputation as Africa's Kingdom of Pleasure.

Finally re-discovered and now part of Sun City, the Lost City and the Valley of Waves, fabled to be the Ruins of a glorious ancient civilisation, celebrate and bring to life the legends of this mystical city.

The Lost City is internationally applauded for its wonderfully imaginative theme and exquisite landscaping whilst the fantastic Valley of Waves is one of the world's most exciting waterparks.

WHO SHOULD ATTEND

- Academics
- Business development managers
- Concentrator managers
- Consultants
- Engineers
- Exploration managers
- Geologists
- Hydrogeologists
- Innovation managers
- Mechanical engineers
- Metallurgical managers
- Metallurgical consultants
- Metallurgists
- Mine managers
- Mining engineers
- New business development managers
- Planning managers
- Process engineers
- Product developers
- Production managers
- Project managers
- Pyrometallurgists
- Researchers
- Scientists

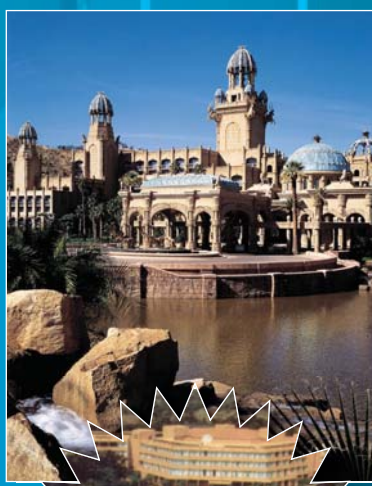

Sponsors

ALICOCO MINERAL TECHNOLOGY
ERIEZ
Mineral Technologies
Saveway
MULTOTEC
DERRICK
Polypipe
WEIR

Announcement and Call for Papers

SAIMM THE SOUTHERN AFRICAN INSTITUTE OF MINING AND METALLURGY

Camielah Jardine, Conference Co-ordinator
Tel: 27 (11) 834-1273/7
Fax 27 (11) 838-5923 or 833-8156
E-mail: camielah@saimm.co.za

Conference Announcement

science & technology
Department:
Science and Technology
REPUBLIC OF SOUTH AFRICA

ami
advanced metals initiative

SAIMM
THE SOUTHERN AFRICAN INSTITUTE OF MINING AND METALLURGY

Ferrous 2016
FERROUS AND BASE METALS DEVELOPMENT NETWORK CONFERENCE 2016

19–21 October 2016

Southern Sun Elangeni Maharani, KwaZulu-Natal, South Africa

BACKGROUND

Through its Advanced Metals Initiative (AMI) the South African Department of Science and Technology (DST) promotes research, development and innovation across the entire value chain of the advanced metals field. The goal of this initiative is to achieve sustainable local mineral beneficiation and to increase the downstream value addition of advanced metals in a sustainable manner. The achievement of this is envisioned to be through human capital development on post-graduate and post-doctoral level, technology transfer, localization and ultimately, commercialisation.

The AMI comprises four networks, each focussing on a different group of metals. These are Light Metals, Precious Metals, Nuclear Materials and Ferrous and Base Metals (i.e. iron, steel, stainless steels, superalloys, copper, brass, etc.).

The AMI FMDN 2016 Conference aims to bring together stakeholders from the mineral sector, academia, steel industry, international research institutions and government in order to share and debate the latest trends, research and innovations, specifically in the areas of energy, petrochemical, corrosion, materials for extreme environments and transport, local mineral beneficiation and advanced manufacturing related to these materials.

Keynote speakers to be invited include international specialists in the fields of ferrous metals, computational materials science, high temperature corrosion and mineral beneficiation.

The Ferrous and Base Metals Development Network (FMDN) of the DST's Advanced Metals Initiative (AMI) programme will host the AMI's annual conference in 2016. The conference seeks to share insight into the state of R&D under the AMI-FMDN programmes and explore and debate the following broad themes:

- Development of high performance ferrous and base metal alloys for application in the energy and petrochemical industries
- Development of corrosion resistant ferrous and base metal alloys
- Development of lightweight and/or durable steels for cost-effective transportation and infrastructure, and
- Panel discussions on possible future value-adding R&D programmes under FMDN within the South African National Imperatives.

OBJECTIVES

Insight into ferrous and base metal materials R&D for application in the areas of energy, petrochemical, corrosion, extreme environments, improved processing technologies and advanced alloys for the transport industry in South Africa and globally.

EXHIBITION/SPONSORSHIP

Sponsorship opportunities are available. Companies wishing to sponsor or exhibit should contact the Conference Co-ordinator.

WHO SHOULD ATTEND

Stakeholders from the energy, petrochemical, corrosion and transportation industries where ferrous (i.e. iron, steel, stainless steels, superalloys, etc.) and base (i.e. copper, brass, etc.) metals are used in their infrastructure. Also included in this invitation are local and international Higher Education Institutions (HEIs), Government Departments and Science Councils that are involved and/or have interest in R&D in these areas.

MINTEK
Specialists in mineral and metallurgical technology

necsa
We're in your world

CSIR
our future through science

For further information contact:
Head of Conferencing, Raymond van der Berg
SAIMM, P O Box 61127, Marshalltown 2107
Tel: +27 11 834-1273/7 ·Fax: +27 11 833-8156 or +27 11 838-5923
E-mail: raymond@saimm.co.za · Website: http://www.saimm.co.za

INTERNATIONAL ACTIVITIES

2016

9–10 June 2016 — New technology and innovation in the Minerals Industry Colloquium
Emperors Palace, Johannesburg
Contact: Camielah Jardine
Tel: +27 11 834-1273/7, Fax: +27 11 838-5923/833-8156
E-mail: camielah@saimm.co.za, Website: http://www.saimm.co.za

27–28 June 2016 — The 2nd School on Manganese Ferroalloy Production
Mintek, Johannesburg
Contact: Raymond van der Berg
Tel: +27 11 834-1273/7, Fax: +27 11 838-5923/833-8156
E-mail: raymond@saimm.co.za, Website: http://www.saimm.co.za

19–20 July 2016 — Innovations in Mining Conference 2016
'Redesigning the Mining and Mineral Processing Cost Structure'
Holiday Inn Bulawayo
Contact: Raymond van der Berg
Tel: +27 11 834-1273/7, Fax: +27 11 838-5923/833-8156
E-mail: raymond@saimm.co.za, Website: http://www.saimm.co.za

25–26 July 2016 —Production of Clean Steel
Mintek, Randburg
Contact: Camielah Jardine
Tel: +27 11 834-1273/7, Fax: +27 11 838-5923/833-8156
E-mail: camielah@saimm.co.za, Website: http://www.saimm.co.za

31 July–3 August 2016 — Hydrometallurgy Conference 2016
'Sustainability and the Environment' in collaboration with MinProc and the Western Cape Branch
Belmont Mount Nelson Hotel, Cape Town
Contact: Raymond van der Berg
Tel: +27 11 834-1273/7, Fax: +27 11 838-5923/833-8156
E-mail: raymond@saimm.co.za, Website: http://www.saimm.co.za

8 August 2016 — South African Underground Coal Gasification Association
2nd Underground Coal Gasification Network Workshop
CDH Sandton, Johannesburg
Contact: Shehzaad Kauchali
Email: shehzaad.kauchali@wits.ac.za
Website: http://www.saucga.org.za

9–12 August 2016 — Thirty Third Annual International Pittsburgh Coal Conference 2016
International Convention Centre, Cape Town, South Africa
Contact: Raquel (South Africa)
Tel: +27 11 475-2750 or +27 82 509-6485
Email: pcc@@ap22ude.co.za
Contact: H.M. Peck (International)
Tel: +1(412) 624-7440, Fax: +1(412) 624-1480
Email: ipcc@pitt.edu, Website: http://www.pccpitt.org

16–18 August 2016 — The Tenth International Heavy Minerals Conference '*Expanding the horizon*'
Sun City, South Africa
Contact: Camielah Jardine
Tel: +27 11 834-1273/7, Fax: +27 11 838-5923/833-8156
E-mail: camielah@saimm.co.za, Website: http://www.saimm.co.za

31 August–2 September 2016 — MINESafe Conference Striving for Zero Harm
Emperors Palace, Hotel Casino Convention Resort
Contact: Raymond van der Berg
Tel: +27 11 834-1273/7, Fax: +27 11 838-5923/833-8156
E-mail: raymond@saimm.co.za, Website: http://www.saimm.co.za

12–13 September 2016 — Mining for the Future 2016
'The Future for Mining starts Now'
Electra Mining, Nasrec, Johanannesburg
Contact: Camielah Jardine
Tel: +27 11 834-1273/7, Fax: +27 11 838-5923/833-8156
E-mail: camielah@saimm.co.za, Website: http://www.saimm.co.za

12–14 September 2016 — 8th International Symposium on Ground Support in Mining and Underground Construction
Kulturens Hus – Conference & Congress, Luleå, Sweden
Contact: Erling Nordlund
Tel: +46-920493535, Fax: +46-920491935
E-mail: erling.nordlund@ltu.se, Website:
http://groundsupport2016.com

19–21 October 2016 — AMI Ferrous and Base Metals Development Network Conference 2016
Southern Sun Elangeni Maharani, KwaZulu-Natal, South Africa
Contact: Raymond van der Berg
Tel: +27 11 834-1273/7, Fax: +27 11 838-5923/833-8156
E-mail: raymond@saimm.co.za, Website: http://www.saimm.co.za

25 October 2016 — The Young Professionals Week, 14th Annual Student Colloquium
Mintek, Randburg
Contact: Raymond van der Berg
Tel: +27 11 834-1273/7, Fax: +27 11 838-5923/833-8156
E-mail: raymond@saimm.co.za, Website: http://www.saimm.co.za

2017

9–10 March 2017 — 3rd Young Professionals Conference
Innovation Hub, Pretoria, South Africa
Contact: Camielah Jardine
Tel: +27 11 834-1273/7, Fax: +27 11 838-5923/833-8156
E-mail: camielah@saimm.co.za, Website: http://www.saimm.co.za

25–28 June 2017 — Emc 2017: European Metallurgical Conference
Leipzig, Germany
Contact: Paul-Ernst-Straße
Tel: +49 5323 9379-0, Fax: +49 5323 9379-37
E-mail: EMC@gdmg.de, Website: http://emc.gdmb.de

27–29 June 2017 —4th Mineral Project Valuation
Mine Design Lab, Chamber of Mines Building, The University of the Witwatersrand, Johannesburg
Contact: Raymond van der Berg
Tel: +27 11 834-1273/7, Fax: +27 11 838-5923/833-8156
E-mail: raymond@saimm.co.za, Website: http://www.saimm.co.za

2–7 October 2017 —AfriRock 2017: ISRM International Symposium 'Rock Mechanics for Africa'
Cape Town Convention Centre, Cape Town
Contact: Raymond van der Berg
Tel: +27 11 834-1273/7, Fax: +27 11 838-5923/833-8156
E-mail: raymond@saimm.co.za, Website: http://www.saimm.co.za

Company Affiliates

The following organizations have been admitted to the Institute as Company Affiliates

3 M South Africa

AECOM SA (Pty) Ltd

AEL Mining Services Limited

Air Liquide (PTY) Ltd

AMEC Mining and Metals

AMIRA International Africa (Pty) Ltd

ANDRITZ Delkor(Pty) Ltd

Anglo Operations Ltd

Anglo Platinum Management Services (Pty) Ltd

Aurecon South Africa (Pty) Ltd

Aveng Moolmans (Pty) Ltd

Axis House (Pty) Ltd

Bafokeng Rasimone Platinum Mine

Barloworld Equipment -Mining

BASF Holdings SA (Pty) Ltd

BCL Limited

Becker Mining (Pty) Ltd

BedRock Mining Support (Pty) Ltd

Bell Equipment Company (Pty) Ltd

Blue Cube Systems (Pty) Ltd

Caledonia Mining Corporation

CDM Group

CGG Services SA

Chamber of Mines

Concor Mining

Concor Technicrete

Council for Geoscience Library

CSIR-Natural Resources and the Environment

Data Mine SA

Department of Water Affairs and Forestry

Digby Wells and Associates

Downer EDI Mining

DRA Mineral Projects (Pty) Ltd

DTP Mining

Duraset

Elbroc Mining Products (Pty) Ltd

Engineering and Project Company Ltd

eThekwini Municipality

Exxaro Coal (Pty) Ltd

Exxaro Resources Limited

FLSmidth Minerals (Pty) Ltd

Fluor Daniel SA (Pty) Ltd

Franki Africa (Pty) Ltd Johannesburg

Fraser Alexander Group

Geobrugg Southern Africa

GIBB (Pty) Ltd

Glencore

Goba (Pty) Ltd

Hall Core Drilling (Pty) Ltd

Hatch (Pty) Ltd

Herrenknecht AG

HPE Hydro Power Equipment (Pty) Ltd

IMS Engineering (Pty) Ltd

Ivanhoe Mines SA

JENNMAR South Africa

Joy Global Inc. (Africa)

Kadumane Manganese Resources

Leco Africa (Pty) Limited

Longyear South Africa (Pty) Ltd

Lonmin Plc

Magnetech (Pty) Ltd

Magotteaux(PTY) LTD

MBE Minerals SA Pty Ltd

MCC Contracts (Pty) Ltd

MDM Technical Africa (Pty) Ltd

Metalock Industrial Services Africa (Pty)Ltd

Metorex Limited

Metso Minerals (South Africa) (Pty) Ltd

Minerals Operations Executive (Pty) Ltd

MineRP Holding (Pty) Ltd

Mintek

MIP Process Technologies

Modular Mining Systems Africa (Pty) Ltd

MSA Group (Pty) Ltd

Multotec (Pty) Ltd

Murray and Roberts Cementation

Nalco Africa (Pty) Ltd

Namakwa Sands (Pty) Ltd

New Concept Mining (Pty) Limited

Northam Platinum Ltd - Zondereinde

PANalytical (Pty) Ltd

Paterson and Cooke Consulting Engineers (Pty) Ltd

Polysius A Division Of Thyssenkrupp Industrial Solutions (Pty) Ltd

Precious Metals Refiners

Rand Refinery Limited

Redpath Mining (South Africa) (Pty) Ltd

Rosond (Pty) Ltd

Royal Bafokeng Platinum

Roymec Tecvhnologies (Pty) Ltd

Runge Pincock Minarco Limited

Rustenburg Platinum Mines Limited

Salene Mining (Pty) Ltd

Sandvik Mining and Construction Delmas (Pty) Ltd

Sandvik Mining and Construction RSA(Pty) Ltd

SANIRE

Sasol Mining(Pty) Ltd

Sebilo Resources (Pty) Ltd

SENET (Pty) Ltd

Senmin International (Pty) Ltd

Smec SA

SMS Siemag South Africa (Pty) Ltd

Sound Mining Solutions (Pty) Ltd

South 32

SRK Consulting SA (Pty) Ltd

Technology Innovation Agency

Time Mining and Processing (Pty) Ltd

Tomra Sorting Solutions Mining (Pty) Ltd

Ukwazi Mining Solutions (Pty) Ltd

Umgeni Water

VBKOM Consulting Engineers

Webber Wentzel

Weir Minerals Africa

WorleyParsons (Pty) Ltd

Forthcoming SAIMM events...

EXHIBITS/SPONSORSHIP
Companies wishing to sponsor and/or exhibit at any of these events should contact the conference co-ordinator as soon as possible

For the past 120 years, the Southern African Institute of Mining and Metallurgy, has promoted technical excellence in the minerals industry. We strive to continuously stay at the cutting edge of new developments in the mining and metallurgy industry. The SAIMM acts as the corporate voice for the mining and metallurgy industry in the South African economy. We actively encourage contact and networking between members and the strengthening of ties. The SAIMM offers a variety of conferences that are designed to bring you technical knowledge and information of interest for the good of the industry. Here is a glimpse of the events we have lined up for 2016. Visit our website for more information.

SAIMM
THE SOUTHERN AFRICAN INSTITUTE OF MINING AND METALLURGY

For further information contact:
Conferencing, SAIMM
P O Box 61127, Marshalltown 2107
Tel: (011) 834-1273/7
Fax: (011) 833-8156 or (011) 838-5923
E-mail: raymond@saimm.co.za

SAIMM DIARY

2016

- **COLLOQUIUM**
  New technology and innovation in the Minerals Industry Colloquium
  9–10 June 2016, Emperors Palace, Johannesburg
- **SCHOOL**
  The 2nd School on Manganese Ferroalloy Production
  27–28 June 2016, Mintek, Johannesburg
- **CONFERENCE**
  Innovations in Mining Conference 2016
  19–20 July 2016, Holiday Inn Bulawayo
- **SCHOOL**
  Production of Clean Steel
  25–26 July 2016, Mintek, Randburg
- **CONFERENCE**
  Hydrometallurgy Conference 2016 *'Sustainability and the Environment'* in collaboration with MinProc and the Western Cape Branch
  31 July–3 August 2016, Belmont Mount Nelson Hotel, Cape Town
- **CONFERENCE**
  The Tenth International Heavy Minerals Conference *'Expanding the horizon'*
  16–18 August 2016, Sun City, South Africa
- **CONFERENCE**
  MINESafe Conference Striving for Zero Harm
  31 August–2 September 2016, Emperors Palace, Hotel Casino Convention Resort,
- **CONFERENCE**
  Mining for the Future 2016 *'The Future for Mining starts Now'*
  12–13 September 2016, Electra Mining, Nasrec, Johannesburg
- **CONFERENCE**
  AMI Ferrous and Base Metals Development Network Conference 2016
  19–21 October 2016, Southern Sun Elangeni Maharani, KwaZulu-Natal
- **COLLOQUIUM**
  The Young Professionals Week
  14th Annual Student Colloquium
  25 October 2016, Mintek, Randburg

2017

- **CONFERENCE**
  3rd Young Professionals Conference
  9–10 March 2017, Innovation Hub, Pretoria
- **CONFERENCE**
  4th Mineral Project Valuation School
  27–29 June 2017, The University of the Witwatersrand, Johannesburg
- **SYMPOSIUM**
  ISRM International Symposium *'Rock Mechanics for Africa'*
  2–7 October 2017, Cape Town Convention Centre, Cape Town

The best blast, on time, every time

The future of mining is electronic initiation

DetNet continues to strive towards excellence in electronic initiation. As a world leader in our field, we aim to deliver the latest technology, consistent quality, and improved loading and fragmentation, all to ensure mining becomes more sustainable today and into the future. You can rely on DetNet to provide the best blast, on time, every time.

detnet™

detnet.com

the future of electronic initiation